Fully Distributed Time-varying Formation and Containment Control for Multi-agent / Multi-robot Systems

Wei Jiang

Fully Distributed Time-varying Formation and Containment Control for Multi-agent / Multi-robot Systems

Wei Jiang

N° d'ordre: | 3 | 6 | 4 |

CENTRALE LILLE

THÈSE

Présentée en vue
d'obtenir le grade de

DOCTEUR

En

Spécialité : Automatique, Génie Informatique, Traitement du Signal et Image

Par

Wei JIANG

DOCTORAT DÉLIVRÉ PAR CENTRALE LILLE

Titre de la thèse :

Contrôle de la formation et du confinement variable dans le temps et entièrement distribué pour les systèmes multi-agents/ multi-robots

Fully Distributed Time-varying Formation and Containment Control for Multi-agent / Multi-robot Systems

---

Soutenue le 27 novembre 2018 devant le jury d'examen :

Président	Youcef MEZOUAR	Professeur, Université Clermont Auvergne, France
Rapporteur	António M. PASCOAL	Professeur, Université Lisbonne, Portugal
Rapporteur	Zhengtao DING	Professeur, Université Manchester, UK
Membre	Carolina ALBEA SÁNCHEZ	Professeur Associé, Université Toulouse III, France
Membre	Youcef MEZOUAR	Professeur, Université Clermont Auvergne, France
Membre	Marc DOUILLY	PhD, STELIA Aerospace, France
Directeur de thèse	Ahmed RAHMANI	Professeur, École Centrale de Lille, France

Thèse préparée au Centre de Recherche en Informatique, Signal et Automatique de Lille
CRIStAL, UMR CNRS 9189 - Centrale Lille
Ecole Doctorale SPI 072

Je dédie ce travail

à mes chers parents,

à ma chère petite soeur,

à mon directeur,

à mes chèr(e)s ami(e)s,

et aux gens qui apparaissent dans ma vie en France.

Acknowledgement

This research work has been realized in École Centrale de Lille, in "Centre de Recherche en Informatique, Signal et Automatique de Lille (CRIStAL)", with the research team "Méthodes & Outils pour la Conception Intégrée de Systèmes (MOCIS)".

I have to express my feelings to my dear parents and my little sister. They are the ones who always love me, support me and wait for me there. Without them, I may possibly lose the strongest motivation to finish my PhD career with good quality.

My supervisor, Ahmed who will always have my gratitude, gives me a great freedom to research. This is very important for an independent researcher. My thanks will also go to the associated professor, Guoguang Wen who gave me good guidances about how to write, submit and rectify articles. What is more, I was very lucky to meet, live and work with some professors or associated professors in CRIStAL, Centrale Lille during these three years, especially Prof. Yunhe Meng, Prof. Yongguang Yu and associated professor Kun Liu. I learned a lot from them. As a team member, I always try to cooperate with my colleagues: Dr. Youwei Dong, Dr. Xing Chu, Dr. Yan Wei and PhD candidates Wei Hu and Thanh Bình Do. The time working with them is good.

I would like to thank the MOCIS team colleagues who gave me really good advices to improve the quality of my thesis defense power point.

Every Wednesday evening. as soon as I'm available, Cafe de Paris will be where I go to practice my French language and meet nice people there, especially my friend Marie-thé Del. I have developed some good friends all over the Europe like Dr. Kun Yang in Oslo, Dr, Zhifan Jiang, Zheng Chang, Tianqi Zhu, Xuemei Liu, Yongbin Zeng and Qixing Lu, etc in France, which makes my life much easier and happier. These friendships will always be in my heart. My brother, Jianrui Wang, he knows where he is from my side, and will always be there.

The research is very important, of course; but life should still be organized and experienced with high quality, especially in France. Buying a car to travel around the Europe, playing golf to relax myself, going to the gym regularly, drinking the vin rouge, blanc and champagne, and shopping really make me feel happy. I met some girls, Chinese and French, with which the time makes me become maturer,

stronger, more considerate and responsible. These memories will be cherished from always. Mostly, thank you, Manon, for bringing me the beautiful happy time once.

After three year's work, day and night, I get to know myself, to accept my true love to the research and will try the best to continue.

Finally, I would like to present my sincere gratitude to all the jury members. Your huge affirmations to my work will be the enormous motivations for me to continue producing not bad fruits, with or without reputation. Particularly, I would like to express my respect to Prof. Zhengtao Ding whose deep understanding of my work and professional English writing suggestions make this thesis much better.

Thank you all!

Contents

List of Figures

List of Tables

Abbreviations and Notations

List of abbreviations

ARE	Algebraic Riccati Equation	LMI	Linear Matrix Inequality
APESO	Adaptive Predictive Extended State Observer	LTI	Linear Time-Invariant
ESO	Extended State Observer	NCS	Networked Control Systems
FC	Formation-Containment	OCT	Output Consensus Tracking
FSA	Finite Spectrum Assignment	TDS	Time-Delay System
IF	Informed Follower	TVFT	Time-Varying Formation Tracking
IL	Informed Leader	UF	Uninformed Follower
LKF	Lyapunov-Krasovskii Functional	UL	Uninformed Leader

List of notations

$\mathbb{R}^n$	Set of the n-dimensional Euclidean vector space
$\mathbb{R}^{m\times n}$	Set of the $m \times n$ real matrix space
I_n	The n-dimensional identity matrix
$0_{n\times m}$	The $n \times m$ matrix with each entry being 0
$\mathbf{1}$	The column vector with all entries being 1
$\otimes$	The Kronecker product
$\text{diag}\{a_1, \ldots, a_n\}$	The diagonal matrix with the diagonal elements being $a_1, \ldots, a_n$
M-matrix	The quare matrix $A = [a_{ij}]$ is nonsingular M-matrix if $a_{ij} \leq 0, \forall i \neq j$
$\lambda_{min}(P)$	Smallest eigenvalue of the real symmetric matrix P
$\lambda_{max}(P)$	Largest eigenvalue of the real symmetric matrix P
$P > (\geq) 0$	The matrix P is positive (nonnegative) definite
$\mathbb{N}$	The set of natural numbers
$\mathbf{I}[a, b]$	$\mathbf{I}[a, b] = \{a, a + 1, \ldots, b\} \forall\, integer\, a \leq b$
$\det(P)$	The determinant of a square matrix P
$\text{trace}(P)$	The sum of the elements on the main diagonal of P
$\|x\|$	The 2-norm of a vector x
$\|x\|_\infty$	The infinity norm of a vector x, $\|x\|_\infty \leq \|x\|$
$\|x\|$	The absolute value of a scaler x
$L_p(a, b), p \in \mathbb{N}$	The space of functions $\phi : (a, b) \to \mathbb{R}^n$ with the norm $\|\phi\|_{L_p} = \left[\int_a^b \|\phi(\theta)\|^p d\theta\right]^{\frac{1}{p}}$
$x_t(\theta)$	For $x : \mathbb{R} \to \mathbb{R}^n, x_t(\theta) \triangleq x(t + \theta), \theta \in [-h, 0], h > 0$

Chapter 1

General introduction

Contents

1.1 Motivations

This thesis is dedicated to the fully distributed cooperative control (consensus, formation, containment) for large-scale multi-agent systems (MASs)/multi-robot systems (MRSs), from undirected to directed communication topology, from homogeneous to heterogeneous general linear time-invariant (LTI) dynamics, considering constant/time-varying input/output delays and external matched/mismatched disturbances.

The MASs are systems that consist of multiple agents with several sensors/ actuators and with the capability to communicate with other agents to execute coordinated tasks. The theories proposed in this thesis can be applied to MRSs of which the types are multiple mobile robots that can move around in the environment, such as ground aerial or underwater vehicles. Those robots with nonlinear dynamics need to be linearized to adopt the proposed theories in this study.

1.1.1 Why cooperative control

Distributed cooperative control, which can be characterized as a group of decision-making autonomous agents seeking a collective objective based on their local sensed information and limited inter-agent information, has attracted much research interest in the past decades (Albea, Seuret & Zaccarian, 2016, Almeida, Silvestre & Pascoal, 2014, Aranda, Mezouar, López-Nicolás & Sagüés, 2018, Ding, 2017, Jadbabaie, Lin & Morse, 2003, Li, Duan, Chen & Huang, 2010, Olfati-Saber & Murray, 2004, Ren & Beard, 2005).

In laboratory experiments, the common test domains of multiple mobile robot systems are foraging and coverage, flocking and formations, RoboCup multi-robot soccer (shown in Fig. 1.1 (a)), box pushing and cooperative manipulation, etc. Many real-world applications can benefit from those laboratory experiments such as container management in ports (Alami *et al.*, 1998), search and rescue (Murphy, 2000), hazardous waste cleanup (Parker *et al.*, 1998), agriculture, and warehouse management (Hazard *et al.*, 2006), surveillance, reconnaissance and security (Everett *et al.*, 2000), underwater robotic systems (Fig. 1.1 (b) in Abreu *et al.* (2015)), future combat systems, distributed reconfigurable sensor networks and so on. The detailed discussions about the applications can refer to the work of Parker (2008) and references therein.

The motivation for cooperative control of MASs can be summarized as follows:

1. While single agent performing solo missions will yield some benefits, greater benefits will come from the cooperation of teams of agents.

2. It is much cheaper to build some robots/vehicles that have limited function than a single powerful robot/vehicle.

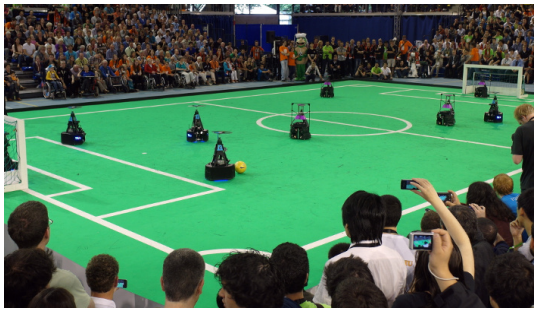

(a) Mobile robot teams competing in soccer.

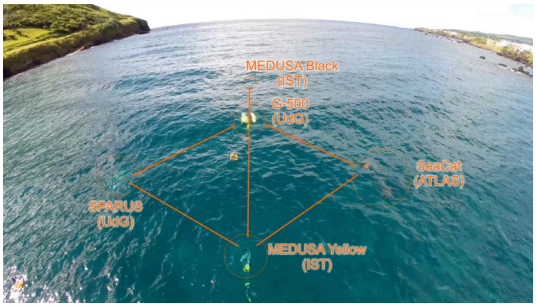

(b) Cooperative Formation Control in the EC MORPH Project (Abreu *et al.*, 2015)

Figure 1.1: Laboratory and real-world cooperative control examples.

3. Multiple robots/vehicles can solve problems faster than only one and increase robustness through redundancy.

1.1.2 Why fully distributed control

The overall control architecture of MASs/MRSs has a significant influence on the robustness and scalability of the system. And the most common architectures are centralized, hierarchical, distributed, and hybrid. The advantages and disadvantages have been discussed extensively by Parker (2008). Especially, the motivation for distributed control is: (i) no agent knows the state/control of all other agents; (ii) the control law for each agent must be distributed so that the overall computational complexity of the problem is acceptable for many agents; (iii) this control architecture could be highly robust to failure as no agent is responsible for the control of any other agent. However, most distributed controllers designed in the existing works (Antonelli *et al.*, 2014, Kim *et al.*, 2011, Meng *et al.*, 2017, Seyboth *et al.*, 2016, Wu *et al.*, 2017, Yaghmaie *et al.*, 2016, Zhang *et al.*, 2018b) of the literature cannot apply to large-scale systems. The reason is that the designed parameters inside those controllers are related to some global information of the system as follows:

- The knowledge of Laplacian matrix $\mathcal{L}$ of communication topology, e.g., the minimum eigenvalue $\lambda_{min}(\mathcal{L})$.
- The total number N of agents in the system.

For instance, Antonelli *et al.* (2014) put forward a distributed controller-observer schema for time-varying formation control of MRSs with first-order dynamics. Each follower needs the knowledge of the total number N (the global information)

of robots in the whole system, meaning that the protocol cannot apply to large-scale swarm systems (number N of agents is very large and sometimes not known to every agent). Yaghmaie *et al.* (2016) solved the output regulation problem of linear heterogeneous MASs via output and state feedback where the distributed controller is related to one parameter matrix

$$\tilde{H} = H \otimes I_p, H = \text{diag}\{\frac{1}{d_i + g_i}\}(\mathcal{L} + G). \tag{1.1}$$

One can see that the controller needs the knowledge of $\mathcal{L}$. The theory and experiment on formation-containment control of multiple multirotor unmanned aerial vehicle (UAV) systems was investigated by Dong *et al.* (2018). The gain matrices $K_l = [k_{l1}, k_{l2}], (l = 1, 2, 3)$ in the controller should satisfy some constraints such as

$$k_{12} + Re(\lambda_i)k_{32} < 0 \tag{1.2}$$

where λ_i is the eigenvalue of $\mathcal{L}$. It means without the knowledge of $\mathcal{L}$, this controller cannot be designed either.

Why is the information of $\mathcal{L}$ so important? Because $\mathcal{L}$ represents the communication topology among MASs/MRSs. If the distributed controller needs some information of $\mathcal{L}$, e.g. $\lambda_{min}(\mathcal{L})$ which is a piece of global information, then the controller is not applicable to large-scale systems because the agent number will be very large.

For example, if there are 1000 agents, then the dimension of $\mathcal{L}$ will be 1000×1000. So it takes time and resources to calculate $\lambda_{min}(\mathcal{L})$ for each agent. What is worse, if there is a small change in the communication topology, such as the link among agents increasing or decreasing, then each agent should know this change, which is not fully distributed and is very difficult to realize this scenario in reality. **This is why we propose the fully distributed controllers in Part I of this thesis to remove this constraint, i.e. the fully distributed controller is designed to be applied to large-scale systems.**

Since each agent only needs to communicate with its neighbors and parameters in protocols do not depend on any global information, no matter how many agents in the whole system or how many changes in the communication topology, each agent only needs to get information from its parent agent and send information to its child agent. It means each agent does not need any information (e.g., $\lambda_{min}(\mathcal{L})$) about the whole system. **So the method in this thesis is easy for application on large-scale systems.**

In total, the computational advantage of such a fully distributed attribute is that in large-scale systems, each agent does not need to know the information of $\mathcal{L}$, does not need to calculate $\lambda_{min}(\mathcal{L})$, and does not need to know the whole number

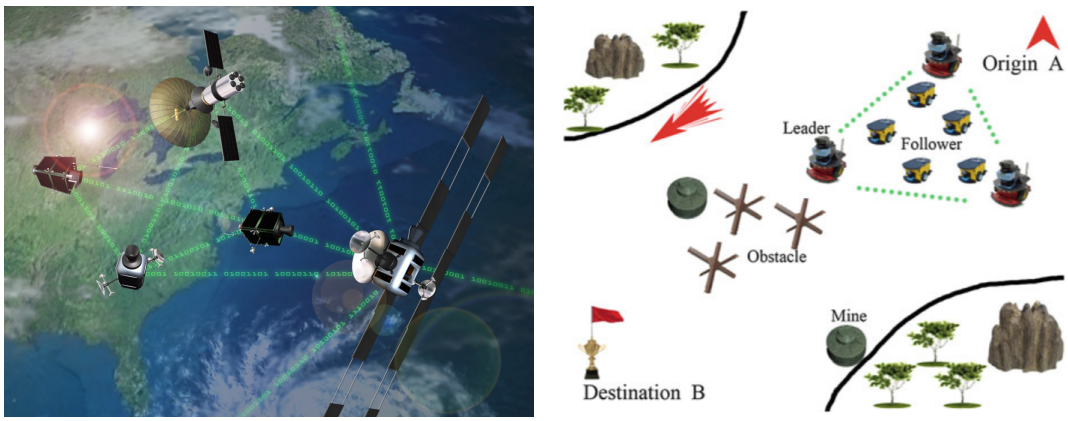

(a) The F6 concept by DARPA.

(b) Cooperative migration of multiple robots in the hazardous environment (Dong, 2015).

Figure 1.2: Formation and containment control examples

of the large-scale system. Therefore, designing the control protocol with the fully distributed property is important, necessary and challenging.

1.1.3 Why time-varying formation-containment control

Various cooperative control problems of MASs (e.g., consensus, formation or containment) have attracted much research interest in the past decades. As one of the most important issues, formation control has been paid much attention due to its broad potential applications such as target enclosing (López-Nicolás, Aranda & Mezouar, 2017, Zhang & Liu, 2016), surveillance (Nigam *et al.*, 2012), cooperative localization (Hurtado *et al.*, 2004), load transportation (Bai & Wen, 2010), sea testing by heterogeneous autonomous marine vehicles (Abreu *et al.*, 2015) and so on. Figure 1.2 (a) shows the promising effort to develop formation-flying satellites consisted of the Future, Fast, Flexible, Fractionated Free-Flying Spacecrafts, or System F6 by DARPA (2006). The time-invariant formation control problems have been studied substantially in Brinón-Arranz *et al.* (2014a), Lin *et al.* (2005), Liu & Jiang (2013), Peng *et al.* (2013), Tanner (2004), Wang & Xin (2013). Time-varying formation (TVF) control, which can be interpreted that the MAS/MRS is able to change its formation shapes in certain circumstances and keep being stable simultaneously, was studied by Antonelli *et al.* (2014), Rahimi *et al.* (2014) and Dong & Hu (2016) and other researchers recently. Changing formation shapes can be necessary for two reasons: covering the larger area or avoiding collisions with obstacles.

Containment control (see Fig. 3.7 as an example), whose objective is to drive the states of multiple followers into the convex hull spanned by multiple leaders,

has been investigated a lot in recent years (Haghshenas *et al.*, 2015, Liu *et al.*, 2012, Wen *et al.*, 2016). The motivation comes from some natural phenomena with many potential and important applications. For instance, a small portion of agents equipped with expensive sensors can be introduced as leaders to deal with the complicated surroundings and to form a safe region at the same time, such that followers without those expensive sensors can move inside that region. Then the whole system can move safely and the total cost is not very expensive. This kind of control method is especially important when the number of followers is very large. Figure 1.2 (b) gives an example for the leaders and followers to arrive at the destination with avoiding the obstacles and mines by adopting the containment control method.

Above all, combining the containment control and TVF control together to form the time-varying formation-containment (FC) control, whose objective is to make leaders achieve the predefined formation shapes and drive followers into the convex hull spanned by leaders, is very interesting and challenging.

1.1.4 Why heterogeneity

At the beginning, some of the earliest works related to MASs/MRSs deal with the large scale of homogeneous agents/robots, called swarms which obtain inspirations from biological societies (particularly ants, bees, fishes and birds) to develop similar behaviors to accomplish impressive group tasks (see Fig. 1.3). In multiple mobile robot systems, the homogeneous linear dynamics can be described as

$$\dot{x}_i(t) = Ax_i(t) + Bu_i(t), y_i(t) = Cx_i(t), \quad i \in \mathbf{I}[1, N] \tag{1.3}$$

where $x_i(t) \in \mathbb{R}^n$, $u_i(t) \in \mathbb{R}^p$ and $y_i(t) \in \mathbb{R}^q$ are the state, control input and measured output, respectively. $A \in \mathbb{R}^{n\times n}, B \in \mathbb{R}^{n\times p}$ and $C \in \mathbb{R}^{q\times n}$ are constant matrices. N is the number of agents.

In swarm systems, individual robots are usually unaware of the actions of other robots, other than information on proximity. Dong (2015) finished a good thesis about formation and containment control of high-order LTI swarm systems. However, all the controllers inside his work need the information of Laplacian matrix $\mathcal{L}$. The point is that when the number of agents is not large, it is not expensive for each agent to know the whole communication topology to calculate $\mathcal{L}$. But when the number becomes very large as in the swarm system, it is nearly impossible for each agent to know the whole topology. The cost will be very high to calculate $\mathcal{L}$, especially if there exists a small change in the communication topology, as we have stated out in detail in Section 1.1.2. In a word, the work in Dong (2015) is not fully distributed for swarm systems.

In contrast, heterogeneous agents/robots in which team members may vary significantly in their dynamics and capabilities, gain researchers' attention more

(a) Ants move a leaf together.

(b) Swarm bees.

(c) Swarm fishes.

(d) Swarm birds.

Figure 1.3: Swarm examples from the nature.

and more (Almeida *et al.*, 2014, Kim *et al.*, 2011, Lunze, 2012, Meng *et al.*, 2017, Mu & Shi, 2018, Rezaei & Menhaj, 2018, Seyboth *et al.*, 2016, Tian & Zhang, 2012, Wieland *et al.*, 2011, Zhang *et al.*, 2018b). Agent/robot heterogeneity could be defined in terms of variety in its behavior, morphology, performance quality, size, and cognition (Parker, 2008). The motivation to investigate heterogeneity can be three folds:

1. From designing aspect, with heterogeneity, different robots can have different capabilities to finish a cooperative task with less cost, e.g., Fig. 1.4 shows the localization, reconnaissance and surveillance task by aerial-ground robots.

2. From engineering aspect, sometimes it is too difficult do equip the same robots with all the necessary calculating, sensing and executing equipments to finish a specific cooperative task.

3. It is nearly impossible to build a truly homogeneous systems in reality.

(a) Heterogeneous aerial-ground robots performing cooperative task (Sukhatme *et al.*, 2001).

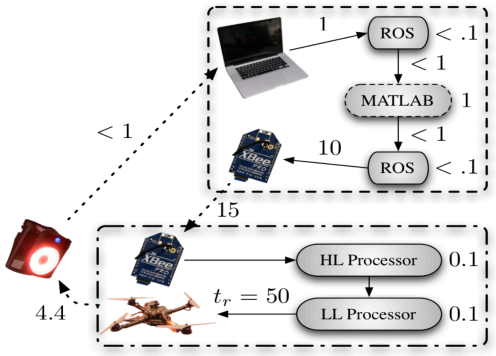

(b) Latencies (ms) in the experimental system from Mellinger (2012). HL: High Lever, LL: Low Lever.

Figure 1.4: Heterogeneity and delay researches.

In this thesis, the heterogeneous LTI dynamics is described as

$$\dot{x}_i(t) = A_i x_i(t) + B_i u_i(t), y_i(t) = C_i x_i(t), \quad i \in \mathbf{I}[1, N] \tag{1.4}$$

where $x_i(t) \in \mathbb{R}^{n_i}$, $u_i(t) \in \mathbb{R}^{p_i}$ and $y_i(t) \in \mathbb{R}^q$. $A_i \in \mathbb{R}^{n_i \times n_i}, B_i \in \mathbb{R}^{n_i \times p_i}$ and $C_i \in \mathbb{R}^{q \times n_i}$ are constant matrices.

1.1.5 Why input/output delay

Time-delay systems (TDS) are also called systems with aftereffect or dead-time, hereditary systems, equations with deviating argument or differential-difference equations. They belong to the class of functional differential equations which are infinite-dimensional, as opposed to ordinary differential equations (Richard, 2003). Normally, delays are known to deteriorate the stability. However, for some systems, they can have a stabilizing effect. A well-known example is as follows:

$$\ddot{y}(t) + y(t) - y(t - \tau) = 0. \tag{1.5}$$

When $\tau = 0$, (1.5) is unstable as (1.5) changes to $\ddot{y}(t) = 0$. But (1.5) will be stable when $\tau = 1$ as (1.5) changes to $\ddot{y}(t) + \dot{y}(t) = 0$ because the approximation $\dot{y}(t) \backsimeq [y(t) - y(t - \tau)]\tau^{-1}$ explains the damping effect.

On the other hand, delays are strongly involved in challenging areas of communication and information technologies: stability of networked control system (NCS) or high-speed communication networks (Richard, 2003). Fig. 1.4 (b) displays the different latencies happened in the control loop of a quadrotor. One can

see about 80ms delay consisted of the communication, computation and sensor delays. For systems with very slow dynamics, such a delay would not influence the control performance greatly. But for unstable systems with fast dynamics like flying robots, the presence of small delay could still destabilize the whole system. So the research on TDS is of great importance and always captures the attention of the control community.

Specifically, there are four kinds of delay formats occurring in the MAS: state, output, communication (Ghabcheloo *et al.*, 2009) and input. The input delay inside MASs arises from the processing and connecting queuing time for the packets arriving at each agent (Tian & Liu, 2009, Zhou & Lin, 2014), communication latencies, sensor measurements or computation time (Léchappé, 2015). To some extent, the input delay system

$$\dot{x}_i(t) = Ax_i(t) + Bu_i(t-\tau) \tag{1.6}$$

can represent some kinds of state or communication delay systems. For example, if $u_i(t) = K_1 x_i(t)$ with K_1 being a feedback matrix, then (1.6) changes to $\dot{x}_i(t) = Ax_i(t)+BK_1x_i(t-\tau)$ which is a state delay system. And if $u_i(t) = K_1 \sum_{j=1}^{N} l_{ij}x_j(t)$ with l_{ij} defined in (1.38) as the element of $\mathcal{L}$ denoting the communication topology in the MASs, then (1.6) changes to $\dot{x}_i(t) = Ax_i(t)+BK_1 \sum_{j=1}^{N} l_{ij}x_j(t-\tau)$ which can be regarded as a communication delay system (see the truncated predictor feedback controller (21) in Zhou & Lin (2014) as a detailed example). Note that very recent works by Jenabzadeh & Safarinejadian (2018), Ni *et al.* (2017), Wang *et al.* (2018a), Yuan (2018), Zhang *et al.* (2018a), Zhu & Jiang (2015), Zuo *et al.* (2017) and Zhang *et al.* (2018c) have investigated the distributed cooperative control for MASs considering constant/time-varying uniform/nonuniform input delays, which confirms that it is a trendy direction. **That is why another part of this thesis is concentrated on dealing with the input delay.**

It should be noted here that except Wang *et al.* (2018a), all the above control inputs are designed without considering the output delay. It is known that implementing an output-based approach is quite important as the full state information is not always available in practice. As the delay effect is usually unavoidable, studying the output delay is meaningful and necessary. This is the motivation of investigating the output delay.

In addition to the delay effect, the external disturbance is a source of systems' poor performance and instability, and is inevitable (Jenabzadeh & Safarinejadian, 2018). To sum up, **the objective of this thesis is to develop the fully distributed controllers to address the cooperative (consensus, TVF, time-varying FC) control problems for large-scale systems considering the heterogeneity, input/output delays and matched/mismatched disturbances.**

Facing this challenging objective, the thesis has been organized in two parts:

- The first part proposes new TVF shape formats for homogeneous and heterogeneous MASs, respectively. Then it presents how the fully distributed controllers can be designed to solve TVF and FC control problems.

- The second part focuses on the factors which can degrade the control performance in reality, i.e., input/output delays and disturbances by designing the fully distributed controllers at the same time.

1.2 Overview of formation/containment control

Distributed cooperative control has been researched for decades. The motivation is clearly stated out in the Sections 1.1.1 and 1.1.2. As one of the fundamental problems in the cooperative control of MASs, consensus control has been investigated extensively in the literature (Jadbabaie *et al.*, 2003, Li *et al.*, 2010, Olfati-Saber & Murray, 2004, Ren, 2007, Ren & Beard, 2005). Specifically, Olfati-Saber & Murray (2004) introduced the theoretical framework of posing and solving the consensus problem for networked dynamic systems and then, Ren (2007) showed that many existing virtual structure, leader–follower and behavior-based formation control methods could be unified in the framework of consensus-based methods. A unified framework to extend conventional observers to distributed observers by exchanging estimated state information was proposed by Li *et al.* (2010) to solve the consensus problem and the synchronization problem of complex networks. Detailed information about the recent study of consensus designing for MAS can be found in the survey paper Cao *et al.* (2013) and references therein.

As consensus control usually deals with at most one leader, containment control, whose main objective is to drive the states of the followers into the convex hull spanned by multi-leaders, has been investigated a lot in recent years. The motivation comes from some natural phenomena with many potential and important applications as stated out in Section 1.1.3. The stationary and dynamic leader cases were considered respectively for containment control of mobile agents with first-order dynamics under undirected communication topology by Ji *et al.* (2008). Then the results were improved to multiple stationary or dynamic leaders in fixed and switching directed networks for single-integrator dynamics in Cao *et al.* (2012). Distributed containment control for double-integrator dynamics in the presence of both stationary and dynamic leaders was investigated in Cao *et al.* (2011) where the communication topology is directed when leaders are static or have the same velocity, and it will become undirected among followers when leaders move with different velocities. The similar result was presented in Liu *et al.* (2012) with the control protocol being not fully distributed due to the requirement of eigenvalue information of Laplacian matrix $\mathcal{L}$ which is a piece of global information for each

follower. Most of the previous references deal with first or second order dynamics and assume that the relative state measurements of neighbor agents can be utilized for designing control protocols. However, the full state information of dynamic agents is usually unavailable in practice. Hence, implementing an output approach is quite important. The observer-type containment protocols for general linear MAS based on only relative output measurements of neighbor agents were proposed in Li *et al.* (2013) and Wen *et al.* (2016), but they are still not fully distributed since the parameters in protocols depend on the $\lambda_{min}(\mathcal{L})$ information. In addition, the fully distributed containment control problem of high-order MAS with nonlinear dynamics was addressed in Wang *et al.* (2017b), but the control protocol is base on relative state information.

The attention should be paid here that the above works about the containment control problems are only related to the case of homogeneous MAS, in which all the agents have identical dynamics. Well, since there are different kinds of agents in the real world, heterogeneous dynamic systems are more applicable than homogeneous ones. In Zheng & Wang (2014), the containment problem of heterogeneous agents under directed communication topology is divided into two cases: a linear protocol with leaders and followers being the first-order and second-order integrator respectively; a nonlinear protocol with leaders and followers being second-order and first-order integrator respectively. Haghshenas *et al.* (2015) presented a distributed dynamic state feedback control scheme based on output regulation framework to handle heterogeneous containment problem for linear MASs which consist of non-identical followers and identical leaders. The communication topology of the whole system is directed, but the topology among followers is strongly connected which is a more stringent topology compared with a directed one containing a spanning tree. It is worth remarking that the control protocols in these two works use the absolute/relative state information and are not fully distributed. Chu *et al.* (2016) proposed a fully distributed adaptive protocol based on the output regulation approach for heterogeneous linear MASs, but the dynamics of all the leaders are the same. So designing a fully distributed protocol based on output measurements of neighbor agents under the directed communication topology to solve the containment problem for heterogeneous systems, where each of the leaders or followers can have different dimensions and different dynamics, is still open (Oh *et al.*, 2015), very necessary, practical and quite challenging in real applications. **This challenge is solved in Chapter 3.**

Another reminder is that the above-mentioned results on containment control always suppose no interactions among leaders and take no account of leaders' collective behaviors. However, in the real world, due to the requirement of performing extremely complex and difficult tasks, sometimes leaders should exchange information between each other to achieve and keep a formation shape. **Therefore, the research of FC control is quite realistic and important, which is the topic in Chapter 3.**

Before moving on to the FC control issue, the discussion of formation control is necessary. The time-invariant formation control problems have been studied substantially in Brinón-Arranz *et al.* (2014a), Lin *et al.* (2005), Liu & Jiang (2013), Peng *et al.* (2013), Tanner (2004), Wang & Xin (2013). For example, Liu & Jiang (2013) focused on the distributed leader-follower formation control of unicycle robots by using local relative positions of neighbors. The drawback is all the followers need to know the leader's velocity and acceleration information which can be regarded as a heavy communication burden for the whole system. Brinón-Arranz *et al.* (2014a) dealt with the adaptive leader-follower formation control of autonomous marine vehicles whose prototype was developed by Pascoal *et al.* (1997) for underwater inspection and ocean data acquisition in coastal areas. The virtual vehicle idea, which comes from Encarnaçao & Pascoal (2001), is adopted with the constant triangular formation technique. The controller in Brinón-Arranz *et al.* (2014a) uses the full absolute state information for the feedback control because of no communication among leaders and followers. Then, the relative position is used in controller design with the help of undirected and connected graph theory in Soares *et al.* (2016) where the formation is not fixed since a method to change the formation spacing by varying the bias vector as a function of the measured wind speed. Note that the researched formation shapes in Soares *et al.* (2016) are simple as line or rectangular.

TVF control was studied in Antonelli *et al.* (2014), Brinón-Arranz *et al.* (2014b), Soares *et al.* (2016) and Dong & Hu (2016), etc. For instance, in Brinón-Arranz *et al.* (2014b), the time-varying shape was defined by three affine transformations (translation, scaling, rotation) and the controller was designed by using the absolute state measurements under the undirected graph to address the TVF tracking problem. Antonelli *et al.* (2014) put forward a distributed controller-observer schema for TVF tracking control of MRSs with first-order dynamics. The proposed solution works for strongly connected topology which is a stricter constraint compared with the directed spanning tree topology. Moreover, each follower needs the knowledge of the total number (the global information) of robots in the whole system, meaning that the protocol is not fully distributed. In Dong & Hu (2016), the desired TVF shape was described by piecewise continuously differentiable vectors, and the absolute/relative state measurements were used to design the controller under switching topologies. However, the coupling strength parameter in the control protocol depends on the minimal positive eigenvalue (the global information) of Laplacian matrices associated to all the switching topologies. Therefore, the control protocol is not fully distributed as well. The work in Dong & Hu (2016) is related to the formation stabilization issue; the formation tracking control, which includes some higher lever applications such as enclosing a target or tracking the trajectory of an actual/virtual leader, was investigated in Ghommam *et al.* (2016) and Dong *et al.* (2017). Ghommam *et al.* (2016) studied the formation tracking control of multiple under-actuated quadrotors where the reference trajectory is only

accessible to a small portion of quadrotors using filtering design and backstepping techniques. But the formation shape is constant and again, the control protocol is not fully distributed due to its dependence on the communication topology information. Note here that the aforementioned works on the formation control have considered the case of homogeneous MAS; there are also several interesting results available on the heterogeneous case in the literature. For instance, Peymani *et al.* (2014) solved the $\mathcal{H}_\infty$ almost time-invariant formation stabilization problem with output regulation for general linear heterogeneous MAS with tracking the virtual reference trajectory at the same time. A solution to the TVF tracking problem for a collaborative heterogeneous unmanned aerial and ground vehicles was presented in Rahimi *et al.* (2014). However, each follower needs the virtual leader's position and velocity information, which is a heavy communication burden that we should try to avoid. Abreu *et al.* (2015) introduced the EC MORPH project which focused on the implementation and at sea testing of the systems responsible for relative navigation and time-invariant formation control of a group of heterogeneous autonomous marine vehicles. It assumes the leader moves at a constant velocity, along a path composed of segments which are either lines or constant-curvature arcs. Hence, designing a fully distributed control protocol based on output measurements of neighbor agents with directed communication topology for heterogeneous TVF tracking problem is challenging and quite important in real applications, **which is the topic in Chapter 2**.

Above all, combining the containment control and TVF control together to form the time-varying FC control for heterogeneous MASs is very interesting. Similar as the above analysis, the research on this topic evolves from the first-order (Ferrari-Trecate *et al.*, 2006), second-order (Dimarogonas *et al.*, 2006, Han *et al.*, 2016), homogeneous general linear (Dong *et al.*, 2016) to heterogeneous general linear (Wang *et al.*, 2018c) dynamics, and from the undirected (Dimarogonas *et al.*, 2006, Ferrari-Trecate *et al.*, 2006, Wang *et al.*, 2017e), Wang *et al.* (2018c) to directed (Dong *et al.*, 2016, Han *et al.*, 2016) graph. The the protocols in (Dong *et al.*, 2016, Wang *et al.*, 2017f) and Wang *et al.* (2018c) are not fully distributed.

Motivated by the above analysis, **one purpose of this thesis is to utilize the fully distributed adaptive observer method to study the time-varying FC control problem for heterogeneous MASs in cooperative output regulation framework under directed communication topology.** The cooperative output regulation technique, which can be used to deal with heterogeneous dynamics, has been widely investigated in consensus problems in Ding (2015a), Su *et al.* (2013), Wang *et al.* (2010), Wieland & Allgöwer (2009), Wieland *et al.* (2011), to name a few. For instance, Wieland *et al.* (2011) proposed an internal model principle to investigate leaderless output consensus problem of heterogeneous linear MAS. Su & Huang (2012) solved the cooperative output regulation of the same system via a dynamic full information control law. In Ding (2015a), the

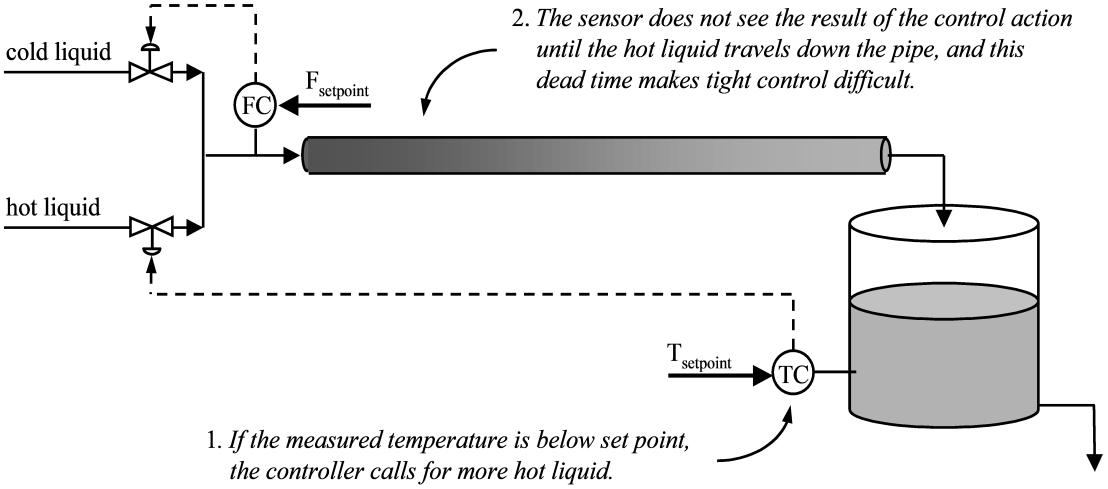

Figure 1.5: Example of "distance" temperature control (Henry, 2016).

adaptive consensus output regulation of several classes of nonlinear MAS was discussed. Note here that control protocols in Wang *et al.* (2010), Su *et al.* (2013) and Su & Huang (2012) explicitly depend on certain nonzero eigenvalues of Laplacian matrix of communication topology, which means being not fully distributed.

1.3 Overview of methods dealing with delays

Fig 1.5 shows how the dead time (delay) influences the control performance. The objective is to maintain temperature in the tank by adjusting the flow rate of hot/cold liquid entering the pipe. Because of this delay (time of the hot/cold liquid traveling through the pipe), there will be large oscillations in temperature around the set point. This problem was firstly successfully solved by Smith by proposing a frequency approach named Smith predictor in Smith (1957) and Smith (1959).

Smith Predictor (SP)

The idea of SP is to design an inner loop (Fig. 1.6) to calculate the prediction $y_{ideal}(t)$ of delayed output $y(t)$ as if there were no time delay. Fig. 1.7 is the corresponding transfer function block diagram. $\tilde{g}(s)$ is the best estimation of the process transfer function $g(s)$ without delay τ, and $\tilde{\tau}$ is the estimation of τ. $\tilde{g}(s)$ and $\tilde{\tau}$ will be used for controller design. If the estimation is perfect, i.e.,

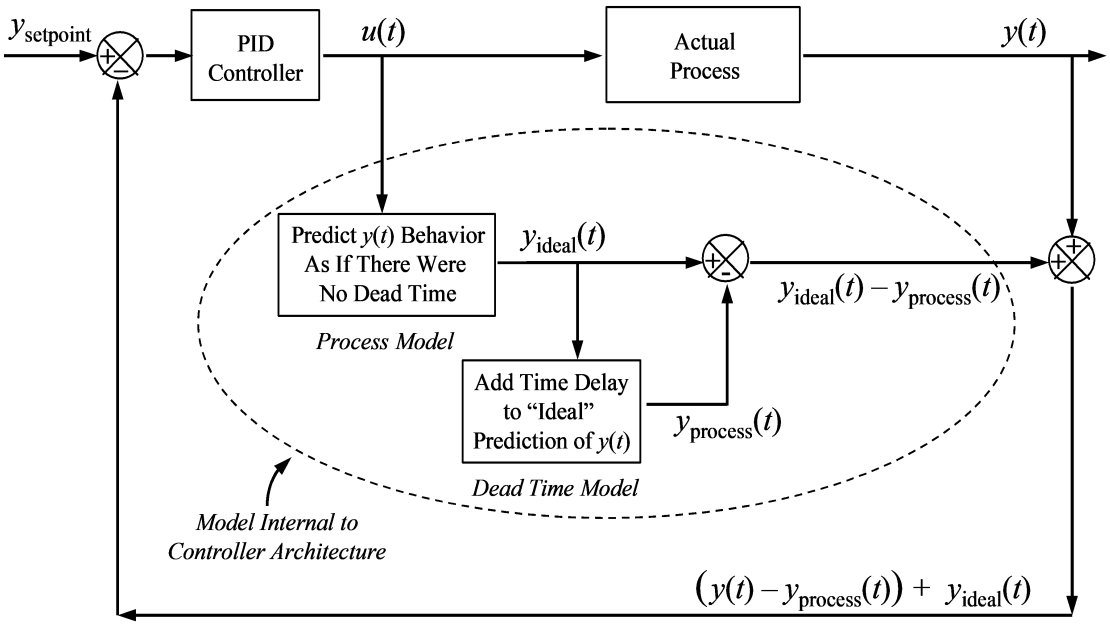

Figure 1.6: Smith predictor block diagram description (Henry, 2016).

$\tilde{g}(s) = g(s), \tilde{\tau} = \tau$, then

$$g_c^*(s) = \frac{m(s)}{\varepsilon(s)} = \frac{g_c(s)}{1 + g_c(s)\tilde{g}(s)(1 - e^{-\tilde{\tau}s})} = \frac{g_c(s)}{1 + g_c(s)g(s)(1 - e^{-\tau s})}. \tag{1.7}$$

After some algebraic calculations, the closed loop transfer function is

$$G_{CL} = \frac{y(s)}{y_{sp}(s)} = \frac{g_c(s)g(s)}{1 + g_c(s)g(s)} e^{-\tau s} = \frac{g_c(s)\tilde{g}(s)}{1 + g_c(s)\tilde{g}(s)} e^{-\tilde{\tau}s}, \tag{1.8}$$

which means SP moves the delay out of the feedback loop if the model is exact.

In the following of this thesis, we assume the agent's delayed dynamics is LTI and exact, which means

$$\dot{x}(t) = Ax(t) + Bu(t - \tau) \tag{1.9}$$

represents agent's real exact dynamics with $x \in \mathbb{R}^n$ and (A, B) being controllable. It is well known that SP can only stabilize the open-loop stable plants. Then some modified SPs like the "finite spectrum assignment" (Kwon & Pearson, 1980, Manitius & Olbrot, 1979, Olbrot, 1978), "reduction" (Artstein, 1982) and "PDE backstepping" (Krstic, 2009) approaches are proposed to stabilize the open-loop unstable plants, which will be introduced in the following.

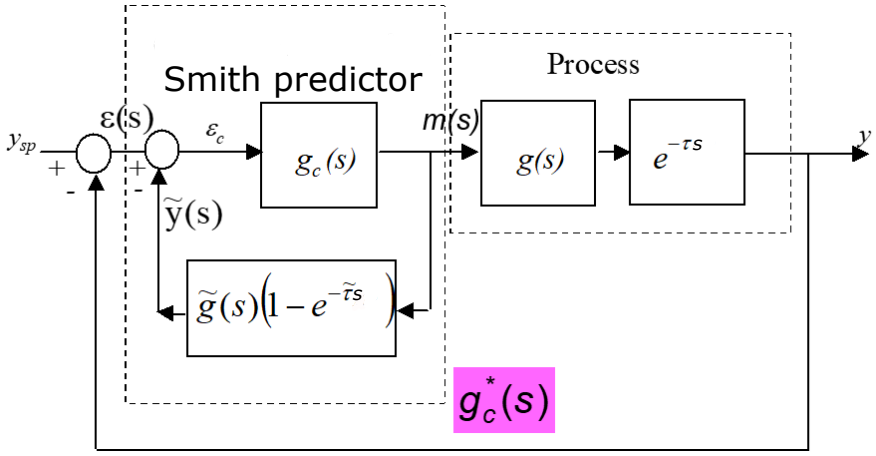

Figure 1.7: Smith predictor transfer function block diagram.

Finite Spectrum Assignment (FSA) approach

The idea of FSA is to design the control input

$$u(t) = Kx(t+\tau) \tag{1.10}$$

so that the dynamics (1.9) changes to

$$\dot{x}(t) = (A+BK)x(t), \tag{1.11}$$

which can be controlled by assigning the spectrum of $(A+BK)$ thanks to K. This is why it is called the FSA approach. (1.10) is the predictive feedback controller as it needs the future state information $x(t+\tau)$, which is impossible at moment t in real implementations. Remind that for any initial condition $x(t_0)$ and $t \geq t_0$, the solution of (1.9) is

$$x(t) = e^{A(t-t_0)}x(t_0) + \int_{t_0}^{t} e^{A(t-s)}Bu(s-\tau)ds. \tag{1.12}$$

Then $x(t+\tau)$ can be calculated as

$$x(t+\tau) = e^{A\tau}x(t) + \int_{t-\tau}^{t} e^{A(t-s)}Bu(s)ds. \tag{1.13}$$

So the input

$$u(t) = K\left[e^{A\tau}x(t) + \int_{t-\tau}^{t} e^{A(t-s)}Bu(s)ds\right] \tag{1.14}$$

is implementable in reality, but it is infinite-dimensional because of the distributed delay term involving the historical input information $\int_{t-\tau}^{t} e^{A(t-s)}Bu(s)ds$ (Krstic, 2009). Be careful that this controller is true only after $u(t)$ in (1.14) "kicks in" at $t = \tau$ as $\dot{x}(t) = (A + BK)x(t), t \geq \tau$. During the time interval $[0, \tau]$, agent's state is governed by

$$x(t) = e^{At}x(0) + \int_0^t e^{A(t-s)}Bu(s-\tau)ds, \forall t \in [0, \tau]. \tag{1.15}$$

Reduction approach

Artstein (1982) introduced this approach by proposing a state predictor

$$Z(t) = x(t) + \int_{t-\tau}^{t} e^{A(t-s-\tau)}Bu(s)ds. \tag{1.16}$$

such that the dynamics (1.9) changes to

$$\dot{Z}(t) = AZ(t) + e^{-A\tau}Bu(t) \tag{1.17}$$

which is input delay free with the delay τ being a parameter. Banks *et al.* (1971) proved that (A, B) is controllable $\Leftrightarrow$ $(A, e^{-A\tau}B)$ is controllable. We also give our proof in Lemma 1.9. The reduction approach is similar as the FSA as $Z(t) = e^{-A\tau}x(t+\tau)$. However, the former has some advantages compared with the latter, e.g., in the application to cooperative control of heterogeneous MASs whose dynamics are as follows:

$$\dot{x}_i(t) = A_i x_i(t) + B_i u_i(t), \quad i \in \mathbf{I}[1, N] \tag{1.18}$$

where $x_i \in \mathbb{R}^n$ but $A_i \neq A_j, i, j \in \mathbf{I}[1, N]$. Specifically, we have

$$\begin{aligned} Z_i(t) - Z_j(t) =& x_i(t) - x_j(t) \\ &+ \int_{t-\tau}^{t} [e^{A_i(t-s-\tau)}Bu_i(s) - e^{A_j(t-s-\tau)}Bu_j(s)]ds, \\ x_i(t+\tau) - x_j(t+\tau) =& e^{A_i\tau}x_i(t) - e^{A_j\tau}x_j(t) \\ &+ \int_{t-\tau}^{t} [e^{A_i(t-s)}Bu_i(s) - e^{A_j(t-s)}Bu_j(s)]ds. \end{aligned} \tag{1.19}$$

It is obvious that for Artstein's reduction approach, the relative state $x_i(t) - x_j(t)$ can be used for distributed controller design, whereas for FSA, only the absolute state $x_i(t)$ can be used. **This point of difference is demonstrated in Chapter 5.2.**

It is interesting to ask the real difference between the original SP and the modified SPs such as FSA and reduction approaches. If one develop the original SP in the state space (1.9), then the control input becomes (Krstic, 2009)

$$u(t) = K\left[x(t) + \int_0^t e^{A(t-s)}Bu(s)ds - \int_{-\tau}^{t-\tau} e^{A(t-\tau-s)}Bu(s)ds\right], \tag{1.20}$$

which seems more complicated than (1.14) developed by FSA. Besides, the original SP can only be used for open-loop stable systems.

PDE Backstepping approach

Observing that neither the FSA nor Artstein's reduction approach equips researchers a tool for the stability analysis, Krstic (2009) proposed a PDE backstepping technique with a Lyapunov-Krasovskii functional (LKF) to give an exponential stability analysis for the closed-loop system.

The idea is to model the delay in (1.9) by the following "transport PDE" or the first-order hyperbolic PDE as

$$\begin{aligned} \frac{\partial \chi(a,t)}{\partial t} =& \frac{\partial \chi(a,t)}{\partial a}, \\ \chi(\tau,t) =& u(t) \end{aligned} \tag{1.21}$$

with the solution

$$\chi(a,t) = u(t+a-\tau) \tag{1.22}$$

and the output

$$\chi(0,t) = u(t-\tau). \tag{1.23}$$

Then the dynamics (1.9) can be rewritten as

$$\dot{x}(t) = Ax(t) + B\chi(0,t). \tag{1.24}$$

Equations (1.21)-(1.24) construct an ODE-PDE cascade that is driven by the input u from the boundary of the PDE (Fig. 1.8). Then the following backstepping transformation

$$w(a,t) = \chi(a,t) - Ke^{Aa}x(t) - \int_0^a Ke^{A(a-s)}B\chi(s,t)ds \tag{1.25}$$

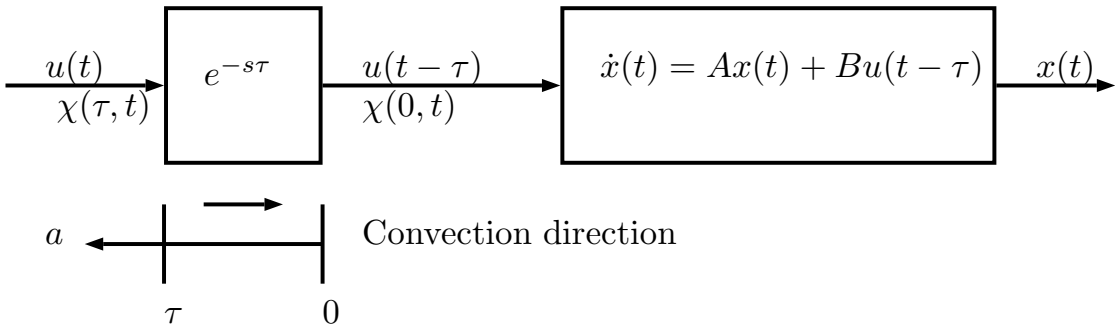

Figure 1.8: Transfer function block diagram.

is implemented to transform the system (1.21)-(1.24) into

$$\begin{aligned} \dot{x}(t) =&(A+BK)x(t)+Bw(0,t),\\ \frac{\partial w(a,t)}{\partial t} =&\frac{\partial w(a,t)}{\partial a},\\ w(\tau,t) =&0. \end{aligned} \tag{1.26}$$

The detail of derivation process of $w(a,t)$ in (1.25) can be referred to Krstic (2009). The exponential stability is proved by consider the following LKF

$$V(t)=x^T(t)Px(t)+\frac{b}{2}\int_0^\tau (1+a)w(a,t)^2da \tag{1.27}$$

where b is a constant. Recall that based on (1.21), (1.25) and (1.26), the explicit expression of control input is

$$\begin{aligned} u(t)=\chi(\tau,t) =&Ke^{A\tau}x(t)+\int_0^\tau Ke^{A(\tau-s)}Bu(t+s-\tau)ds\\ =&Ke^{A\tau}x(t)+\int_{t-\tau}^t Ke^{A(t-s)}Bu(s)ds \end{aligned} \tag{1.28}$$

which is exactly the input (1.14) designed by FSA. This is the first result extending the Lyapunov analysis to predictive feedbacks by using the PDE backstepping technique. However, when the system encounters the external unknown disturbances as follows:

$$\dot{x}(t)=Ax(t)+Bu(t-\tau)+d(t) \tag{1.29}$$

with $d(t)\in\mathbb{R}^n$ being the unknown disturbance, it is necessary to adopt another method since the unknown disturbance $d(t)$ cannot be compensated completely.

Other integral term-based approaches

In order to control the system (1.29), based on the FSA and reduction approaches, Léchappé *et al.* (2015) proposed a new state predictor

$$\begin{aligned} x_{\hat{p}}(t) =& x_p(t) + x(t) - x_p(t-\tau), \\ x_p(t) =& x(t+\tau) = e^{A\tau}x(t) + \int_{t-\tau}^{t} e^{A(t-s)}Bu(s)ds, t \geq 0, \\ x_p(t-\tau) =& x_p(0), t \in \mathbf{I}[0,\tau] \end{aligned} \tag{1.30}$$

so that the constant unknown disturbance $d(t) = constant$ can be perfectly compensated by the control input $u(t) = Kx_{\hat{p}}(t)$.

For the bounded time-varying and known input delay system ($\tau \in \mathbf{I}[0,\bar{\tau}]$ with $\bar{\tau}$ being the upper bound):

$$\dot{x}(t) = Ax(t) + Bu(t-\tau(t)), \tag{1.31}$$

based on the FSA approach, Nihtila (1991) proposed another state predictor

$$x(r(t)) = e^{A(r(t)-t)}x(t) + \int_{t-\tau(t)}^{t} e^{A(r(t)-r(s))}B\dot{r}(s)u(s)ds \tag{1.32}$$

where $r(t)$ is the inverse function of $\eta(t) = t - \tau(t)$, i.e., $\eta(r(t)) = t$. To guarantee the existence of $r(t)$, $\tau(t)$ should satisfy $|\dot{\tau}(t)| \leq \delta < 1$ which is known as the slowly-varying delay (Fridman, 2014). One can see that $r(t) = t + \tau(r(t)) > t$, so $x(r(t))$ is clearly the state predictor. Then the explicit state-feedback input can be designed as $u(t) = Kx(r(t))$. A parameter-adaptive design for a scalar system with known time-varying input delay was investigated earlier by Nihtila (1989).

To understand this inverse mechanism more clearly, we take the constant input delay as an example. In this case, $\eta(t) = t - \tau \Rightarrow r(t) = t + \tau$, then (1.32) changes to $x(t+\tau) = e^{A\tau}x(t) + \int_{t-\tau}^{t} e^{A(t-s)}Bu(s)ds$ which is the same as (1.13) developed by the FSA approach.

Inspired by the work of Nihtila (1991), Krstic (2010) extended the PDE backstepping approach from the known constant input delay case (1.21) to the known time-varying input case.

Based on above introductions and analysis, the integral term in (1.14), (1.16), (1.25) or (1.32) should be carefully dealt with. Take $\vartheta(t) = \int_{t-\tau}^{t} e^{A(t-s)}Bu(s)ds$ as an example. Actually, for open-loop stable dynamics, there is no need to execute integral discretization to compute the $\vartheta(t)$ in reality (Furukawa & Shimemura,

1983, Watanabe & Ito, 1981). The reason is as follows:

$$\begin{aligned}\vartheta(t) =& e^{At}\vartheta^{'}(t) + \int_0^t e^{A(t-s)}Bu(s)ds - e^{A\tau}\left[e^{A(t-\tau)}\vartheta^{'}(t) + \int_0^{t-\tau} e^{A(t-\tau-s)}Bu(s)ds\right] \\ =& \vartheta^{'}(t) - e^{A\tau}\vartheta^{'}(t-\tau)\end{aligned} \tag{1.33}$$

where $\vartheta^{'}(t)$ is the solution of

$$\dot{\vartheta}^{'}(t) = A\vartheta^{'}(t) + Bu(t). \tag{1.34}$$

For open-loop unstable dynamics, the integral term $\vartheta(t)$ must be carefully executed because it may destabilize the closed system (Engelborghs *et al.*, 2001, Van Assche *et al.*, 1999). So in order to calculate $\vartheta(t)$ by integral discretization, please refer to Léchappé (2015) on Page 22 for details in which the trapezoidal rule is used.

In the Matlab simulations of this thesis, we use Matlab function **"integral(fun,xmin,xmax,'ArrayValued',true)"** to calculate the matrix integral term $\vartheta(t)$ for open-loop unstable MASs.

To sum up, because of the existence of the integral terms which contain the historical input information, all the above controllers are memory controllers in which different state predictors are designed. As it is stated out in Mirkin & Raskin (2003), *the state prediction is a fundamental concept for delay systems, much like the state observation is for systems with incomplete state measurements.* The memory controllers are especially beneficial for open-loop unstable systems with large input delays. Here, only the big breakthroughs are introduced. For more details, please refer to the survey papers (Gu & Niculescu, 2003, Richard, 2003) and books (Fridman, 2014, Krstic, 2009, Zhong, 2006)

In this thesis, one of the contributions is that by employing the FSA/reduction approaches, the fully distributed controllers are successfully and firstly designed for cooperative control of homogeneous and heterogeneous MASs considering the input delay and disturbances.

Truncated Predictor Feedback (TPF) approach

The TPF approach, which is originally proposed by Lin & Fang (2007) and further developed in Yoon & Lin (2013), Zhou & Lin (2014), has the advantage that the requirement for integral terms in (1.14), (1.16), (1.25) or (1.32) can be removed, making the controller be implemented more easily in reality. However, it requires the open-loop system to satisfy the following constraints:

- can be polynomially unstable but definitely not exponentially unstable for arbitrarily large constant and known input delay (Zhou & Lin, 2014),

- can be exponentially unstable for not arbitrarily large time-varying and known input delay (Yoon & Lin, 2013).

Another point is that the control input is not utilized efficiently and sufficiently as the value of input is usually quite small due to the incorporation of low gain feedback technique, resulting in possibly sluggish control performance.

Sequential Sub-predictor (SSP) approach

In order to drop off the integral terms, e.g., $\vartheta(t)$ in (1.33), Najafi *et al.* (2013) proposed a new state predictor which is based on delayed state observer

$$\dot{\bar{x}}(t) = A\bar{x}(t) + Bu(t) + L(\bar{x}(t-\tau) - x(t)) \tag{1.35}$$

with its prediction error defined as $e(t) = \bar{x}(t-\tau) - x(t)$ for $\tau \in \mathbf{I}[0, \bar{\tau}]$ with $\bar{\tau}$ being sufficiently small. **This new state predictor is adopted and modified in Appendix A of this thesis considering time-varying input/output delays.** For a long time-delay in unstable systems, a series of coupled predictors (SSPs) are designed. Each of them is responsible for the prediction of one small portion of the delay, such that the predictors collectively predict the states for this long time-delay.

Descriptor approach

For the system with the following dynamics

$$\dot{x}(t) = Ax(t) + Lx(t-\tau), \tag{1.36}$$

Fridman (2001) proposed the descriptor approach which describes (1.36) in the equivalent descriptor form:

$$\dot{x}(t) = y(t),\ y(t) = Ax(t) + Lx(t-\tau), \tag{1.37}$$

and regard $[x^T(t), y^T(t)]^T$ as an augmented state for the LKF design. Then a linear matrix equality (LMI) can be derived to decide the upper bound $\bar{\tau}$ of delay τ. The input saturation problem is investigated in Liu & Fridman (2014) by giving a special analysis on the first internal $t \in \mathbf{I}[0, \tau(t)]$ using this approach. **The descriptor approach is adopted and modified in Chapter 6 and Appendix A to deal with the time-varying output delay.**

To sum up, the above TPF, SSP, descriptor based controllers are memory free controllers as they drop off the integral terms for controller design, which is an advantage for the real applications in reality as the discretization calculation of

integral terms should be carefully executed, especially for open-loop unstable systems. **Remind that the main objective of this thesis is to develop fully distributed controllers for large-scale systems.** Since the TPF has special requirement for the open-loop dynamics as stated previously, the FSA and reduction approaches are preferred to design controllers which are also fully distributed in Chapters 4, 5, 6. The SSP is really attractive and is used in Appendix A to deal with time-varying input/output delays. Regret is that the controller in Appendix A is not fully distributed till now (needs future work). That is why we cannot design fully distributed controllers based on SSP in Chapters 4, 5 and 6. Descriptor approach is mainly used for stability analysis with LKFs and is used in Chapters6 and Appendix A to deal with time-varying output delay (not input delay).

The detailed overview about the latest results of cooperative control for the MASs/MRSs considering the input/output delays and disturbances will be provided in **Part** II.

1.4 The structure of thesis

This thesis is divided into two parts:

- The first part is dedicated to the presentation of two points: (i) the newly proposed time-varying shape formats for homogeneous and heterogeneous MASs respectively; (ii) how to design fully distributed controllers for large-scale systems by the output-based observer method.

- The second part reveals one core technique behind the TVF and FC control—consensus, and studies its behaviors considering the constant/time-varying input/output delays, matched/mismatched disturbances by designing predictive and adaptive controllers with fully distributed property.

A detailed organization is shown in Fig. 1.9. The contributions are stated throughout the presentation of each chapter. **Note that the theorems in frame boxes are the main contributions of this work**.

Part I is dedicated to the presentation of the new definitions of TVF control with the fully distributed property, which is one of the main contributions. Another main contribution is to reveal the essence of linking the TVF tracking control and containment control together to achieve the time-varying FC control for heterogeneous large-scale MASs/MRSs.

In **Chapter** 2, a unified framework of TVF control design for general linear MASs based on an observer viewpoint from undirected to directed topology and from stabilization to tracking is proposed. A first version of this method has been published in Jiang *et al.* (2017) for the undirected communication topology.

An extension to the directed topology from TVF stabilization to tracking control is also given in detail. The original idea lies in the proposition of a new TVF shape format definition (see Fig. 1.10 (a)) and the methodology of designing fully distributed controllers for homogeneous MASs. The observer-based method with output measurements is used and formal convergence proofs are given. A numerical simulation is provided to verify the theoretical results.

In **Chapter** 3, the distributed output time-varying FC control problem for heterogeneous linear MASs under the directed communication topology based on output regulation framework from the observer viewpoint is researched. All agents can have different dynamics and different state dimensions. Firstly, another new TVF shape format is proposed, which is different from the format for homogeneous MASs in **Chapter** 2. Then, the TVF tracking control problem for heterogeneous MASs is addressed by designing the newly fully distributed observer. After that, the time-varying FC problem is solved. One big contribution lies in how to find the link to go from TVF tracking to time-varying FC with controllers always

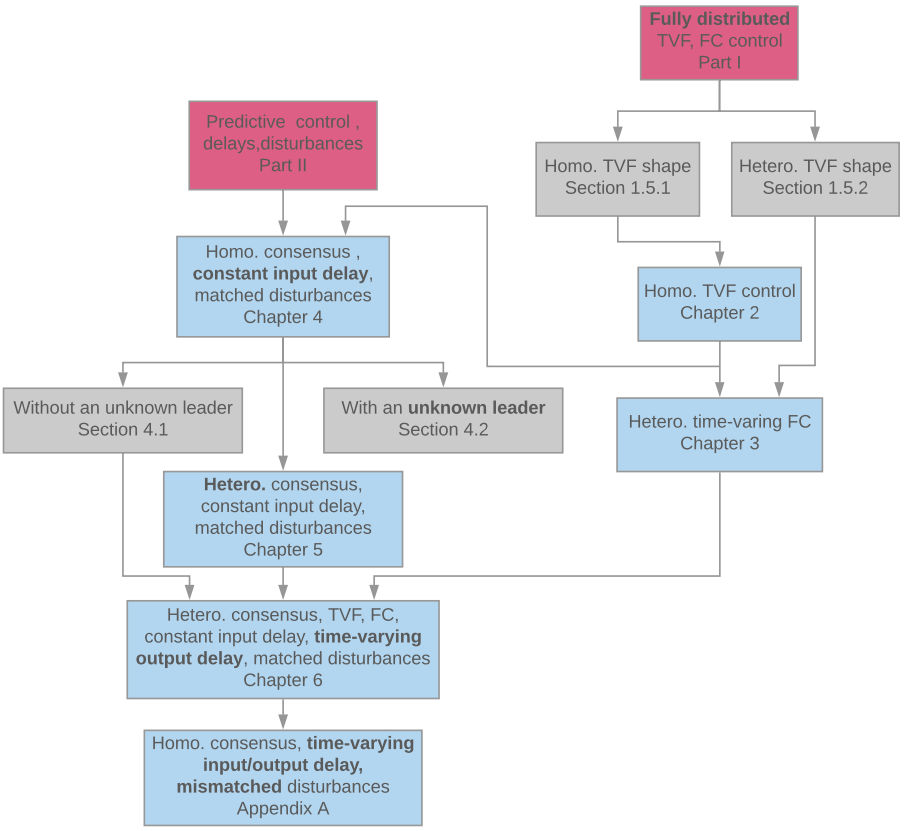

Figure 1.9: Organization of thesis (Homo.:homogeneous; Hetero.:heterogeneous).

being fully distributed. Simulations including an application to heterogeneous multiple nonholonomic mobile robots are demonstrated to verify the effectiveness of theoretical results. A convergence rate analysis is also provided. The content of this chapter is partially summed up in Jiang *et al.* (2018c).

Part II presents that the consensus control could be viewed as one of the core techniques for time-varying formation and containment control after the analysis of results of **Part** I. The main objective is to firstly develop predictive and adaptive controllers to have better consensus control performance considering the constant/time-varying input/output delays and external matched/mismatched disturbances, and then to extend above results to TVF and time-varying FC control. The stable analysis is presented by the Lyapunov function or Lyapunov-Krasovskii functional with sufficient conditions derived in terms of the algebraic Riccati equation and linear matrix inequality. All results in this part work for the directed communication topology.

Chapter 4 deals with the consensus tracking problem of disturbance rejection/attenuation for constant input-delayed linear MASs. First, in **Section** 4.1, when the leader has no control input, a novel adaptive predictive extended state observer (APESO) using only relative state information of neighboring agents is designed based on the FSA approach to achieve disturbance-rejected consensus tracking. Then, in **Section** 4.2, the result is extended to disturbance-attenuated case where the leader has bounded control input which is only known by a portion of followers (the unknown leader). The basic idea is to design a new state predictor to transform the delayed MAS into the delay-free one, and to design a new disturbance observer to compensate the disturbance effect. The detailed procedures to deal with the unknown leader is also presented. The main contribution focuses on the design of APESO protocols with fully distributed property. This work is presented in Jiang *et al.* (2018a).

Chapter 5 extends the result of Section 4.1 by linking the result of Chapter 3 to address the output consensus tracking (OCT) problem for heterogeneous linear MASs using the observer approach. First, in **Section** 5.1, we study the OCT problem considering only the constant input delay. Based on the FSA approach and the output regulation theory, another novel state predictor and an adaptive protocol, which requires only the states of designed observers of neighbors and the leader's output information, are proposed to tackle the input delay effect. Then, in **Section** 5.2, in order to achieve the disturbance rejection, the followers are constrained to have the same state dimension so that the above protocol can be redesigned based on Arstein's reduction approach, by adding one novel APESO to estimate the disturbance and the redesigned state predictor simultaneously. This work is given in Jiang *et al.* (2018d). All the results are verified by simulations of MASs and multi-vehicle systems.

Chapter 6 extends the results in Chapter 5 to consider the time-varying output delay. The descriptor approach introduced in Chapter 1.3 is used to analyze

the stability by means of Lyapunov-Krasovskii functionals. Detailed comparisons about how to design parameters to have better control performance dealing with time-varying output delay are given. Finally, how to design fully distributed controllers dealing with cooperative control problems from consensus to TVF, then to time-varying FC for heterogeneous LTI MASs, is demonstrated.

In **Appendix** A, an attempt to solve consensus tracking control for homogeneous LTI MASs considering the time-varying input/output delays and mismatched disturbances is completed by proposing the distributed control protocol without integral terms inside. The detailed comparisons are provided to give a thinking about how to get better disturbance attenuation performance when facing mismatched disturbances.

Some of the results presented in this thesis have been published or are under revision process for publication in journals and conferences.

Journal papers

1. Wei Jiang, Zhaoxia Peng, Ahmed Rahmani, Wei Hu and Guoguang Wen, *Distributed consensus of linear MASs with an unknown leader via a predictive extended state observer considering input delay and disturbances*, Neurocomputing, 315, 465-476, 2018.
   Jiang *et al.* (2018a)

2. Wei Jiang, Guoguang Wen, Zhaoxia Peng, Tingwen Huang and Ahmed Rahmani, *Fully distributed formation-containment control of heterogeneous linear multi-agent systems*, IEEE Transactions on Automatic Control, accepted.
   Jiang *et al.* (2018c)

3. Wei Jiang, Guoguang Wen, Ahmed Rahmani, Tingwen Huang, Zhongkui Li and Zhaoxia Peng, *Observer-based fully distributed output consensus tracking of heterogeneous linear multi-agent systems with input delay and disturbances*, IEEE Transactions on Cybernetics, submitted.
   Jiang *et al.* (2018d)

4. Wei Jiang, Ahmed Rahmani and Guoguang Wen, *Fully distributed time-varying formation-containment control for large-scale nonholonomic vehicles with an unknown real leader*, International Journal of Control, submitted.
   Jiang *et al.* (2018b)

Conference papers

1. Wei Jiang, Guoguang Wen, Yunhe Meng and Ahmed Rahmani, *Distributed adaptive time-varying formation tracking for linear multi-agent systems: A dynamic output approach*, Chinese Control Conference, Dalian, China, 2017.
   Jiang *et al.* (2017)

Part I

Fully distributed formation/containment control

It has been shown in literature review that research on fully distributed cooperative control for large-scale systems is very necessary and challenging. Recall that one focus of this thesis is develop TVF and time-varying FC controllers. So in this part, some graph theories related to MASs/MRSs is firstly introduced with necessary mathematical knowledge. Then the new TVF shape propositions for homogeneous/heterogeneous systems are demonstrated in detail. After that, Chapter 2 illustrates how to design fully distributed controllers step by step for homogeneous systems, and finally for heterogeneous systems in Chapter 3.

1.5 Preliminaries

1.5.1 Graph theory

The fixed connections between N agents can be represented by a fixed and weighted graph $\mathcal{G} = (\mathcal{V}, \mathcal{E}, \mathcal{A})$, where $\mathcal{V}$ and $\mathcal{E}$ denote the nodes and edges, respectively. $\mathcal{A} = [a_{ij}] \in \mathbb{R}^{N\times N}$ denotes the adjacency matrix where $a_{ij} = 1$ if there exists a path from agent j to agent i, and $a_{ij} = 0$ otherwise. An edge $(i, j) \in \mathcal{E}$ in graph $\mathcal{G}$ means that agent j can receive information from agent i but not necessarily conversely. The Laplacian matrix $\mathcal{L} = [l_{ij}] \in \mathbb{R}^{N\times N}$ is normally defined as

$$\begin{cases} l_{ii} = \sum_{j\neq i} a_{ij}, \\ l_{ij} = -a_{ij}, \qquad i \neq j. \end{cases} \tag{1.38}$$

A graph is said to be undirected if $(i, j) \in \mathcal{E}$ implies $(j, i) \in \mathcal{E}$ for any $i, j \in \mathcal{V}$. An undirected graph is **connected** if there exists a path between each pair of distinct nodes. A directed path from node i to j is a sequence of edges $(i, i_1), (i_1, i_2), \ldots, (i_k, j)$ with different nodes $i_s, s = 1, 2, \ldots, k$. A digraph (i.e., directed graph) is **strongly connected** if there is a directed path from each node to each other node. A digraph contains a directed **spanning tree** if there is a node from which a directed path exists to each other node. A digraph has a directed spanning tree if it is strongly connected, but not vice versa. More graph theories can be found in Godsil & Royle (2001).

Lemma 1.1 (Ren & Beard (2005)) *The Laplacian matrix $\mathcal{L}$ of a directed communication topology $\mathcal{G}$ has at least one zero eigenvalue with $\mathbf{1}$ as a right eigenvector, and has all nonzero eigenvalues with positive real parts. Furthurmore, zero is a simple eigenvalue of $\mathcal{L}$ if and only if $\mathcal{G}$ contains a directed spanning tree.*

Lemma 1.2 (Mei *et al.* (2014)) *Suppose that $\mathcal{G}$ is strongly connected. Then there exists a positive vector $r = [r_1^T, \ldots, r_N^T] > 0$ such that $r^T\mathcal{L} = 0$, and $\hat{\mathcal{L}} = R\mathcal{L}+\mathcal{L}R$ is the symmetric Laplacian matrix associated with an undirected connected graph where $R = \text{diag}\{r_1, \ldots, r_N\}$. Moreover, $\min_{\chi^T x=0, x\neq 0} \frac{x^T\hat{\mathcal{L}}x}{x^Tx} > \frac{\lambda_2(\hat{\mathcal{L}})}{N}$, where $\lambda_2(\hat{\mathcal{L}})$ denotes the **algebraic connectivity** of $\hat{\mathcal{L}}$, i,e. the smallest positive eigenvalue of $\hat{\mathcal{L}}$, and χ is any vector with positive entries.*

1.5.2 Mathematical knowledge

If A is an $m \times n$ matrix and B is a $p \times q$ matrix, then the Kronecker product $A \otimes B$ is the $mp \times nq$ block matrix:

$$A \otimes B = \begin{bmatrix} a_{11}B & \cdots & a_{1n}B \\ \vdots & \ddots & \vdots \\ a_{m1}B & \cdots & a_{mn}B \end{bmatrix}$$

The properties of Kronecker product are:

- $A \otimes (B + C) = A \otimes B + A \otimes C$;
- $(A + B) \otimes (C + D) = AC \otimes (BD)$;
- $(A \otimes B)^T = A^T \otimes B^T$;
- $(A \otimes B)^{-1} = A^{-1} \otimes B^{-1}$;

Suppose the eigenvalues of $S \in \mathbb{R}^{n\times n}$ and $T \in \mathbb{R}^{m\times m}$ are $\lambda_1, \ldots, \lambda_n$ and $\mu_1, \ldots, \mu_m$, respectively, then the eigenvalues of $S \otimes T$ are $\lambda_i\mu_j, i \in \mathbf{I}[1, n], j \in \mathbf{I}[1, m]$. If $S \in \mathbb{R}^{n\times n}$ and $T \in \mathbb{R}^{n\times n}$ are two symmetric positive definite matrices, then $\lambda_{max}(ST) \leq \lambda_{max}(S)\lambda_{max}(T)$.

The matrix $A = [a_{ij}] \in \mathbb{R}^{N\times N}$ is called a nonsingular M-matrix if $a_{ij} \leq 0, \forall i \neq j$, and all eigenvalues of A have positive real parts. $\text{diag}\{a_1, \ldots, a_n\}$ denotes a diagonal matrix with the diagonal elements being $a_1, \ldots, a_n$. $\det(A)$ is the determinant of a square matrix A, and $\text{trace}(A)$ is the sum of elements on the main diagonal of A. For any integer $a \leq b$, denote $\mathbf{I}[a, b] = \{a, a + 1, \ldots, b\}$.

Lemma 1.3 (Corless & Leitmann (1981)) *For a system $\dot{x} = f(x, t)$ where $f(\cdot)$ is locally Lipschitz in x and piecewise continuous in t, suppose that there exists a continuously differentiable function $V(x, t) \geq 0$ satisfying*

$$\begin{aligned} \mathcal{K}_1(\|x\|) \leq V(x, t) \leq & \mathcal{K}_2(\|x\|) \\ \dot{V}(x, t) \leq & -\mathcal{K}_3(\|x\|) + \Xi, \end{aligned}$$

where $\Xi > 0$ is a constant, $\mathcal{K}_1, \mathcal{K}_2$ belong to class $\mathcal{K}_\infty$ functions, and $\mathcal{K}_3$ belongs to class $\mathcal{K}$ function. The solution $x(t)$ of $\dot{x} = f(x,t)$ is uniformly ultimately bounded.

Lemma 1.4 (Young's inequality (Bernstein, 2009)) *If $a \geq 0, b \geq 0, p > 0, q > 0$ are real numbers satisfying $\frac{1}{p} + \frac{1}{q} = 1$, then $ab \leq \frac{a^p}{p} + \frac{b^q}{q}$.*

Lemma 1.5 (Khalil (1996)) *If a real function $V(t)$ satisfies $\dot{V}(t) \leq -aV(t)+b$, where a, b are positive constants, then*

$$V(t) \leq (V(0) - \frac{b}{a})e^{-at} + \frac{b}{a}.$$

Lemma 1.6 (Leibniz differentiation rule (Flanders, 1973)) *Let $f(x,t)$ be a function such that both $f(x,t)$ and its partial derivative $f_x(x,t)$ are continuous in t and x in some region of the (x,t)-plane, including $a(x) \leq t \leq b(x), x_0 \leq x \leq x_1$. Also suppose that the functions $a(x)$ and $b(x)$ are both continuous and both have continuous derivatives for $x_0 \leq x \leq x_1$. Then, for $x_0 \leq x \leq x_1$,*

$$\frac{d}{dx}\left(\int_{a(x)}^{b(x)} f(x,t)\,dt\right) = f(x,b(x)) \cdot \frac{d}{dx}b(x) - f(x,a(x)) \cdot \frac{d}{dx}a(x) + \int_{a(x)}^{b(x)} \frac{\partial}{\partial x} f(x,t)\,dt.$$

Lemma 1.7 (Jensen's inequality (Gu *et al.*, 2003)) *Let $\phi \in L_2[-h(t), 0]$, $h(t) > 0$ be a continuous function and $R \in \mathbb{R}^{n\times n} > 0$, then on has*

$$\int_{-h(t)}^{0} \phi^T(s) R \phi(s) ds \geq \frac{1}{h(t)} \int_{-h(t)}^{0} \phi^T(s) ds R \int_{-h(t)}^{0} \phi(s) ds. \tag{1.39}$$

Lemma 1.8 (Schur complement (Boyd *et al.*, 1994)) *For given matrices A, B, C, the following holds:*

$$D = \begin{bmatrix} A & B \\ B^T & C \end{bmatrix} < 0 \Longleftrightarrow C < 0 \,\&\, A - BC^{-1}B^T < 0. \tag{1.40}$$

Here $A - BC^{-1}B^T$ is the Schur complement of block C of D.

Lemma 1.9 *If (A, B) is controllable, then $(A, e^{-A\tau}B)$ is controllable.*

Proof. Define $\mathcal{C} := (B \quad AB \quad \dots \quad A^{n-1}B)$ and $\mathcal{C}_1 := (e^{-A\tau}B \quad Ae^{-A\tau}B \quad \dots \quad A^{n-1}e^{-A\tau}B)$. Based on $Ae^{-A\tau} = e^{-A\tau}A$, we get $\mathcal{C}_1 = e^{-A\tau}\mathcal{C}$. It is known that $\det(e^{-A\tau}) = e^{\text{trace}(-A\tau)} > 0$, which means $e^{-A\tau}$ is invertible, i.e., $rank(e^{-A\tau}) =$

n. Then $rank(\mathcal{C}_1) = rank(e^{-A\tau}\mathcal{C}) = rank(\mathcal{C})$. Since (A, B) is controllable, i.e., $rank(\mathcal{C}) = n$, thus we have $rank(\mathcal{C}_1) = n$ meaning that $(A, e^{-A\tau}B)$ is controllable.

Lemma 1.10 (Qu (2009)) *For a nonsingular M-matrix A, there exists a positive diagonal matrix $G = \text{diag}\{g_1, \ldots, g_N\} > 0$ such that $GA + A^T G > 0$.*

1.6 Time-varying formation shape

1.6.1 TVF shape for homogeneous systems

Consider the identical general LTI dynamics of agent i in the MAS as

$$\begin{array}{rcl} \dot{x}_i(t) & = & Ax_i(t) + Bu_i(t), \\ y_i(t) & = & Cx_i(t), \quad i \in \mathbf{I}[0, N] \end{array} \tag{1.41}$$

where $x_i(t) \in \mathbb{R}^n$, $u_i(t) \in \mathbb{R}^p$ and $y_i(t) \in \mathbb{R}^q$ are the state, control input and measured output, respectively. $A \in \mathbb{R}^{n\times n}, B \in \mathbb{R}^{n\times p}$ and $C \in \mathbb{R}^{q\times n}$ are constant matrices. Agent 0 is the leader and agents $1, \ldots, N$ are the followers.

Definition 1.11 *The TVF tracking means the relative offset vector (here is $h_i(t)$, $i \in \boldsymbol{I}[1, N]$ in Fig. 1.10 (a)) between the leader and follower is time-varying.*

On the contrary, if $h_i(t)$ is a constant, then the formation tracking is time-invariant. For each follower i, for the first time, we propose to design the TVF shape information as $h(t) = [h_1^T(t), \ldots, h_N^T(t)]^T \in \mathbb{R}^{Nn}$ with $h_i(t) \in \mathbb{R}^n$ being piecewise continuously differentiable for the homogeneous MAS as follows:

$$\dot{h}_i(t) = (A + BK_1)h_i(t), i \in \mathbf{I}[1, N] \tag{1.42}$$

where K_1 is a constant matrix to be designed. Designing K_1 give us a freedom to design any TVF shape satisfying the Eq. (1.42).

Remark 1.12 *An example in Fig. 1.10 (a) is used to explain the output TVF tracking control. Followers form an octagon shape and track the leader simultaneously. $Ch_i(t)$ denotes the desired relative offset vector of follower i relative to the leader. In Fig. 1.10 (a), the follower i rotates around the leader, and its reference trajectory comes from the leader's output and $Ch(t)$, i.e., $y_0(t)+Ch_i(t), i \in \boldsymbol{I}[1, N]$.*

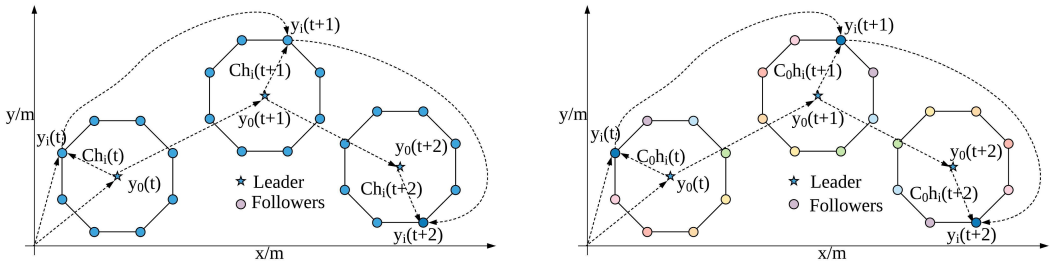

(a) Homogeneous. (b) Heterogeneous.

Figure 1.10: TVF tracking examples for homogeneous/heterogeneous MASs.

Remark 1.13 *It is not arbitrary or random to choose the TVF shape information $h(t)$ since it must be compatible with each agent's dynamics according to Eq. (1.42). Actually the application of K_1 provides more flexibility for $h(t)$. The TVF shape will become constant in many existing works if $A+BK_1 = 0$. K_1 is also dispensable for MASs. For example, by choosing $K_1 = 0$, $h(t)$ will be only related to each follower's dynamic matrix A, i.e., $\dot{h}_i(t) = Ah_i(t)$, which is a severe constraint when designing $h(t)$. Above all, K_1 has the function of expanding the feasible output TVF shape set described by Eq. (1.42).*

Definition 1.14 *The MAS (1.41) is said to achieve the output TVF tracking control if for any given initial states $x_i(0), i \in \boldsymbol{I}[0, N]$, there exists*

$$\lim_{t\to\infty} \|y_i(t) - y_0(t) - Ch_i(t)\| = 0. \tag{1.43}$$

Remark 1.15 *The Definition 1.14 reveals that the objective is to make all the followers reach an agreement on leader's output $y_0(t)$ while keep the offset $h(t)$ with respect to $y_0(t)$. If (1.43) is satisfied, thus for any $i, j \in \boldsymbol{I}[1, N]$, $\lim_{t\to\infty}[(y_i(t) - y_j(t)) - C(h_i(t) - h_j(t))] = 0$, which means the desired formation specified by $h(t)$ is achieved. Then considering the leader's tracked trajectory, it may locate inside or outside of the formation shape $h(t)$. In the assumption that $\lim_{t\to\infty} \sum_{i=1}^{N} h_i(t) = 0$, from (1.43) it generates $\lim_{t\to\infty} \left(\sum_{i=1}^{N} y_i(t)/N - y_0(t)\right) = 0$, which means the leader $y_0(t)$ lies inside the formation shape $h(t)$. Moreover, in the case where $h(t) \equiv 0$, the TVF tracking problem becomes the well-known consensus tracking*

problem. Therefore, consensus tracking problem can be regarded as the special case of the TVF tracking problem.

1.6.1.1 Example

Here, we take the simulation in Section 2.6 to illustrate the TVF shape changing mechanism. Consider a group of agents consisting of a leader labelled 0 and six followers labelled from 1 to 6. Suppose that the state of agent i is described as $x_i(t) = (x_{i1}(t), \ldots, x_{i6}(t))^T \in \mathbb{R}^6$. A and B are given as follows:

$$A = \begin{bmatrix} 0 & 0 & 0 & 1 & 0 & 0 \\ 0 & 0 & 0 & 0 & 1 & 0 \\ 0 & 0 & 0 & 0 & 0 & 1 \\ -1 & 0 & 0 & 0 & 0 & 0 \\ 0 & -1 & 0 & 0 & 0 & 0 \\ 0 & 0 & -1 & 0 & 0 & 0 \end{bmatrix}, \quad B = \begin{bmatrix} 0 & 0 & 0 \\ 0 & 0 & 0 \\ 0 & 0 & 0 \\ 1 & 0 & 0 \\ 0 & 1 & 0 \\ 0 & 0 & 1 \end{bmatrix}.$$

Choosing $C = [I_5, 0_{5\times 1}]$. Inspired by our previous work (Jiang *et al.*, 2017), design $h_i = [h_{i1}, \ldots, h_{i6}]^T$ as

$$\begin{aligned} h_{i1} =& -r\cos(wt + (i-1)\pi/3) + r\sin(wt + (i-1)\pi/3), \\ h_{i2} =& 2r\sin(wt + (i-1)\pi/3), \\ h_{i3} =& 2r\cos(wt + (i-1)\pi/3), \\ h_{i4} =& wr\cos(wt + (i-1)\pi/3) + wr\sin(wt + (i-1)\pi/3), \\ h_{i5} =& 2wr\cos(wt + (i-1)\pi/3), \\ h_{i6} =& -2wr\sin(wt + (i-1)\pi/3),\ i \in \mathbf{I}[1,6]. \end{aligned} \tag{1.44}$$

where w describes the frequency of followers rotating around the leader and r describes the TVF shape size. The TVF shapes for followers are described as the parallel hexagon shape when $t \in [0, 50) \cup [150, 200]$, the parallelogram shape when $t \in [50, 100)$ and the triangle shape when $t \in [100, 150)$ in the following:

$$h(t) = \begin{cases} [h_1^T, h_2^T, h_3^T, h_4^T, h_5^T, h_6^T]^T & 0 \le t < 50, \\ [h_1^T, (\frac{h_1+h_3}{2})^T, h_3^T, h_4^T, (\frac{h_4+h_6}{2})^T, h_6^T]^T & 50 \le t < 100, \\ [h_1^T, (\frac{h_1+h_3}{2})^T, h_3^T, (\frac{h_3+h_5}{2})^T, h_5^T, (\frac{h_5+h_1}{2})^T]^T & 100 \le t < 150, \\ [h_1^T, h_2^T, h_3^T, h_4^T, h_5^T, h_6^T]^T & 150 \le t \le 200. \end{cases}$$

It is obvious that $\lim_{t\to\infty} \sum_{i=1}^{6} h_i(t) = 0$, meaning that the six followers will keep TVF shapes around the leader when the desired formation tracking is achieved.

From (1.42) we get

$$K_1 = \begin{bmatrix} -3 & 0 & 0 & 0 & 0 & 0 \\ 0 & -3 & 0 & 0 & 0 & 0 \\ 0 & 0 & -3 & 0 & 0 & 0 \end{bmatrix}.$$

Set $r = 2, w = 2$. The TVF shape changing results is shown in Fig. 1.11. Furthermore, if the parameter r is a function of time t, i.e., $r(t)$, then the shape size will also change: when r becomes larger, the shape will expand and vice versa.

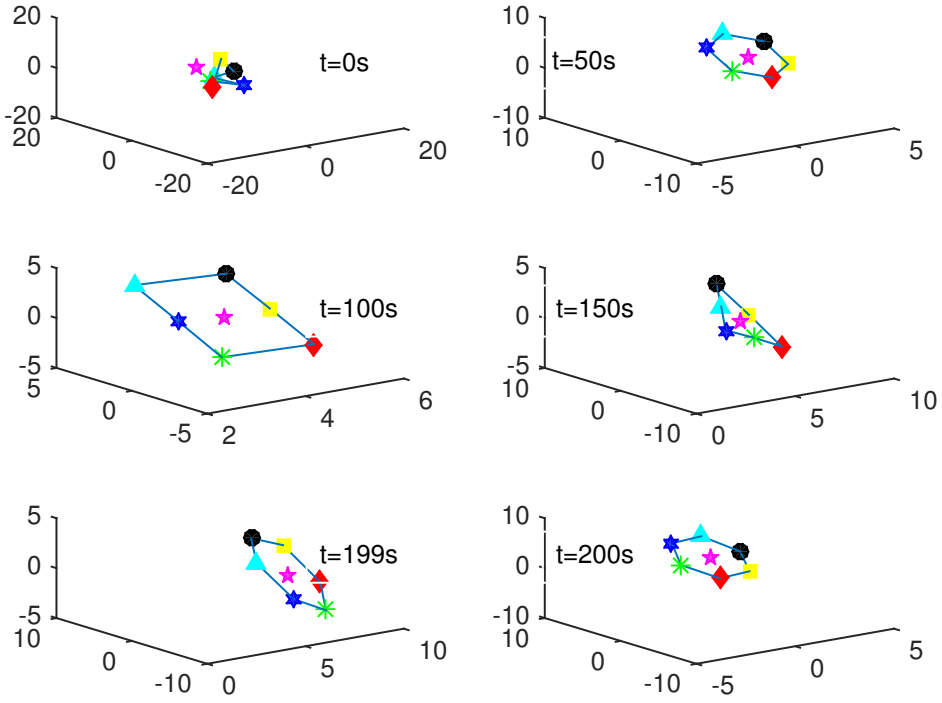

Figure 1.11: An example about how the time-varying shapes change.

1.6.2 TVF shape for heterogeneous systems

This section, a new TVF shape format for heterogeneous MAS/MRS is proposed. Different from (1.41), consider a group of heterogeneous follower agents as follows:

$$\begin{aligned} \dot{x}_i(t) &= A_i x_i(t) + B_i u_i(t), \\ y_i(t) &= C_i x_i(t), \quad i \in \mathbf{I}[1, N] \end{aligned} \tag{1.45}$$

where $x_i(t) = [x_{i1}(t), \ldots, x_{in_i}(t)]^T \in \mathbb{R}^{n_i}$, $u_i(t) \in \mathbb{R}^{p_i}$ and $y_i(t) \in \mathbb{R}^q$ are the state, control input and measured output of the i-th agent, respectively. $A_i \in \mathbb{R}^{n_i \times n_i}$, $B_i \in \mathbb{R}^{n_i \times p_i}$ and $C_i \in \mathbb{R}^{q \times n_i}$ are constant matrices. The leader indexed by 0 provides motion reference information followed by followers, and its dynamics is

$$\dot{x}_0(t) = A_0 x_0(t), \; y_0(t) = C_0 x_0(t) \tag{1.46}$$

where $A_0 \in \mathbb{R}^{n \times n}, C_0 \in \mathbb{R}^{q \times n}$, and $x_0(t) \in \mathbb{R}^n$, $y_0(t) \in \mathbb{R}^q$ are the state and output of the leader, respectively.

For the first time, we propose the TVF shape $h(t) = [h_1(t)^T, \ldots, h_N(t)^T]^T$ with $h_i(t) \in \mathbb{R}^n$ being piecewise continuously differentiable for the heterogeneous MAS as follows:

$$\dot{h}_i(t) = A_h h_i(t), \; i \in \mathbf{I}[1, N] \tag{1.47}$$

where $A_h \in \mathbb{R}^{n \times n}$ satisfying

$$\begin{array}{rcl} X_{hi} A_h & = & A_i X_{hi} + B_i U_{hi}, \\ C_0 & = & C_i X_{hi}, \quad i \in \mathbf{I}[1, N]. \end{array} \tag{1.48}$$

Remark 1.16 *This is a new format of TVF shape proposal for heterogeneous MASs. When A_h is designed, $(X_{hi}, U_{hi}), i \in \boldsymbol{I}[1, N]$ are the solutions of (1.48). Note that A_h is different from A_0. The detail could be referred to Chapter 3.*

Remark 1.17 *Since the MAS is non-identical and in particular, each agent may have different state dimensions, we cannot expect to achieve the state TVF tracking control. The output TVF tracking control scenario is shown in Fig. 1.10 (b) as an example (different colors mean the different dynamics). $C_0 h_i(t)$ denotes the desired relative offset vector of $y_i(t)$ relative to $y_0(t)$. In Fig. 1.10 (b), the follower i rotates around the leader, and its reference trajectory comes from the leader's output and $C_0 h(t)$, i.e., $y_0(t) + C_0 h_i(t), i \in \boldsymbol{I}[1, N]$.*

1.6.3 Summary

Contributions

- √ Propose a new TVF shape format (1.42) for homogeneous MASs.
- √ Propose a new TVF shape format (1.47), (1.48) for heterogeneous MASs.

Chapter 2

A unified framework of time-varying formation

Contents

This chapter presents a unified framework of TVF controller design for homogeneous LTI MASs based on an observer viewpoint from undirected to directed topology, from stabilization to tracking and from a leader without input to a one with bounded input. The followers can form a TVF shape which is specified by piecewise continuously differential vectors. The leader's trajectory, which is available to only a subset of followers, is also time-varying. For the undirected formation tracking and directed formation stabilization cases, only the relative output measurements of neighbors are required to design control protocols; for the directed formation tracking case, the agents need to be introspective (i.e. agents have partial knowledge of their own states) and the output measurements are required. Furthermore, considering the real applications, the leader with bounded input case is studied.

The distributed protocols in this chapter are independent of any global information, rely on agent dynamics and only the output measurements, thereby are fully distributed. The comparisons with some existing works are summarized as follows:

- A unified framework of TVF control design from the distributed observer viewpoint is presented. We reveal how to design observers to tackle TVF control problems from undirected to directed topology, from stabilization to tracking and from a leader without input to a one with bounded input.
- The protocols of majority of existing works are not fully distributed, where the protocol parameters are related to the minimal positive eigenvalue of the Laplacian matrix (Dong & Hu, 2016, Dong *et al.*, 2016, Ghommam *et al.*, 2016) or every follower needs the knowledge of the number of all robots (Antonelli *et al.*, 2014). In this thesis, we design the protocols in a fully distributed fashion.
- Compared with most literature dealing with time-invariant formation control with first order dynamics (Sakurama, 2016), second order dynamics (Wang & Xin, 2013), Liu & Jiang (2013), general linear dynamics (Peymani *et al.*, 2014) or TVF control with first order dynamics (Antonelli *et al.*, 2014), this chapter studies the TVF control with general linear dynamics.
- The output measurements, which are more applicable in real industry than the state ones in Antonelli *et al.* (2014), Dong & Hu (2016) that are sometimes unavailable in reality, are utilized here. Different from Liu & Jiang (2013), Rahimi *et al.* (2014) where all the followers need to know the leader's information, in this thesis, only a small portion of followers need the leader's information, which can reduce communication cost greatly especially in the case of large number of followers.

Section 2.1 solved the formation stabilization and tracking problems under undirected topology based only on relative output measurements. After that, we modified the protocol of Section 2.1 to address the same problem under directed topology in Section 2.2. Unfortunately, the designed protocol is not perfect since every follower needs to know the leader's output, which is a heavy communication burden for the whole system. In order to relax this constraint and make the control effect perfect, the protocol design for TVF tracking problem under directed topology is divided into three steps. Firstly, the TVF stabilization problem under directed topology is solved in Section 2.3 in which we do not take the leader into consideration. Then in Section 2.4, we tackle the TVF tracking problem under directed topology with a leader of no control input, i.e. $u_0(t) = 0$. Finally, the extended case of a leader with bounded input, i.e. $u_0(t) \neq 0$, is studied in Section 2.5.

In this chapter, the identical general linear dynamics of MASs is the same as in (1.41), which may be regarded as the linearized model of some nonlinear systems, such as the unicycle mobile robot in Chapter 3.3.2. For reading convenience, we rewrite it here:

$$\begin{aligned} \dot{x}_i(t) &= Ax_i(t) + Bu_i(t), \\ y_i(t) &= Cx_i(t), \quad i \in \mathbf{I}[0, N]. \end{aligned} \tag{2.1}$$

Without loss of generality, suppose that agents in (2.1) indexed by $1, \ldots, N$ are the followers denoted as $\mathbb{F} = \{1, \ldots, N\}$ and the agent indexed by 0 is the leader whose output information is only available to a small portion of followers. Moreover, the leader does not receive any information from the followers.

In the following, first the leader is regarded without control input, i.e. $u_0(t) = 0$, which is a common assumption in many existing works on the distributed cooperative control of linear MAS (Cai *et al.*, 2017, Wen *et al.*, 2016, Wu *et al.*, 2017, Yaghmaie *et al.*, 2016, Zhang *et al.*, 2018b).

However, as we know, where the whole system moves is decided by the leader and that is why the leader exists. Then where will the leader move? The answer is that a desired dynamic trajectory command is given to the leader to ask the leader to finish the desired trajectory tracking or that the leader moves anywhere it could, which requires the leader's control input to be nonzero. Furthermore, $u_0(t) = 0$ means the leader is a virtual one and the desired trajectory has severe limitations because of the equation $\dot{x}_0(t) = Ax_0(t)$ as the system matrix A is unchangeable. In real applications, the leader needs to regulate the final consensus trajectory. So its control input $u_0(t)$ will not be affected by followers. In this chapter, we deal with the consensus control in a fully distributed fashion, which means $u_0(t)$ will not be accessible to any follower. This is more difficult than the case of $u_0(t) = 0$. The leader with bounded control input $u_0(t)$ will be presented in Section 2.5.

The TVF shape information $h(t)$ is proposed in Chapter 1.6.1. In order to reach TVF control, a variety of protocols based on absolute or relative states have been proposed, e.g., in Dong *et al.* (2017), Wang *et al.* (2016a). For instance, a TVF protocol based on absolute/relative state information of neighboring agents is given in Wang *et al.* (2016a) as

$$u_i(t) = K_1 x_i(t) + K_2 \sum_{i \in N_i} c_{ij}(t) a_{ij} [(x_i(t) - x_j(t)) - (h_i(t) - h_j(t))]. \tag{2.2}$$

However, the state information in (2.2) in most practical applications may not be always available, whereas output information is accessible all the time. **So the output-based adaptive observer-type protocols are proposed in this chapter. The term (t) is omitted in the following for writing convenience.** Each follower can get access to the relative output measurements as

$$y_{ij} = y_i - y_j, \; y_{i0} = y_i - y_0, \quad i, j \in \mathbb{F}. \tag{2.3}$$

Assumption 2.1 *(A,B) is stabiliszable.*

Assumption 2.2 *(A, C) is detectable.*

2.1 Undirected formation tracking

Assumption 2.3 *The communication subgraph $\tilde{\mathcal{G}}$ among followers is undirected with the adjacency matrix $\tilde{\mathcal{A}}$ and Laplacian matrix $\tilde{\mathcal{L}}_1$. The graph $\mathcal{G}$ of the whole system contains a spanning tree with the adjacency matrix $\mathcal{A}$ and Laplacian matrix $\mathcal{L}$ where the leader acts as the root node.*

The objective here is to design the fully distributed protocol to make followers form the TVF shape and track the leader simultaneously based only on relative output measurements. To do this, the protocol for each follower i is proposed as

$$\begin{aligned} u_i =& K_1 h_i + K_2 v_i, \\ \dot{v}_i =& (A + BK_2)v_i + F\left[\sum_{j=1}^{N} a_{ij}c_{ij}(\bar{c}_{ij} - y_{ij}) + d_i c_i(\bar{c}_i - y_{i0})\right], \\ \dot{c}_{ij} =& k_{ij}a_{ij}(\bar{c}_{ij} - y_{ij})^T\Gamma(\bar{c}_{ij} - y_{ij}), \\ \dot{c}_i =& k_i d_i(\bar{c}_i - y_{i0})^T\Gamma(\bar{c}_i - y_{i0}), i \in \mathbb{F} \end{aligned} \tag{2.4}$$

where

$$\bar{c}_i = C(v_i + h_i), \quad \bar{c}_{ij} = \bar{c}_i - \bar{c}_j, \tag{2.5}$$

y_{ij}, y_{i0} are defined in (2.3) and K_1, K_2 are the feedback gain matrices. $v_i \in \mathbb{R}^n$ is the observer state and a_{ij} is the (i, j)-th entry of adjacency matrix $\tilde{\mathcal{A}}$ (graph theory can be referred to Chapter 1.5.1). $c_{ij}(t)$ denotes the time-varying coupling weight between follower i and j with $c_{ij}(0) = c_{ji}(0) > 0$, and $c_i > 0$ denotes the coupling weight between follower i and the leader. $k_{ij} = k_{ji}, k_i$ are positive constants and $F \in \mathbb{R}^{n\times q}, \Gamma \in \mathbb{R}^{q\times q}$ are the feedback gain matrices to be determined. d_i satisfies $d_i = 1$ if follower i can get information from the leader, otherwise $d_i = 0$.

Remark 2.4 *The adaptive coupling weights $c_{ij}(t)$ and $c_i(t)$ can release the constraint that some protocols need to know the minimal positive eigenvalue of the Laplacian matrix $\mathcal{L}$, e.g. in Dong & Hu (2016), Dong et al. (2017) and Wen et al. (2016). In other words, $c_{ij}(t)$ and $c_i(t)$ can make the protocol fully distributed.*

Define the TVF tracking error

$$\tilde{x}_i = x_i - h_i - x_0 \tag{2.6}$$

and the observer estimating error

$$e_i = \tilde{x}_i - v_i. \tag{2.7}$$

It is clear that e_i means the error between $\tilde{x}_i$ and observer v_i. We will design F and Γ to make the followers form TVF and track the leader's trajectory simultaneously, namely, (1.43) is satisfied. The following theorem presents a result of designing the adaptive protocol (2.4) for solving the TVF tracking problem.

Theorem 2.5 (Jiang *et al.* (2017)) *The fully distributed TVF tracking problem is solved with Assumptions 2.1, 2.2 and 2.3 under the protocol (2.4) if $A + BK_2$ is Hurwitz, $\Gamma = I$ and $F = -PC^T$, where $P^{-1} > 0$ is a solution to the following LMI:*

$$P^{-1}A + A^T P^{-1} - 2C^T C < 0. \tag{2.8}$$

Moreover, the coupling weights $c_{ij}(t), c_i(t), i, j \in \mathbb{F}$ converge to some finite steady-state values.

Proof. From $y_i(t) - y_0(t) - Ch_i(t) = C\tilde{x}_i$, it follows (1.43) that the objective is to prove $\lim_{t\to\infty} \tilde{x}_i = 0, i \in \mathbf{I}[1, N]$. Using (2.1), (1.42), the formation tracking error dynamic $\tilde{x}_i$ is

$$\dot{\tilde{x}}_i = A\tilde{x}_i + BK_2 v_i. \tag{2.9}$$

Using (2.9) for (2.4), the system can be rewritten in the following form

$$\begin{aligned} \dot{e}_i &= Ae_i + FC\left[\textstyle\sum_{j=1}^N a_{ij}c_{ij}(e_i - e_j) + d_i c_i e_i\right], \\ \dot{c}_{ij} &= k_{ij}a_{ij}(e_i - e_j)^T C^T \Gamma C(e_i - e_j), \\ \dot{c}_i &= k_i d_i e_i^T C^T \Gamma C e_i. \end{aligned} \tag{2.10}$$

Consider the Lyapunov function candidate

$$V = \sum_{i=1}^N e_i^T P^{-1} e_i + \sum_{i=1}^N \sum_{j=1, j\neq i}^N \frac{(c_{ij} - \alpha)^2}{2k_{ij}} + \sum_{i=1}^N \frac{(c_i - \alpha)^2}{k_i} \tag{2.11}$$

where α is a constant to be determined. The time derivative of V along the dynamics (2.10) is

$$\begin{aligned}\dot{V} =&2\sum_{i=1}^{N} e_i^T P^{-1} A e_i + 2\sum_{i=1}^{N}(c_i-\alpha) d_i e_i^T C^T \Gamma C e_i + 2\sum_{i=1}^{N} e_i^T P^{-1} F C \\ &\times [\sum_{j=1}^{N} a_{ij} c_{ij}(e_i - e_j) + d_i c_i e_i] + \sum_{i=1}^{N}\sum_{j=1,j\neq i}^{N}(c_{ij}-\alpha) a_{ij}(e_i-e_j)^T C^T \Gamma C (e_i - e_j).\end{aligned} \tag{2.12}$$

Because of $k_{ij} = k_{ji}, c_{ij}(0) = c_{ji}(0)$ and $a_{ij} = a_{ji}$ due to the property of undirected graph among followers with Γ being symmetric, it follows from protocol (2.4) that $c_{ij} = c_{ji}, \forall t \geq 0$. Then

$$\sum_{i=1}^{N}\sum_{j=1,j\neq i}^{N}(c_{ij}-\alpha) a_{ij}(e_i-e_j)^T C^T \Gamma C (e_i-e_j) = 2\sum_{i=1}^{N}\sum_{j=1,j\neq i}^{N}(c_{ij}-\alpha) a_{ij} e_i^T C^T \Gamma C (e_i-e_j). \tag{2.13}$$

Substituting $F = -PC^T, \Gamma = I$ and (2.13) into (2.12) then

$$\begin{aligned}\dot{V} =&\sum_{i=1}^{N} e_i^T (P^{-1}A + A^T P^{-1}) e_i - 2\alpha \sum_{i=1}^{N} d_i e_i^T C^T C e_i \\ &- 2\alpha \sum_{i=1}^{N}\sum_{j=1,j\neq i}^{N} a_{ij} e_i^T C^T C (e_i - e_j) \\ =&e^T (I_N \otimes (P^{-1}A + A^T P^{-1}) - 2\alpha \hat{\mathcal{L}} \otimes C^T C) e\end{aligned} \tag{2.14}$$

where $\hat{\mathcal{L}} = \tilde{\mathcal{L}}_1 + \mathcal{D}$. $\tilde{\mathcal{L}}_1$ is the Laplacian matrix corresponding to the graph $\tilde{\mathcal{G}}$, $\mathcal{D} = \text{diag}\{d_1, \ldots, d_N\}$. It is known that $\mathcal{D} > 0$ with at least one diagonal entry being positive since at least one follower can get access to the leader. Then $\hat{\mathcal{L}}$ is positive-defined.

Let $U \in \mathbb{R}^{N\times N}$ be a unitary matrix such that $U^T \hat{\mathcal{L}} U = \Lambda \triangleq \text{diag}\{\lambda_1, \ldots, \lambda_N\}$ where $\lambda_i, i \in \mathbf{I}[1, N]$ are the eigenvalues of $\hat{\mathcal{L}}$. Define $\tilde{e} \triangleq [\tilde{e}_1, \ldots, \tilde{e}_N] = (U^T \otimes I_n) e$. It thus follows from (2.14) that

$$\begin{aligned}\dot{\tilde{e}} =&\tilde{e}^T [I_N \otimes (P^{-1}A + A^T P^{-1}) - 2\alpha\Lambda \otimes C^T C]\tilde{e} \\ =&\sum_{i=1}^{N} \tilde{e}_i^T (P^{-1}A + A^T P^{-1} - 2\alpha\lambda_i C^T C)\tilde{e}_i.\end{aligned} \tag{2.15}$$

Choose α to be sufficiently large such that $\alpha\lambda_i \geq 1, i \in \mathbf{I}[1, N]$. Then it follows

from (2.15) that

$$\begin{aligned}\dot{\tilde{e}} =& \sum_{i=1}^{N} \tilde{e}_i^T (P^{-1}A + A^T P^{-1} - 2C^T C)\tilde{e}_i \\ \leq& 0\end{aligned} \tag{2.16}$$

where the last inequality comes directly from the LMI (2.8). So we can conclude that $V(t)$ is bounded and so are $c_{ij}(t), c_i(t)$. From (2.4) and $\Gamma = I$ it follows $\dot{c}_{ij} > 0, \dot{c}_i > 0$, thus each coupling weight $c_{ij}(t), c_i(t)$ increases monotonically and converges to some finite value finally. Note that $\dot{V} \equiv 0$ is equivalent to $\tilde{e} = 0$, implying $e = 0$. By LaSalle's Invariance principle (Krstic *et al.*, 1995), it follows that $\lim_{t\to\infty} e_i = 0 \Rightarrow v_i \to \tilde{x}_i$ as $t \to \infty$, which means the function of each follower's distributed observer v_i in (2.4) is to estimate its own formation error $\tilde{x}_i$. From (2.9), we get

$$\dot{\tilde{x}}_i = (A + BK_2)\tilde{x} - BK_2 e_i. \tag{2.17}$$

Since $A + BK_2$ is Hurwitz and $\lim_{t\to\infty} e_i = 0$, it is easy to see $\lim_{t\to\infty} \tilde{x}_i = 0$. The proof is finished.

2.2 Directed formation tracking with full access to leader

Assumption 2.6 *The graph $\mathcal{G}$ contains a directed spanning tree where the leader acts as the root node.*

As we know, each follower has access to a weighted linear combination of relative outputs between itself and its neighbours. The network measurement for follower i can be synthesised as a single signal:

$$\tilde{y}_i = \sum_{j=1}^{N} a_{ij} y_{ij} + d_i y_{i0}, i \in \mathbb{F} \tag{2.18}$$

where y_{ij} and y_{i0} are defined in (2.3).

In protocol (2.4) of Section 2.1, the key point to solve the formation tracking problem is $c_{ij}(t) = c_{ji}(t)$ thanks to the symmetric property of the adjacency matrix $\tilde{\mathcal{A}}$ of undirected topology $\tilde{\mathcal{G}}$ in Assumption 2.3, namely, $a_{ij} = a_{ji}$. But for the directed topology, $\tilde{\mathcal{A}}$ does not have the symmetric property, i.e. $a_{ij} \neq a_{ji}$. So the parameter $c_{ij}(t)$, which is the time-varying coupling weight between follower i and j, will not be suitable for the protocol design of directed topology. In addition, note that parameter $c_i(t)$ denotes the coupling weight between follower i and the

leader. Based on the above finding, we replace the parameters $c_{ij}(t)$ and $c_i(t)$ by one parameter $c_i(t) > 0$ denoting the time-varying coupling weight associated with the i-th follower, and modify the protocol (2.4) to a new one in the following form

$$\begin{aligned} u_i =& K_1 h_i + K_2 v_i, \\ \dot{v}_i =& (A + BK_2)v_i + F(c_i + \rho_i)\left(\sum_{j=1}^{N} a_{ij}\bar{c}_{ij} + d_i\bar{c}_i - \tilde{y}_i\right) \\ \dot{c}_i =& (\bar{c}_i - y_{i0})^T\Gamma(\bar{c}_i - y_{i0}), i \in \mathbb{F} \end{aligned} \tag{2.19}$$

where $c_i(0) > 0, \bar{c}_i = C(v_i + h_i), \bar{c}_{ij} = \bar{c}_i - \bar{c}_j$, y_{i0} is defined in (2.3) and ρ_i is a smooth function to be determined later. Other parameters are the same as in (2.4).

Theorem 2.7 *The fully distributed TVF tracking problem is solved with Assumptions 2.1, 2.2 and 2.6 under the protocol (2.19) if $A+BK_2$ is Hurwitz, $\Gamma = I$, $F = -PC^T$ and $\rho_i = e_iP^{-1}e_i$, where $P^{-1} > 0$ is a solution to the LMI (2.8). Moreover, the coupling weight $c_i(t), i \in \mathbb{F}$ converge to some finite steady-state values.*

Proof. Recall (2.17) that $\dot{\tilde{x}}_i = (A + BK_2)\tilde{x} - BK_2e_i$. The objective now is to prove $\lim_{t\to\infty} e_i = 0$ such that $\lim_{t\to\infty} \tilde{x}_i = 0, i \in \mathbb{F}$ since $A + BK_2$ is Hurwitz. Using (2.17) and (2.19), the system (2.1) can be rewritten as

$$\begin{aligned} \dot{e}_i &= Ae_i + FC(c_i + \rho_i)(\textstyle\sum_{j=1}^{N} l_{ij}e_i + d_ie_i), \\ \dot{c}_i &= e_i^TC^T\Gamma Ce_i. \end{aligned} \tag{2.20}$$

Let

$$V_1 = \frac{1}{2}\sum_{i=1}^{N} g_i(2c_i + \rho_i)\rho_i + \frac{1}{2}\sum_{i=1}^{N} g_i(c_i - \alpha)^2 \tag{2.21}$$

where $g_i > 0, i \in \mathbb{F}$ is defined in Lemma 1.10. It follows from $c_i(0) > 0$ and $\dot{c}_i(t) > 0$ that $c_i(t) > 0, \forall t > 0$. α is a positive constant to be determined. Noting

further that $\rho_i \geq 0$, thus V_1 is positive definite. Then

$$\begin{aligned}\dot{V}_1 =& \sum_{i=1}^{N}[g_i(c_i+\rho_i)\dot{\rho}_i + g_i\rho_i\dot{c}_i + g_i(c_i-\alpha)\dot{c}_i] \\ =& e^T[G(\hat{c}+\hat{\rho})\otimes(P^{-1}A + A^TP^{-1}) + (\hat{c}+\hat{\rho})(G\hat{\mathcal{L}} + \hat{\mathcal{L}}^TG)(\hat{c}+\hat{\rho}) \\ & \otimes P^{-1}FC + G(\hat{c}+\hat{\rho}-\alpha I)\otimes C^T\Gamma C]e \\ \leq& e^T[G(\hat{c}+\hat{\rho})\otimes(P^{-1}A + A^TP^{-1}) - \lambda_0(\hat{c}+\hat{\rho})^2 \\ & \otimes C^TC + G(\hat{c}+\hat{\rho}-\alpha I)\otimes C^TC]e\end{aligned} \tag{2.22}$$

where $\hat{c} = \text{diag}\{c_1,\ldots,c_N\}$, $\hat{\rho} = \text{diag}\{\rho_1,\ldots,\rho_N\}$, $\mathcal{D} = \text{diag}\{d_1,\ldots,d_N\}$ and $\hat{\mathcal{L}} = \tilde{\mathcal{L}}_1 + \mathcal{D}$. The Laplacian matrix $\tilde{\mathcal{L}}_1$ is corresponding to the subgraph $\tilde{\mathcal{G}}$ among followers. Then $\hat{\mathcal{L}}$ is a M-matrix with the whole graph $\mathcal{G}$ satisfying Assumption 2.6, which means all eigenvalues of $\hat{\mathcal{L}}$ have positive real parts (Hong *et al.*, 2006). Furthermore, from Lemma 1.10 there exists $G = \text{diag}\{g_1,\ldots,g_N\} > 0$ such that $G\hat{\mathcal{L}} + \hat{\mathcal{L}}^TG \geq \lambda_0 I$ where λ_0 is the smallest positive eigenvalue of $G\hat{\mathcal{L}} + \hat{\mathcal{L}}^TG$. Using Lemma 1.4 we get

$$e^T[G(\hat{c}+\hat{\rho})\otimes C^TC]e \leq e^T[(\frac{\lambda_0}{2}(\hat{c}+\hat{\rho})^2 + \frac{G^2}{2\lambda_0})\otimes C^TC]e. \tag{2.23}$$

Substituting (2.23) into (2.22) we have

$$\dot{V}_1 \leq e^T[G(\hat{c}+\hat{\rho})\otimes(P^{-1}A + A^TP^{-1}) - (\frac{\lambda_0}{2}(\hat{c}+\hat{\rho})^2 - \frac{G^2}{2\lambda_0} + \alpha G)\otimes C^TC]e. \tag{2.24}$$

Choosing $\alpha \geq \max_{i\in\mathbb{F}}\frac{5g_i}{\sqrt{2\lambda_0}}$, we obtain

$$\dot{V}_1 \leq e^T[G(\hat{c}+\hat{\rho})\otimes(P^{-1}A + A^TP^{-1} - 2C^TC)]e \leq 0 \tag{2.25}$$

where the last inequality comes directly from the LMI (2.8). Then $V_1(t)$ is bounded and so is $c_i(t)$. Each coupling weight $c_i(t)$ increases monotonically and converges to some finite value finally. Note that $\dot{V}_1 \equiv 0$ is equivalent to $e = 0$. By LaSalle's Invariance principle (Krstic *et al.*, 1995), it follows that $\lim_{t\to\infty} e_i = 0$ such that $v_i \to \tilde{x}_i$ as $t \to \infty$, which means the function of each follower's distributed observer v_i in (2.19) is to estimate its own TVF tracking error $\tilde{x}_i$.

Since $A + BK_2$ is Hurwitz and $\lim_{t\to\infty} e_i = 0$, from (2.17) we have $\lim_{t\to\infty}\tilde{x}_i = 0, i \in \mathbb{F}$, i.e., the distributed TVF tracking problem under the directed topology satisfying Assumption 2.6 is solved. The proof is finished.

Remark 2.8 *Note that in order to calculate $c_i(t)$ in protocol (2.19), each follower*

i requires the knowledge of y_{i0} in (2.3), namely the relative output measurement between the follower i and the leader. It means every follower needs to know the leader's output information, in other words, $d_i > 0, \forall i \in \mathbb{F}$, which is a stringent communication constraint and will increase communication burden heavily. We will solve the TVF tracking problem where the leader's output information is only available to a small subset of followers in the following sections.

2.3 Directed formation stabilization

Assumption 2.9 *The communication graph $\mathcal{G}$ is strongly connected.*

Definition 2.10 *The MAS (2.1) is said to achieve the output TVF stabilization if for any given initial states $x_i(0), i \in \mathbb{F}$, there exists*

$$\lim_{t\to\infty} \|(y_i(t) - y_j(t)) - C(h_i(t) - h_j(t))\| = 0. \tag{2.26}$$

In Section 2.2 we solved the leader-follower TVF tracking problem with directed spanning tree topology, but it requires each follower to know the leader's output information. In order to relax this severe constraint, we start to solve the formation stabilization problem first, namely without the leader. The inspiration comes from the last section. Recall the equation of adaptive parameter c_i in protocol (2.19) as

$$\dot{c}_i = (\tilde{x}_i - v_i)^T C^T \Gamma C (\tilde{x}_i - v_i).$$

Remark 2.11 *It is obvious that the observer v_i in (2.19) is used to estimate the formation tracking error $\tilde{x}_i = x_i - h_i - x_0$ in (2.6). For the formation stabilization problem without the leader, it is natural to design v_i to estimate*

$$\bar{x}_i = x_i - h_i. \tag{2.27}$$

Our goal in this section is to design the fully distributed protocol based only on the relative output measurements to make the system form a shape, namely, making agents i and j satisfy formation stabilization condition (2.26). Similar as the network measurement (2.18), we define two signals as

$$\psi_i = \sum_{j=1}^{N} a_{ij}(v_i - v_j),\ \eta_i = \sum_{j=1}^{N} a_{ij}(\bar{x}_i - \bar{x}_j). \tag{2.28}$$

Denote $\psi = [\psi_1^T, \ldots, \psi_N^T]^T, \eta = [\eta_1^T, \ldots, \eta_N^T]^T$, then $\eta = (\mathcal{L} \otimes I_n)\bar{x}$, where $\mathcal{L}$ is the Laplacian matrix corresponding to the graph $\mathcal{G}$ satisfying Assumption 2.9. Based on Lemma 1.1, $\mathcal{L}$ has a zero eigenvalue and other eigenvalues with positive real parts. From Definition 2.10, the TVF stabilization problem is solved if $\lim_{t\to\infty} \eta = 0$. So η can be viewed as formation stabilization error in this section.

The fully distributed adaptive protocol based only on relative output measurements is proposed for each agent i as

$$\begin{aligned} u_i =& K_1 h_i + K_2 v_i, \\ \dot{v}_i =& (A + BK_2)v_i + F(c_i + \rho_i)\sum_{j=1}^{N} a_{ij}(\bar{c}_{ij} - y_{ij}), \\ \dot{c}_i =& \left[\sum_{j=1}^{N} a_{ij}(\bar{c}_{ij} - y_{ij})\right]^T \Gamma \sum_{j=1}^{N} a_{ij}(\bar{c}_{ij} - y_{ij}) \end{aligned} \tag{2.29}$$

where $y_{ij} = y_i - y_j, \bar{c}_i = C(v_i + h_i), \bar{c}_{ij} = \bar{c}_i - \bar{c}_j$ and other parameters are defined similarly as protocol (2.19). By substituting (2.28) into (2.29) we can write protocol (2.29) as

$$\begin{aligned} u_i =& K_1 h_i + K_2 v_i, \\ \dot{v}_i =& (A + BK_2)v_i + F(c_i + \rho_i)C(\psi_i - \eta_i), \\ \dot{c}_i =& [C(\psi_i - \eta_i)]^T \Gamma C(\psi_i - \eta_i). \end{aligned} \tag{2.30}$$

Note that the term $C(\psi_i - \eta_i)$ implies that each agent needs to receive observers' virtual outputs Cv_j and agents' relative output measurements $C\bar{x}_j$ from its neighbors via the communication graph $\mathcal{G}$ satisfying Assumption 2.9. Let $\varrho_i = \psi_i - \eta_i, \varrho = [\varrho_1^T, \ldots, \varrho_N^T]^T$, then we combine (2.1), (2.28), (2.29) and get

$$\begin{aligned} \dot{\psi} =& [I_N \otimes (A + BK_2)]\psi + [\mathcal{L}(\hat{c} + \hat{\rho}) \otimes FC]\varrho, \\ \dot{\eta} =& [I_N \otimes (A + BK_2)]\eta + (I_N \otimes BK_2)\varrho, \\ \dot{\varrho} =& [I_N \otimes A + \mathcal{L}(\hat{c} + \hat{\rho}) \otimes FC]\varrho. \end{aligned} \tag{2.31}$$

Theorem 2.12 *Suppose Assumptions 2.1, 2.2 and 2.9 hold, the fully distributed TVF stabilization problem is solved under the protocol (2.29) if $A+BK_2$ is Hurwitz, $\Gamma = I$, $F = -Q^{-1}C^T$ and $\rho_i = \varrho_i^T Q \varrho_i$, where $Q > 0$ is a solution to the LMI*

$$QA + A^T Q - 2C^T C < 0. \tag{2.32}$$

And $c_i(t)$ converge to some finite steady-state values.

Proof. First, we prove that $\lim_{t\to\infty} \varrho = 0$. To this end, similar as (2.21) in Theorem 2.7, let

$$V_2 = \frac{1}{2}\sum_{i=1}^{N} r_i(2c_i + \rho_i)\rho_i + \frac{1}{2}\sum_{i=1}^{N} r_i(c_i - \alpha)^2 \tag{2.33}$$

where $r = [r_1^T, \ldots, r_N^T]^T, r_i > 0$ is the left eigenvector of $\mathcal{L}$ associated with the zero eigenvalue and other parameters are the same as in Theorem 2.7. Then,

$$\begin{aligned}\dot{V}_2 =& \varrho^T[R(\hat{c}+\hat{\rho}) \otimes (QA + A^T Q) + R(\hat{c}+\hat{\rho}-\alpha I) \otimes C^T \Gamma C \\ &+ (\hat{c}+\hat{\rho})\tilde{\mathcal{L}}(\hat{c}+\hat{\rho}) \otimes QFC]\varrho\end{aligned} \tag{2.34}$$

where $R = \text{diag}\{r_1, \ldots, r_N\}$ and $\tilde{\mathcal{L}} = R\mathcal{L} + \mathcal{L}^T R$. Denote $\tilde{\varrho} = [(\hat{c}+\hat{\rho}) \otimes I_n]\varrho$. Considering $\varrho = \psi - \eta = (\mathcal{L} \otimes I_n)(v - \bar{x}), r^T \mathcal{L} = 0$, then

$$\tilde{\varrho}^T[(\hat{c}+\hat{\rho})^{-1} r \otimes \mathbf{1}] = (v - \bar{x})^T(\mathcal{L}^T r \otimes \mathbf{1}) = 0.$$

Since each entry of r is positive, then each entry of $[(\hat{c}+\hat{\rho})^{-1} r \otimes \mathbf{1}]$ is also positive. From Lemma 1.2,

$$\tilde{\varrho}^T(\tilde{\mathcal{L}} \otimes I_n)\tilde{\varrho} > \frac{\lambda_2(\tilde{\mathcal{L}})}{N}\tilde{\varrho}^T\tilde{\varrho} = \frac{\lambda_2(\tilde{\mathcal{L}})}{N}\varrho^T[(\hat{c}+\hat{\rho})^2 \otimes I_n]\varrho.$$

Similar as (2.23) in Theorem 2.7, using Lemma 1.4 we get

$$\varrho^T[R(\hat{c}+\hat{\rho}) \otimes C^T C]\varrho \leq \varrho^T[(\frac{\lambda_2(\tilde{\mathcal{L}})}{2N}(\hat{c}+\hat{\rho})^2 + \frac{N}{2\lambda_2(\tilde{\mathcal{L}})}R^2) \otimes C^T C]\varrho.$$

Combining above two inequalities with (2.34) and choosing $\alpha \geq \frac{5N\lambda_{max}(R)}{2\lambda_2(\tilde{\mathcal{L}})}$, we have

$$\dot{V}_2 \leq \varrho^T[R(\hat{c}+\hat{\rho}) \otimes (QA + A^TQ - 2C^TC)]\varrho \leq 0 \tag{2.35}$$

where the last inequality comes from LMI (2.32). So $V_2(t)$ is bounded, and $c_i(t)$ increases monotonically and converges to some finite value finally. Similar as the proof in Theorem 2.7, $\lim_{t\to\infty} \varrho = 0$ can be proved. From the second equation in (2.31) and $A+BK_2$ is Hurwitz, we can prove $\lim_{t\to\infty} \eta = 0$, i.e. the fully distributed TVF stabilization problem with the directed strongly connected topology is solved.

Remark 2.13 *From (2.28) it is easy to get $\psi = (\mathcal{L} \otimes I_n)v, \eta = (\mathcal{L} \otimes I_n)\bar{x}$ and $\varrho = (\mathcal{L} \otimes I_n)(v - \bar{x})$. $\lim_{t\to\infty} \varrho = 0$ means that the error between observer v_i and formation stabilization error $\bar{x}_i$ of each agent i will go to zero eventually. Similarly, $\lim_{t\to\infty} \eta = 0$ means that the formation stabilization error $\bar{x}_i$ of each agent i will reach consistent eventually. Obviously, the observer v_i of each agent i will also reach consistent eventually. Note that (2.29) is a consensus-based formation stabilization protocol. From Corollary 1 of Olfati-Saber & Murray (2004), we know that the group decision value of formation is a function of each agent's initial state $x_i(0), i \in \boldsymbol{I}[1, N]$. The group decision value decides where the leaderless formation to go, which means there is no precisely explicit equation defining where the leaderless formation to go. It is necessary and applicable to solve the leader-follower TVF tracking problem with directed topology when only a small subset of followers know leader's output information, which will be presented in next section.*

2.4 Directed formation tracking with partial access to leader

During the process of solving the TVF stabilization problem with directed topology in Section 2.3, an observer v_i that estimates formation stabilization error is introduced to design the protocol (2.29) based on the following structure

$$\left.\begin{array}{l}\lim\limits_{t\to\infty}\varrho_i=0\Rightarrow v_i-\bar{x}_i\to v_j-\bar{x}_j\\ \lim\limits_{t\to\infty}\psi_i=0\Rightarrow v_i\to v_j\end{array}\right\}\Rightarrow \bar{x}_i\to\bar{x}_j, t\to\infty.$$

In this section for the formation tracking problem, similar to that structure, we introduce two observers to design the fully distributed protocol as follows

$$\begin{aligned}u_i=&K_1h_i+K_2v_i,\\ \dot{w}_i=&Aw_i+Bu_i-BK_1h_i+F[Cw_i-(y_i-Ch_i)],\\ \dot{v}_i=&Av_i+Bu_i-BK_1h_i+FC(c_i+\rho_i)(\psi_i-\eta_i)+F[Cw_i-(y_i-Ch_i)],\\ \dot{c}_i=&(\psi_i-\eta_i)^TC^T\Gamma C(\psi_i-\eta_i), i\in\mathbb{F}.\end{aligned}\tag{2.36}$$

Here $\psi_i=\sum_{j=0}^N a_{ij}(v_i-v_j), \eta_i=\sum_{j=0}^N a_{ij}(w_i-w_j)$, which is similar to (2.28). And $w_0=Aw_0+F(Cw_0-y_0), v_0=0$ meaning that the leader has only one observer w_0 to estimate its state x_0. Note here that $a_{i0}>0$ means follower i can receive information from the leader and cannot if $a_{i0}=0$, which shows that only a subset of followers can get the leader's output information. The local observer w_i is designed to estimate $\bar{x}_i=x_i-h_i$ in (2.27), while the distributed observer v_i is used to make formation tracking error $\tilde{x}_i=\bar{x}_i-x_0$ in (2.6) converge to zero. Here we assume that each agent is introspective as termed in Peymani *et al.* (2014), which means each one has access to its own output.

Under Assumption 2.6, the Laplacian matrix of graph $\mathcal{G}$ can be partitioned as $\mathcal{L}=\begin{bmatrix}0 & 0_{1\times N}\\ \mathcal{L}_2 & \mathcal{L}_1\end{bmatrix}$, where $\mathcal{L}_1\in\mathbb{R}^{N\times N}, \mathcal{L}_2\in\mathbb{R}^{N\times 1}$. It is easy to confirm that $\mathcal{L}_1$ is a nonsingular M-matrix. Denote $w=[w_1^T,\ldots,w_N^T]^T, v=[v_1^T,\ldots,v_N^T]^T$ and $\varrho_i=\psi_i-\eta_i, i\in\mathbb{F}$, then

$$\begin{aligned}\psi=&(\mathcal{L}_1\otimes I_n)v,\\ \eta=&(\mathcal{L}_1\otimes I_n)(w-\mathbf{1}\otimes w_0),\\ \varrho=&(\mathcal{L}_1\otimes I_n)(v-w+\mathbf{1}\otimes w_0).\end{aligned}\tag{2.37}$$

Our goal is try to prove that

$$\left.\begin{array}{l}\varrho_i = 0 \Rightarrow w_i - v_i \to w_0 \\ \psi_i = 0 \Rightarrow v_i \to 0\end{array}\right\} \Rightarrow w_i \to w_0 \left.\begin{array}{l} \\ \\ w_i \to \bar{x}_i, \quad w_0 \to x_0\end{array}\right\} \Rightarrow \bar{x}_i \to x_0$$

where $\bar{x}_i - x_0 = x_i - h_i - x_0$ is the same as formation tracking error $\tilde{x}_i$ in the proof of Theorem 2.7. In this section, similar as (2.18), define a signal as

$$\hat{x}_i = \sum_{j=1}^{N} a_{ij}(\bar{x}_i - \bar{x}_j) + a_{i0}(\bar{x}_i - x_0) \tag{2.38}$$

where $\bar{x}_i = x_i - h_i$ and $\hat{x} = [\hat{x}_1^T, \ldots, \hat{x}_N^T]^T$, then $\hat{x} = (\mathcal{L}_1 \otimes I_n)(\bar{x} - \mathbf{1} \otimes x_0)$. It is easy to see that the TVF tracking problem with the directed topology is solved if and only if $\lim_{t\to\infty} \hat{x} = 0$. Substituting (2.36), (2.37) into (2.1), we get

$$\begin{aligned}\dot{\hat{x}} =& (I_N \otimes A)\hat{x} + (I_N \otimes BK_2)\psi, \\ \dot{\eta} =& (I_N \otimes A)\eta + (I_N \otimes BK_2)\psi + (I_N \otimes FC)(\eta - \hat{x}), \\ \dot{\psi} =& [I_N \otimes (A + BK_2)]\psi + [\mathcal{L}_1(\hat{c} + \hat{\rho}) \otimes FC]\varrho + (I_N \otimes FC)(\eta - \hat{x}) \\ & + (\mathcal{L}_1 \otimes FC)[\mathbf{1} \otimes (w_0 - x_0)], \\ \dot{c}_i =& (\psi_i - \eta_i)^T C^T \Gamma C(\psi_i - \eta_i), \quad i \in \mathbb{F}.\end{aligned} \tag{2.39}$$

Defining $\bar{x}_0 = w_0 - x_0$ as the leader's state estimation error, $\zeta = [\zeta_1^T, \ldots, \zeta_N^T]^T = \eta - \hat{x}$ and $\varrho = \psi - \eta$, we obtain

$$\begin{aligned}\dot{\zeta} =& [I_N \otimes (A + FC)]\zeta, \\ \dot{\varrho} =& [I_N \otimes A + \mathcal{L}_1(\hat{c} + \hat{\rho}) \otimes FC]\varrho + (\mathcal{L}_1 \otimes FC)(\mathbf{1} \otimes \bar{x}_0), \\ \dot{c}_i =& \varrho_i^T C^T \Gamma C \varrho_i, \quad i \in \mathbb{F}.\end{aligned} \tag{2.40}$$

The following theorem presents a result of designing protocol (2.36) to solve the TVF tracking problem with only a small subset of followers knowing the leader's output information.

Theorem 2.14 *The fully distributed TVF tracking problem is solved with Assumptions 2.1, 2.2 and 2.6 under the protocol (2.36) if $A+BK_2$ is Hurwitz, $\Gamma = I$, $F = -Q^{-1}C^T$ and $\rho_i = \varrho_i^T Q \varrho_i$, where $Q > 0$ satisfies the LMI (2.32). And $c_i(t), i \in \mathbb{F}$ converge to some finite steady-state values.*

Proof. First, we prove that $\lim_{t\to\infty}\varrho=0$ and $\lim_{t\to\infty}\bar{x}_0=0$. To this end, let

$$V_3=\frac{1}{2}\sum_{i=1}^{N}g_i(2c_i+\rho_i)\rho_i+\frac{1}{2}\sum_{i=1}^{N}g_i(c_i-\alpha)^2+\gamma\bar{x}_0^TQ\bar{x}_0 \tag{2.41}$$

where γ is a positive constant to be determined later and other parameters are the same as in the proof of Theorem 2.7. Similarly, V_3 is positive definite with respect to ϱ_i, c_i and $\bar{x}_0$. Then

$$\begin{aligned}\dot{V}_3\leq&\varrho^T[G(\hat{c}+\hat{\rho})\otimes(QA+A^TQ)-\lambda_0^{'}(\hat{c}+\hat{\rho})^2\otimes C^TC+G(\hat{c}+\hat{\rho}-\alpha I)\otimes C^TC]\varrho\\&-\gamma\bar{x}_0^TW\bar{x}_0-2\varrho^T[G(\hat{c}+\hat{\rho})\mathcal{L}_1\otimes C^TC](\mathbf{1}\otimes\bar{x}_0)\end{aligned} \tag{2.42}$$

where $\lambda_0^{'}>0$ is the smallest eigenvalue of $G\mathcal{L}_1+\mathcal{L}_1^TG$, and $W=-(QA+A^TQ-2C^TC)$ is a positive definite matrix according to (2.32). By using Lemma 1.4 and $\mathcal{L}_1\mathbf{1}=-\mathcal{L}_2$, we can get

$$\varrho^T[G(\hat{c}+\hat{\rho})\otimes C^TC]\varrho\leq\varrho^T[(\frac{\lambda_0^{'}}{3}(\hat{c}+\hat{\rho})^2+\frac{3G^2}{4\lambda_0^{'}})\otimes C^TC]\varrho$$

and

$$\begin{aligned}&-2\varrho^T[G(\hat{c}+\hat{\rho})\mathcal{L}_1\otimes C^TC](\mathbf{1}\otimes\bar{x}_0)\\&\leq\frac{\lambda_0^{'}}{3}\varrho^T[(\hat{c}+\hat{\rho})^2\otimes C^TC]\varrho+\frac{3}{\lambda_0^{'}}\bar{x}_0^T(G\mathcal{L}_2\mathcal{L}_2^TG\otimes C^TC)\bar{x}_0\\&\leq\frac{\lambda_0^{'}}{3}\varrho^T[(\hat{c}+\hat{\rho})^2\otimes C^TC]\varrho+\frac{3\lambda_{max}(C^TC)\mathcal{L}_2^TGG\mathcal{L}_2}{\lambda_0^{'}\lambda_{min}(W)}\bar{x}_0^TW\bar{x}_0,\end{aligned}$$

where $\mathcal{L}_2^TGG\mathcal{L}_2$ is a scalar and $\frac{W}{\lambda_{min}(W)}\geq I$ is used to arrive at the last inequality. Substituting above two inequalities into (2.42), we get

$$\begin{aligned}\dot{V}_3\leq&\varrho^T[G(\hat{c}+\hat{\rho})\otimes(QA+A^TQ)-(\frac{\lambda_0^{'}}{3}(\hat{c}+\hat{\rho})^2-\frac{3G^2}{4\lambda_0^{'}}+\alpha G)\otimes C^TC]\varrho\\&+(-\gamma+\frac{3\lambda_{max}(C^TC)\mathcal{L}_2^TGG\mathcal{L}_2}{\lambda_0^{'}\lambda_{min}(W)})\bar{x}_0^TW\bar{x}_0.\end{aligned}$$

Choosing $\alpha\geq\frac{15\lambda_{max}(G)}{4\lambda_0^{'}}$ and $\gamma=1+\frac{3\lambda_{max}(C^TC)\mathcal{L}_2^TGG\mathcal{L}_2}{\lambda_0^{'}\lambda_{min}(W)}$, we obtain

$$\dot{V}_3\leq-\varrho^T[G(\hat{c}+\hat{\rho})\otimes W]\varrho-\bar{x}_0^TW\bar{x}_0\leq0 \tag{2.43}$$

where the last inequality comes from $W > 0$. Similar as the proof in Theorem 2.7, it is easy to verify that $\varrho_i, \bar{x}_0$ and c_i are bounded, and the coupling weight $c_i(t)$ converges to some finite value.

Next we show the convergence of ζ in (2.40). Thanks to $F = -Q^{-1}C^T$, it follows from LMI (2.32) that

$$(A + FC)^T Q + Q(A + FC) = A^T Q + QA - 2C^T C < 0.$$

Therefore, $(A + FC)$ is Hurwitz and ζ converges to zero.

Then we try to verify the convergence of ψ in (2.39). Based on $\lim_{t\to\infty} \varrho = 0, \lim_{t\to\infty} \bar{x}_0 = 0, \lim_{t\to\infty} \zeta = 0$ and $(A + BK_2)$ being Hurwitz, from (2.39) we can conclude that $\lim_{t\to\infty} \psi = 0$.

Furthermore, based on $\lim_{t\to\infty} \zeta = 0, \lim_{t\to\infty} \psi = 0$, from (2.39) we can conclude that $\lim_{t\to\infty} \eta = 0$.

Finally, due to $\hat{x} = \eta - \zeta$, based on $\lim_{t\to\infty} \eta = 0$ and $\lim_{t\to\infty} \zeta = 0$, we obtain $\lim_{t\to\infty} \hat{x} = 0$. Recalling that $\hat{x} = (\mathcal{L}_1 \otimes I_n)(\bar{x} - \mathbf{1} \otimes x_0)$ and $\mathcal{L}_1$ is a M-matrix with all eigenvalues having positive real parts, we obtain $\lim_{t\to\infty}(\bar{x}_i - x_0) = \lim_{t\to\infty}(x_i - h_i - x_0) = 0$, which means the distributed TVF tracking problem considering the leader of no input under directed spanning tree topology is solved where only a small subset of followers know leader's output information.

Remark 2.15 *Compared with the TVF research (Dong & Hu, 2016), where only the stabilization problem is solved, our control protocol in this subsection solves the TVF tracking problem and furthermore, is fully distributed due to the application of adaptive parameter $c_i(t)$, while the protocol in Dong & Hu (2016) is not since its parameter depends on the smallest positive eigenvalue information of Laplacian matrices. The second improvement is that we use output measurements which are more applicable in reality than the state ones utilised in Dong & Hu (2016). Thirdly, the protocol in Dong & Hu (2016) requires (A, B) to be controllable while we require (A, B) to be stabilisable, which is a more relaxed condition for system dynamics. Finally, the algorithm in Dong & Hu (2016) needs to check the TVF feasibility condition first, which is more complicated compared with our TVF shape proposition $h(t)$ in (1.42).*

2.5 Directed formation tracking with bounded leader input

In the previous sections, we dealt with TVF tracking control problem without leader's input for general linear MAS. In this section, we extend our analysis to address formation tracking issue with leader's control input $u_0(t)$.

Assumption 2.16 *The leader's control input satisfies $\|u_0(t)\| \leq \epsilon$, where ϵ is a positive constant.*

From the protocol (2.36) in Section 2.4, the following fully distributed adaptive protocol based on the absolute/relative output measurements is proposed as

$$\begin{aligned}
u_i =&K_1 h_i + K_2 v_i - \beta z(B^T S\eta_i),\\
\dot{w}_i =&Aw_i + Bu_i - BK_1 h_i + F[Cw_i - (y_i - Ch_i)],\\
\dot{v}_i =&Av_i + B[u_i - \beta z(B^T Q(\psi_i - \eta_i))] - BK_1 h_i\\
&+ FC(c_i + \rho_i)(\psi_i - \eta_i) + FC(w_i - \bar{x}_i),\\
\dot{c}_i =&(\psi_i - \eta_i)^T C^T \Gamma C(\psi_i - \eta_i), i \in \mathbb{F}
\end{aligned} \tag{2.44}$$

where $c_i(0) \geq 1$, $S > 0$, $\psi_i = \sum_{j=0}^{N} a_{ij}(v_i - v_j), \eta_i = \sum_{j=0}^{N} a_{ij}(w_i - w_j), i \in \mathbb{F}$ and $w_0 = Aw_0 + Bu_0 + F(Cw_0 - y_0), v_0 = 0$. The positive constant β is to be determined later and other parameters are the same as in (2.36) of Section 2.4. The nonlinear function $z(\cdot)$ is defined as

$$z(x) = \begin{cases} \frac{x}{\|x\|} & \text{if } \|x\| \neq 0,\\ 0 & \text{if } \|x\| = 0. \end{cases} \tag{2.45}$$

Similar as in Section 2.4, combine (2.44) with (2.1) then

$$\begin{aligned}
\dot{\hat{x}} =&(I_N \otimes A)\hat{x} + (I_N \otimes BK_2)\psi - (\mathcal{L}_1 \otimes B)(\beta M(\eta) + \mathbf{1} \otimes u_0),\\
\dot{\eta} =&(I_N \otimes A)\eta + (I_N \otimes BK_2)\psi + (I_N \otimes FC)(\eta - \hat{x}) - (\mathcal{L}_1 \otimes B)(\beta M(\eta) + \mathbf{1} \otimes u_0),\\
\dot{\psi} =&[I_N \otimes (A + BK_2)]\psi + [\mathcal{L}_1(\hat{c} + \hat{\rho}) \otimes FC]\varrho + (I_N \otimes FC)(\eta - \hat{x})\\
&+ (\mathcal{L}_1 \otimes FC)[\mathbf{1} \otimes (w_0 - x_0)] - (\mathcal{L}_1 \otimes B)\beta[M(\eta) + Z(\varrho)], i \in \mathbb{F}
\end{aligned} \tag{2.46}$$

where $Z(\varrho) = [z(B^T Q(\psi_1 - \eta_1))^T, \ldots, z(B^T Q(\psi_N - \eta_N))^T]^T$,

$M(\eta) = [z(B^T S\eta_1)^T, \ldots, z(B^T S\eta_N)^T]^T$, and

$$\begin{aligned}\dot{\zeta} =&[I_N \otimes (A + FC)]\zeta,\\ \dot{\varrho} =&[I_N \otimes A + \mathcal{L}_1(\hat{c} + \hat{\rho}) \otimes FC]\varrho + (\mathcal{L}_1 \otimes FC)(\mathbf{1} \otimes \bar{x}_0)\\ &- (\mathcal{L}_1 \otimes B)(\beta Z(\varrho) - \mathbf{1} \otimes u_0),\\ \dot{c}_i =&\varrho_i^T C^T \Gamma C \varrho_i, i \in \mathbb{F}.\end{aligned} \tag{2.47}$$

The following theorem presents a result of designing protocol (2.44) to solve the TVF tracking problem with leader's bounded input under directed topology.

Theorem 2.17 *Suppose Assumptions 2.1, 2.2, 2.6 and 2.16 hold, the fully distributed TVF tracking problem with leader's bounded input is solved under the protocol (2.44) if $A + BK_2$ is Hurwitz, $\Gamma = I$, $F = -Q^{-1}C^T$ and $\rho_i = \varrho_i^T Q \varrho_i$, where $Q > 0$ is a solution to the LMI (2.32). $\beta \geq \epsilon$ and $S > 0$ satisfies*

$$S(A + BK_2) + (A + BK_2)^T S < 0. \tag{2.48}$$

The coupling weight $c_i(t), i \in \mathbb{F}$ converge to some finite steady-state values.

Proof. First, based on the proof of Theorem 2.14, the convergence of ζ in (2.47) is addressed. Then in order to prove $\lim_{t\to\infty} \varrho = 0$, let

$$V_4 = \frac{1}{2}\sum_{i=1}^{N} g_i(2c_i + \rho_i)\rho_i + \frac{1}{2}\sum_{i=1}^{N} g_i(c_i - \alpha)^2 + \gamma \bar{x}_0^T Q \bar{x}_0. \tag{2.49}$$

By choosing the same parameters α and γ as in the proof of Theorem 2.14, we get

$$\dot{V}_4 \leq -\varrho^T[G(\hat{c} + \hat{\rho}) \otimes W]\varrho - \bar{x}_0^T W \bar{x}_0 - 2\varrho^T[G(\hat{c} + \hat{\rho})\mathcal{L}_1 \otimes QB](\beta Z(\varrho) - \mathbf{1} \otimes u_0). \tag{2.50}$$

Note that

$$\begin{aligned}\varrho_i^T QBz(B^T Q\varrho_i) =&\varrho_i^T QB\frac{B^T Q\varrho_i}{\|B^T Q\varrho_i\|} = \|B^T Q\varrho_i\|,\\ \varrho_i^T QBz(B^T Q\varrho_j) \leq&\|\varrho_i^T QB\| \left\|\frac{B^T Q\varrho_j}{\|B^T Q\varrho_j\|}\right\| = \|B^T Q\varrho_i\|,\end{aligned}$$

then

$$\begin{aligned}-\varrho^T[G(\hat{c}+\hat{\rho})\mathcal{L}_1\otimes QB]\beta Z(\varrho) &= -\sum_{i=1}^{N} g_i(c_i+\rho_i)\beta\varrho_i^T QB\\ &\times[\sum_{j=1}^{N} a_{ij}(z(B^TQ\varrho_i)-z(B^TQ\varrho_j))+a_{i0}z(B^TQ\varrho_i)]\\ &\leq -\sum_{i=1}^{N} g_i(c_i+\rho_i)\|B^TQ\varrho_i\|a_{i0}\beta.\end{aligned} \tag{2.51}$$

On the other hand, using $\mathcal{L}_1\mathbf{1}=-\mathcal{L}_2$, we get

$$\begin{aligned}\varrho^T[G(\hat{c}+\hat{\rho})\mathcal{L}_1\otimes QB](\mathbf{1}\otimes u_0) &= \sum_{i=1}^{N} g_i(c_i+\rho_i)\varrho_i^T QBa_{i0}u_0\\ &\leq \sum_{i=1}^{N} g_i(c_i+\rho_i)\|B^TQ\varrho_i\|a_{i0}\epsilon.\end{aligned} \tag{2.52}$$

Substitute (2.51) and (2.52) into (2.50) with $\beta\geq\epsilon$, then

$$\begin{aligned}\dot{V}_4 &\leq -\varrho^T[G(\hat{c}+\hat{\rho})\otimes W]\varrho-\bar{x}_0^TW\bar{x}_0\\ &= -\xi^T(I_{N+1}\otimes W)\xi\leq 0\end{aligned} \tag{2.53}$$

where the last inequality comes from $W=-(QA+A^TQ-2C^TC)>0$ and $\xi=[\varrho^T(\sqrt{G(\hat{c}+\hat{\rho})}\otimes I_n),\bar{x}_0^T]^T$. Similar as the proof in Theorem 2.14, it is easy to verify that $V_4,\varrho_i,\bar{x}_0,c_i$ are bounded and $c_i(t)$ converges to some finite value.

By the definition of ξ and the bounded property of $\varrho_i,\bar{x}_0$, we can get that ξ is bounded. In addition, since $u_0(t)$ is bounded in Assumption 2.16, $\dot{\varrho}$ in (2.47) is bounded, too. Recall that $\dot{\bar{x}}_0=\dot{w}_0-\dot{x}_0=(A+FC)\bar{x}_0$ is also bounded, which furthermore implies that $\dot{\xi}$ is bounded.

Integrate (2.53) then

$$\int_0^\infty \xi^T(I_{N+1}\otimes W)\xi dt\leq V_4(0)-V_4(\infty).$$

Since $V_4(\infty)$ is finite due to $\dot{V}_4\leq 0$ and $V_4(t)>0$, we get that $\int_0^\infty\xi^T(I_{N+1}\otimes W)\xi dt$ has a finite limit.

In fact, $2\xi^T(I_{N+1}\otimes W)\dot{\xi}$ is bounded because of the boundedness of ξ and $\dot{\xi}$, which in turn proves that $\xi^T(I_{N+1}\otimes W)\xi$ is uniformly continuous.

Finally, $\int_0^\infty\xi^T(I_{N+1}\otimes W)\xi dt$ is differentiable and has a finite limit as $t\to\infty$, and $\xi^T(I_{N+1}\otimes W)\xi$ is uniformly continuous. Then by Barbalat's Lemma (Khalil, 1996) we get $\xi^T(I_{N+1}\otimes W)\xi\to 0$ as $t\to\infty$, which means $\lim_{t\to\infty}\xi=0$ such that

$\lim_{t\to\infty}\varrho = 0$.

Next, to prove $\lim_{t\to\infty}\eta = 0$, we consider the following Lyapunov function candidate

$$V_5 = \eta^T(I_N \otimes S)\eta + \gamma_1\zeta^T(I_N \otimes Q)\zeta + \gamma_2 V_4 \tag{2.54}$$

where γ_1, γ_2 are positive constants to be determined later. V_5 is positive definite with respect to $\eta, \zeta, \varrho, c_i$ and $\bar{x}_0$. Combining (2.46) and (2.47), the derivative of V_5 is

$$\begin{aligned}\dot{V}_5 =& -\eta^T(I_N \otimes \bar{W})\eta - \gamma_1\zeta^T(I_N \otimes W)\zeta + 2\eta^T(I_N \otimes SBK_2)\varrho \\ &+ 2\eta^T(I_N \otimes SFC)\zeta - 2\eta^T(L_1 \otimes SB)(\beta M(\eta) + \mathbf{1} \otimes u_0) + \gamma_2\dot{V}_4\end{aligned} \tag{2.55}$$

where $\bar{W} = -[S(A+BK_2)+(A+BK_2)^TS] > 0$ and $W = -(QA+A^TQ-2C^TC) > 0$. Similarly by using Lemma 1.4, we have

$$\begin{aligned}2\eta^T(I_N \otimes SBK_2)\varrho \leq& \frac{1}{4}\eta^T(I_N \otimes \bar{W})\eta + \frac{4\lambda_{max}(K_2^TB^TSSBK_2)}{\lambda_{min}(\bar{W})}\varrho^T\varrho, \\ 2\eta^T(I_N \otimes SFC)\zeta \leq& \frac{1}{4}\eta^T(I_N \otimes \bar{W})\eta + \frac{4\lambda_{max}(K_2^TB^TSSBK_2)}{\lambda_{min}(\bar{W})}\zeta^T\zeta.\end{aligned} \tag{2.56}$$

Due to $c_i(0) \geq 1$, $\dot{c}_i \geq 0$ and $\rho_i = \varrho_i^TQ\varrho_i \geq 0$ we get $(\hat{c}+\hat{\rho}) > I$. Choosing $\gamma_1 \geq \frac{4\lambda_{max}(C^TF^TSSFC)}{\lambda_{min}(\bar{W})\lambda_{min}(W)}, \gamma_2 \geq \frac{4\lambda_{max}(K_2^TB^TSSBK_2)}{\lambda_{min}(\bar{W})\lambda_{min}(W)\lambda_{min}(G)}$ and substituting (2.53), (2.56) into (2.55), we obtain

$$\dot{V}_5 = -\frac{1}{2}\eta^T(I_N \otimes \bar{W})\eta - 2\eta^T(\mathcal{L}_1 \otimes SB)(\beta M(\eta) + \mathbf{1} \otimes u_0). \tag{2.57}$$

Similar as in (2.51) and (2.52), we can prove that

$$-2\eta^T(\mathcal{L}_1 \otimes SB)(\beta M(\eta) + \mathbf{1} \otimes u_0) \leq 0.$$

Finally,

$$\dot{V}_5 = -\frac{1}{2}\eta^T(I_N \otimes \bar{W})\eta \leq 0.$$

Therefore, V_5 is bounded and so is η. It is easy to verify that $\lim_{t\to\infty}\eta = 0$. Due to $\lim_{t\to\infty}\zeta = 0$ and $\hat{x} = \eta - \zeta$, we get $\lim_{t\to\infty}\hat{x} = 0$. Similar as the proof of Theorem 2.14, the distributed adaptive TVF tracking problem considering the leader's bounded input with directed spanning tree topology is solved.

Remark 2.18 *Compared with the previous protocols without leader's input, the nonlinear components $z(B^TS\eta_i)$ and $z(B^TQ\varrho_i)$ in protocol (2.44) are used to deal*

with the leader's bounded input. It is worth noting that the technique utilised in the proof are partially motivated by Lv et al. (2015) where the distributed output feedback consensus problem for general linear MAS has been studied by using a sequential observer design approach.

Remark 2.19 *Since function (2.45) is nonsmooth, the whole control protocol (2.44) is discontinuous dealing with the leader's bounded input $u_0(t)$. In fact, from Section 2.4 to 2.5, we regard $u_0(t)$ as one kind of disturbances and use function (2.45) to compensate it. The discontinuous protocol (2.44) can be modified to be continuous with the following smooth function $z(x)$*

$$z_i(x) = \begin{cases} \frac{x}{\|x\|} & \text{if } \|x\| > \sigma_i, \\ \frac{x}{\sigma_i} & \text{if } \|x\| \leq \sigma_i \end{cases} \tag{2.58}$$

and $\dot{c}_i = (\psi_i - \eta_i)^T C^T \Gamma C(\psi_i - \eta_i) - \varepsilon_i(c_i(t) - 1)$, where $\varepsilon_i, \sigma_i, i \in \mathbb{F}$ are small positive constants. It is worth noting that this modified continuous protocol's control effect will be uniformly ultimately bounded while protocol (2.44) make the TVF tracking error converge to zero asymptotically. Since this chapter focus on proposing the unified framework of TVF control design from undirected to directed topology, from stabilization to tracking and from a leader without input to the one with bounded input $u_0(t)$, we will not go into the proving detail about the modified protocol in this chapter. However, the detail can be referred to Chapter 4.2.

2.6 Simulations

An example is presented to illustrate that the fully distributed adaptive controller (2.44) successfully achieve the TVF tracking with the leader of bounded input. Consider a group of agents consisting of a leader labelled 0 and six followers labelled from 1 to 6, where the communication topology $\mathcal{G}$ is shown in Fig. 2.1(a) satisfying Assumption 2.6. Suppose that the state of agent i in (2.1) is described as $x_i(t) = (x_{i1}(t), \ldots, x_{i6}(t))^T \in \mathbb{R}^6$. A and B in (2.1) are given as

follows

$$A = \begin{bmatrix} 0 & 0 & 0 & 1 & 0 & 0 \\ 0 & 0 & 0 & 0 & 1 & 0 \\ 0 & 0 & 0 & 0 & 0 & 1 \\ -1 & 0 & 0 & 0 & 0 & 0 \\ 0 & -1 & 0 & 0 & 0 & 0 \\ 0 & 0 & -1 & 0 & 0 & 0 \end{bmatrix}, \quad B = \begin{bmatrix} 0 & 0 & 0 \\ 0 & 0 & 0 \\ 0 & 0 & 0 \\ 1 & 0 & 0 \\ 0 & 1 & 0 \\ 0 & 0 & 1 \end{bmatrix}.$$

Choosing $C = [I_5, 0_{5\times 1}]$, then it is easy to verify that (A, B, C) is stabilisable and detectable. Inspired by our previous work (Jiang *et al.*, 2017), definite

$$\begin{aligned} h_{i1} =& - r\cos(wt + (i-1)\pi/3) + r\sin(wt + (i-1)\pi/3), \\ h_{i2} =& 2r\sin(wt + (i-1)\pi/3), \\ h_{i3} =& 2r\cos(wt + (i-1)\pi/3), \\ h_{i4} =& wr\cos(wt + (i-1)\pi/3) + wr\sin(wt + (i-1)\pi/3), \\ h_{i5} =& 2wr\cos(wt + (i-1)\pi/3), \\ h_{i6} =& - 2wr\sin(wt + (i-1)\pi/3),\ i \in \mathbf{I}[1, 6]. \end{aligned}$$

where $r = 2, w = 2$ for followers and $h_i = [h_{i1}, \ldots, h_{i6}]^T$. The TVF shapes for followers are described as the parallel hexagon shape when $t \in [0, 50) \cup [150, 200]$, the parallelogram shape when $t \in [50, 100)$ and the triangle shape when $t \in [100, 150)$ in the following

$$h(t) = \begin{cases} [h_1^T, h_2^T, h_3^T, h_4^T, h_5^T, h_6^T]^T & 0 \le t < 50, \\ [h_1^T, (\frac{h_1+h_3}{2})^T, h_3^T, h_4^T, (\frac{h_4+h_6}{2})^T, h_6^T]^T & 50 \le t < 100, \\ [h_1^T, (\frac{h_1+h_3}{2})^T, h_3^T, (\frac{h_3+h_5}{2})^T, h_5^T, (\frac{h_5+h_1}{2})^T]^T & 100 \le t < 150, \\ [h_1^T, h_2^T, h_3^T, h_4^T, h_5^T, h_6^T]^T & 150 \le t \le 200. \end{cases}$$

It is obvious that $\lim_{t\to\infty} \sum_{i=1}^{6} h_i(t) = 0$, meaning that the six followers will keep TVF shapes around the leader when the desired formation tracking is achieved.

Define the leader's bounded input as $u_0(t) = [e^{-t} + 1, e^{-2t}, 2 + sin(\frac{t}{2})]^T$ and $\beta = 4$. From (1.42) we get

$$K_1 = \begin{bmatrix} -3 & 0 & 0 & 0 & 0 & 0 \\ 0 & -3 & 0 & 0 & 0 & 0 \\ 0 & 0 & -3 & 0 & 0 & 0 \end{bmatrix}.$$

Solving LMI (2.32) gives a solution

$$Q = \begin{bmatrix} 7.314 & -0.000 & -0.000 & -0.000 & 0.000 & 0.000 \\ -0.000 & 7.314 & -0.000 & -0.000 & 0.000 & -0.000 \\ -0.000 & -0.000 & 7.412 & -0.000 & 0.000 & -0.487 \\ -0.000 & -0.000 & -0.000 & 7.314 & -0.000 & -0.000 \\ 0.000 & 0.000 & 0.000 & -0.000 & 7.314 & -0.000 \\ 0.000 & -0.000 & -0.487 & -0.000 & -0.000 & 7.412 \end{bmatrix}.$$

Thus the feedback gain matrix in (2.44) is obtained as

$$F = \begin{bmatrix} -0.1367 & -0.0000 & -0.0000 & -0.0000 & 0.0000 \\ -0.0000 & -0.1367 & -0.0000 & -0.0000 & 0.0000 \\ -0.0000 & -0.0000 & -0.1355 & -0.0000 & 0.0000 \\ -0.0000 & -0.0000 & -0.0000 & -0.1367 & -0.0000 \\ 0.0000 & 0.0000 & 0.0000 & -0.0000 & -0.1367 \\ 0.0000 & -0.0000 & -0.0089 & -0.0000 & -0.0000 \end{bmatrix}.$$

Assign eigenvalue of $A + BK_2$ as $-1, -5, -10 + 10j, -10 - 10j, -20, -50$ with $j^2 = -1$, then

$$K_2 = \begin{bmatrix} -111.3 & 21.8 & 10.7 & -13.8 & -11.3 & -11.0 \\ 56.3 & -159.0 & -10.9 & -1.8 & -25.5 & -2.5 \\ 107.6 & -78.1 & -71.1 & 29.2 & -32.4 & -56.7 \end{bmatrix}.$$

Substituting K_2 into (2.48), we get

$$S = \begin{bmatrix} 2319.3 & -422.9 & -383.7 & 21.1 & -7.4 & 21.7 \\ -422.9 & 2453.7 & 186.0 & -11.3 & 9.3 & -16.2 \\ -383.7 & 186.0 & 1167.9 & -6.1 & 3.1 & 3.9 \\ 21.1 & -11.3 & -6.1 & 24.6 & -0.7 & -0.2 \\ -7.4 & 9.3 & 3.1 & -0.7 & 19.5 & -1.0 \\ 21.7 & -16.2 & 3.9 & -0.2 & -1.0 & 16.9 \end{bmatrix}.$$

Set the initial states $x_{ij}(0) = 10\delta - 5, c_i(0) = 2\delta + 1, i, j = 1, \ldots, 6$ for followers and $x_{0j}(0) = 10\delta - 5, j = 1, \ldots, 6$ for the leader, where δ is a pseudorandom value with a uniform distribution on the interval $(0, 1)$.

The coupling weights shown in Fig. 2.1(b) converge to some finite values. Fig. 2.2(a) shows the TVF tracking error $x_i - h_i - x_0$, meaning that the output TVF tracking problem is indeed solved. Fig. 2.2(b) describes the leader's state estimation error $\bar{x}_0 = w_0 - x_0$ (top) and followers' formation stabilization estimation error $w_i - \bar{x}_i$, respectively, which means the distributed observers are designed correctly. Fig. 2.3 depicts the position snapshots of followers and the

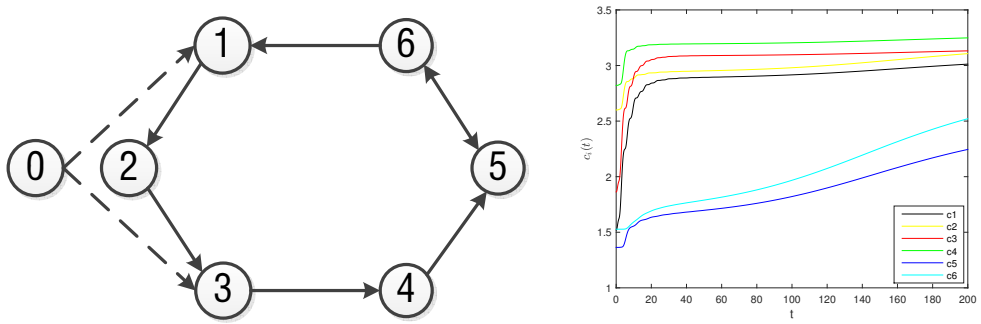

(a) (b)

Figure 2.1: (a) The communication topology $\mathcal{G}$; (b)The coupling weights $c_i(t)$.

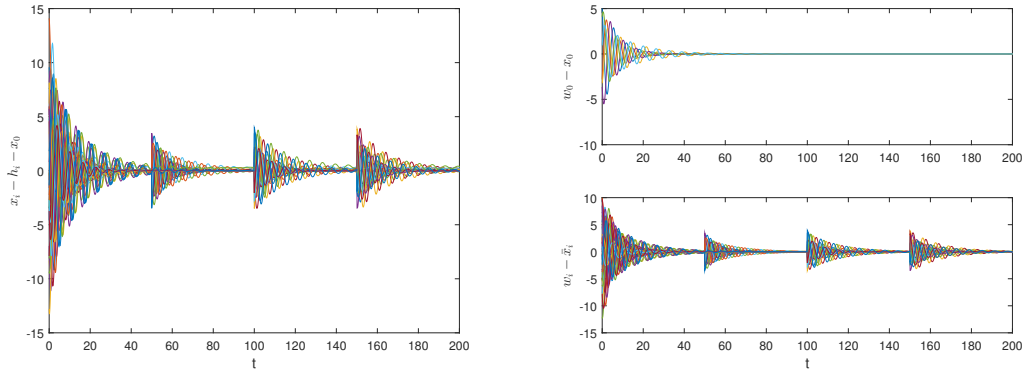

(a) $\tilde{x}_i = x_i - h_i - x_0$. (b) $\bar{x}_0 = w_0 - x_0$ (top) and $w_i - \bar{x}_i$ (bottom).

Figure 2.2: The control errors.

leader at different timestamps. Six followers form formation shapes with random initial positions and keep tracking the leader which is located at the shape center at the same time. The TVF shapes change from parallel hexagon to parallelogram, then triangle and finally back to parallel hexagon. From $t = 199s$ and $t = 200s$, we can see the shape keeps rotating around the leader, which means it is time-varying. The leader's trajectory is time-varying as well. It is worth noting that the presented results can be applied to target enclosing problems with regarding the leader as the target.

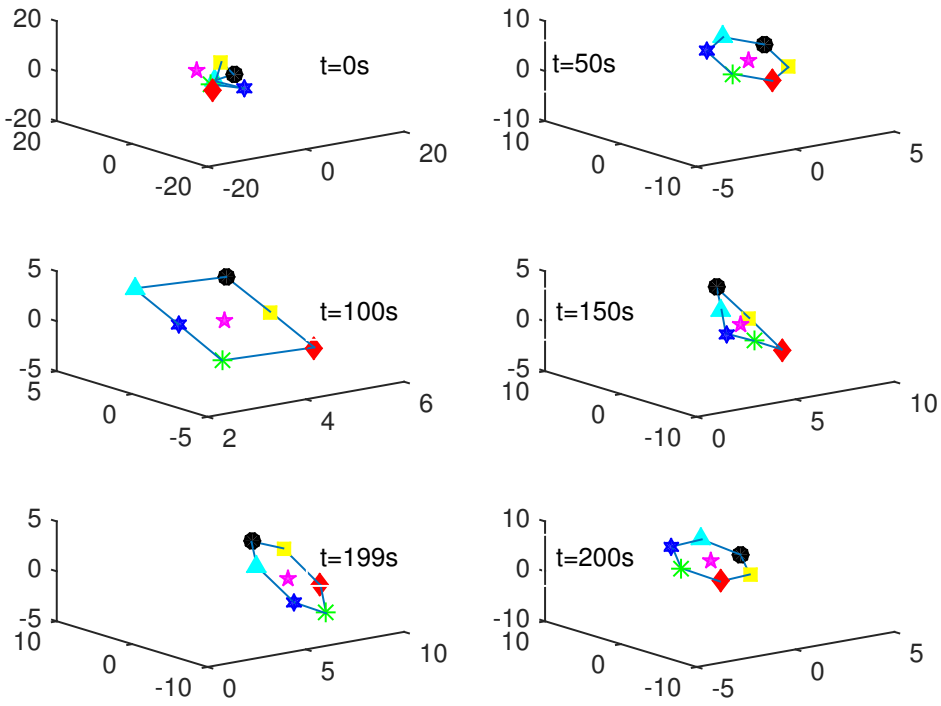

Figure 2.3: Position snapshots of six followers (circle, square, diamond, asterisk, hexagon, triangle) and the leader (pentagram) forming the shape from parallel hexagon to parallelogram, then triangle and finally back to parallel hexagon.

2.7 Summary

Contributions

- √ Demonstration of the unified framework of TVF control protocol design from undirected to directed topology, from formation stabilization to tracking, and from with a leader of no input to with one of bounded input whose information is only available to a small subset of followers.
- √ Presentation of fully distributed adaptive observer-type protocols design for TVF control problems.
- √ Use of the absolute/relative output measurements designing protocols, more available in practice compared with absolute/relative state ones.

Chapter 3

Heterogeneous formation-containment

Contents

This chapter addresses the distributed time-varying formation-containment (FC) control problem for heterogeneous general linear MASs (the virtual leader, multi-leaders and followers in Fig. 3.1) based on the output regulation framework from an observer viewpoint under the directed topology which contains a spanning tree. All agents can have different dynamics and different state dimensions. A new format of TVF shape is proposed. The multi-leaders are required to achieve the TVF with tracking the virtual leader whose output is only available to a subset of them, and only need to send the information of their designed observers and TVF shapes to their neighboring followers. A new class of distributed adaptive observer-based controllers is designed with the mild assumption that both leaders and followers are introspective (i.e., agents have knowledge of their own outputs). The simulation to multiple mobile robot systems is also provided to verify the effectiveness of theoretical results.

Specifically, a new definition of TVF shape for heterogeneous MASs is proposed. Then, the protocol which consists of the fully distributed adaptive observer and

Luenberger observer, is firstly designed to solve the TVF tracking problem in Section 3.1. After that, the link to the extension of heterogeneous FC control is further discovered in Section 3.2. To our best knowledge, this is the first work designing the fully distributed controllers with the proposition of a new format of TVF shape, to address the TVF tracking and time-varying FC control problems for heterogeneous general linear MASs. Main contributions can be stated as follows:

- A new format of TVF shape is proposed for heterogeneous MASs.
- This chapter reveals the essence of linking the TVF tracking and containment control together to achieve the heterogeneous FC control.
- Compared with the latest results in Wang *et al.* (2017f) and Wang *et al.* (2018c) where parameters need to be chosen based on the Laplacian matrix and the TVF shape has to be designed based on the virtual leader's dynamics, the controllers here are fully distributed and the TVF shape can be designed independently.
- Different from heterogeneous containment control results (Chu *et al.*, 2016, Haghshenas *et al.*, 2015) with identical leaders or result (Zheng & Wang, 2014) with both identical leaders and identical followers, each agent in our system can have different dynamics.
- For heterogeneous MASs, the communication topology here is directed satisfying Assumption 3.7, which is an improvement compared with Rahimi *et al.* (2014) where the virtual leader needs to send its information to all followers, Haghshenas *et al.* (2015) that is directed and strongly connected among followers, Wang *et al.* (2017f) that is undirected and connect among followers, or Wang *et al.* (2017e) and Wang *et al.* (2018c) that are undirected among leaders and followers.

Since there are many variables in this chapter, some may coincide with those in the previous chapter. Fortunately, these variables will be defined clearly here.

In this chapter, the $N+L$ non-identical general linear dynamics is the same as in (1.45). For reading convenience, we rewrite it here:

$$\begin{array}{rcl} \dot{x}_i(t) & = & A_i x_i(t) + B_i u_i(t), \\ y_i(t) & = & C_i x_i(t), \quad i \in \mathbf{I}[1, N+L] \end{array} \tag{3.1}$$

where $x_i(t) = [x_{i1}(t), \ldots, x_{in_i}(t)]^T \in \mathbb{R}^{n_i}$, $u_i(t) \in \mathbb{R}^{p_i}$ and $y_i(t) \in \mathbb{R}^q$ are the state, control input and measured output of the i-th agent, respectively. $A_i \in \mathbb{R}^{n_i \times n_i}$, $B_i \in \mathbb{R}^{n_i \times p_i}$ and $C_i \in \mathbb{R}^{q \times n_i}$ are constant matrices.

Without loss of generality, suppose that agents in (3.1) indexed by $1, \ldots, N$ are the leaders denoted as $\mathbb{L} \triangleq \{1, \ldots, N\}$, and agents indexed by $N+1, \ldots, N+L$

are the followers denoted as $\mathbb{F} \triangleq \{N+1, \ldots, N+L\}$. The virtual leader indexed by 0 provides motion reference information followed by leaders, and its dynamics is the same as in (1.46):

$$\dot{x}_0(t) = A_0 x_0(t), \; y_0(t) = C_0 x_0(t) \tag{3.2}$$

where $A_0 \in \mathbb{R}^{n\times n}, C_0 \in \mathbb{R}^{q\times n}$, and $x_0(t) \in \mathbb{R}^n$, $y_0(t) \in \mathbb{R}^q$ are the state and output of the virtual leader, respectively. Note that only a small subset of leaders can get information from the virtual leader.

Assumption 3.1 *(A_i, B_i, C_i), $i \in \boldsymbol{I}[1, N+L]$ are stabilizable and detectable. (A_0, C_0) is detectable.*

Remark 3.2 *Here for the heterogeneous linear MASs, the virtual leader's dynamics in the output FC control has the same formulation as the **virtual exosystem** generated by the internal model (A_0, C_0) in the output synchronization (Wieland et al., 2011) or as the **exosystem** in classical output regulation. Since the leaders will form a shape to move and the followers will achieve the containment control, for the naming convenience, we name the dynamics (3.2) as the virtual leader which will provide the reference trajectory for leaders to achieve formation tracking. Besides, the leader is considered without the control input $u_0(t)$, which is a common assumption in consensus tracking problems (Cai et al., 2017, Wu et al., 2017, Yaghmaie et al., 2016, Zhang et al., 2018b).*

The TVF shape information $h(t)$ for the heterogeneous MAS is proposed in Chapter 1.6.2. For reading convenience, we rewrite it here:

$$\dot{h}_i(t) = A_h h_i(t), \; i \in \mathbb{L} \tag{3.3}$$

where $A_h \in \mathbb{R}^{n\times n}$ satisfying

$$\begin{array}{rcl} X_{hi} A_h &=& A_i X_{hi} + B_i U_{hi}, \\ C_0 &=& C_i X_{hi}, \quad i \in \mathbb{L} \cup \mathbb{F}. \end{array} \tag{3.4}$$

Remark 3.3 *We propose a new format of TVF shape for heterogeneous MASs. When A_h is designed, (X_{hi}, U_{hi}) is the solution of (3.4). Note that A_h is different from A_0 which is a big improvement compared with existing works.*

Definition 3.4 (Rockafellar (2015)) *A set $K \subset \mathbb{R}^q$ is said to be convex if $(1-\delta)x + \delta y \in K$ whenever $x \in K, y \in K$ and $0 < \delta < 1$. The convex hull of a finite set of points $y_i, i \in \boldsymbol{I}[1,N]$ is the minimal convex set containing all points $y_i, i \in \boldsymbol{I}[1,N]$, denoted by $co(y_l) = col\{y_1, \ldots, y_N\}$. Particularly, $co(y_l) = \left\{\sum_{i=1}^N \alpha_i y_i | \alpha_i \in \mathbb{R}, \alpha_i \geq 0, \sum_{i=1}^N \alpha_i = 1\right\}$.*

Similar as Definition 1.14, The definition of output FC control of heterogeneous MAS is given as follows.

Definition 3.5 *Heterogeneous MASs (3.1) is said to achieve output time-varying FC control if for any given initial states $x_i(0), i \in \mathbb{L} \cup \mathbb{F} \cup \{0\}$, there exists*

$$\lim_{t\to\infty} \|y_i(t) - y_0(t) - C_0 h_i(t)\| = 0, i \in \mathbb{L}, \tag{3.5}$$

$$\lim_{t\to\infty} \inf_{y \in co(y_l)} \|y_i(t) - y\| = 0, i \in \mathbb{F}. \tag{3.6}$$

Remark 3.6 *Since the MAS is non-identical and in particular, each agent may have different state dimensions, we cannot expect to achieve the state FC control. The output FC control scenario is shown in Fig. 3.1 as an example. Followers move inside the convexed hull (here is an octagon) formed by multi-leaders which are influenced by the virtual leader to achieve the TVF tracking. $C_0 h_i(t)$ denotes the desired relative offset vector of $y_i(t)$ relative to $y_0(t)$. In Fig. 3.1, the leader i rotates around the virtual leader, and its reference trajectory comes from the virtual leader's output and $C_0 h(t)$, i.e., $y_0(t) + C_0 h_i(t), i \in \mathbb{L}$. From (3.2) and (3.3), we can see both the virtual leader and the relative distance is time-varying.*

As the virtual leader's information is only accessible to a subset of leaders, without loss of generality, inspired by Li *et al.* (2016), assume that leaders indexed by $1, \ldots, M (1 \leq M \leq N)$ (named *informed leaders*: ILs) have direct access to the virtual leader and the rest (named *uninformed leaders*: ULs) do not.

Assumption 3.7 *For each UL $i, i \in \boldsymbol{I}[M+1, N]$, there exists at least one IL $i, i \in \boldsymbol{I}[1, M]$ which has a direct path to that UL. And for each follower $i, i \in \mathbb{F}$, there exists at least one leader $i, i \in \mathbb{L}$ which has a direct path to that follower.*

In the case of only one IL, the Assumption 3.7 means the graph $\mathcal{G}$ is a directed spanning tree with the IL acting as the root node. In order to decrease the number of communication channels, and thanks to the accessibility of IL $i, i \in \mathbf{I}[1, M]$ to

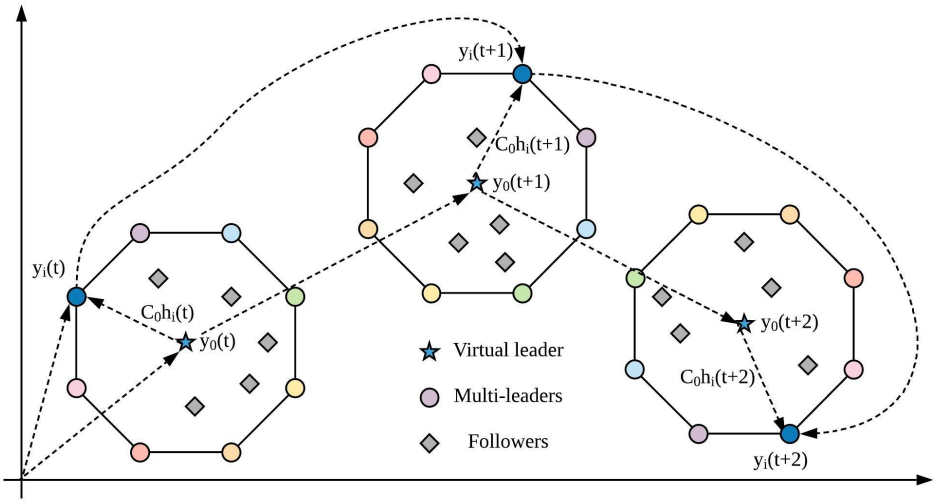

Figure 3.1: An example of the FC control for timestamps $t, t+1, t+2$ (TVF tracking for multi-leaders and containment for followers).

the virtual leader, we assume that ILs do not receive information from other agents. Then the Laplacian matrix of $\mathcal{G}$ can be partitioned as

$$\mathcal{L} = \begin{bmatrix} 0_{M\times M} & 0_{M\times(N-M)} & 0_{N\times L} \\ \mathcal{L}_2 & \mathcal{L}_1 & \\ & \mathcal{L}_3 & \mathcal{L}_4 \end{bmatrix}, \tag{3.7}$$

where $\mathcal{L}_1 \in \mathbb{R}^{(N-M)\times(N-M)}, \mathcal{L}_2 \in \mathbb{R}^{(N-M)\times M}, \mathcal{L}_3 \in \mathbb{R}^{L\times N}, \mathcal{L}_4 \in \mathbb{R}^{L\times L}$. Under Assumption 3.7, all the eigenvalues of $\mathcal{L}_1, \mathcal{L}_4$ have positive real parts. It is also easy to confirm that both $\mathcal{L}_1$ and $\mathcal{L}_4$ are nonsingular M-matrices Qu (2009).

Lemma 3.8 (Qu (2009), Theorem 4.25) *For the nonsingular M-matrices $\mathcal{L}_1, \mathcal{L}_4$, there exist positive diagonal matrices $G \triangleq \mathrm{diag}\{\bar{g}_1\}^{-1}, G' \triangleq \mathrm{diag}\{\bar{g}_2\}^{-1}$ such that $G\mathcal{L}_1 + \mathcal{L}_1^T G > 0$ and $G'\mathcal{L}_4 + \mathcal{L}_4^T G' > 0$ where $\bar{g}_1 = [g_{M+1}, \ldots, g_N]^T = \mathcal{L}_1^{-1}\mathbf{1}_{N-M}, \bar{g}_2 = [g_{N+1}, \ldots, g_{N+L}]^T = \mathcal{L}_4^{-1}\mathbf{1}_L$.*

Since the leaders only get information from neighboring leaders or the virtual leader, It is natural to research the heterogeneous TVF control first, then extend to FC case.

3.1 Heterogeneous TVF control

Hereafter, the variable t will be omitted, e.g., $x = x(t)$ if there is no confusion. To achieve the TVF with tracking the virtual leader, from $y_i - y_0 - C_0 h_i = y_i - C_0(h_i + x_0)$ in (3.5), we see that every leader requires the virtual leader's state information x_0 for the feedback control. To accomplish this goal, the observer $v_i \in \mathbb{R}^n$ is utilized to estimate the x_0 information. Denote the observer error as $\tilde{v}_i = v_i - x_0, i \in \mathbb{L}$.

For ILs, the following Luenberger-like observer is designed

$$\dot{v}_i = A_0 v_i + F(y_0 - C_0 v_i), i \in \mathbf{I}[1, M]. \tag{3.8}$$

It is easy to get $\dot{\tilde{v}}_i = (A_0 - FC_0)\tilde{v}_i$. By using the pole placement method in linear control theory to get the feedback gain matrix $F \in \mathbb{R}^{n\times q}$ such that $A_0 - FC_0$ is Hurwitz, we get that $\lim_{t\to\infty} \tilde{v}_i = 0, i \in \mathbf{I}[1, M]$.

For ULs, the fully distributed adaptive observer is established as follows:

$$\begin{aligned} \dot{v}_i =& A_0 v_i + K(c_i + \rho_i)\eta_i, \\ \dot{c}_i =& \eta_i^T \Gamma \eta_i, i \in \mathbf{I}[M+1, N] \end{aligned} \tag{3.9}$$

where $\eta_i = \sum_{j=1}^{N} a_{ij}(v_i - v_j),$, c_i denotes the time-varying coupling weight associated with the i-th uninformed leader, $K \in \mathbb{R}^{n\times n}, \Gamma \in \mathbb{R}^{n\times n}$ are the feedback gain matrices to be determined and so is $\rho_i(\cdot)$.

Lemma 3.9 *Suppose Assumptions 3.1-3.7 hold and $c_i(0) > 0, i \in \boldsymbol{I}[M+1, N]$. Then, the observer error $\lim_{t\to\infty} \tilde{v}_i = \lim_{t\to\infty}(v_i - x_0) = 0, i \in \mathbb{L}$ if F in (3.8) is chosen such that $A_0 - FC_0$ is Hurwitz, $\rho_i = \eta_i^T P \eta_i, i \in \boldsymbol{I}[M+1, N]$ in (3.9), $K = -P, \Gamma = P^2$ and $P > 0$ is a solution to the algebraic Riccati equation (ARE)*

$$A_0^T P + P A_0 - P^2 + I_n = 0. \tag{3.10}$$

Moreover, $c_i(t)$ converge to some finite steady-state values.

Proof. See the Appendix.

Remark 3.10 *Lemma 3.9 shows that the observers (3.8) and (3.9) can estimate x_0 to make leaders achieve TVF tracking under the directed graph satisfying Assumption 3.7. The observer (3.9) always exists since the ARE (3.10) has a unique solution $P > 0$ based on the reality that (A_0, I_n) is controllable. It is worth mentioning that the technique used in this proof is partially motivated by Li et al.*

(2016) where the cooperative output regulation problem for MASs has been studied by designing an observer which can be viewed as $\dot{v}_i = A_0 v_i + (c_i + \rho_i)\eta_i$ *in this note. The difference is that we add an important parameter* $K = -P$ *in* (3.9). *The proof is different and, is explained more clearly thanks to* K. *What is more, the new format of TVF shape* $h_i(t)$ *in* (3.3) *is also proposed, which is not covered in Li* et al. *(2016).*

Remark 3.11 *If we do not separate the leaders as ILs and ULs, then another observer can be designed as follows:*

$$\begin{aligned}\dot{v}_i =& A_0 v_i + K(c_i + \rho_i) C_0 \eta_i,\\ \eta_i =& \sum_{j=1}^{N} a_{ij}(v_i - v_j) + a_{i0}(v_i - x_0(t)),\\ \dot{c}_i =& \eta_i^T \Gamma \eta_i, \rho_i = \eta_i^T P \eta_i, i \in \boldsymbol{I}[1, N]\end{aligned} \tag{3.11}$$

to estimate x_0 *for all multiple leaders. The difference is that compared with the Luenberger-like observer* (3.8), *this observer* (3.11) *for the IL* $i, i \in \boldsymbol{I}[1, M]$ *is more complicated. Another disadvantage is that the virtual leader's state* x_0 *rather than output* y_0, *is needed for observer construction. This is the reason we choose the setting of ILs and ULs for the system* (3.1).

At this stage, we have $\lim_{t\to\infty} v_i = \lim_{t\to\infty} x_0, i \in \mathbb{L}$. To solve the heterogeneous TVF control problem, the following proof is based on the classic output regulation theory for which some assumptions are stated out as in Almeida *et al.* (2014), Haghshenas *et al.* (2015) and Li *et al.* (2016).

Assumption 3.12 $Re(\lambda) \geq 0, \forall\, \lambda \in \sigma(A_0)$, *where* $\sigma(A_0)$ *denotes the spectrum of* A_0.

Assumption 3.13 *There exist solutions* $(X_i \in \mathbb{R}^{n_i \times n}, U_i \in \mathbb{R}^{p_i \times n})$ *for the following regulation equation for each agent* i*:*

$$\begin{aligned} X_i A_0 &= A_i X_i + B_i U_i,\\ C_0 &= C_i X_i. \end{aligned} \tag{3.12}$$

Remark 3.14 *Assumption 3.12 is made without loss of generality (see Huang, 2004, Remark 1.3). The leader cannot affect the dynamic behavior of system* (3.1)

asymptotically if $Re(\lambda) < 0$. *The solvability of the regulation function in Assumption 3.12 is guaranteed if rank* $\begin{bmatrix} A_i - \lambda I & B_i \\ C_i & 0 \end{bmatrix} = n_i + q, \forall \lambda \in \sigma(A_0)$ *(see Huang, 2004, Theorem 1.9).*

Here we assume that each leader $i, i \in \mathbb{L}$ is introspective as termed in Peymani *et al.* (2014), which means each one has access to its own output. Then the control input is designed as

$$\begin{aligned} u_i =& K_{1i}\hat{v}_i + K_{2i}v_i + K_{3i}h_i, \\ \dot{\hat{v}}_i =& A_i\hat{v}_i + B_iu_i + F_i(y_i - C_i\hat{v}_i), i \in \mathbb{L} \end{aligned} \tag{3.13}$$

where the observer $\hat{v}_i \in \mathbb{R}^{n_i}$ is used to estimate the leader's state x_i. K_{1i}, K_{2i}, K_{3i} and F_i are the gain matrices to be determined later. Denote $A = \text{diag}\{A_1, \ldots, A_N\}$ and the same to B, C, K_1, K_2, K_3.

Theorem 3.15 (Jiang *et al.* (2018c)) *Suppose Assumptions 3.1, 3.7, 3.12 and 3.13 hold and* $c_k(0) > 0, k \in \boldsymbol{I}[M+1, N]$. *For any initial states* $x_j(0), j \in \mathbb{L} \cup \{0\}$, *the heterogeneous TVF tracking problem for leaders is solved by the fully distributed controller (3.13), and observers (3.8), (3.9) constructed by Lemma 3.9, if* F_i, K_{1i} *are chosen such that* $A_i - F_iC_i, A_i + B_iK_{1i}$ *are Hurwitz and* $K_{2i} = U_i - K_{1i}X_i, K_{3i} = U_{hi} - K_{1i}X_{hi}$, *where* $(X_{hi}, U_{hi}), (X_i, U_i), i \in \mathbb{L}$ *are the solutions of (3.4) and (3.12).*

Proof. See the Appendix.

Remark 3.16 *Here, using the cooperative output regulation framework allows us to consider heterogeneous systems. In contrast to the homogeneous formation protocols in Antonelli* et al. *(2014), Dong & Hu (2016), Dong* et al. *(2017), Ghommam* et al. *(2016) which require the knowledge of graph information or system's total robot number, the protocols (3.8), (3.9) and (3.13) in this note depend only on agent dynamics and its own output, and thereby is fully distributed. Compared with the heterogeneous time-invariant formation stabilization control Peymani* et al. *(2014), our case deals with TVF tracking task, which is a higher level. And the communication burden is less heavier than the heterogeneous TVF tracking results Rahimi* et al. *(2014) where all followers need the virtual leader's position and velocity information. It is worth noting that the result of this section can be regarded as the solution to the heterogeneous TVF tracking control problem.*

3.2 Heterogeneous time-varying FC control

From Assumption 3.7, there exists at least one leader $i, i \in \mathbb{L}$ that has a direct path to follower $i, i \in \mathbb{F}$. Then,

Lemma 3.17 (Wen *et al.* (2016)) *Based on Assumption 3.7, all the eigenvalues of $\mathcal{L}_4$ have positive real parts, each entry of $-\mathcal{L}_4^{-1}\mathcal{L}_3$ is nonnegative, and each row sum of $-\mathcal{L}_4^{-1}\mathcal{L}_3$ equals to one.*

From Definition 3.4 and based on Lemma 3.17, the leaders' convex hull can be represented as $co(y_l) = (-\mathcal{L}_4^{-1}\mathcal{L}_3 \otimes I_q)y_l, y_l = [y_1^T, \ldots, y_N^T]^T$. Due to the TVF tracking error $\lim_{t\to\infty} e = 0 \Rightarrow \lim_{t\to\infty} y_l = (I \otimes C_0)(h + \mathbf{1} \otimes x_0)$ in (3.32) of Theorem 3.15, from (3.6) we find that $(-\mathcal{L}_4^{-1}\mathcal{L}_3 \otimes I_n)(h + \mathbf{1} \otimes x_0)$ is vital for followers to achieve containment.

The idea is to design another two observers to estimate $(-\mathcal{L}_4^{-1}\mathcal{L}_3 \otimes I_n)(\mathbf{1} \otimes x_0)$ and $(-\mathcal{L}_4^{-1}\mathcal{L}_3 \otimes I_n)h$, respectively. So the following fully distributed adaptive observer $w_i \in \mathbb{R}^n$ is proposed to estimate the $(-\mathcal{L}_4^{-1}\mathcal{L}_3 \otimes I_n)(\mathbf{1} \otimes x_0)$ information

$$\begin{aligned} \dot{w}_i =& A_0 w_i + K^{'}(d_i + \varrho_i)\theta_i, \\ \dot{d}_i =& \theta_i^T \Gamma^{'} \theta_i,\ i \in \mathbb{F} \end{aligned} \tag{3.14}$$

where $\theta_i = \sum_{j=1}^{N} a_{ij}(w_i - v_j) + \sum_{j=N+1}^{N+L} a_{ij}(w_i - w_j)$. d_i denotes the time-varying coupling weight associated with the i-th follower, $K^{'} \in \mathbb{R}^{n\times n}, \Gamma^{'} \in \mathbb{R}^{n\times n}$ and $\varrho_i(\cdot)$ are to be determined. From $\theta_i = \sum_{j=1}^{N} l_{ij}v_j + \sum_{j=N+1}^{N+L} l_{ij}w_j$, we have,

$$\theta = (\mathcal{L}_3 \otimes I_n)v + (\mathcal{L}_4 \otimes I_n)w \tag{3.15}$$

where $w = [w_{N+1}^T, \ldots, w_{N+L}^T]^T$. Since $\lim_{t\to\infty} v = \mathbf{1} \otimes x_0$ in Lemma 3.9 and $\mathcal{L}_4$ is nonsingular, then we have $\lim_{t\to\infty} w = (-\mathcal{L}_4^{-1}\mathcal{L}_3 \otimes I_n)(\mathbf{1} \otimes x_0)$ if and only if $\lim_{t\to\infty} \theta = 0$.

To this end, the objective is to prove $\lim_{t\to\infty} \theta = 0$.

Lemma 3.18 *Suppose Assumptions 3.1,3.7 hold and $d_i(0) > 0$. Then, the followers' observers $\lim_{t\to\infty} w = (-\mathcal{L}_4^{-1}\mathcal{L}_3 \otimes I_n)(\boldsymbol{1} \otimes x_0)$ if $\varrho_i = \theta_i^T P \theta_i, i \in \mathbb{F}$, $K^{'} = -P, \Gamma^{'} = P^2$ and $P > 0$ is a solution to the ARE (3.10). Moreover, the coupling weights $d_i(t)$ converge to some finite steady-state values.*

Proof. See the Appendix.

Another fully distributed adaptive observer $\hat{h}_i \in \mathbb{R}^n$ is proposed to estimate the $(-\mathcal{L}_4^{-1}\mathcal{L}_3 \otimes I_n)h$ as follows:

$$\begin{aligned}\dot{\hat{h}}_i =& A_h\hat{h}_i + K''(d_i' + \varrho_i')\theta_i',\\ \dot{d}_i' =& \theta_i'^T\Gamma''\theta_i',\ i \in \mathbb{F}\end{aligned} \tag{3.16}$$

where $\theta_i' = \sum_{j=1}^{N} a_{ij}(\hat{h}_i - h_j) + \sum_{j=N+1}^{N+L} a_{ij}(\hat{h}_i - \hat{h}_j)$.

Lemma 3.19 *Suppose Assumptions 3.1,3.7 hold and $d_i'(0) > 0$. Then, the followers' observers $\lim_{t\to\infty}\hat{h} = (-\mathcal{L}_4^{-1}\mathcal{L}_3 \otimes I_n)h$ if $\varrho_i' = \theta_i'^T P'\theta_i', i \in \mathbb{F}$, $K'' = -P', \Gamma'' = P'^2$ and $P' > 0$ is a solution to the following ARE:*

$$A_h^T P' + P' A_h - P'^2 + I_n = 0. \tag{3.17}$$

Proof. The proof is similar as the proof of Lemma 3.18 and is omitted here.

Remark 3.20 *The reason we design two observers w_i and $\hat{h}_i$ is that the matrices A_0 and A_h are different.*

Finally, we come to solve the heterogeneous FC control problem. Similar as the protocol (3.13) , followers are assumed to be introspective and the distributed protocol is provided as

$$\begin{aligned}u_i =& K_{1i}\hat{w}_i + K_{2i}w_i + K_{3i}\hat{h}_i,\\ \dot{\hat{w}}_i =& A_i\hat{w}_i + B_iu_i + F_i(y_i - C_i\hat{w}_i), i \in \mathbb{F}\end{aligned} \tag{3.18}$$

where $\hat{w}_i$ is used to estimate the follower's state x_i and $K_{1i}, K_{2i}, K_{3i}, F_i, i \in \mathbb{F}$ are similar as those in (3.13). Denote $\bar{K}_1 = \text{diag}\{K_{1(N+1)}, \ldots, K_{1(N+L)}\}$ and $\bar{K}_2, \bar{K}_3$ are similar. $\bar{A} = \text{diag}\{A_{N+1}, \ldots, A_{N+L}\}$ and $\bar{B}, \bar{C}$ are similar.

Theorem 3.21 (Jiang *et al.* (2018c)) *Consider Assumptions 3.1, 3.7, 3.12 and 3.13 hold and $c_k(0) > 0, k \in \boldsymbol{I}[M+1, N], d_m(0) > 0, d_m'(0) > 0, m \in \mathbb{F}$. Based on Theorem 3.15, for any initial states $x_j(0), j \in \mathbb{L}\cup\mathbb{F}\cup\{0\}$, the heterogeneous output time-varying FC control problem is solved by the controller (see Fig. 3.2) consisting of the input (3.18) and the fully distributed observers (3.14) and (3.16) constructed in Lemma 3.18 and 3.19, if $A_i - F_iC_i, A_i + B_iK_{1i}$ are Hurwitz, $K_{2i} = U_i - K_{1i}X_i, K_{3i} = U_{hi} - K_{1i}X_{hi}$, where $(X_{hi}, U_{hi}), (X_i, U_i), i \in \mathbb{L}\cup\mathbb{F}$ are solutions of (3.4) and (3.12).*

Proof. See the Appendix.

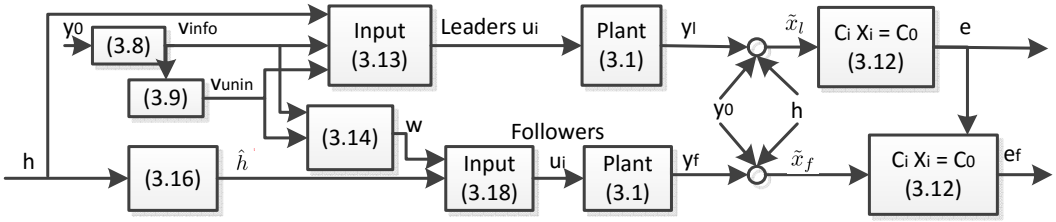

Figure 3.2: Block diagram of the FC controller (variables from the proofs).

Remark 3.22 *In contrast to the latest results Wang* et al. *(2017f) and Wang* et al. *(2018c) in which the protocols are not fully distributed with undirected communication topology among followers to address heterogeneous FC control problem, a distinctive feature of our whole controller here is that protocols are fully distributed under the directed topology.*

Remark 3.23 *The whole picture is that leaders achieve TVF tracking without any influence from followers, and only send their observer states v_i and TVF shape information $h_i, i \in \mathbb{L}$ to their neighboring followers which can move inside the convex hull $co(y_l)$ spanned by leaders. In essence, the protocols* (3.14) *and* (3.16) *reveal how the TVF tracking and containment link together to achieve the FC control.*

3.3 Simulations

The effectiveness of the proposed theories is proved in this section by two numerical examples. The first example is to show that the fully distributed het-

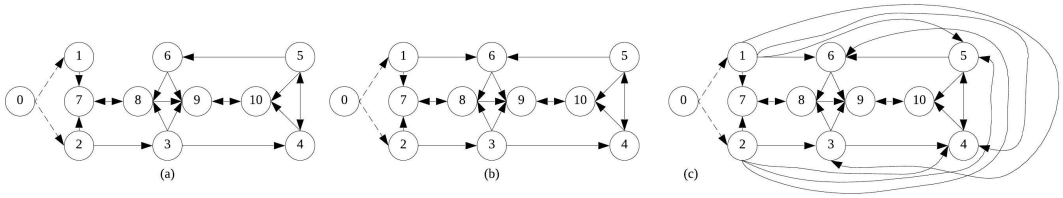

Figure 3.3: Three different graphs of FC control.

erogeneous time-varying FC problem has been successfully solved where all agents can have different dynamics. Then, an application to two different types of mobile robots is provided in the second example.

Example 1. Denote $M = 2, N = 6, L = 4$ and the communication topology $\mathcal{G}$ is shown in Fig. 3.3 satisfying Assumption 3.7. Consider the following different dynamics with different dimensions as

$$\begin{aligned}
&A_i^{'} = \begin{bmatrix} 0 & 1 \\ a(i) & b(i) \end{bmatrix}, B_i^{'} = \begin{bmatrix} d(i) & 0 \\ 0 & d(i+1) \end{bmatrix}, C_i^{'} = \begin{bmatrix} 1 & 0 \\ 0 & 1 \end{bmatrix}, \\
&A_i^{''} = \begin{bmatrix} 0 & 1 & 0 \\ 0 & 0 & 1 \\ 0 & a(i) & d(i) \end{bmatrix}, B_i^{''} = \begin{bmatrix} b(i) & 0 & 0 \\ 0 & b(i+1) & 0 \\ 0 & 0 & b(i) \end{bmatrix}, \\
&C_i^{''} = \begin{bmatrix} 1 & 0 & 0 \\ 0 & 1 & 0 \end{bmatrix}, C_i^{''''} = \begin{bmatrix} 1 & 0 & 0 & 0 \\ 0 & 1 & 0 & 0 \end{bmatrix}, \\
&A_i^{''''} = \begin{bmatrix} 0 & 1 & 0 & 0 \\ 0 & 0 & 1 & 0 \\ 0 & 0 & 0 & 1 \\ 0 & a(i) & b(i) & d(i) \end{bmatrix}, B_i^{''''} = \begin{bmatrix} b(i) & 0 & 0 & 0 \\ 0 & b(i+1) & 0 & 0 \\ 0 & 0 & c(i) & 0 \\ 0 & 0 & 0 & c(i+1) \end{bmatrix},
\end{aligned} \tag{3.19}$$

where $a = [1, 2, 3, 4, 5, 6]^T$, $b = [1, 2, 2, 4, 4, 8, 10]^T$, $c = [2, 4, 5, 6, 8, 10, 1]^T$ and $d = [2, 2, 4, 5, 1, 8, 6]^T$. The corresponding states are described as $x_i^{'} \in \mathbb{R}^2$, $x_i^{''} \in \mathbb{R}^3$ and $x_i^{''''} \in \mathbb{R}^4$. Choose the dynamics of leaders as $A_1 = A_1^{''}, A_2 = A_2^{'}, A_3 = A_3^{'}, A_4 = A_4^{'}, A_5 = A_5^{''''}, A_6 = A_6^{''''}$ and the dynamics of followers as $A_7 = A_2^{''}, A_8 = A_5^{'}, A_9 = A_6^{'}, A_{10} = A_3^{''''}$. The corresponding $B_i, C_i, i \in \mathbf{I}[1, 10]$ are chosen similarly. The virtual leader's dynamics is (A_0, C_0) with $f = 5$ as follows:

$$A_0 = \begin{bmatrix} 0 & 0 & 2 & 0 \\ -3 & 0 & 0 & 1 \\ -f & 0 & 0 & 1 \\ 0 & -f^3 & 0 & 0 \end{bmatrix}, C_0 = \begin{bmatrix} 1 & 0 & 0 & 0 \\ 0 & 1 & 0 & 0 \end{bmatrix}.$$

It is easy to verify that $(A_i, B_i, C_i), i \in \mathbf{I}[1, 10]$ are stabilizable and detectable, and (A_0, C_0) is detectable. Set

$$A_h = \begin{bmatrix} 0_{2\times 2} & I_2 \\ \text{diag}\{-w^2, -w^2\} & 0_{2\times 2} \end{bmatrix},$$

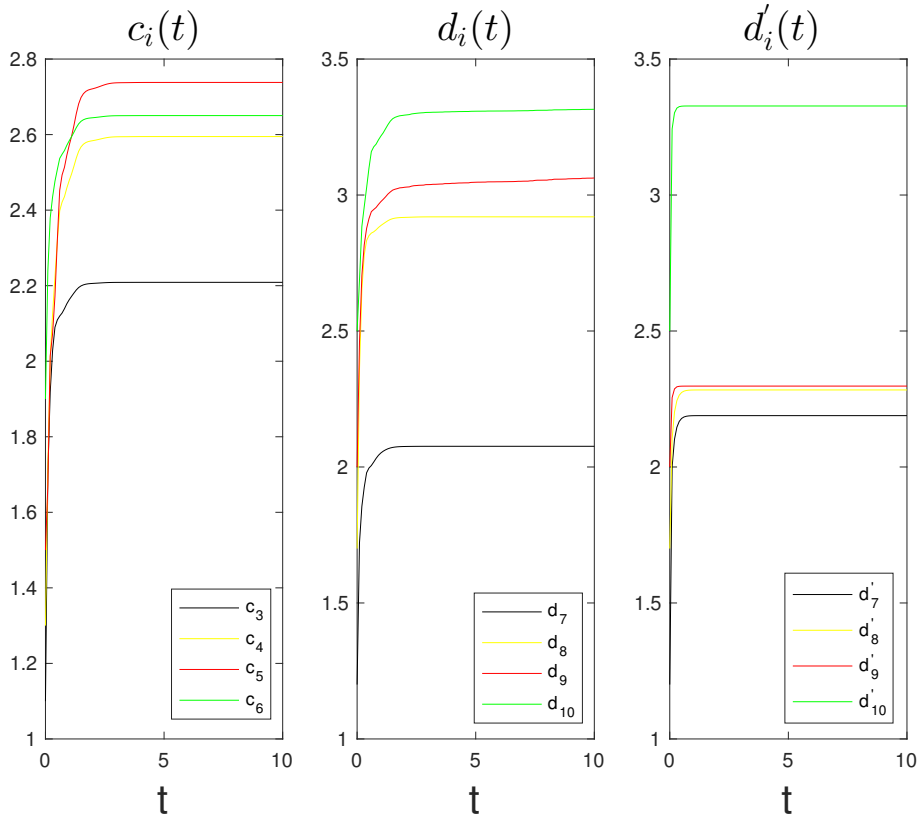

Figure 3.4: The coupling weights $c_i(t), i \in \mathbf{I}[3,6]$ for uninformed leaders and $d_i(t), d_i^{'}(t), i \in \mathbf{I}[7,10]$ for followers for graph Fig. 3.3(b).

then similar as (1.44), the TVF shape information $h(t)$ can be designed as

$$\begin{aligned}
h_{i1} =& r\sin(wt+(i-1)\pi/3) - r\cos(wt+(i-1)\pi/3),\\
h_{i2} =& 2r\sin(wt+(i-1)\pi/3),\\
h_{i3} =& rw\sin(wt+(i-1)\pi/3) + rw\cos(wt+(i-1)\pi/3),\\
h_{i4} =& 2rw\cos(wt+(i-1)\pi/3), i \in \mathbf{I}[1,6]
\end{aligned}$$

which satisfies (3.3). Choose $r=3, w=2$. We can verify that $\lim_{t\to\infty}\sum_{i=1}^{6} h_i(t) = 0$ meaning that the six leaders will rotate around the virtual leader which locates in the center of the time-varying shape. Solving AREs (3.10) and (3.17) gets P and $P^{'}$. And $K, K^{'}, K^{''}, \Gamma, \Gamma^{'}, \Gamma^{''}$ can be calculated accordingly.

Using pole placement method, assign eigenvalues of $A_0 - FC_0$ as -2,-5,-8,-10. Similarly, assign poles -5,-8,-10 for agents 1,7, poles -5,-10 for agents 2,3,4,8,9, and poles -2,-5,-8,-10 for agents 5,6,10. Then, we get $F, F_i, K_{1i}, i \in \mathbf{I}[1,10]$ respectively.

Solving (3.12) gets

$$X_i = \begin{bmatrix} I_2 & 0_{2\times 2} \\ -f^2 \quad 0 & 0_{1\times 2} \end{bmatrix}, i = 1, 7, X_j = \begin{bmatrix} I_2 & 0_{2\times 2} \\ -f^2 \quad 0 & 0 \quad 0 \\ 0 \quad 0 & -f^2 \quad 0 \end{bmatrix},$$
$$j = 5, 6, 10, X_k = \begin{bmatrix} I_2 & 0_{2\times 2} \end{bmatrix}, k = 2, 3, 4, 8, 9.$$

Thus, $U_i = B_i^{-1}(X_i A_0 - A_i X_i)$, and $K_{2i} = U_i - K_{1i}X_i, i \in \mathbf{I}[1, 10]$. To get the solution of (3.4), X_{hi} can be obtained by replacing f in X_i as w.

Remark 3.24 *In this example, to solve the output regulation equation (3.12), the X_i is firstly calculated and then U_i. The reason of designing $A_i, i \in \boldsymbol{I}[0, 6]$ is for the convenience of calculating the corresponding X_i. Then, designing B_i as the diagonal matrix is for the easiness of calculating U_i. However, if the U_i is firstly set, then, the first equation in (3.12) becomes a Sylvester equation and can be solved by the Matlab command: sylvester.*

All the initial conditions $x_i(0), i \in \mathbf{I}[0, 10], c_j(0), j \in \mathbf{I}[3, 6]$ and $d_k(0), d_k'(0), k \in \mathbf{I}[7, 10]$ are chosen as follows: $x_0(0) = [2.1, -0.7, 1, 1]^T$,
$x_1(0) = [-1.4, -1.3, -0.3]^T, x_2(0) = [-1.6, -0.1]^T$,
$x_3(0) = [0.8, 0.6]^T, x_4(0) = [-1.9, -0.7]^T$,
$x_5(0) = [0.1, 0.6, 0.2, -0.4]^T, x_6(0) = [1.3, 0.9, -0.4, 1.9]^T$,
$x_7(0) = [-1.6, 0.4, -0.1]^T, x_8(0) = [0.1, -0.4]^T$,
$x_9(0) = [1.3, 1.9]^T, x_{10}(0) = [0.8, 0.8, 0.7, 0.6]^T$,
$c_3(0) = 1.1, c_4(0) = 1.3, c_5(0) = 1.5, c_6(0) = 1.9$,
$d_7(0) = d_7'(0) = 1.2, d_8(0) = d_8'(0) = 1.7, d_9(0) = d_9'(0) = 2, , d_{10}(0) = d_{10}'(0) = 2.5$.

Figs. 3.5 (b,d,f) mean the heterogeneous output time-varying FC control problem is indeed solved. Figs. 3.5 (a,c,e) illustrate that the fully distributed adaptive observers are designed correctly. The coupling weights in Fig. 3.4 converge to some finite values.

3.3.1 Convergence rate analysis

1) We recall the Laplacian matrix (3.7) of communication topology as

$$\mathcal{L} = \begin{bmatrix} 0_{M\times M} & 0_{M\times(N-M)} & 0_{N\times L} \\ \mathcal{L}_2 & \mathcal{L}_1 & \\ & \mathcal{L}_3 & \mathcal{L}_4 \end{bmatrix},$$

where $\mathcal{L}_1 \in \mathbb{R}^{(N-M)\times(N-M)}, \mathcal{L}_2 \in \mathbb{R}^{(N-M)\times M}, \mathcal{L}_3 \in \mathbb{R}^{L\times N}, \mathcal{L}_4 \in \mathbb{R}^{L\times L}$.

	$\lambda(\mathcal{L}_1)$	$\frac{1}{g_i}, i \in \mathbf{I}[M+1, N]$
(a)	**0.1332** + 0.0000i	0.1111
	1.5000 + 0.6067i	0.1250
	1.5000 - 0.6067i	0.1429
	2.8668 + 0.0000i	0.2000
(b)	**0.2451** + 0.0000i	0.2000
	1.8774 + 0.7449i	0.2500
	1.8774 - 0.7449i	0.3333
	3.0000 + 0.0000i	0.5000
(c)	**2.0000** + 0.0000i	2.0000
	3.1226 + 0.7449i	2.0000
	3.1226 - 0.7449i	2.0000
	4.7549 + 0.0000i	2.0000

Table 3.1: The eigenvalues of $\lambda(\mathcal{L}_1)$ and $\frac{1}{g_i}, i \in \mathbf{I}[M+1, N]$.

2), Form Eq. (3.30) of the proof in Lemma 3.9, we have

$$\dot{V}_8 \leq -\eta^T[G(\hat{c}+\hat{\rho}) \otimes I_n]\eta, \tag{3.20}$$

which means the matrix G is related to the convergence rate of the Lyapunov function V. From Lemma 3.8 that $G \triangleq \text{diag}\{\frac{1}{g_{M+1}}, \ldots, \frac{1}{g_N}\}$ with $[g_{M+1}, \ldots, g_N]^T = \mathcal{L}_1^{-1}\mathbf{1}_{N-M}$, we can conclude that the matrix $\mathcal{L}_1$ is related to the convergence rate of the Lyapunov function V_8, then the convergence rate of the TVF tracking error.

Similarly, from Eq. (3.40) of the proof in Lemma 3.18, we can conclude that the matrix $\mathcal{L}_4$ is related to the convergence rate of the containment error.

3), It is stated in Tanner *et al.* (2005) that the smallest positive eigenvalue of Laplacian matrix is the algebraic connectivity of the graph, because it is directly related to how the nodes are interconnected. So we think the convergence rate is related to $\lambda_{min}(\mathcal{L}_1)$ and $\lambda_{min}(\mathcal{L}_4)$. We take the three simulations related to different value of $\lambda_{min}(\mathcal{L}_1)$.

Fig. 3.3 shows three different graphs. We can see that the information flow from informed leaders 1,2 to uninformed leaders 3,4,5,6 become more and more from (a) to (c). Consequently, from Table 3.1, we can see that from (a) to (c), $\frac{1}{g_i}, i \in \mathbf{I}[M+1, N]$ become larger when the $\lambda_{min}(\mathcal{L}_1)$ become larger. It means from (a) to (c), the convergence rate of FC control becomes faster and faster, based on $\dot{V}_8 \leq -\eta^T[G(\hat{c}+\hat{\rho}) \otimes I_n]\eta$, and $G \triangleq \text{diag}\{\frac{1}{g_{M+1}}, \ldots, \frac{1}{g_N}\}$.

4), The Fig. 3.5 shows three simulations with the same initial condition for communicating graphs in Fig. 3.3. For graph (a), it takes almost 7 simulation seconds to achieve convergence; for graph (b) almost 4 simulation seconds; for

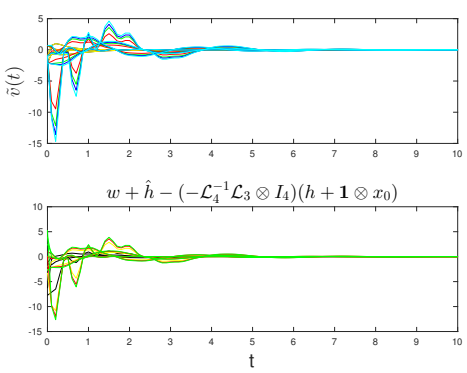

(a) Observer estimating error for graph (a)

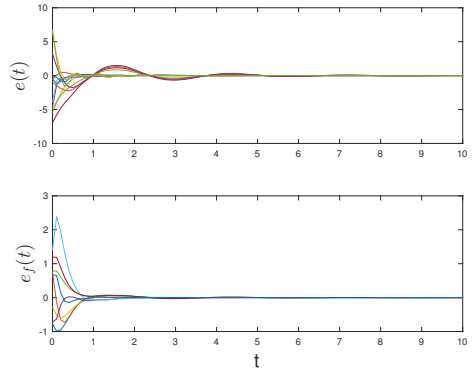

(b) TVF and containment error for graph (a)

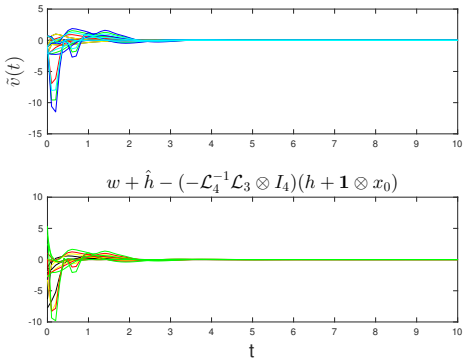

(c) Observer estimating error for graph (b)

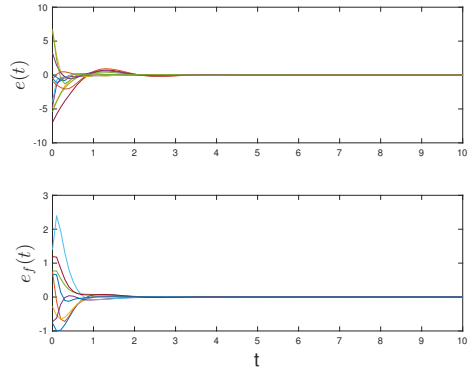

(d) TVF and containment error for graph (b)

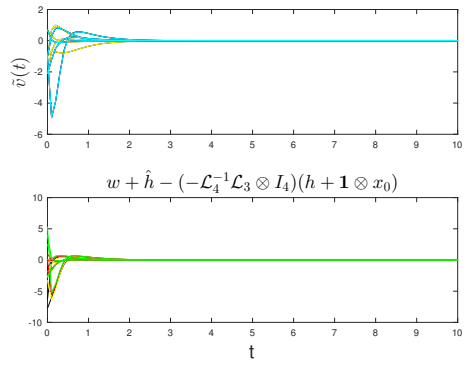

(e) Observer estimating error for graph (c)

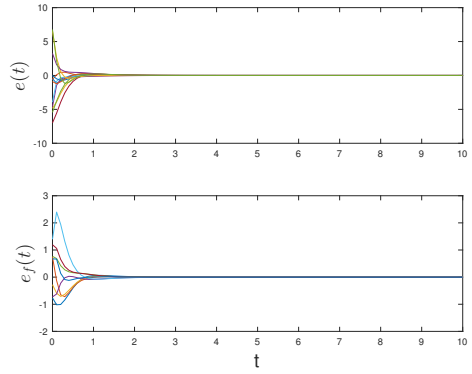

(f) TVF and containment error for graph (c)

Figure 3.5: The convergence rate comparisons for observer estimating error (left), and the TVF tracking and containment error (right) for graphs Fig. 3.3 (a), (b) (c).

graph (c) almost 2.5 simulation seconds. Based on Table 3.1, it validates the conclusion that the topology structure is reflected on the convergence speed of the tracking performance. Specifically, when $[g_{M+1},\ldots,g_N]^T = \mathcal{L}_1^{-1}\mathbf{1}_{N-M}$ is smaller meaning that $\frac{1}{g_i}, i \in \mathbf{I}[M+1,N]$ become larger, the convergence rate is faster. The same conclusion applies to containment control, i.e., when $[g_{N+1},\ldots,g_{N+L}]^T = \mathcal{L}_4^{-1}\mathbf{1}_L$ is smaller, the convergence rate is faster. So we give the following remark.

Remark 3.25 *The topology structure is reflected on the convergence speed of the tracking performance. From Lemma 3.9 and based on (3.30), (3.40), we can conclude that the matrices $\mathcal{L}_1, \mathcal{L}_4$ are related to the convergence rate of the FC control. Specifically, when $\mathcal{L}_1^{-1}\mathbf{1}_{N-M}$ and $\mathcal{L}_4^{-1}\mathbf{1}_L$ are smaller, the convergence rate is faster.*

3.3.2 Application to multi-robot systems

Example 2. The heterogeneous MAS have many applications in reality. Heterogeneous dynamics is also very common, e.g., different vehicles with different dynamics and abilities are normal in our living life. Thinking one scenario, in order to make some autonomous vehicles without necessary sensors (referred as followers) avoid collide with surrounding obstacles, autonomous vehicles equipped with all sensors (referred as leaders) can form a formation shape moving safely and make followers move inside the convex hull formed by those leaders. Then the whole multi-vehicle system operates safely.

Here, we set $f = 0.1, w = 0.1, r = 20$ for the virtual leader dynamics (A_0, C_0) and TVF shape information $h(t)$ as in Example 1.

Consider two types of mobile vehicles with the same graph in Fig. 3.3 (b). The first type comes from the linearized dynamics of the Caltech wireless tested multiple vehicles Gupta* *et al.* (2005) as follows:

$$\bar{A}_1 = \begin{bmatrix} & 0_{3\times 3} & & & I_3 & \\ 0 & 0 & -0.2003 & 0.2003 & 0 & 0 \\ 0 & 0 & 0.2003 & 0 & 0.2003 & 0 \\ 0 & 0 & 0 & 0 & 0 & -1.6129 \end{bmatrix},$$

$$\bar{B}_1 = \begin{bmatrix} 0 & 0 & 0 & 0.9441 & 0.9441 & -28.7097 \\ 0 & 0 & 0 & 0.9441 & 0.9441 & 28.7097 \end{bmatrix}^T$$

where $x_i = (x_{i1},\ldots,x_{i6})^T \in \mathbb{R}^6$. x_{i1}, x_{i2} and x_{i3} are the positions along the x and y coordinates and orientation of the i-th vehicle, respectively. Choose $\bar{C}_1 = [I_2, 0_{2\times 4}]$ and we get $(\bar{A}_1, \bar{B}_1, \bar{C}_1)$ is stabilizable and detectable. Similarly, assigning poles -2,-5,-6,-8,-10,-20 to $\bar{A}_1 - \bar{F}_1\bar{C}_1$ and $\bar{A}_1 + \bar{B}_1\bar{K}_{11}$ so as to be Hurwitz. The solution

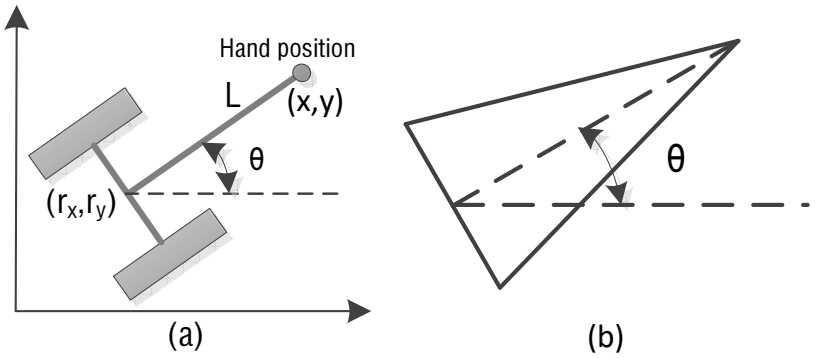

Figure 3.6: (a) Hand position. (b) The vehicle orientation presentation in Fig. 3.7.

to (3.4) and (3.12) is

$$\bar{X}_1 = \begin{bmatrix} & I_2 & & 0_{2\times 2} \\ -1.0 & -0.0025 & -16.0 & -4.5 \\ 0 & 0 & 2 & 0 \\ -3 & 0 & 0 & 1 \\ 1.6 & 0.0045 & -2.0 & -16.0 \end{bmatrix}, \bar{X}_{h1} = \begin{bmatrix} I_2 & & 0_{2\times 2} & \\ 0.025 & -0.025 & -0.5 & 0.5 \\ 0_{2\times 2} & & I_2 & \\ 0.005 & -0.005 & 0.025 & -0.025 \end{bmatrix},$$

$$\bar{U}_1 = \begin{bmatrix} -0.2604 & -0.0007 & -1.4824 & 1.0663 \\ -0.1637 & 0.0001 & -1.4830 & 0.0990 \end{bmatrix},$$

$$\bar{U}_{h1} = \begin{bmatrix} -0.0028 & -0.0025 & 0.0523 & 0.0538 \\ -0.0025 & -0.0028 & 0.0538 & 0.0523 \end{bmatrix}.$$

The second type of mobile vehicle dynamics is as follows:

$$\begin{pmatrix} \dot{r}_{xi} \\ \dot{r}_{yi} \\ \dot{\theta}_i \\ \dot{\bar{v}}_i \\ \dot{\bar{w}}_i \end{pmatrix} = \begin{pmatrix} \bar{v}_i \cos(\theta_i) \\ \bar{v}_i \sin(\theta_i) \\ \bar{w}_i \\ 0 \\ 0 \end{pmatrix} + \begin{pmatrix} 0 & 0 \\ 0 & 0 \\ 0 & 0 \\ \frac{1}{m_i} & 0 \\ 0 & \frac{1}{J_i} \end{pmatrix} \begin{pmatrix} F_i \\ \tau_i \end{pmatrix} \tag{3.21}$$

where(r_{xi}, r_{yi}) is the Cartesian position of the i-th vehicle, θ_i its orientation, and $\bar{v}_i, \bar{w}_i$ are its linear and angular speed, m_i its mass, J_i its moment of inertia, and F_i, τ_i its applied force and torque. Define $\bar{u}_i = [F_i, \tau_i]^T$ as the control input.

As shown in Lawton *et al.* (2003), we focus on the vehicle's "hand" position

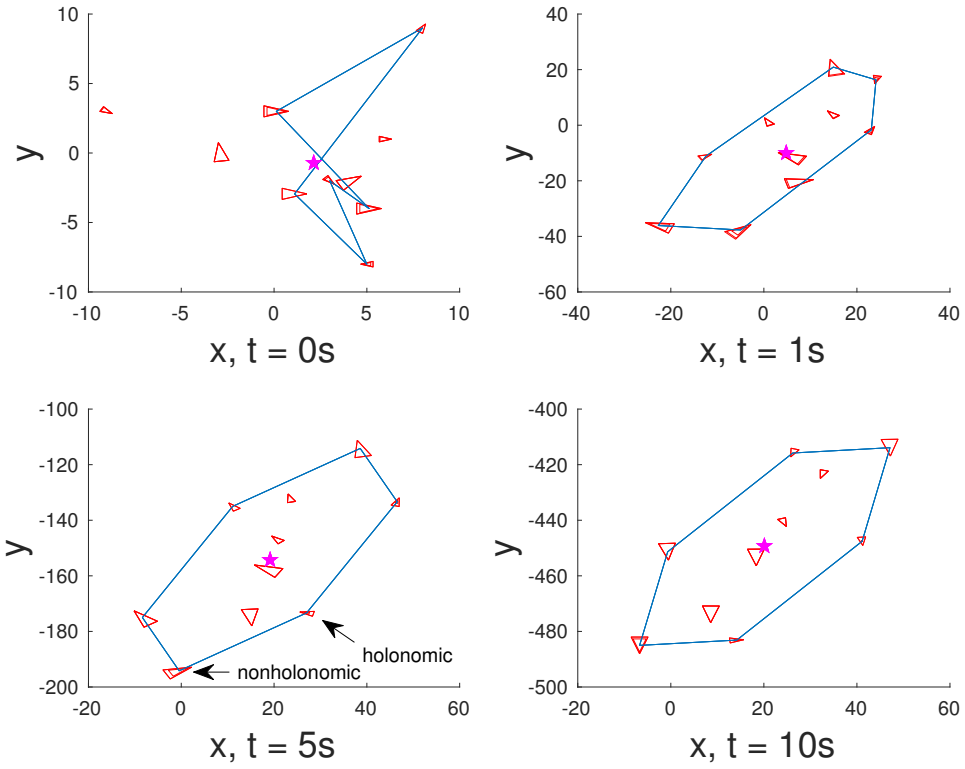

Figure 3.7: The snapshots of heterogeneous multi-vehicle system with orientations.

$s_i = (x_i, y_i)$ which lies a distance L_i along the line that is normal to the wheel axis and intersects the wheel axis at the center point (r_{xi}, r_{yi}), as shown in Fig. 3.6 (a). Therefore, the hand position is defined as $\begin{pmatrix} x_i \\ y_i \end{pmatrix} = \begin{pmatrix} r_{xi} \\ r_{yi} \end{pmatrix} + L_i \begin{pmatrix} \cos(\theta_i) \\ \sin(\theta_i) \end{pmatrix}$. Using the output feedback linearizing technique Lawton *et al.* (2003), we have

$$\bar{u}_i = \begin{pmatrix} \frac{1}{m_i}\cos(\theta_i) & -\frac{L_i}{J_i}\sin(\theta_i) \\ \frac{1}{m_i}\sin(\theta_i) & \frac{L_i}{J_i}\cos(\theta_i) \end{pmatrix}^{-1} \left[u_i - \begin{pmatrix} -\bar{v}_i\bar{w}_i\sin(\theta_i) - L_i\bar{w}_i^2\cos(\theta_i) \\ \bar{v}_i\bar{w}_i\cos(\theta_i) - L_i\bar{w}_i^2\sin(\theta_i) \end{pmatrix} \right] \tag{3.22}$$

where u_i is the linearized control input. Then the input output dynamics of each vehicle can be described as a double integrator system

$$\ddot{s}_i = u_i \tag{3.23}$$

which can be rewritten in a state space form as $\bar{A}_2 = \begin{bmatrix} 0 & I_2 \\ 0 & 0 \end{bmatrix}$, $\bar{B}_2 = \begin{bmatrix} 0 \\ I_2 \end{bmatrix}$. Set

$\bar{C}_2 = [I_2, 0_{2\times 2}]$ and we get $(\bar{A}_2, \bar{B}_2, \bar{C}_2)$ is stabilizable and detectable. Define the same parameter $m_i = 10.1\,kg$, $J_i = 0.13\,kg\,m^2$ and $L_i = 0.12\,m$ as in Lawton *et al.* (2003). Similarly, assigning poles -2,-6,-8,-20 to $\bar{A}_2 - \bar{F}_2\bar{C}_2$ and $\bar{A}_2 + \bar{B}_2\bar{K}_{12}$ so as to be Hurwitz. The solution to (3.4) and (3.12) is

$$\bar{X}_2 = \begin{bmatrix} I_2 & 0_{2\times 2} \\ 0 & 0 & 2 & 0 \\ -3 & 0 & 0 & 1 \end{bmatrix}, \bar{U}_2 = \begin{bmatrix} -0.2000 & 0 & 0 & 2.0000 \\ 0 & -0.0010 & -6.0000 & 0 \end{bmatrix},$$
$$\bar{X}_{h2} = I_4, \bar{U}_{h2} = \begin{bmatrix} -0.1000 & 0 & 0 & 1.0000 \\ 0 & -0.0010 & 0 & 0 \end{bmatrix}.$$

Similarly as in Example 1, Choose vehicles 1,3,4,7,8 with dynamics $(\bar{A}_1, \bar{B}_1, \bar{C}_1)$ and vehicles 2,5,6,9,10 with linearized dynamics $(\bar{A}_2, \bar{B}_2, \bar{C}_2)$. Set the initial positions, orientation and velocities as $x_0(0) = [2.1, -0.7, 1, 1]^T$,
$x_1(0) = [8, 9, \pi/3, 0, 0, 0]^T, x_2(0) = [1, -3, \pi/6, 0, 0]^T$,
$x_3(0) = [5, -8, \pi, 0, 0, 0]^T, x_4(0) = [3, -2, -\pi/4, 0, 0, 0]^T$,
$x_5(0) = [5, -4, 0, 0, 0]^T, x_6(0) = [0, 3, 0, 0, 0]^T$,
$x_7(0) = [6, 1, 0, 0, 0, 0]^T, x_8(0) = [-9, 3, -\pi/6, 0, 0, 0]^T$,
$x_9(0) = [-3, 0, \pi/4, 0, 0]^T, x_{10}(0) = [4, -2, 0, 0, 0]^T$.

The initial positions and the movement snapshots of the multi-vehicle system at different timestamps are depicted in Fig. 3.7. Note here that the orientation angle θ of each vehicle is represented as in Fig. 3.6 (b). In Fig. 3.7 the pentagram represents the virtual leader, and the smaller and bigger triangles represent the holonomic Caltech vehicles and nonholonomic vehicles, respectively. Six heterogeneous leader vehicles form the parallel hexagon shape and keep tracking the virtual leader which is located at the shape center eventually, and four heterogeneous follower vehicles move inside the shape achieving containment control at the same time. From $t = 5s$ and $t = 10s$, we can see the shape keeps rotating around the virtual leader, which means it is time-varying.

It is worth noting here that by using output $y = Cx$ measurement in this example, only vehicles' position information (without any velocity information) is needed to achieve heterogeneous FC control.

Proof appendix

Proof of Lemma 3.9. Due to $\eta_i = \sum_{j=1}^N l_{ij}(v_j - x_0) = \sum_{j=1}^N l_{ij}\tilde{v}_j, i \in \mathbf{I}[M+1, N]$ in (3.9), rewrite the observer error $\tilde{v} = [\tilde{V}_2^T, \tilde{V}_1^T]^T$, where $\tilde{V}_1 = [\tilde{v}_{M+1}^T, \ldots, \tilde{v}_N^T]^T$ for ULs and $\tilde{V}_2 = [\tilde{v}_1^T, \ldots, \tilde{v}_M^T]^T$ for ILs. Then, $\eta = [\eta_{M+1}^T, \ldots, \eta_N^T]^T$ is

$$\eta = (\mathcal{L}_1 \otimes I_n)\tilde{V}_1 + (\mathcal{L}_2 \otimes I_n)\tilde{V}_2. \tag{3.24}$$

Since $\mathcal{L}_1$ is nonsingular and $\lim_{t\to\infty}\tilde{V}_2 = 0$ for ILs in (3.8), then for ULs, $\lim_{t\to\infty}\tilde{V}_1 = 0$ if and only if $\lim_{t\to\infty}\eta = 0$ which is the objective of following proof. From (3.9) and (3.24) we obtain

$$\dot{\eta} = [I_{N-M}\otimes A_0 + \mathcal{L}_1(\hat{c}+\hat{\rho})\otimes K]\eta - (\mathcal{L}_2\otimes FC_0)\tilde{V}_2, \tag{3.25}$$

where $\hat{c} \triangleq \text{diag}\{c_{M+1},\ldots,c_N\}$, $\hat{\rho} \triangleq \text{diag}\{\rho_{M+1},\ldots,\rho_N\}$.

Let

$$V_6 = \frac{1}{2}\sum_{i=M+1}^{N}\frac{1}{g_i}[(2c_i+\rho_i)\rho_i + (c_i-\alpha)^2] \tag{3.26}$$

where $g_i > 0, i \in \mathbf{I}[M+1, N]$ from Lemma 3.8. It follows from $c_i(0) > 0, \dot{c}_i(t) \geq 0$ that $c_i(t) > 0, \forall t > 0$. α is a positive constant to be determined. Noting further that $\rho_i \geq 0$, it is not difficult to see V_6 is positive definite. Based on Lemma 3.8, we have $G\mathcal{L}_1 + \mathcal{L}_1^T G \geq \lambda_0 I$ with $\lambda_0 = \lambda_{min}(G\mathcal{L}_1 + \mathcal{L}_1^T G) > 0$. Then,

$$\begin{aligned}
\dot{V}_6 =& \sum_{i=1}^{N}[\frac{1}{g_i}(c_i+\rho_i)\dot{\rho}_i + \frac{1}{g_i}\rho_i\dot{c}_i + \frac{1}{g_i}(c_i-\alpha)\dot{c}_i] \\
=& \eta^T[G(\hat{c}+\hat{\rho})\otimes(PA_0 + A_0^T P) + G(\hat{c}+\hat{\rho}-\alpha I)\otimes\Gamma + (\hat{c}+\hat{\rho}) \\
& \times (G\mathcal{L}_1 + \mathcal{L}_1^T G)(\hat{c}+\hat{\rho})\otimes PK]\eta - 2\eta^T[G(\hat{c}+\hat{\rho})\mathcal{L}_2\otimes PFC_0]\tilde{V}_2 \\
\leq& \eta^T[G(\hat{c}+\hat{\rho})\otimes(PA_0 + A_0^T P) - \lambda_0(\hat{c}+\hat{\rho})^2\otimes P^2 + G(\hat{c}+\hat{\rho}-\alpha I) \\
& \otimes P^2]\eta - 2\eta^T[G(\hat{c}+\hat{\rho})\mathcal{L}_2\otimes PFC_0]\tilde{V}_2.
\end{aligned} \tag{3.27}$$

By using Young's inequality, we can get

$$\eta^T[G(\hat{c}+\hat{\rho})\otimes P^2]\eta \leq \eta^T[(\frac{\lambda_0}{2}(\hat{c}+\hat{\rho})^2 + \frac{G^2}{2\lambda_0})\otimes P^2]\eta$$

and

$$\begin{aligned}
& -2\eta^T[G(\hat{c}+\hat{\rho})\mathcal{L}_2\otimes PFC_0]\tilde{V}_2 \\
\leq& \frac{1}{4}\eta^T(\lambda_0(\hat{c}+\hat{\rho})^2\otimes P^2)\eta + \frac{4}{\lambda_0}\|G\mathcal{L}_2\otimes FC_0\|^2\|\tilde{V}_2\|^2.
\end{aligned}$$

Substituting them into (3.27) yields

$$\begin{aligned}\dot{V}_6 \leq & \eta^T\{G(\hat{c}+\hat{\rho})\otimes(PA_0+A_0^TP)-[\frac{\lambda_0}{4}(\hat{c}+\hat{\rho})^2\\ & -\frac{G^2}{2\lambda_0}+\alpha G]\otimes P^2\}\eta+\frac{4}{\lambda_0}\|G\mathcal{L}_2\otimes FC_0\|^2\|\tilde{V}_2\|^2\\ \leq & \eta^T\{G(\hat{c}+\hat{\rho})\otimes(PA_0+A_0^TP)-[\frac{\lambda_0}{4}(\hat{c}+\hat{\rho})^2\\ & +\frac{G^2}{\lambda_0}]\otimes P^2\}\eta+\frac{4}{\lambda_0}\|G\mathcal{L}_2\otimes FC_0\|^2\|\tilde{V}_2\|^2\\ \leq & \eta^T[G(\hat{c}+\hat{\rho})\otimes(PA_0+A_0^TP-P^2)]\eta+\frac{4}{\lambda_0}\|G\mathcal{L}_2\otimes FC_0\|^2\|\tilde{V}_2\|^2.\end{aligned}$$

Based on the fact that $a+b\geq 2\sqrt{ab}, \forall a,b\in\mathbb{R}^+$, we have chosen $\alpha\geq\frac{3}{2\lambda_0}\max\frac{1}{g_i}, i\in\mathbf{I}[M+1,N]$ to get the last two inequalities.

Define $V_7=\tilde{V}_2^T(I_M\otimes Q)\tilde{V}_2$, where $Q>0$ satisfies

$$(A_0-FC_0)^TQ+Q(A_0-FC_0)=-I_n. \tag{3.28}$$

Combined with $\dot{\tilde{V}}_2=[I_M\otimes(A_0-FC_0)]\tilde{V}_2$, we obtain

$$\dot{V}_7=-\tilde{V}_2^T\tilde{V}_2=-\|\tilde{V}_2\|^2. \tag{3.29}$$

Based on the above analysis, consider the following Lyapunov function candidate $V_8=V_6+\gamma V_7$, where γ is a positive constant to be determined later. Then,

$$\begin{aligned}\dot{V}_8 \leq & \eta^T[G(\hat{c}+\hat{\rho})\otimes(PA_0+A_0^TP-P^2)]\eta\\ & +\frac{4}{\lambda_0}\|G\mathcal{L}_2\otimes FC_0\|^2\|\tilde{V}_2\|^2-\gamma\|\tilde{V}_2\|^2\\ \leq & -\eta^T[G(\hat{c}+\hat{\rho})\otimes I_n]\eta\leq 0\end{aligned} \tag{3.30}$$

where the inequality comes from ARE (3.10) and the choice of $\gamma\geq\frac{4}{\lambda_0}\|G\mathcal{L}_2\otimes FC_0\|^2$. So we can conclude that $V_8(t)$ is bounded and so are ρ_i, c_i and $\tilde{V}_2$. From (3.9) and $\Gamma=P^2$ it follows $\dot{c}_i(t)\geq 0$, thus each coupling weight $c_i(t)$ increases monotonically and converges to some finite value finally. Note that $\dot{V}_8\equiv 0$ is equivalent to $\eta=0$. By LaSalle's Invariance principle Krstic *et al.* (1995), it follows $\lim_{t\to\infty}\eta=0$.

Proof of Theorem 3.15. Firstly, we prove the convergence of the observer $\hat{v}_i$. Define the estimation error as $\psi_i=\hat{v}_i-x_i, i\in\mathbb{L}$. Similar as the convergence proof of $\tilde{v}_i, i\in\mathbf{I}[1,M]$, we have $\dot{\psi}_i=(A_i-F_iC_i)\psi_i$. Since $A_i-F_iC_i$ is Hurwitz,

we get that $\lim_{t\to\infty}\psi_i = 0$.

Next, denote $\tilde{x}_l = \mathfrak{x}_l - \mathfrak{X}_l(\mathbf{1}\otimes x_0) - \mathfrak{X}_{hl}h$, where $\mathfrak{x}_l = [x_1^T,\ldots,x_N^T]^T, \mathfrak{X}_l = \mathrm{diag}\{X_1,\ldots,X_N\}, \mathfrak{X}_{hl} = \mathrm{diag}\{X_{h1},\ldots,X_{hN}\}$. Then from (3.1), (3.2), (3.3), (3.13),

$$\begin{aligned}\dot{\tilde{x}}_l =&(A+BK_1)[\tilde{x}_l + \mathfrak{X}_l(\mathbf{1}\otimes x_0) + \mathfrak{X}_{hl}h] + BK_1\psi_l + BK_2v\\ &+ BK_3h - \mathfrak{X}_l(I\otimes A_0)(\mathbf{1}\otimes x_0) - \mathfrak{X}_{hl}(I\otimes A_h)h\end{aligned}$$

where $v = [v_1^T,\ldots,v_N^T]^T, \psi_l = [\psi_1^T,\ldots,\psi_N^T]^T$. Since $(X_{hi},U_{hi}),(X_i,U_i), i\in\mathbb{L}$ are the solutions of(3.4) and (3.12), after calculation we get

$$\begin{aligned}\dot{\tilde{x}}_l =&(A+BK_1)\tilde{x}_l + BK_1\mathfrak{X}_l(\mathbf{1}\otimes x_0) + BK_1\mathfrak{X}_{hl}h + BK_1\psi_l\\ &+ BK_2v + BK_3h - BU(\mathbf{1}\otimes x_0) - BU_hh\end{aligned}$$

where $U = \mathrm{diag}\{U_1,\ldots,U_N\}$, $U_h = \mathrm{diag}\{U_{h1},\ldots,U_{hN}\}$. Choose $K_{2i} = U_i - K_{1i}X_i$, $K_{3i} = U_{hi} - K_{1i}X_{hi}$, then

$$\dot{\tilde{x}}_l = (A+BK_1)\tilde{x}_l + BK_1\psi_l + BK_2(v-\mathbf{1}\otimes x_0). \tag{3.31}$$

Select $K_{1i}, i\in\mathbb{L}$ such that $A_i + B_iK_{1i}$ is Hurwitz. From Lemma 3.9 we know $\lim_{t\to\infty}(v-\mathbf{1}\otimes x_0) = 0$. So based on $\lim_{t\to\infty}\psi_i = 0$, we obtain $\lim_{t\to\infty}\tilde{x}_l = 0$.

From (3.5) in Definition 3.5, define the TVF tracking error $e_i = y_i - y_0 - C_0h_i, e = [e_1^T,\ldots,e_N^T]^T$. From $\tilde{x}_l = x_l - \mathfrak{X}_l(\mathbf{1}\otimes x_0) - \mathfrak{X}_{hl}h$ we have

$$e = C\tilde{x}_l + C\mathfrak{X}_l(\mathbf{1}\otimes x_0) + C\mathfrak{X}_{hl}h - (I\otimes C_0)(h+\mathbf{1}\otimes x_0). \tag{3.32}$$

Thanks to $C_iX_i = C_0$, $C_iX_{hi} = C_0, i\in\mathbb{L}$ and $\lim_{t\to\infty}\tilde{x}_l = 0$, we conclude that $\lim_{t\to\infty}e = 0$, i.e., the heterogeneous TVF tracking for leaders is achieved.

Proof of Lemma 3.18. Denote $\hat{d}\triangleq\mathrm{diag}\{d_{N+1},\ldots,d_{N+L}\}$ and $\hat{\varrho}\triangleq\mathrm{diag}\{\varrho_{N+1},\ldots,\varrho_{N+L}\}$. From (3.14), (3.15), we obtain

$$\begin{aligned}\dot{\theta} =&(\mathcal{L}_4\otimes I_n)[(I_L\otimes A_0)w + (\hat{d}+\hat{\varrho})\otimes K'\theta] + (\mathcal{L}_3\otimes I_n)\dot{v}\\ =&[I_L\otimes A_0 + \mathcal{L}_4(\hat{d}+\hat{\varrho})\otimes K']\theta - (\mathcal{L}_3\otimes A_0)v + (\mathcal{L}_3\otimes I_n)\dot{v}.\end{aligned} \tag{3.33}$$

Denote $v_{unin} = [v_{M+1}^T,\ldots,v_N^T]^T$, $v_{info} = [v_1^T,\ldots,v_M^T]^T$ for all ULs and ILs,

respectively. From (3.8) and (3.9) we get

$$\begin{aligned}\dot{v} &= \begin{bmatrix}\dot{v}_{info}\\ \dot{v}_{unin}\end{bmatrix} = \begin{bmatrix}(I_M \otimes A_0)v_{info} - (I_M \otimes FC_0)\tilde{V}_2\\ (I_{N-M} \otimes A_0)v_{unin} + [(\hat{c}+\hat{\rho}) \otimes K]\eta\end{bmatrix}\\ &= (I_N \otimes A_0)\begin{bmatrix}v_{info}\\ v_{unin}\end{bmatrix} - \begin{bmatrix}(I_M \otimes FC_0)\tilde{V}_2\\ -((\hat{c}+\hat{\rho}) \otimes K)\eta\end{bmatrix}\\ &= (I_N \otimes A_0)v - \begin{bmatrix}(I_M \otimes FC_0)\tilde{V}_2\\ -((\hat{c}+\hat{\rho}) \otimes K)\eta\end{bmatrix}.\end{aligned} \tag{3.34}$$

Substituting (3.34) into (3.33), we have

$$\dot{\theta} = [I_L \otimes A_0 + \mathcal{L}_4(\hat{d}+\hat{\varrho}) \otimes K']\theta - (\mathcal{L}_3 \otimes I_n)\begin{bmatrix}(I_M \otimes FC_0)\tilde{V}_2\\ ((\hat{c}+\hat{\rho}) \otimes P)\eta\end{bmatrix}. \tag{3.35}$$

What is quite interesting here is that (3.35) is similar as (3.25) in which $\lim_{t\to\infty}\tilde{V}_2 = 0$ and $\lim_{t\to\infty}\eta = 0$. It is equal to say that because $I_{N-M} \otimes A_0 + \mathcal{L}_1(\hat{c}+\hat{\rho}) \otimes K$ is Hurwitz and $\lim_{t\to\infty}\tilde{V}_2 = 0$, so we get $\lim_{t\to\infty}\eta = 0$. It proves that $\tilde{V}_2$ has no influence to the final convergence of η to 0 in (3.25). Similarly here, due to $\lim_{t\to\infty}\tilde{V}_2 = 0$ and $\lim_{t\to\infty}\eta = 0$ in (3.35), $\lim_{t\to\infty}\theta = 0$ if $I_L \otimes A_0 + \mathcal{L}_4(\hat{d}+\hat{\varrho}) \otimes K'$ is Hurwitz.

Next, we prove that $I_L \otimes A_0 + \mathcal{L}_4(\hat{d}+\hat{\varrho}) \otimes K'$ is Hurwitz. To get that, we eliminate $(\mathcal{L}_3 \otimes I_n)\begin{bmatrix}(I_M \otimes FC_0)\tilde{V}_2\\ ((\hat{c}+\hat{\rho}) \otimes P)\eta\end{bmatrix}$ in (3.35) for simplicity, and have

$$\dot{\theta} = [I_L \otimes A_0 + \mathcal{L}_4(\hat{d}+\hat{\varrho}) \otimes K']\theta, \quad i \in \mathbb{F}. \tag{3.36}$$

Similar as the Proof of Lemma 3.9, let

$$V_9 = \frac{1}{2}\sum_{i=N+1}^{N+L}\frac{1}{g_i}[(2d_i + \varrho_i)\varrho_i + (d_i - \beta)^2] \tag{3.37}$$

where $g_i > 0, i \in \mathbf{I}[N+1, N+L]$ and $G'\mathcal{L}_4 + \mathcal{L}_4^T G' \geq \lambda_0' I$ with $\lambda_0' = \lambda_{min}(G'\mathcal{L}_4 + \mathcal{L}_4^T G') > 0$ based on Lemma 3.8. The properties of other parameters are similar

as in (3.26). Then

$$\begin{aligned}\dot{V}_9 =&\theta^T[G^{'}(\hat{d}+\hat{\varrho})\otimes(PA_0+A_0^TP)+G^{'}(\hat{d}+\hat{\varrho}-\beta I)\otimes\Gamma^{'}\\&+(\hat{d}+\hat{\varrho})(G^{'}\mathcal{L}_4+\mathcal{L}_4^TG^{'})(\hat{d}+\hat{\varrho})\otimes PK^{'}]\theta\\\leq&\theta^T[G^{'}(\hat{d}+\hat{\varrho})\otimes(PA_0+A_0^TP)\\&-\lambda_0^{'}(\hat{d}+\hat{\varrho})^2\otimes P^2+G^{'}(\hat{d}+\hat{\varrho}-\beta I)\otimes P^2]\theta\end{aligned}\tag{3.38}$$

By using Young's inequality, we can get

$$\theta^T[G^{'}(\hat{d}+\hat{\varrho})\otimes P^2]\theta\leq\theta^T[(\frac{\lambda_0^{'}}{2}(\hat{d}+\hat{\varrho})^2+\frac{G^{'2}}{2\lambda_0^{'}})\otimes P^2]\theta.\tag{3.39}$$

Substituting (3.39) into (3.38) yields

$$\begin{aligned}\dot{V}_9\leq&\theta^T\{G^{'}(\hat{d}+\hat{\varrho})\otimes(PA_0+A_0^TP)-[\frac{\lambda_0^{'}}{2}(\hat{d}+\hat{\varrho})^2\\&-\frac{G^{'2}}{2\lambda_0^{'}}+\beta G^{'}]\otimes P^2\}\theta\\\leq&\theta^T[G^{'}(\hat{d}+\hat{\varrho})\otimes(PA_0+A_0^TP-P^2)]\theta\leq 0\end{aligned}\tag{3.40}$$

where we have chosen $\beta\geq\frac{1}{\lambda_0^{'}}\max\frac{1}{g_i}, i\in\mathbb{F}$ and ARE (3.10) to get the last two inequalities. So we can conclude that $V_9(t)$ is bounded and so are ϱ_i and d_i. Following the similar analysis in the proof of Lemma 3.9, we can conclude that $\lim_{t\to\infty}\theta=0$ in (3.35), which is equal to say that $I_L\otimes A_0+\mathcal{L}_4(\hat{d}+\hat{\varrho})\otimes K^{'}$ is Hurwitz. $d_i(t)$ increases monotonically and converges to some finite value finally. From (3.15) and based on $\lim_{t\to\infty}v=\lim_{t\to\infty}(\mathbf{1}\otimes x_0)$ in Lemma 3.9, we obtain the observer $\lim_{t\to\infty}w=(-\mathcal{L}_4^{-1}\mathcal{L}_3\otimes I_n)(\mathbf{1}\otimes x_0)$.

Proof of Theorem 3.21. Firstly, we prove the convergence of Luenberger observer $\hat{w}_i$. Define the estimation error as $\psi_i=\hat{w}_i-x_i, i\in\mathbb{F}$. Similar as the convergence proof of $\hat{v}_i, i\in\mathbb{L}$ in Theorem 3.15, since $A_i-F_iC_i, i\in\mathbb{F}$ is Hurwitz, we get that $\lim_{t\to\infty}\psi_i=0, i\in\mathbb{F}$.

Next we show the heterogeneous FC control is achieved. Denote $\tilde{x}_f=\mathfrak{x}_f-\mathfrak{X}_f(-\mathcal{L}_4^{-1}\mathcal{L}_3\otimes I_n)(\mathbf{1}\otimes x_0)-\mathfrak{X}_{hf}(-\mathcal{L}_4^{-1}\mathcal{L}_3\otimes I_n)h$, where $\mathfrak{x}_f=[x_{N+1}^T,\ldots,x_{N+L}^T]^T$ with $\mathfrak{X}_f$ and $\mathfrak{X}_{hf}$ being defined similarly. Then from (3.1), (3.2), (3.3), (3.18), we obtain

$$\begin{aligned}\dot{\tilde{x}}_f=&(\bar{A}+\bar{B}\bar{K}_1)[\tilde{x}_f+\mathfrak{X}_f(-\mathcal{L}_4^{-1}\mathcal{L}_3\otimes I_n)(\mathbf{1}\otimes x_0)+\mathfrak{X}_{hf}(-\mathcal{L}_4^{-1}\mathcal{L}_3\otimes I_n)h]\\&+\bar{B}\bar{K}_1\psi_f+\bar{B}\bar{K}_2w+\bar{B}\bar{K}_3\hat{h}-\mathfrak{X}_f(-\mathcal{L}_4^{-1}\mathcal{L}_3\otimes I_n)(I_N\otimes A_0)(\mathbf{1}\otimes x_0)\\&-\mathfrak{X}_{hf}(-\mathcal{L}_4^{-1}\mathcal{L}_3\otimes I_n)(I_N\otimes A_0)h\end{aligned}$$

where $\hat{h} = [\hat{h}_{N+1}^T, \ldots, \hat{h}_{N+L}^T]^T, \psi_f = [\psi_{N+1}^T, \ldots, \psi_{N+L}^T]^T$. Choose $K_{2i} = U_i - K_{1i}X_i, K_{3i} = U_{hi} - K_{1i}X_{hi}, i \in \mathbb{F}$. Similar as the calculation in the proof of Theorem 3.15, we get

$$\begin{aligned}\dot{\tilde{x}}_f =&(\bar{A} + \bar{B}\bar{K}_1)\tilde{x}_f + \bar{B}\bar{K}_1\psi_f + \bar{B}\bar{K}_2[w - (-\mathcal{L}_4^{-1}\mathcal{L}_3 \otimes I_n)(\mathbf{1} \otimes x_0)] \\ &+ \bar{B}\bar{K}_3[\hat{h} - (-\mathcal{L}_4^{-1}\mathcal{L}_3 \otimes I_n)h].\end{aligned} \tag{3.41}$$

Select K_{1i} such that $A_i + B_iK_{1i}, i \in \mathbb{F}$ is Hurwitz. From Lemma 3.18 and 3.19, we know $w \to (-\mathcal{L}_4^{-1}\mathcal{L}_3 \otimes I_n)(\mathbf{1} \otimes x_0)$ and $\hat{h} \to (-\mathcal{L}_4^{-1}\mathcal{L}_3 \otimes I_n)h$ as $t \to \infty$. So based on $\lim_{t\to\infty} \psi_f = 0$, we obtain $\lim_{t\to\infty} \tilde{x}_f = 0$.

From (3.6) in Definition 3.5, define the heterogeneous containment error for follower i as $e_i = y_i - y, y \in co(y_l), i \in \mathbb{F}$, then $e_f = [e_{N+1}^T, \ldots, e_{N+L}^T]^T = y_f - (-\mathcal{L}_4^{-1}\mathcal{L}_3 \otimes I_q)y_l$. From the definition of heterogeneous TVF tracking error $e = y_l - (I_N \otimes C_0)(h + \mathbf{1} \otimes x_0)$ in (3.32), we have

$$\begin{aligned}e_f =&\bar{C}\tilde{x}_f + \bar{C}\mathfrak{X}_f(-\mathcal{L}_4^{-1}\mathcal{L}_3 \otimes I_n)(\mathbf{1} \otimes x_0) + \bar{C}\mathfrak{X}_{hf}(-\mathcal{L}_4^{-1}\mathcal{L}_3 \otimes I_n)h \\ &- (-\mathcal{L}_4^{-1}\mathcal{L}_3 \otimes I_q)[e + (I_N \otimes C_0)(h + \mathbf{1} \otimes x_0)].\end{aligned} \tag{3.42}$$

Based on $\lim_{t\to\infty} e = 0$ in the proof of Theorem 3.15 and $\lim_{t\to\infty} \tilde{x}_f = 0$, similar as the calculation of (3.32), we get $\lim_{t\to\infty} e_f = 0$, i.e., the fully distributed heterogeneous output time-varying FC control problem is solved.

3.4 Summary

Contributions

- √ Reveal the essence of linking the heterogeneous TVF tracking and containment control together to achieve the heterogeneous FC control, i.e. Eqs. (3.33), (3.34) and (3.35).
- √ Propose a new format of TVF shape which can be designed independently, not based on the virtual leader's dynamics.
- √ Fully distributed controllers for FC control of heterogeneous general linear MASs are for the first time designed, which can be applied to large-scale systems.

Part II

Cooperative control with delays and disturbances

Introduction

After our work about fully distributed controller design for TVF and time-varying FC control problems is done in **Part** I, we find out that if we put the TVF shape propositions and the fully distributed property away, the controllers in **Part** I will become similar as most of other existing works, which are consensus-based formation or containment controllers. It means the consensus controller technique could be regarded as one key technique behind formation or containment control techniques. The difference is that the consensus controller structure is much simpler. So in this part, we decide to research on consensus control first, then go to more and more complicated scenarios, i.e., TVF, time-varying FC.

The consensus or synchronization problem, which is a fundamental cooperative control problem of linear MASs, has been researched extensively during the past decades. One of the main focuses in consensus problems is how to deal with different agent dynamics, i.e., from single-integrator (Olfati-Saber & Murray, 2004), double-integrator (Ren, 2007), to general linear dynamics (Li *et al.*, 2010, Scardovi & Sepulchre, 2009).

It should be pointed out that the above works deal with homogeneous dynamics. From a practical point of view, the heterogeneous MAS consisting of different dynamics and different state dimensions is more applicable in reality and therefore, recently, it has been investigated broadly varying from double integrator UGVs and unicycle dynamics UAVs (Tanner & Christodoulakis, 2007) to the first-order and second-order systems (Liu & Liu 2011, 2013, Zheng *et al.* 2011), heterogeneous high-order (Rezaei & Menhaj, 2018, Tian & Zhang, 2012) and general liner systems (Lunze 2012, Mu & Shi 2018, Seyboth *et al.* 2015, 2016, Wieland *et al.* 2011). Since the state consensus is not achievable for the heterogeneous MAS if the state dimensions are different, the output regulation theory is adopted to solve the *output consensus problem* which is a terminology presented in Kim *et al.* (2011). Nowadays, more complicated situations associated with output consensus for heterogeneous MASs are considered, e.g., the uncertain linear dynamics (Kim *et al.*, 2011, Lunze, 2012, Yaghmaie *et al.*, 2016), the aperiodic sampled-data communications (Zhang *et al.*, 2018b), the switching topology (Meng *et al.*, 2017), the communication delay (Liu & Liu, 2011, Tian & Zhang, 2012) and the uncertain leader (Cai *et al.*, 2017, Wu *et al.*, 2017), to name a few. Among the above-mentioned references, the protocols (Kim *et al.*, 2011, Meng *et al.*, 2017, Seyboth *et al.*, 2016, Wu *et al.*, 2017, Yaghmaie *et al.*, 2016, Zhang *et al.*, 2018b) are related to the eigenvalue information of the Laplacian matrix of communication topology which is a piece of global information, thus those protocols are not fully distributed. It is worthy to emphasize here that in the large-scale system, it is nearly impossible for each agent to know the eigenvalue information to design its controller. Therefore, designing the control protocol with the fully distributed property is important, necessary and challenging. **To our best knowledge,**

the output consensus tracking (OCT) problem for heterogeneous linear MAS considering the input/output delays and disturbances has not been fully addressed in current existing literatures, which is one of the researching topics of this part.

As we know, the delay effect can deteriorate the convergence of consensus controller from being stable to unstable. The motivation of researching on TDSs is stated out in Chapter 1.1.5. In addition to the delay effect, the disturbance is another main factor to influence the system's convergent performance. One of the fundamental ideas is to design an observer mechanism to estimate the disturbance, and then incorporate the designed observer into input controller to compensate the effect of disturbance. This disturbance observer technique was firstly presented for a robotic system in the late 1980s, where an observer was proposed to estimate external disturbance in Nakao *et al.* (1987). Recently, this technique was applied on MASs to deal with external disturbances in considerable works (Cao *et al.* 2015, Wang *et al.* 2016b, 2017d, 2018b). **The controllers in those works can be categorized in the domain of disturbance observer based control (DOBC) theory which is also the interest of this part in this thesis**. The disturbance attenuation and rejection problems have been investigated thoroughly for the single agent and the homogeneous MASs. Readers could refer to the survey paper (Chen *et al.*, 2016, Guo & Cao, 2014, Madoński & Herman, 2015) for details.

For **homogeneous MASs**, Tian & Liu (2009) solved the robust leader-following consensus of second-order MASs with diverse input delays by using the frequency-domain method. The state consensus of linear MASs with communication and input delays was investigated in Zhou & Lin (2014) while the drawbacks are that the open-loop dynamics of agents need to be not exponentially unstable and that the protocols are not fully distributed. The reason is that the parameters inside control protocols are related to the Laplacian matrix of communication topology which is a piece of global information. Recently, the work in Ponomarev *et al.* (2018) was about the leaderless consensus issue using the discrete-time predictor feedback technique. However, the disturbance which may deteriorate the controlling stability is not considered and the protocol is not fully distributed as well. The leaderless consensus (Wang & Ding, 2016, Zuo *et al.*, 2017) and leader-follower consensus (Wang *et al.* 2017a, 2018a) considering constant input/output delay and matched disturbances were investigated. The drawback is that the latter results assume the leader without control input (not an unknown leader whose input is nonzero). In addition, all the above four latest results are not fully distributed. Another latest work concerning the fully distributed consensus tracking with disturbance rejection problem is in Sun *et al.* (2018) where the leader is treated without control input too, which means that the leader's dynamics is known once its initial state is known. In Chapter 4.2, we deal further with an unknown leader. What is more, the work Sun *et al.* (2018) does not consider the time-delay effect that exists commonly in networked control systems and that can deteriorate the

system stability heavily. **In Chapter 4, the work covers the control input delay problem**.

It should be pointed out that those above works focus on the homogeneous dynamics. In terms of delays for **heterogeneous MASs**, Liu & Liu (2013) adopted a dynamical consensus algorithm for the first-order and second-order system based on frequency-domain analysis. However, the communication topology needs to be undirected, which consumes obviously much more energies than the directed topology. Seyboth *et al.* (2016) formulated the reference tracking and disturbance signals as a distributed output regulation problem and presented a distributed regulator for heterogeneous linear MASs. However, the protocol is not fully distributed.

From the above analysis, we can see that using the frequency-domain method to tackle heterogeneous general linear MASs considering the input delay under the directed topology is very difficult. In the time-domain, the FSA and model reduction approaches introduced in Chapter 1.3 are usually utilized with the introduction of a state predictor to transform the homogeneous input-delay system into a delay-free one. But for the heterogeneous MASs, given that each agent's state could be of any state dimension, **how to design the corresponding novel state predictor to achieve the output consensus is one main challenge and is for the first time solved in Chapter 5 as one of the main contributions**.

Among above works, the output delay is usually not considered. The challenge is that the classic Luenberger observer can be used to estimate the normal output, but not the delayed output. **We use the descriptor approach introduced in Chapter 1.3 to deal with time-varying output delay in Chapter 6**. It is nice to declare that the controllers in Chapter 6, which deals with constant input delay, time-varying output delay and matched disturbance, are still fully distributed for heterogeneous LTI MASs.

All the work until now, only the matched disturbances, which are in the same channels as the control inputs, are considered. In reality, mismatched disturbances, which do not appear in the same channels as control inputs, exist widely in MASs. For example, in multi-missile systems, the lumped disturbance torques caused by unmodelled dynamics, external winds, and parameter variations, affect the missiles directly rather than through the input channels (Chen, 2003). And for multi-hydraulic manipulator systems, the environmental forces and manipulator model uncertainties are in different channels from actuator inputs (Zeng & Sepehri, 2005). As mismatched disturbances influence agents via different channels (not input channel), these disturbances cannot be directly suppressed by feedback controllers, meaning that dealing with the mismatched disturbances is more challenging. Recently, the research on consensus control of MASs with mismatched disturbances differs from the dynamics such as linear high-order (Wang, Li & Lam, 2016b), nonlinear high-order (Wang, Wen & Huang (2017c), Wang, Li & Chen (2018b)). The communication topology in above three works is undirected,

and the important delay effects are not considered there. Inspired by Najafi *et al.* (2013), **Appendix A gives an attempt to tackle the consensus tracking problem for homogeneous general linear MASs considering the time-varying input/output delays and mismatched disturbances under directed communication topology**.

The structure of this part can be reminded in Fig 3.8.

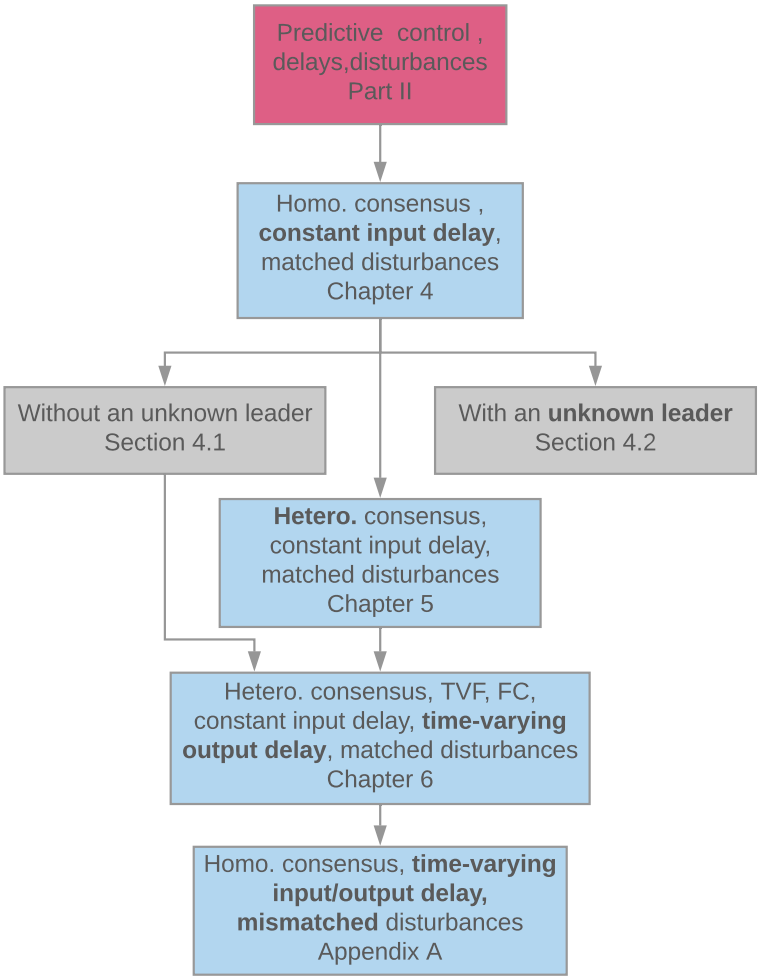

Figure 3.8: Organization of Part II (Homo.:homogeneous; Hetero.:heterogeneous).

Chapter 4

Constant input delay & matched disturbances

Contents

In this chapter, the problem of disturbance rejection/attenuation for constant-input delayed LTI MASs with the directed communication topology is tackled, where the FSA approach introduced in Chapter 1.3 is adopted to transform the delayed MAS into the delay-free one. First, when the leader has no control input, a novel adaptive predictive extended state observer (APESO) using only relative state information of neighboring agents is designed to achieve disturbance-rejected consensus tracking. The stabilization analysis is presented via the Lyapunov function and sufficient conditions are derived in terms of LMIs. Then the result is extended to disturbance-attenuated case where the leader has bounded control input which is only known by a portion of followers. Different from Chapter 2.5 which uses discontinuous function (2.45) to deal with leader's bounded input, in Section 4.2, the continuous function (4.24) is utilized instead. The main contribution focuses on the design of APESO protocols with the fully distributed property. To our best knowledge, this is the first time proposing the fully distributed controller to address the consensus tracking problem with an unknown leader under the directed communication topology considering the input delay and disturbances.

Since there are many variables in this chapter, some may coincide with those in the previous chapter. Fortunately, these variables will be defined clearly here.

In this chapter, a group of $N+1$ agents with identical linear dynamics is described as

$$\dot{x}_i(t) = Ax_i(t) + Bu_i(t-\tau) + Ew_i(t), \quad i \in \mathbf{I}[0, N] \tag{4.1}$$

where $x_i(t) = [x_{i1}(t), \ldots, x_{in}(t)]^T \in \mathbb{R}^n$ and $u_i(t) \in \mathbb{R}^p$ are the state, control input of the i-th agent, respectively. $A \in \mathbb{R}^{n\times n}, B \in \mathbb{R}^{n\times p}$ and $E \in \mathbb{R}^{n\times s}$ are constant matrices. τ is the system's control input delay. $w_i(t) \in \mathbb{R}^s$ is the corresponding external disturbance which is generated by the following exosystem

$$\dot{w}_i(t) = Sw_i(t), \quad i \in \mathbf{I}[0, N] \tag{4.2}$$

with $S \in \mathbb{R}^{s\times s}$ being a known constant matrix.

Assumption 4.1 *$\tau > 0$ is constant and known.*

Assumption 4.2 *(A, B) is controllable.*

Similar as in Chapter 2, agents in (4.1) indexed by $1, \ldots, N$ are the followers denoted as $\mathbb{F} \triangleq \{1, \ldots, N\}$ and agent 0 is the leader which receives no information from the followers. Note that the leader's state information is only available to a subset of followers. The leader is regarded without the control input in Section 4.1, i.e., $u_0(t) = 0$. Furthermore, as the reason to deal with leader whose input is nonzero, i.e., $u_0(t) \neq 0$, is stated out clearly in Chapter 2, in Section 4.2, we deal with the disturbance-attenuating consensus control in a fully distributed fashion, which is more difficult than the case of $u_0(t) = 0$.

The communication topology satisfies Assumption 2.6 where the Laplacian matrix $\mathcal{L}$ can be partitioned as $\mathcal{L} = \begin{bmatrix} 0 & 0_{1\times N} \\ \mathcal{L}_2 & \mathcal{L}_1 \end{bmatrix}$, where $\mathcal{L}_1 \in \mathbb{R}^{N\times N}, \mathcal{L}_2 \in \mathbb{R}^{N\times 1}$. Under Assumption 2.6, all the eigenvalues of $\mathcal{L}_1$ have positive real parts. It is also easy to confirm that $\mathcal{L}_1$ is a nonsingular M-matrix.

Assumption 4.3 *There exists a matrix $F \in \mathbb{R}^{p\times s}$ such that $E = BF$, meaning that the disturbance is matched. The eigenvalues of S are distinct and on the imaginary axis. (S, E) is observable.*

The assumption of eigenvalues of S assures the external disturbance $w_i(t), i \in \mathbf{I}[0, N]$ to be the non-vanishing harmonic disturbance including constants and sinusoidal functions, which is commonly used for the output regulation and disturbance rejection. In addition, the matched disturbances could be relaxed and be transformed to unmatched ones in some circumstances (Isidori, 2013). The detailed explanation of Assumption 4.3 can be refered to the Remark 1 in Ding (2015b).

If $w_i(t), i \in \mathbf{I}[0, N]$ is known, the disturbance rejection is quite straightforward by adding the term $-F(w_i(t) - w_0(t))$ in the control input $u_i(t)$. The key issue here is to design fully distributed observers to estimate those unknown disturbances under the directed graph $\mathcal{G}$ satisfying Assumption 2.6. The disturbance state $w_i(t)$ is expected to be observable from the system state measurement $x_i(t), i \in \mathbf{I}[0, N]$. For this purpose, inspired by Ding (2015b), we propose the following lemma.

Lemma 4.4 (Jiang *et al.* (2018a)) *If (S, E) is observable, then the pair (A_T, T) is observable, with $A_T = \begin{bmatrix} A & e^{A\tau}E \\ 0 & S \end{bmatrix}$ and $T = \begin{bmatrix} I & 0 \end{bmatrix}$.*

Proof. Let us prove the result by seeking a contradiction. Assume that (A_T, T) is not observable, there exists an eigenvalue λ_i of A_T, such that the matrix

$$\begin{bmatrix} \lambda_i I - A & -e^{A\tau}E \\ 0 & \lambda_i I - S \\ I & 0 \end{bmatrix}$$

is rank deficient, i.e., there exists a nonzero vector $\eta = [\eta_1^T, \eta_2^T]^T \in \mathbb{R}^{(n+s)}$ such that

$$\begin{bmatrix} \lambda_i I - A & -e^{A\tau}E \\ 0 & \lambda_i I - S \\ I & 0 \end{bmatrix} \begin{bmatrix} \eta_1 \\ \eta_2 \end{bmatrix} = 0.$$

This implies that

$$\eta_1 = 0, \begin{bmatrix} -e^{A\tau}E \\ \lambda_i I - S \end{bmatrix} \eta_2 = 0. \tag{4.3}$$

Since $\eta_1 = 0$, we get $\eta_2 \neq 0$.

It is known that $\det(e^{A\tau}) = e^{\text{trace}(A\tau)} > 0$, which means $e^{A\tau}$ is invertible, i.e., $rank(e^{A\tau}) = n$. From $-e^{A\tau}E\eta_2 = 0$ in (4.3) we have $\begin{bmatrix} -E \\ \lambda_i I - S \end{bmatrix} \eta_2 = 0$, which implies, together with $\eta_2 \neq 0$, that (S, E) is not observable. This is a contradiction, meaning that (A_T, T) must be observable.

Since (A_T, T) is observable, there exists a positive definite matrix P that satisfies the following LMI:

$$PA_T + A_T^T P - 2T^T T < 0. \tag{4.4}$$

This chapter mainly focuses on how to design fully distributed adaptive protocols to address consensus tracking problems the constant considering input delay and matched disturbances with the directed communication topology. Section 4.1 solves the consensus tracking problem with the leader of no control input based

only on relative state measurements. After that, the extended case of the leader with bounded input is studied in Section 4.2.

Define the consensus tracking error as $\tilde{x}_i(t) = x_i(t) - x_0(t)$. The objective here is to prove the convergence of $\tilde{x}_i(t)$ for any initial state $x_0(0)$ and $x_i(0), i \in \mathbb{F}$.

4.1 Homogeneous consensus tracking control without $u_0(t)$

The dynamics of $\tilde{x}_i(t)$ is

$$\dot{\tilde{x}}_i(t) = A\tilde{x}_i(t) + Bu_i(t-\tau) + E\bar{w}_i(t), i \in \mathbb{F} \tag{4.5}$$

where $\bar{w}_i(t) = w_i(t) - w_0(t)$. Here, we concern about the disturbance rejection $\bar{w}_i(t)$ and control input delay $u_i(t-\tau)$.

Firstly, if there is no input delay and suppose the disturbance $w_i, i \in \mathbf{I}[0, N]$ is known, the method of disturbance rejection is quite easy by adding a term $-F\bar{w}_i(t)$ in $u_i, i \in \mathbb{F}$. So the key technique is to estimate $\bar{w}_i(t)$ by designing a fully distributed disturbance observer $\hat{w}_i(t)$. This is one of main contributions in this chapter and will be explained in detail later.

Then, in terms of input delay $u_i(t-\tau), i \in \mathbb{F}$, inspired by the FSA approach introduced in Chapter 1.3 which can be utilized and modified to transform the system (4.1) with a delayed input into a delay-free system, the variable transformation for each follower i is designed as follows:

$$\tilde{Z}_i(t) = e^{A\tau}\tilde{x}_i(t) + \int_{t-\tau}^{t} e^{A(t-s)}[Bu_i(s) + Ee^{S\tau}\hat{w}_i(s)]ds. \tag{4.6}$$

Remark 4.5 *Here, the link between the consensus tracking error $\tilde{x}_i(t)$ and transformed variable $\tilde{Z}_i(t)$ is established, which is one main difficulties in this chapter.*

Let us define an augmented state $Z_i(t) = [\tilde{Z}_i(t)^T, \bar{w}_i(t)^T]^T$ and apply the transformation (4.6) on system (4.5), then

$$\dot{Z}_i(t) = \underbrace{\begin{bmatrix} A & e^{A\tau}E \\ 0 & S \end{bmatrix}}_{A_T} Z_i(t) + \underbrace{\begin{bmatrix} B \\ 0 \end{bmatrix}}_{\bar{B}} u_i(t) + \begin{bmatrix} Ee^{S\tau} \\ 0 \end{bmatrix} \hat{w}_i(t) - \begin{bmatrix} e^{A\tau}Ee^{S\tau} \\ 0 \end{bmatrix} \hat{w}_i(t-\tau) \tag{4.7}$$

where $A_T \in \mathbb{R}^{(n+s)\times(n+s)}, \bar{B} \in \mathbb{R}^{(n+s)\times p}$.

The idea is to design the fully distributed ESO as $\bar{Z}_i(t) = [v_i^T(t), \hat{w}_i^T(t)]^T, i \in \mathbb{F}$ to estimate the extended state $Z_i(t) = [\tilde{Z}_i^T(t), \bar{w}_i^T(t)]^T$, which will be elaborated in detail in the following. According to (4.7), the control input for each follower i could be designed as

$$u_i(t) = (\underbrace{\begin{bmatrix} K_1 & 0 \end{bmatrix}}_{\bar{K}_1} - \underbrace{\begin{bmatrix} 0 & Fe^{S\tau} \end{bmatrix}}_{\bar{F}})\bar{Z}_i(t), i \in \mathbb{F} \tag{4.8}$$

such that

$$\dot{\tilde{Z}}_i(t) = (A + BK_1)\tilde{Z}_i(t) + BK_1\tilde{v}_i(t) - e^{A\tau}Ee^{S\tau}\tilde{w}_i(t-\tau) \tag{4.9}$$

where $\tilde{v}_i(t) = v_i(t) - \tilde{Z}_i(t)$ and $\tilde{w}_i(t) = \hat{w}_i(t) - \bar{w}_i(t)$ are observer estimating errors, and $K_1 \in \mathbb{R}^{p\times n}$ is a constant matrix to be designed later.

On the other hand, where is the link among consensus tracking error $\tilde{x}_i(t)$, transformed variable $\tilde{Z}_i(t)$, the ESO $\bar{Z}_i(t)$ and the designed control input $u_i(t)$? The answer is to substitute the designed control input (4.8) into the transformed delay-free system (4.6), generating

$$\tilde{Z}_i(t) = e^{A\tau}\tilde{x}_i(t) + \int_{t-\tau}^{t} e^{A(t-s)}BK_1v_i(s)ds \tag{4.10}$$

which have

$$\|e^{A\tau}\tilde{x}_i(t)\| \leq \|\tilde{Z}_i(t)\| + \tau(\max_{-\tau\leq\theta\leq 0}\|e^{A\theta}\|)\|B\|\|K_1\|\|v_{i,t}(\theta)\|$$

where $v_{i,t}(\theta) := v_i(t+\theta), -\tau \leq \theta \leq 0$. Thus, $e^{A\tau}\tilde{x}_i(t) \to 0$ as $\tilde{Z}_i(t) \to 0$ and $v_i(t) \to 0$. It is known that $det(e^{A\tau}) = e^{tr(A\tau)} > 0$, which means $e^{A\tau}$ is invertible, i.e., $rank(e^{A\tau}) = n$. So the objective here changes to design the ESO $\bar{Z}_i(t)$ such that $\lim_{t\to\infty} v_i(t) = 0, \lim_{t\to\infty}\tilde{Z}_i(t) = 0$ such that $\lim_{t\to\infty}\tilde{x}_i(t) = 0$.

Similar as the network measurement (2.18), the signal denoting weighted linear combination of relative states between agent i and its neighbors is

$$\xi_i(t) = \sum_{j=1}^{N} a_{ij}(x_i(t) - x_j(t)) + a_{i0}(x_i(t) - x_0(t)), i \in \mathbb{F} \tag{4.11}$$

where a_{ij} is the (i,j)-th entry of adjacency matrix $\mathcal{A}$ of graph $\mathcal{G}$. Especially, $a_{i0} = 1$ means the follower i can get information from the leader and cannot otherwise. It is easy to calculate $\xi_i(t) = \sum_{j=1}^{N} a_{ij}[(x_i(t) - x_0(t)) - (x_j(t) - x_0(t))] + a_{i0}\tilde{x}_i(t) = \sum_{j=1}^{N} a_{ij}(\tilde{x}_i(t) - \tilde{x}_j(t)) + a_{i0}\tilde{x}_i(t)$. By using relative state information, denote a

signal similar to (4.11) as

$$\begin{aligned}\varrho_i(t) =& a_{i0}\left[v_i(t)-\int_{t-\tau}^{t}e^{A(t-s)}(Bu_i(s)+Ee^{S\tau}\hat{w}_i(s))ds\right]-e^{A\tau}\xi_i(t)\\ &+\sum_{j=1}^{N}a_{ij}\left\{v_i(t)-v_j(t)-\int_{t-\tau}^{t}e^{A(t-s)}\left[B(u_i(s)-u_j(s))+Ee^{S\tau}(\hat{w}_i(s)-\hat{w}_j(s))\right]ds\right\}\\ &=\sum_{j=0,j\neq i}^{N}a_{ij}\left[v_i(t)-e^{A\tau}\tilde{x}_i(t)-\int_{t-\tau}^{t}e^{A(t-s)}(Bu_i(s)+Ee^{S\tau}\hat{w}_i(s))ds\right]\\ &\quad-\sum_{j=1,j\neq i}^{N}a_{ij}\left[v_j(t)-e^{A\tau}\tilde{x}_j(t)-\int_{t-\tau}^{t}e^{A(t-s)}(Bu_j(s)+Ee^{S\tau}\hat{w}_j(s))ds\right]\\ &=\sum_{j=0,j\neq i}^{N}a_{ij}(v_i(t)-\tilde{Z}_i(t))-\sum_{j=1,j\neq i}^{N}a_{ij}(v_j(t)-\tilde{Z}_j(t))\\ &=l_{ii}\tilde{v}_i(t)+\sum_{j=1,j\neq i}^{N}l_{ij}\tilde{v}_j(t)\\ &=\sum_{j=1}^{N}l_{ij}\tilde{v}_j(t).\end{aligned}\tag{4.12}$$

Remark 4.6 *The signal $\varrho_i(t)$, which will be used in the control protocol design, only needs the relative state information $\xi_i(t)$, the adaptive observer state $v_j(t)$, the stored history of control input $u_j(t-\tau)$ and disturbance observer state $\hat{w}_j(t-\tau)$ of its neighbor $j, j\in\mathbb{F}$ via the communication topology $\mathcal{G}$ on the time interval $[t-\tau,t]$. In real applications, the integral discretization can be used to calculate integral terms. Please refer to Léchappé (2015) on Page 22 for details in which the trapezoidal rule is used. In the Matlab simulations of this thesis, the Matlab function* ***"integral(fun,xmin,xmax,'ArrayValued',true)"*** *is utilized to calculate the matrix integral terms.*

The fully distributed adaptive ESO is designed as

$$\dot{\bar{Z}}_i(t)=\underbrace{\begin{bmatrix}A+BK_1 & 0\\ 0 & S\end{bmatrix}}_{\bar{A}_1}\bar{Z}_i(t)+\underbrace{\begin{bmatrix}K\\ K'\end{bmatrix}}_{\bar{A}_2}(c_i(t)+\rho_i(t))\varrho_i(t)\tag{4.13}$$

where $K\in\mathbb{R}^{n\times n}$ and $K'\in\mathbb{R}^{s\times n}$ will be determined later. $c_i(t)$ denotes the time-varying coupling weight associated with the i-th follower and is used to make the

whole controller fully distributed. $\rho_i(t)$ represents the smooth and nonnegative function. Both $c_i(t)$ and $\rho_i(t)$ are scalers and will be designed later. From (4.9) and (4.13), we have

$$\begin{aligned}\dot{\tilde{v}}_i(t) =&A\tilde{v}_i(t) + e^{A\tau}Ee^{S\tau}\tilde{w}_i(t-\tau) + K(c_i(t)+\rho_i(t))\varrho_i(t),\\ e^{S\tau}\dot{\tilde{w}}_i(t-\tau) =&Se^{S\tau}\tilde{w}_i(t-\tau) + e^{S\tau}K'(c_i(t-\tau)+\rho_i(t-\tau))\varrho_i(t-\tau),\ i\in\mathbb{F}.\end{aligned}$$

Denote $e_i(t) = \begin{bmatrix}\tilde{v}_i(t)\\ e^{S\tau}\tilde{w}_i(t-\tau)\end{bmatrix}, \bar{K} = \begin{bmatrix}K\\ e^{S\tau}K'\end{bmatrix}$. Note here that our objective is to prove $\lim_{t\to\infty}\tilde{x}_i(t) = 0$, so it is equal to have $c_i(t-\tau) = c_i(t), \rho_i(t-\tau) = \rho_i(t)$ and $\varrho_i(t-\tau) = \varrho_i(t)$ when $t\to\infty$, then

$$\dot{e}_i(t) = A_T e_i(t) + \bar{K}(c_i(t)+\rho_i(t))\sum_{j=1}^{N} l_{ij}Te_j(t)$$

where $T = [I\ 0]\in\mathbb{R}^{n\times(n+s)}$. Similar to (4.11) and (4.12), denote a signal as

$$\hat{e}_i(t) = \sum_{j=1}^{N} l_{ij}e_j(t). \tag{4.14}$$

The analysis of $\hat{e}_i(t)$ is similar as Remark 4.6. Define $\hat{e}(t) = [\hat{e}_1^T(t),\dots,\hat{e}_N^T(t)]^T$, $\hat{c}(t) = \mathrm{diag}\{c_1(t),\dots,c_N(t)\}, \hat{\rho}(t) = \mathrm{diag}\{\rho_1(t),\dots,\rho_N(t)\}$ and $e(t) = [e_1^T(t),\dots,e_N^T(t)]^T$, then

$$\begin{aligned}\dot{\hat{e}}(t) =&(\mathcal{L}_1\otimes I_{n+s})\dot{e}(t)\\ =&[I_N\otimes A_T + \mathcal{L}_1(\hat{c}(t)+\hat{\rho}(t))\otimes\bar{K}T]\hat{e}(t).\end{aligned} \tag{4.15}$$

The $c_i(t)$ and $\rho_i(t)$ are designed as follows

$$\begin{aligned}\dot{c}_i(t) =&\hat{e}_i^T(t)\Gamma\hat{e}_i(t),\\ \rho_i(t) =&\hat{e}_i^T(t)P\hat{e}_i(t),\ i\in\mathbb{F}\end{aligned} \tag{4.16}$$

where $c_i(0) > 0$. $\Gamma\in\mathbb{R}^{(n+s)\times(n+s)}$ and $P\in\mathbb{R}^{(n+s)\times(n+s)}$ are the feedback gain matrices to be determined in the following.

Theorem 4.7 (Jiang *et al.* (2018a)) *For the network-connected system with dynamics (4.1) and (4.2), the fully distributed controller of (4.8), (4.13) and (4.16) solves the disturbance-rejecting consensus problem considering the control input delay under Assumptions 4.1-4.3 and 2.6 if $A+BK_1$ is Hurwitz, $\Gamma = T^TT, \bar{K} = -P^{-1}T^T$ and $P>0$ is a solution to the LMI (4.4). Moreover, the coupling weight $c_i(t), i \in \mathbb{F}$ converge to some finite steady-state values.*

Proof. In the proof, we omit symbol (t) for the convenience in writing if there is no special statements.

Let

$$V_{10} = \frac{1}{2}\sum_{i=1}^{N} g_i(2c_i+\rho_i)\rho_i + \frac{1}{2}\sum_{i=1}^{N} g_i(c_i-\beta)^2 \tag{4.17}$$

where $G = \mathrm{diag}\{g_1,\ldots,g_N\} > 0$ is a positive definite matrix such that $G\mathcal{L}_1 + \mathcal{L}_1^T G > 0$. Since $\mathcal{L}_1$ is a nonsingular M-matrix, thus G exists based on Lemma 1.10. Particularly, $g_i, i \in \mathbf{I}[1,N]$ can be constructed as $[g_1,\ldots,g_N]^T = (\mathcal{L}_1^T)^{-1}[1,\ldots,1]^T$ (Li *et al.*, 2015). It is easy to get $c_i(t) > 0, \forall t \geq 0$ based on $\dot{c}_i(t) \geq 0, c_i(0) > 0$ in (4.16). β is a positive constant to be determined. Noting further that $\rho_i \geq 0$, so V_{10} is positive definite. Then

$$\begin{aligned}
\dot{V}_{10} =& \hat{e}^T[G(\hat{c}+\hat{\rho})\otimes(PA_T + A_T^TP) + G(\hat{c}+\hat{\rho}-\beta I)\otimes\Gamma \\
&+ (\hat{c}+\hat{\rho})(G\mathcal{L}_1 + \mathcal{L}_1^TG)(\hat{c}+\hat{\rho})\otimes P\bar{K}T]\hat{e} \\
\leq& \hat{e}^T[G(\hat{c}+\hat{\rho})\otimes(PA_T + A_T^TP) + G(\hat{c}+\hat{\rho}-\beta I)\otimes T^TT \\
&- \lambda_0(\hat{c}+\hat{\rho})^2\otimes T^TT]\hat{e}
\end{aligned} \tag{4.18}$$

where $\lambda_0 > 0$ is the smallest eigenvalue of $G\mathcal{L}_1 + \mathcal{L}_1^TG$. The inequality comes from $G\mathcal{L}_1 + \mathcal{L}_1^TG \geq \lambda_0 I$ (Lemma 1.10). By using Lemma 1.4 we get

$$\hat{e}^T[G(\hat{c}+\hat{\rho})\otimes T^TT]\hat{e} \leq \hat{e}^T[(\frac{\lambda_0}{2}(\hat{c}+\hat{\rho})^2 + \frac{G^2}{2\lambda_0})\otimes T^TT]\hat{e}. \tag{4.19}$$

Substituting (4.19) into (4.18) yields

$$\begin{aligned}
\dot{V}_{10} \leq& \hat{e}^T\{G(\hat{c}+\hat{\rho})\otimes(PA_T + A_T^TP) - [\frac{\lambda_0}{2}(\hat{c}+\hat{\rho})^2 - \frac{G^2}{2\lambda_0} + \beta G]\otimes T^TT\}\hat{e} \\
\leq& \hat{e}^T[G(\hat{c}+\hat{\rho})\otimes(PA_T + A_T^TP - 2T^TT)]\hat{e} \\
\leq& 0.
\end{aligned} \tag{4.20}$$

Given the fact that $a+b \geq 2\sqrt{ab}, \forall a, b \in \mathbb{R}^+$, we have chosen $\beta \geq \frac{5}{2\lambda_0}\max_{i\in\mathbb{F}} g_i$ to get the second inequality. The last inequality comes from LMI (4.4).

So we can conclude that $V_{10}(t)$ is bounded and so are $\hat{e}_i$ and c_i. It follows from (4.16) and $\Gamma = T^T T$ that $\dot{c}_i(t) \geq 0$, thus the coupling weights $c_i(t), i \in \mathbb{F}$ increase monotonically and converge to some finite values finally, which verifies $\lim_{t\to\infty} c_i(t-\tau) = \lim_{t\to\infty} c_i(t)$. Note that $\dot{V}_{10}(t) \equiv 0$ is equivalent to $\hat{e} = 0$. By LaSalle's Invariance principle (Krstic *et al.*, 1995), it follows that $\hat{e}$ asymptotically converges to zero, i.e., $\lim_{t\to\infty} \hat{e} = 0$. So from (4.16), $\lim_{t\to\infty} \rho = 0$ which verifies $\lim_{t\to\infty} \rho(t-\tau) = \lim_{t\to\infty} \rho(t)$.

Recalling that $\hat{e} = (\mathcal{L}_1 \otimes I_{n+s})e$ in (4.15) and $\mathcal{L}_1$ is nonsingular, we prove $\lim_{t\to\infty} e = 0$. Considering $e^{S\tau}$ is invertible, i.e., $rank(e^{S\tau}) = s$, we have $\lim_{t\to\infty} \tilde{v}_i(t) = 0, \lim_{t\to\infty} \tilde{w}_i(t) = 0$. Since $\varrho = (\mathcal{L}_1 \otimes I_n)\tilde{v}$ from (4.12), it is easy to verify $\lim_{t\to\infty} \varrho(t-\tau) = \lim_{t\to\infty} \varrho(t)$.

Recall (4.9) as

$$\dot{\tilde{Z}}_i = (A + BK_1)\tilde{Z}_i + \tilde{K}e_i \tag{4.21}$$

where $\tilde{K} = [BK_1, -e^{A\tau}E]$ and $e_i = [\tilde{v}_i^T, (e^{S\tau}\tilde{w}_i(t-\tau))^T]^T$. Since $A + BK_1$ is Hurwitz and $\lim_{t\to\infty} e_i = 0$, from (4.21) we have $\lim_{t\to\infty} \tilde{Z}_i = 0, i \in \mathbb{F}$.

Thanks to $\lim_{t\to\infty} \tilde{Z} = 0$ and $\lim_{t\to\infty} \tilde{v}_i = 0$, we have $\lim_{t\to\infty} v_i = 0$. As it is known that $e^{A\tau} > 0$, from (4.10), we prove that the consensus tracking error $\lim_{t\to\infty} \tilde{x}(t) = 0$, i.e., the proof is finished.

Remark 4.8 *It is worth noting that for each follower i, the variable $\varrho_i(t)$ is very important for the fully distributed adaptive ESO design in (4.13). The detailed explanation can be referred to Remark 4.6.*

Remark 4.9 *In contrast to the result Wang et al. (2017a) where the consensus disturbance rejection problem of network-connected dynamic systems with input delay under the undirected communication topology is solved, the distinctive feature of our whole control are twofolds: i) our controller is fully distributed; ii) the communication topology is directed, which could save tremendous communication resources compared with the undirected topology.*

For the case there is no time-delay in the control input, we simply change $\tilde{v}_i, e_i$ as $\tilde{v}_i = v_i - \tilde{x}_i, e_i = [\tilde{v}_i^T, \tilde{w}_i^T]^T$, and modify the control input from (4.8) to the following

$$u_i(t) = \begin{bmatrix} K_1 & -F \end{bmatrix} \bar{Z}_i(t), i \in \mathbb{F}. \tag{4.22}$$

Then the consensus disturbance rejection problem under Assumptions 4.2, 2.6 and 2.6 is solved with the controller of (4.22), (4.13) and (4.16). Specifically, (4.15) changes to

$$\dot{\hat{e}}(t) = [I_N \otimes A_T' + \mathcal{L}_1(\hat{c}(t) + \hat{\rho}(t)) \otimes \bar{K}'T]\hat{e}(t)$$

where $A_T^{'} = \begin{bmatrix} A & E \\ 0 & S \end{bmatrix}$, $\bar{K}' = \begin{bmatrix} K \\ K' \end{bmatrix}$ and $T = \begin{bmatrix} I & 0 \end{bmatrix}$. From Lemma 1 of Ding (2015b) it is known that $(A_T^{'}, T)$ is observable. The other parameters can be calculated similarly as the proof of Theorem 4.7 and the detail is omitted here.

4.2 Homogeneous consensus tracking control with $u_0(t)$

In this section,the consensus tracking problem with leader's control input satisfying Assumption 2.16 is investigated. Correspondingly, Eqs. (4.5) and (4.6) change to

$$\begin{aligned} \dot{\tilde{x}}_i(t) =& A\tilde{x}_i(t) + B(u_i(t-\tau) - u_0(t-\tau)) + E\bar{w}_i(t), \\ \tilde{Z}_i(t) =& e^{A\tau}\tilde{x}_i(t) + \int_{t-\tau}^{t} e^{A(t-s)}[B(u_i(s) - u_0(s)) + Ee^{S\tau}\hat{w}_i(s)]ds. \end{aligned} \tag{4.23}$$

Considering the leader's bounded input $u_0(t)$, the following continuous nonlinear function $z(\cdot)$

$$z_i(x) = \begin{cases} \frac{x}{\|x\|} & \text{if } \|x\| > \sigma_i, \\ \frac{x}{\sigma_i} & \text{if } \|x\| \leq \sigma_i \end{cases} \tag{4.24}$$

is used to compensate the leader's input effect to the whole cooperative system. In this case, the format of control input remains the same as (4.8) as

$$u_i(t) = (\bar{K}_1 - \bar{F})\bar{Z}_i(t), i \in \mathbb{F} \tag{4.25}$$

such that $\tilde{Z}_i(t)$ in (4.23) changes to

$$\dot{\tilde{Z}}_i(t) = (A + BK_1)\tilde{Z}_i(t) + BK_1\tilde{v}_i(t) - e^{A\tau}Ee^{S\tau}\tilde{w}_i(t-\tau) - Bu_0(t). \tag{4.26}$$

The ESO $\bar{Z}_i(t) = [v_i(t)^T, \hat{w}_i(t)^T]^T$ is modified as

$$\begin{aligned} \dot{\bar{Z}}_i(t) =& \bar{A}_1\bar{Z}_i(t) + \bar{A}_2(c_i(t) + \rho_i(t))\varrho_i(t) - \bar{B}\alpha z(\tilde{\zeta}_i(t)), \\ \dot{c}_i(t) =& \hat{e}_i^T(t)\Gamma\hat{e}_i(t) - \epsilon_i(c_i(t) - \beta_1), \\ \rho_i(t) =& \hat{e}_i^T(t)P\hat{e}_i(t),\ i \in \mathbb{F} \end{aligned} \tag{4.27}$$

where $\bar{A}_1, \bar{A}_2$ are defined in (4.13) , $\tilde{\zeta}_i(t) = \bar{B}^T P\hat{e}_i(t)$, $c_i(0) \geq \beta_1 \geq 1$, and $\alpha, \beta_1, \epsilon_i$ are positive constants. Other variable formats are the same as in Section 4.1.

(4.15) changes to the following nonautonomous system $\dot{\hat{e}}(t) = f(\hat{e}(t), t)$ as

$$\begin{aligned}\dot{\hat{e}}(t) =&[I_N \otimes A_T + \mathcal{L}_1(\hat{c}(t) + \hat{\rho}(t)) \otimes \bar{K}T]\hat{e}(t) \\ &- (\mathcal{L}_1 \otimes \bar{B})[\alpha z(\tilde{\zeta}(t)) - \mathbf{1} \otimes u_0(t)].\end{aligned} \tag{4.28}$$

Remark 4.10 *From $\tilde{Z}_i(t)$ in (4.23), $\tilde{\zeta}_i(t) = \bar{B}^T P\hat{e}_i(t)$ and $\varrho_i(t) = a_{i0}\tilde{v}_i(t) + \sum_{j=1}^{N} a_{ij}(\tilde{v}_i(t) - \tilde{v}_j(t))$ with $\tilde{v}_i(t) = v_i(t) - \tilde{Z}_i(t)$ in (4.27), we can see only a subset of followers need the historical information of leader's control input, i.e., $u_0(t-\tau)$.*

Theorem 4.11 (Jiang *et al.* (2018a)) *For the network-connected system with dynamics (4.1) and (4.2), the fully distributed controller of (4.25) and (4.27) solves the consensus disturbance attenuation problem considering the input delay with the leader of bounded input under Assumptions 4.1-4.3, 2.6 and 2.16, if $A + BK_1 = \mathrm{diag}\{p_1, p_2, \ldots, p_n\}$, where $p_i < 0, i \in \boldsymbol{I}[1, n]$ is the eigenvalues of $A + BK_1$, $\Gamma = T^T T, \bar{K} = -P^{-1}T^T$, $\alpha \geq \epsilon$ and $P > 0$ is the solution to the following LMI*

$$PA_T + A_T^T P + \mu P - 2T^T T < 0 \tag{4.29}$$

where $\mu > 1$. The consensus tracking error $\tilde{x}_i(t)$ converges exponentially to the residual set

$$\Pi = \left\{\tilde{x}_i(t) : \|\tilde{x}_i(t)\| \leq \|\tilde{Z}_i(t-\tau)\| + \chi\|E\|\,\|e^{S\tau}\tilde{w}_i(t-\tau)\|\right\} \tag{4.30}$$

where $\chi = \|\int_{-\tau}^{0} e^{As}ds\|$. $\tilde{Z}_i(t)$ and $\tilde{w}_i(t)$ satisfy (4.50) and (4.47) in the following proof, respectively. Besides, $c_i(t), i \in \mathbb{F}$ are uniformly ultimately bounded.

Proof. In the proof, the symbol (t) is omitted. The Lyapunov function candidate is the same as (4.17), and after the same calculation as in the proof of Theorem 4.7, (4.20) changes to

$$\dot{V}_{10} \leq -\hat{e}^T[G(\hat{c} + \hat{\rho}) \otimes \mathcal{H}]\hat{e} - \sum_{i=1}^{N} g_i(c_i - \beta)\epsilon_i(c_i - \beta_1) + \Omega \tag{4.31}$$

where $\mathcal{H} = -(PA_T + A_T^T P - 2T^T T) > 0$ and $\Omega = -2\hat{e}^T[G(\hat{c}+\hat{\rho})\mathcal{L}_1 \otimes P\bar{B}][\alpha z(\tilde{\zeta}(t)) - \mathbf{1} \otimes u_0(t)]$.

Firstly, we come to deal with the leader's bounded input $u_0(t)$ and the nonlinear function $z(\cdot)$ in Ω. Using the Laplacian matrix property $\mathcal{L}_1\mathbf{1} = -\mathcal{L}_2$ and Assumption 2.16, we get

$$\begin{aligned}\hat{e}^T[G(\hat{c}+\hat{\rho})\mathcal{L}_1 \otimes P\bar{B}](\mathbf{1}\otimes u_0(t)) &= \sum_{i=1}^{N}[g_i(c_i+\rho_i)\hat{e}_i^T P\bar{B}a_{i0}u_0(t)] \\ &\leq \sum_{i=1}^{N} g_i(c_i+\rho_i)\|\bar{B}^T P\hat{e}_i\|a_{i0}\epsilon.\end{aligned} \tag{4.32}$$

On the other hand, considering the following three cases.

i) $\|\bar{B}^T P\hat{e}_i\| > \sigma_i, i \in \mathbb{F}$, then

$$\begin{aligned}\hat{e}_i^T P\bar{B}z(\bar{B}^T P\hat{e}_i) =& \hat{e}_i^T P\bar{B}\frac{\bar{B}^T P\hat{e}_i}{\|\bar{B}^T P\hat{e}_i\|} = \|\bar{B}^T P\hat{e}_i\|, \\ \hat{e}_i^T P\bar{B}z(\bar{B}^T P\hat{e}_j) \leq& \|\hat{e}_i^T P\bar{B}\|\left\|\frac{\bar{B}^T P\hat{e}_j}{\|\bar{B}^T P\hat{e}_j\|}\right\| = \|\bar{B}^T P\hat{e}_i\|.\end{aligned}$$

Here is the reason we choose $\tilde{\zeta}_i(t) = \bar{B}^T P\hat{e}_i$, then

$$\begin{aligned}-\hat{e}^T[G(\hat{c}+\hat{\rho})\mathcal{L}_1 \otimes P\bar{B}]\alpha z(\tilde{\zeta}(t)) =& -\sum_{i=1}^{N}\{g_i(c_i+\rho_i)\alpha\hat{e}_i^T P\bar{B}[a_{i0}z(\bar{B}^T P\hat{e}_i) \\ &+ \sum_{j=1}^{N} a_{ij}(z(\bar{B}^T P\hat{e}_i) - z(\bar{B}^T P\hat{e}_j))]\} \\ \leq& -\sum_{i=1}^{N} g_i(c_i+\rho_i)\|\bar{B}^T P\hat{e}_i\|a_{i0}\alpha.\end{aligned} \tag{4.33}$$

Combining (4.33) and (4.32) with $\alpha \geq \epsilon$, we have

$$\Omega \leq 0. \tag{4.34}$$

ii) $\|\bar{B}^T P\hat{e}_i\| \leq \sigma_i, i \in \mathbb{F}$, then

$$\|z(\bar{B}^T P\hat{e}_j)\| = \|\frac{\bar{B}^T P\hat{e}_j}{\sigma_j}\| \leq 1.$$

Due to $a_{ij} = 0/1$ in $\mathcal{A}$ of the graph $\mathcal{G}$, we get

$$\begin{aligned}\Omega &\leq \sum_{i=1}^{N} g_i[2(c_i-\beta_1)+2\rho_i+2\beta_1][a_{i0}\epsilon+(2N-1)\alpha]\sigma_i \\ &\leq \sum_{i=1}^{N}\frac{g_i\epsilon_i}{4}(c_i-\beta_1)^2+\sum_{i=1}^{N}\frac{\lambda_{min}(\mathcal{H})}{2\lambda_{max}(P)}g_i\rho_i^2+\Xi_1'\end{aligned} \tag{4.35}$$

where

$$\Xi_1' = \sum_{i=1}^{N} g_i\sigma_i[a_{i0}\epsilon+(2N-1)\alpha]\left\{2\beta_1+(\frac{4}{\epsilon_i}+\frac{2\lambda_{max}(P)}{\lambda_{min}(\mathcal{H})})\sigma_i[a_{i0}\epsilon+(2N-1)\alpha]\right\}. \tag{4.36}$$

iii) $\hat{e}_i, i \in \mathbb{F}$ satisfy neither case i) nor case ii). Generally, assume $\|\bar{B}^T P\hat{e}_i\| > \sigma_i, i = 1,\ldots,k$, and $\|\bar{B}^T P\hat{e}_i\| \leq \sigma_i, i = k+1,\ldots,N$, then

$$\Omega \leq 2\sum_{i=k+1}^{N} g_i(c_i+\rho_i)[a_{i0}\epsilon+(2N-1)\alpha]\sigma_i. \tag{4.37}$$

Comparing (4.34), (4.35) and (4.37), we find out that Ω satisfies (4.35). Note that

$$\begin{aligned}-(c_i-\beta)(c_i-\beta_1) &= -(c_i-\beta)^2-(c_i-\beta)(\beta-\beta_1) \\ &\leq -\frac{1}{2}(c_i-\beta)^2+\frac{1}{2}(\beta-\beta_1)^2\end{aligned}$$

and

$$\begin{aligned}-(c_i-\beta)(c_i-\beta_1) &= -(c_i-\beta_1)^2-(\beta_1-\beta)(c_i-\beta_1) \\ &\leq -\frac{1}{2}(c_i-\beta_1)^2+\frac{1}{2}(\beta-\beta_1)^2.\end{aligned}$$

Then substituting above two inequalities and (4.35) into (4.31), we obtain

$$\dot{V}_{10} \leq -\frac{1}{2}\hat{e}^T[G(\hat{c}+\hat{\rho})\otimes\mathcal{H}]\hat{e}-\sum_{i=1}^{N}\frac{g_i\epsilon_i}{4}(c_i-\beta)^2+\Xi_1, \tag{4.38}$$

where

$$\Xi_1 = \frac{(\beta-\beta_1)^2}{2}\sum_{i=1}^{N} g_i\epsilon_i+\Xi_1'. \tag{4.39}$$

Thanks to $\mu > 1, P > 0$ and the LMI (4.29), we have $\mathcal{H} > (\mu-1)P > 0$. What is

more, $\sum_{i=1}^{N} \frac{g_i \epsilon_i}{4}(c_i - \beta)^2 \geq 0$, then

$$\dot{V}_{10} \leq -\frac{1}{2}\hat{e}^T[G(\hat{c}+\hat{\rho}) \otimes \mathcal{H}]\hat{e} + \Xi_1. \tag{4.40}$$

Define the continuous function $\mathcal{K}_3(\|\hat{e}\|) = \hat{e}^T[G(\hat{c}+\hat{\rho}) \otimes \mathcal{H}]\hat{e}$. Because of $G(\hat{c}+\hat{\rho}) > 0$ and $\mathcal{H} > 0$, it is easy to verify $\mathcal{K}_3$ belongs to class $\mathcal{K}$ function. Considering $\Xi_1 > 0$, from (4.40) and Lemma 1.3, it is easy to conclude that $\hat{e}(t)$, which is the solution of the nonautonomous system $\dot{\hat{e}} = f(\hat{e}, t)$ in (4.28), is uniformly ultimately bounded.

Secondly, considering $\rho_i \geq 0$, from (4.17) we get

$$\kappa_1 V_{10} \leq \kappa_1 \sum_{i=1}^{N} g_i(c_i + \rho_i)\hat{e}_i^T P \hat{e}_i + \sum_{i=1}^{N} \frac{\kappa_1 g_i}{2}(c_i - \beta)^2 \tag{4.41}$$

where $\kappa_1 > 0$ is a small positive constant to be designed later. Combine (4.38) and (4.41), then

$$\begin{aligned}
\dot{V}_{10} \leq & -\frac{1}{2}\hat{e}^T[G(\hat{c}+\hat{\rho}) \otimes \mathcal{H}]\hat{e} - \sum_{i=1}^{N} \frac{g_i \epsilon_i}{4}(c_i - \beta)^2 + \Xi_1 - \kappa_1 V_{10} \\
& + \kappa_1 \sum_{i=1}^{N} g_i(c_i + \rho_i)\hat{e}_i^T P \hat{e}_i + \sum_{i=1}^{N} \frac{g_i \kappa_1}{2}(c_i - \beta)^2 \\
= & -\kappa_1 V_{10} - \frac{1}{2}\hat{e}^T[G(\hat{c}+\hat{\rho}) \otimes (\mathcal{H} - 2\kappa_1 P)]\hat{e} - \sum_{i=1}^{N} \frac{g_i(\epsilon_i - 2\kappa_1)}{4}(c_i - \beta)^2 + \Xi_1.
\end{aligned} \tag{4.42}$$

Define $\mu = 1 + 2\kappa_1$, then $\mathcal{H} - 2\kappa_1 P > 0$ based on the LMI (4.29). Choose $0 < \kappa_1 \leq \min_{i \in \mathbb{F}} \frac{\epsilon_i}{2}$, then we obtain

$$\dot{V}_{10} \leq -\kappa_1 V_{10} + \Xi_1. \tag{4.43}$$

In light of Lemma 1.5, we could deduce that V_{10} exponentially converges to the residual set $\Pi_1 = \{V_{10} : V_{10} < \frac{\Xi_1}{\kappa_1}\}$ with a convergence rate faster than $e^{-\kappa_1 t}$. From (4.17) and based on $c_i(t) \geq \beta_1 \geq 1$, we have $V_{10} \geq \min_{i \in \mathbb{F}} g_i[\lambda_{min}(P)\|\hat{e}\|^2 + \frac{1}{2}\sum_{i=1}^{N}(c_i - \beta)^2]$. Since $\hat{e}(t)$ is uniformly ultimately bounded and $\beta \geq \frac{5}{2\lambda_0}\max_{i \in \mathbb{F}} g_i$ is a constant, we can conclude that $c_i, i \in \mathbb{F}$ are uniformly ultimately bounded.

Furthermore, note from (4.42) that if $\|\hat{e}\|^2 > \frac{2\Xi_1}{\lambda_{min}(G)\lambda_{min}(\mathcal{H} - 2\kappa_1 P)}$, then $\dot{V}_{10} \leq -\kappa_1 V_{10}$. Therefore, $\hat{e}$ is uniformly ultimately bounded satisfying

$$\|\hat{e}\|^2 \leq \frac{2\Xi_1}{\lambda_{min}(G)\lambda_{min}(\mathcal{H} - 2\kappa_1 P)}. \tag{4.44}$$

Thirdly, recall (4.26) as

$$\dot{\tilde{Z}}_i = (A + BK_1)\tilde{Z}_i + \tilde{K}e_i - Bu_0(t) \tag{4.45}$$

where $\tilde{K} = [BK_1, -e^{A\tau}E]$ and $e_i = [\tilde{v}_i^T, (e^{S\tau}\tilde{w}_i^T(t-\tau))]^T$. Based on Assumption 2.16, $u_0(t)$ is bounded. From (4.14) where $e = (\mathcal{L}_1^{-1} \otimes I)\hat{e}$, we have

$$\|e\| \leq \frac{\|\hat{e}\|}{\lambda_{min}(\mathcal{L}_1)} \tag{4.46}$$

which means e_i is also bounded. In addition to $e_i = [\tilde{v}_i^T, (e^{S\tau}\tilde{w}_i(t-\tau))^T]^T$, we come to conclusion that $e^{S\tau}\tilde{w}(t-\tau)$ is uniformly ultimately bounded satisfying

$$\|e^{S\tau}\tilde{w}(t-\tau)\| \leq \frac{\|\hat{e}\|}{\lambda_{min}(\mathcal{L}_1)}. \tag{4.47}$$

Denote $\delta_i = [\delta_{i1}, \ldots, \delta_{in}]^T = (\tilde{K}e_i - Bu_0(t)) \in \mathbb{R}^n$, Because of

$$\begin{aligned} \|\delta_i\|_\infty =& \|\tilde{K}e_i - Bu_0(t)\|_\infty \leq \|\tilde{K}e_i\|_\infty + \|Bu_0(t)\|_\infty \\ &\leq \|\tilde{K}e_i\| + \|Bu_0(t)\| \leq \|\tilde{K}\|\,\|e_i\| + \|B\|\epsilon, \end{aligned} \tag{4.48}$$

we have $\delta_{ij} \leq \|\delta_i\|_\infty, j \in \mathbf{I}[1,n]$, where $\|\delta_i\|_\infty$ is bounded. Denote another vector $\bar{\delta}_i = [\|\delta_i\|_\infty, \ldots, \|\delta_i\|_\infty]^T \in \mathbb{R}^n$, then (4.45) turns to

$$\dot{\tilde{Z}}_i \leq \mathrm{diag}\{p_1, p_2, \ldots, p_n\}\tilde{Z}_i + \bar{\delta}_i \tag{4.49}$$

where $p_i < 0, i \in \mathbf{I}[1,n]$ is the eigenvalues of $A + BK_1$. Based on Lemma 1.5, we obtain

$$\tilde{Z}_{ij}(t) \leq (\tilde{Z}_{ij}(0) - \frac{\|\delta_i\|_\infty}{|p_j|})e^{-|p_j|t} + \frac{\|\delta_i\|_\infty}{|p_j|}, i \in \mathbf{I}[1,N], j \in \mathbf{I}[1,n] \tag{4.50}$$

which means $\tilde{Z}_i(t)$ is bounded.

Fourthly, the exact prediction at time t of the consensus tracking error $\tilde{x}_i(t)$ of the system (4.23) at time $t+\tau$ is

$$x_{pi}(t) = e^{A\tau}\tilde{x}_i(t) + \int_{t-\tau}^{t} e^{A(t-s)}[B(u_i(s) - u_0(s)) + E\bar{w}_i(s+\tau)]ds$$

for all $t \geq 0$, which, in other words, $x_{pi}(t) = \tilde{x}_i(t+\tau)$. Similarly, $\tilde{Z}_i(t)$ in (4.23)

estimate $\tilde{x}_i(t+\tau)$, and the estimating error is

$$\tilde{x}_i(t) - \tilde{Z}_i(t-\tau) = x_{pi}(t-\tau) - \tilde{Z}_i(t-\tau) = -\int_{t-\tau}^{t} e^{A(t-s)} E e^{S\tau} \tilde{w}_i(s-\tau) ds. \quad (4.51)$$

Then we conclude that the consensus tracking error $\tilde{x}_i(t)$ converges exponentially to the residual set Π in Theorem 4.11. The proof is finished.

Remark 4.12 *From (4.39), the value of Ξ_1 is proportional to the upper bound ϵ of leader's input, α satisfying $\alpha \geq \epsilon$, σ_i in (4.24), the followers' number N, and a_{i0} which means how many followers can receive the leader's information. Then from (4.30), (4.44), (4.46)-(4.48) and (4.50), the upper bound of $\tilde{x}_i(t)$ can be controlled to be small by tuning the above parameters. Specifically, when $\sigma_i \to 0$, then $\Xi_1' \to 0$ in (4.36). Ξ_1' will become smaller when α is smaller. And the first term of Ξ_1 in (4.39) will tend to zero when $\epsilon_i \to 0$. In total, the smaller σ_i, ϵ_i and α which satisfies $\alpha \geq \epsilon$ are chosen, the smaller the upper bound of $\tilde{x}(t)$ will be.*

4.3 Simulations

The Matlab function **"dde23(ddefun,lags,history,tspan)"** is used to simulate the constant input delay.

Example 3. This example verifies Theorem 4.7. Set system (4.1) and (4.2) as

$$A = \begin{bmatrix} -4 & 1 \\ 1 & 0 \end{bmatrix}, B = \begin{bmatrix} 1 & 2 \\ 2 & 1 \end{bmatrix}, S = \begin{bmatrix} 0 & 1 \\ -1 & 0 \end{bmatrix}$$

and $F = I_2, E = BF$. Then (A, B) is controllable and (S, E) is observable. $\lambda_1(A) = -4.2361$ and $\lambda_2(A) = 0.2361$ means that our fully distributed controller can be applied to open-loop unstable linear MASs. The digraph $\mathcal{G}$ is shown in Fig. 2.1(a) satisfying Assumption 2.6. Solving LMI (4.4) gets

$$P = \begin{bmatrix} 0.3554 & 0.0230 & -0.1985 & -0.0195 \\ 0.0230 & 0.5864 & -0.7986 & 0.0854 \\ -0.1985 & -0.7986 & 3.5022 & -0.7468 \\ -0.0195 & 0.0854 & -0.7468 & 2.4724 \end{bmatrix},$$

$K = \begin{bmatrix} -2.9330 & -0.1793 \\ -0.1793 & -2.5040 \end{bmatrix}, K' = \begin{bmatrix} -0.2167 & -0.5906 \\ -0.1049 & -0.1504 \end{bmatrix}$, and then other parameters are calculated accordingly. Using the pole placement method, assign eigenvalues

of $A+BK_1$ as -5,-10 and get $K_1 = [-0.3333, -6.3333; -0.3333, 2.6667]$. Similarly, when there is no input delay, the solution to LMI: $P^{'}A_T^{'} + A_T^{'T}P^{'} - 2T^TT < 0$ is

$$P^{'} = \begin{bmatrix} 0.3337 & 0.0200 & -0.2022 & -0.0351 \\ 0.0200 & 0.6059 & -0.7971 & 0.1013 \\ -0.2022 & -0.7971 & 3.4524 & -0.7308 \\ -0.0351 & 0.1013 & -0.7308 & 2.4451 \end{bmatrix}.$$

Set the initial states as $x_{ij}(0) = 4\delta + 1, w_{ij}(0) = 10\delta - 5$, $c_i(0) = 4\delta + 1, i \in \mathbb{F}$ and $x_{0j}(0) = 3\delta + 5, w_{0j}(0) = 3\delta + 1, j \in \mathbf{I}[1, 2]$, where δ is a pseudorandom value with a uniform distribution on the interval $(0, 1)$.

The input delay is taken as $\tau = 0.09s$ and $u(t) = 0, \forall t \in [-\tau, 0]$. Compared with the values of initial states, the values of disturbances are quite large.

Fig. 4.1 shows the comparing results under the same initial conditions without input delay and with input delay, respectively. The consensus tracking errors are illustrated in Fig. 4.1(a) and 4.1(b) where the delay effect is well compensated. It can be seen from Fig. 4.1(c) and 4.1(d) that at the beginning the delayed system needs larger control input. Fig. 4.1(e) and 4.1(f) present the ESO $\bar{Z}_i(t) = [v_i(t)^T, \hat{w}_i(t)^T]^T$ tracking errors which state clearly the effectiveness of fully distributed adaptive ESO. Particularly, Fig. 4.2 verifies the assumption that $c_i(t-\tau) = c_i(t)$, $\rho_i(t-\tau) = \rho_i(t)$ and $\varrho_i(t-\tau) = \varrho_i(t), i \in \mathbb{F}$ as $t \to \infty$.

Example 4. This example verifies Theorem 4.11 by using an unicycle mobile vehicle model shown in Fig. 3.6 of Chapter 3.3.

Define the leader's bounded input as $u_0(t) = [e^{-t} + 1, 2 + \sin(\frac{t}{2})]^T$ and $\alpha = 4, \beta_1 = 1, \epsilon_i = 0.1, \sigma_i = 0.005, i \in \mathbb{F}$. The initial conditions of disturbances and mobile vehicles are the same as the Example 1 and are shown in Fig. 4.4, respectively. Choose $\mu = 2, Q > I$ and solve LMIs (2.8), then

$$P = \begin{bmatrix} 0.6777 & -0.0000 & -0.3269 & -0.0163 & 0.1231 & -0.0429 \\ -0.0000 & 0.6777 & 0.0163 & -0.3269 & 0.0429 & 0.1231 \\ -0.3269 & 0.0163 & 1.0746 & -0.0000 & -0.4668 & 0.2192 \\ -0.0163 & -0.3269 & -0.0000 & 1.0746 & -0.2192 & -0.4668 \\ 0.1231 & 0.0429 & -0.4668 & -0.2192 & 0.3620 & 0.0000 \\ -0.0429 & 0.1231 & 0.2192 & -0.4668 & 0.0000 & 0.3620 \end{bmatrix},$$

$$K = \begin{bmatrix} -1.7504 & -0.0000 & -0.7320 & 0.0149 \\ -0.0000 & -1.7506 & -0.0149 & -0.7320 \\ -0.7320 & -0.0149 & -3.2478 & -0.0000 \\ 0.0149 & -0.7320 & -0.0000 & -3.2475 \end{bmatrix},$$

$$K^{'} = \begin{bmatrix} -0.3469 & -0.2445 & -3.9919 & -1.7656 \\ 0.2445 & -0.3468 & 1.7658 & -3.9915 \end{bmatrix}.$$

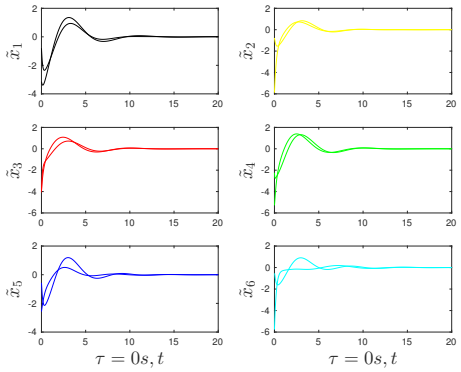

(a) Consensus tracking error without delay.

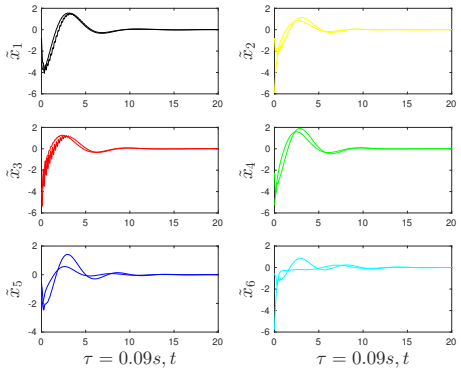

(b) Consensus tracking error with delay.

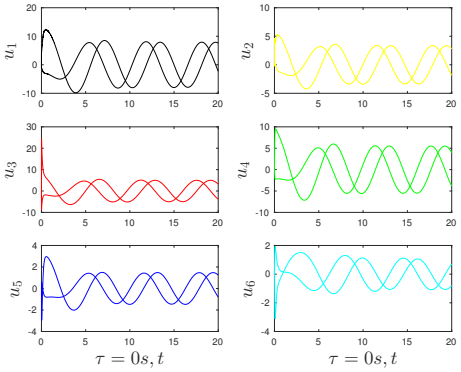

(c) Control input without delay.

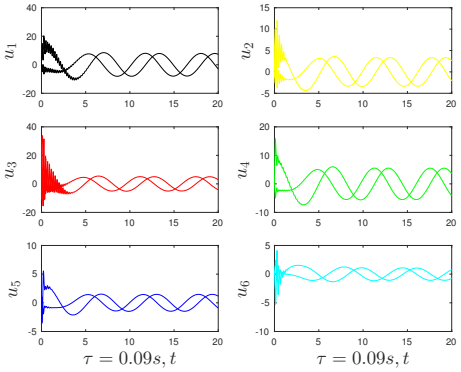

(d) Control input with delay.

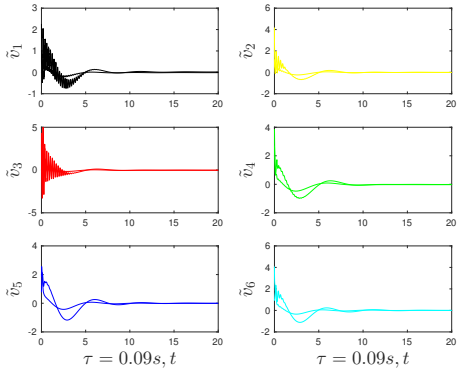

(e) Observer error $\tilde{v} = v - \tilde{Z}$.

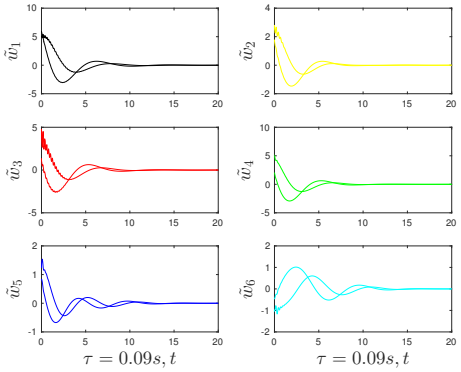

(f) Disturbance observer error $\tilde{w} = \hat{w} - \bar{w}$.

Figure 4.1: Comparison of delay-free and delayed results verifying Theorem 4.7.

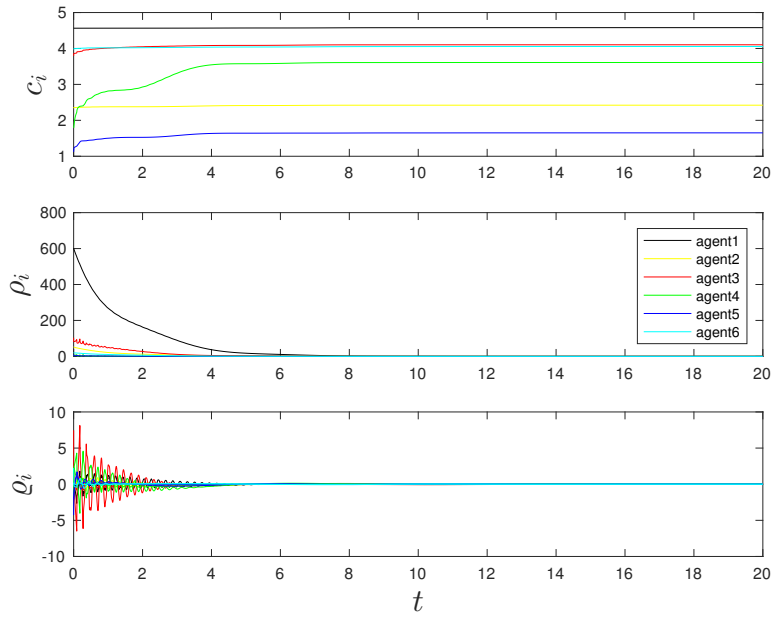

Figure 4.2: Controller parameters c_i (top), ρ_i (center), ϱ_i (bottom).

For the illustration convenience, take the fifth follower as example. From Fig. 4.3 (a), we can see that the consensus tracking error is indeed uniformly ultimately bounded. We can also tune the controller parameters based on Remark 4.12 to control the error as small as possible. Fig. 4.3 (b) still verifies $c_i(t-\tau) = c_i(t), \rho_i(t-\tau) = \rho_i(t)$ and $\varrho_i(t-\tau) = \varrho_i(t), i \in \mathbb{F}$ as $t \to \infty$. In addition, the trajectories of leader and followers are illustrated in Fig. 4.4.

4.4 Summary

Contributions

- √ Design the fully distributed consensus controller for MASs with an unknown leader subject to the constant input delay and matched disturbances under the directed communication topology.
- √ Propose novel adaptive predictive extended state observers using the relative state signals of neighbors.
- √ Present the detail steps about how to design the variables for nonlinear function $z(\cdot)$ in (4.24)

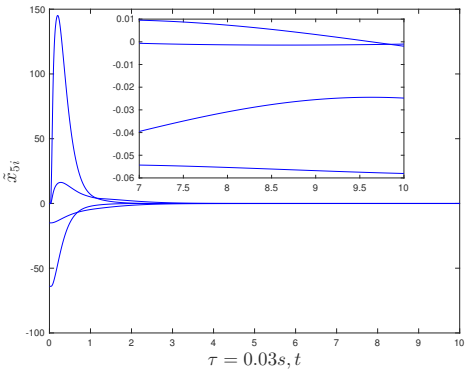

(a) Uniformly ultimately bounded error for the 5th follower.

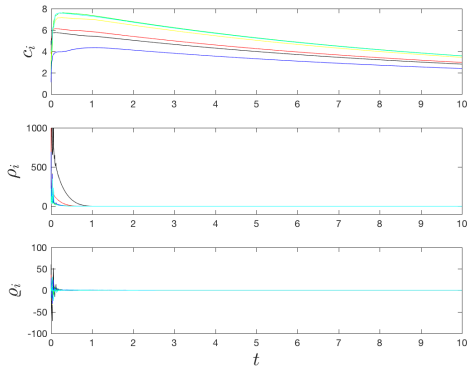

(b) Controller parameters c_i (top), ρ_i (center), ϱ_i (bottom).

Figure 4.3: Consensus tracking with leader's bounded input verifying Theorem 4.11.

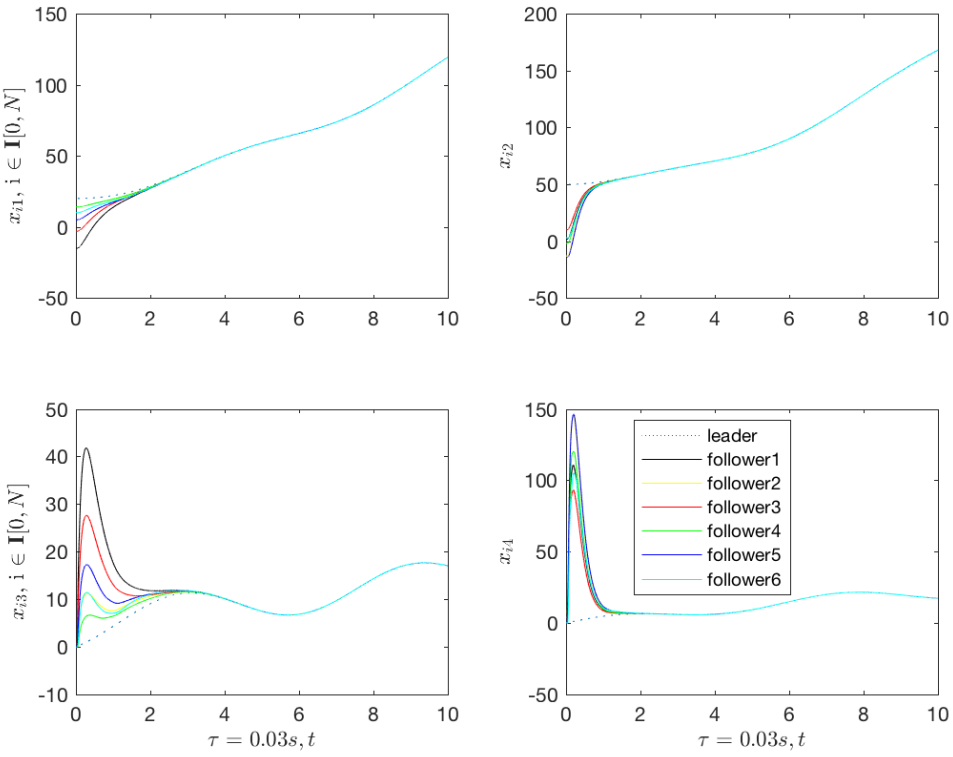

Figure 4.4: State trajectories of the leader and followers.

Chapter 5

Heterogeneous consensus with input delay

Contents

The output consensus tracking (OCT) problem of heterogeneous LTI MASs using the observer approach is investigated. The communication topology contains a fixed directed spanning tree and only a portion of followers can receive the leader's information. First, we study the OCT problem considering the constant input delay and all the agents can have different dynamics and different state dimensions. Based on the FSA approach introduced in Chapter 1.3 and the output regulation theory, a novel state predictor and an adaptive protocol which requires only the states of designed observers of neighbors and the leader's output, are proposed to tackle the input delay effect. Then, to achieve the disturbance rejection, the followers are constrained to have the same state dimension so that the above protocol is redesigned based on the model reduction approach (Artstein, 1982) by adding

another novel APESO to estimate the disturbance and redesigned state predictor simultaneously. The stable analysis is presented by the Lyapunov function with sufficient conditions derived in terms of the ARE and LMI.

Since there are many variables in this chapter, some may coincide with those in the previous chapter. Fortunately, these variables will be defined clearly here.

This chapter gives a detailed presentation showing how to design observers step by step to solve the OCT problem considering the constant input delay and matched disturbances simultaneously. For homogeneous MASs, this problem was solved in Wang *et al.* (2018a) while the parameter inside the protocol is related to the Laplacian matrix of communication topology, indicating that it is not fully distributed. The main contribution of this chapter can be summarized as follows:

- The novel state predictor is proposed in Section 5.1.2 to solve the OCT problem for the heterogeneous general linear MASs for the first time.
- The novel APESO in Section 5.2 is designed to estimate the external disturbance and the redesigned state predictor in a fully distributed fashion.

Consider a group of N followers with non-identical linear dynamics given by

$$\begin{aligned} \dot{x}_i(t) &= A_i x_i(t) + B_i u_i(t-\tau), \\ y_i(t) &= C_i x_i(t), \quad i \in \mathbf{I}[1, N]. \end{aligned} \tag{5.1}$$

Variables and matrices are the same as Eq. (3.1). τ is the known constant input delay.

The leader is indexed by 0 and its dynamics is the same as (1.46) and (3.2), which is

$$\dot{x}_0(t) = A_0 x_0(t), \quad y_0(t) = C_0 x_0(t) \tag{5.2}$$

Note that only a portion of followers can get the leader's information.

Problem 5.1 *Define the OCT error for each follower i as $e_i(t) = y_i(t) - y_0(t)$. Given systems (5.1), (5.2) and a digraph $\mathcal{G}$ considering the constant input delay, design the fully distributed control input $u_i(t)$ such that $\lim_{t\to\infty} e_i(t) = 0, i \in \boldsymbol{I}[1, N]$ for any initial conditions $x_i(0), i \in \boldsymbol{I}[0, N]$.*

Assumption 5.2 *(A_i, B_i), $i \in \boldsymbol{I}[1, N]$ are controllable. (A_0, C_0) is detectable.*

Section 5.1 cover the input delay system (5.1). Specifically, a fully distributed observer $v_{1,i}$ is designed to estimate the leader's state x_0 in Section 5.1.1; then a novel state predictor Z_i is proposed to transform the input-delayed system (5.1) into a delay-free one in Section 5.1.2; after that, the control input design procedure is presented in detail from Section 5.1.3 to 5.1.4. Finally, in Section 5.2, the above novel protocol is redesigned by adding an APESO to deal with the input delay and external disturbances at the same time.

5.1 Consensus with the input delay

5.1.1 Observer $v_{1,i}(t)$ to estimate the leader's state $x_0(t)$

Since not all the followers have the leader's output information, the idea is to design the observer $v_{1,i} \in \mathbb{R}^n$ to estimate x_0 for the state predictor design in Section 5.1.2 and the control input design in Section 5.1.3.

First, inherited from Chapter 3, we share the same ideal about separating followers as informed followers (IFs) indexed from 1 to $M, M \geq 1$ and uninformed followers (UFs) from $M+1$ to N. The IFs can get access to the leader's output y_0 directly and the UFs cannot.

Assumption 5.3 *The graph $\mathcal{G}$ contains a directed spanning tree. In detail, there is a directed path to each IF from the leader which acts as the root node. And for each UF, at least one directed path should exist from the IFs to that UF.*

Then the Laplacian matrix of graph $\mathcal{G}$ can be partitioned as $\mathcal{L} = \begin{bmatrix} 0 & 0_{1\times N} \\ \mathcal{L}_4 & \mathcal{L}_3 \end{bmatrix}$, where $\mathcal{L}_3 = \begin{bmatrix} I_{M\times M} & 0_{M\times(N-M)} \\ \mathcal{L}_2 & \mathcal{L}_1 \end{bmatrix}$, $\mathcal{L}_1 \in \mathbb{R}^{(N-M)\times(N-M)}, \mathcal{L}_2 \in \mathbb{R}^{(N-M)\times M}$. Under Assumption 5.3, $\mathcal{L}_1$ and $\mathcal{L}_3$ are nonsingular M-matrices, so all eigenvalues of $\mathcal{L}_1$ and $\mathcal{L}_3$ have the positive real parts.

Now, for each IF, design the Luenberger-like observer as

$$\dot{v}_{1,i} = A_0 v_{1,i} + F(y_0 - C_0 v_{1,i}), i \in \mathbf{I}[1, M]. \tag{5.3}$$

Denote the observer error as $\tilde{v}_{1,i} = v_{1,i} - x_0, i \in \mathbf{I}[1, N]$. After some calculations, we have $\dot{\tilde{v}}_{1,i} = (A_0 - FC_0)\tilde{v}_{1,i}$. Based on the pole placement method in linear control theory, design $F \in \mathbb{R}^{n\times q}$ such that $A_0 - FC_0$ is Hurwitz, then $\lim_{t\to\infty} \tilde{v}_{1,i} = 0, i \in \mathbf{I}[1, M]$.

For each UF, the following adaptive distributed observer is proposed as

$$\begin{aligned} \dot{v}_{1,i} =& A_0 v_{1,i} + K(c_i + \rho_i)\varrho_i, \\ \dot{c}_i =& \varrho_i^T \Gamma \varrho_i, i \in \mathbf{I}[M+1, N] \end{aligned} \tag{5.4}$$

where $\varrho_i = \sum_{j=1}^N a_{ij}(v_{1,i} - v_{1,j}), \rho_i = \varrho_i^T P \varrho_i$, and $c_i > 0$ can be viewed as the coupling weight associated with the i-th UF. $K \in \mathbb{R}^{n\times n}, P \in \mathbb{R}^{n\times n}, \Gamma \in \mathbb{R}^{n\times n}$ are the feedback gain matrices to be decided later.

Remark 5.4 *ϱ_i means that the UF only needs the observer state $v_{1,j}$ of its neighboring IFs via the digraph $\mathcal{G}$ to estimate the leader's state x_0. In fact, $\varrho_i = \sum_{j=1}^N a_{ij}[(v_{1,i} - x_0) - (v_{1,j} - x_0)] = \sum_{j=1}^N l_{ij}(v_{1,j} - x_0) = \sum_{j=1}^N l_{ij}\tilde{v}_{1,j}$.*

Lemma 5.5 *Consider Assumption 5.3. For the UF $i, i \in \boldsymbol{I}[M+1, N]$, the observer error holds $\lim_{t\to\infty} \tilde{v}_{1,i} = 0$ if $K = -P, \Gamma = P^2$, and $P > 0$ is a solution to the ARE (3.10). Besides, $c_i(t)$ converges to the finite steady-state value.*

The proof is the same as the one of Lemma 3.9 in Chapter 3, so it is omitted here.

5.1.2 The state predictor

This section gives the detail about how to deal with the input delay for heterogeneous linear MASs. To do that, we need the Assumptions 3.12 and 3.13 for the classic output regulation theory which exist in literature such as in Almeida *et al.* (2014), Zhang *et al.* (2018b) and Meng *et al.* (2017).

In terms of the input delay $u_i(t-\tau)$, inspired by the FSA approach, the novel state predictor for each follower is designed as follows:

$$\begin{aligned} Z_i(t) = &\int_{t-\tau}^{t} e^{A_i(t-s)} B_i(u_i(s) - U_i e^{A_0\tau} v_{1,i}(s))ds \\ &+ e^{A_i\tau}(x_i(t) - X_i v_{1,i}(t)), i \in \mathbf{I}[1, N]. \end{aligned} \tag{5.5}$$

Here, the link between x_i and Z_i is established through $v_{1,i}$ and the solution (X_i, U_i) of regulation function (3.12), which is one of the main difficulties. Denote

$$\tilde{x}_i = x_i - X_i v_{1,i}. \tag{5.6}$$

Hereafter, we try to prove the convergence of $\tilde{x}_i \in \mathbb{R}^{n_i}$ for any initial state $x_i(0), i \in \mathbf{I}[0, N]$. The tedious calculation of the derivative of Z_i will be presented. Given $Z_i(t) = f(x_i, v_{1,i})$, the cases of IFs and UFs will be discussed separately.

5.1.2.1 The derivative for the IF $i, i \in \mathbf{I}[1, M]$

From (5.1), (5.3) and (5.5), we have

$$\begin{aligned} \dot{Z}_i =& e^{A_i\tau}\{A_i x_i + B_i u_i(t-\tau) - X_i[A_0 v_{1,i}(t) + F(y_0 - C_0 v_{1,i}(t))]\} \\ &+ B_i u_i(t) - B_i U_i e^{A_0\tau} v_{1,i}(t) - e^{A_i\tau}[B_i u_i(t-\tau) - B_i U_i e^{A_0\tau} v_{1,i}(t-\tau)] \\ &+ A_i \int_{t-\tau}^{t} e^{A_i(t-s)}[B_i u_i(s) - B_i U_i e^{A_0\tau} v_{1,i}(s)]ds. \end{aligned} \tag{5.7}$$

Because of $X_i A_0 = A_i X_i + B_i U_i$ in (3.12), then

$$\begin{aligned} \dot{Z}_i =& A_i Z_i + B_i u_i(t) - B_i U_i e^{A_0\tau} v_{1,i}(t) - e^{A_i\tau} B_i U_i[v_{1,i}(t) - e^{A_0\tau} v_{1,i}(t-\tau)] \\ &+ e^{A_i\tau} X_i F C_0 \tilde{v}_{1,i}(t). \end{aligned} \tag{5.8}$$

The prediction $v_{1,i}(t+\tau)$ in (5.3) at time t is

$$v_{1,i}(t+\tau) = e^{A_0\tau}v_{1,i}(t) - \int_{t-\tau}^{t} e^{A_0(t-s)}FC_0\tilde{v}_{1,i}(s+\tau)ds,$$

which is also

$$v_{1,i}(t) = e^{A_0\tau}v_{1,i}(t-\tau) - \int_{t-\tau}^{t} e^{A_0(t-s)}FC_0\tilde{v}_{1,i}(s)ds. \tag{5.9}$$

Substitute (5.9) into (5.8), then

$$\dot{Z}_i = A_iZ_i + B_iu_i - B_iU_ie^{A_0\tau}v_{1,i} + \Omega_i(t) \tag{5.10}$$

where

$$\Omega_i(t) = e^{A_i\tau}B_iU_i\int_{t-\tau}^{t} e^{A_0(t-s)}FC_0\tilde{v}_{1,i}(s)ds + e^{A_i\tau}X_iFC_0\tilde{v}_{1,i}(t), i \in \mathbf{I}[1,M]. \tag{5.11}$$

As it has been proved that the observer error $\lim_{t\to\infty}\tilde{v}_{1,i}(t) = 0$ for IFs in (5.3), it is obvious that $\lim_{t\to\infty}\Omega_i(t) = 0, i \in \mathbf{I}[1,M]$.

5.1.2.2 The derivative for the UF $i, i \in \mathbf{I}[M+1,N]$

Similar as Section 5.1.2.1, from (5.1), (5.4), (3.12) and (5.5), we get

$$\begin{aligned}\dot{Z}_i =& A_iZ_i + B_iu_i - B_iU_ie^{A_0\tau}v_{1,i}(t) - e^{A_i\tau}B_iU_i(v_{1,i}(t)\\ &- e^{A_0\tau}v_{1,i}(t-\tau)) - e^{A_i\tau}X_iK(c_i+\rho_i)\varrho_i.\end{aligned} \tag{5.12}$$

The prediction of $v_{1,i}(t)$ of (5.4) at time $t-\tau$ is

$$v_{1,i}(t) = e^{A_0\tau}v_{1,i}(t-\tau) + \int_{t-\tau}^{t} e^{A_0(t-s)}K(c_i(s)+\rho_i(s))\varrho_i(s)ds. \tag{5.13}$$

Substitute (5.13) into (5.12), then we obtain (5.10) where

$$\begin{aligned}\Omega_i(t) =& -e^{A_i\tau}B_iU_i\int_{t-\tau}^{t} e^{A_0(t-s)}K(c_i(s)+\rho_i(s))\varrho_i(s)ds\\ &- e^{A_i\tau}X_iK(c_i+\rho_i)\varrho_i(t), i \in \mathbf{I}[M+1,N].\end{aligned} \tag{5.14}$$

As $\lim_{t\to\infty}\varrho_i = 0$ is proved in the proof of Lemma 5.5, we can obtain $\lim_{t\to\infty}\Omega_i(t) = 0, i \in \mathbf{I}[M+1, N]$. Now, based on the analysis of Section 5.1.2, we conclude that

$$\begin{aligned} &\dot{Z}_i = A_i Z_i + B_i u_i - B_i U_i e^{A_0\tau} v_{1,i} + \Omega_i(t), \\ &\lim_{t\to\infty}\Omega_i(t) = 0, i \in \mathbf{I}[1, N]. \end{aligned} \tag{5.15}$$

5.1.3 The design of control inputs $u_i, i \in \mathbf{I}[1, N]$

Based on (5.15), the control input could be designed as

$$u_i = K_{2i} Z_i + U_i e^{A_0\tau} v_{1,i}, i \in \mathbf{I}[1, N] \tag{5.16}$$

such that

$$\dot{Z}_i = (A_i + B_i K_{2i}) Z_i + \Omega_i(t). \tag{5.17}$$

Thanks to $\lim_{t\to\infty}\Omega_i(t) = 0, i \in \mathbf{I}[1, N]$, if $A_i + B_i K_{2i}$ is Hurwitz, then $\lim_{t\to\infty} Z_i = 0$. On the other hand, substituting the designed input (5.16) into the transformed delay-free system (5.5) generates

$$Z_i(t) = e^{A_i\tau}\tilde{x}_i(t) + \int_{t-\tau}^{t} e^{A_i(t-s)} B_i K_{2i} Z_i(s) ds. \tag{5.18}$$

As $e^{A_i\tau}$ is reversible and $\lim_{t\to\infty} Z_i(t) = 0$, $\lim_{t\to\infty}\tilde{x}_i(t) = 0, i \in \mathbf{I}[1, N]$ are proved.

Lemma 5.6 *Consider Assumptions 3.12, 3.13, 5.2 and 5.3. The Problem 5.1 is solved by the fully distributed controller consisting of the input (5.16), the state predictor (5.5) or (5.18), with the Luenberger-like observer (5.3) and adaptive observer (5.4) constructed by Lemma 5.5, if K_{2i} is chosen such that $A_i + B_i K_{2i}$ is Hurwitz and (X_i, U_i) is the solution of (3.12).*

Proof. The proving process here is quite straightforward. From (5.6), the OCT error in Problem 5.1 is

$$e_i = C_i x_i - C_0 x_0 = C_i(\tilde{x}_i + X_i v_{1,i}) - C_0 x_0.$$

Due to $C_i X_i = C_0$ in (3.12), then

$$e_i = C_i\tilde{x}_i + C_0(v_{1,i} - x_0) = C_i\tilde{x}_i + C_0\tilde{v}_{1,i}. \tag{5.19}$$

Thanks to $\lim_{t\to\infty}\tilde{x}_i = 0$ and $\lim_{t\to\infty}\tilde{v}_{1,i} = 0$, we conclude that $\lim_{t\to\infty} e_i = 0$, i.e., the Problem 5.1 is solved.

5.1.4 The thinking behind the control input designing

The attention should be paid here that in (5.18), the expression of Z_i is implicit, which means it is difficult to implement the controller (5.16) in reality. So designing an explicit format of Z_i is preferred. The solution is to propose another observer $v_{2,i} \in \mathbb{R}^{n_i}$ to estimate Z_i. Following (5.15), the control input is redesigned as

$$u_i = K_{2i} v_{2,i} + U_i e^{A_0 \tau} v_{1,i},\ i \in \mathbf{I}[1, N] \tag{5.20}$$

such that

$$\dot{Z}_i = (A_i + B_i K_{2i}) Z_i + B_i K_{2i} (v_{2,i} - Z_i) + \Omega_i(t). \tag{5.21}$$

It is obvious that if observer error $\tilde{v}_{2,i} = v_{2,i} - Z_i$ converges to zero asymptotically, i.e., $\lim_{t\to\infty} \tilde{v}_{2,i} = 0$, then $\lim_{t\to\infty} Z_i = 0$. So the observer $v_{2,i}$ is designed as

$$\dot{v}_{2,i} = (A_i + B_i K_{2i}) v_{2,i} + B_i K_{2i} (v_{2,i} - Z_i). \tag{5.22}$$

Combining the above two equations, we get

$$\dot{\tilde{v}}_{2,i} = (A_i + B_i K_{2i}) \tilde{v}_{2,i} - \Omega_i(t), i \in \mathbf{I}[1, N]. \tag{5.23}$$

Thanks to $\lim_{t\to\infty} \Omega_i(t) = 0$ in (5.15), we have $\lim_{t\to\infty} \dot{\tilde{v}}_{2,i} = 0$. Furthermore, we can get $\lim_{t\to\infty} Z_i = 0$ in (5.21) and $\lim_{t\to\infty} v_{2,i} = 0$ in (5.22). On the other hand, substituting the redesigned control input (5.20) into (5.5) generates

$$Z_i(t) = e^{A_i \tau} \tilde{x}_i(t) + \int_{t-\tau}^{t} e^{A_i (t-s)} B_i K_{2i} v_{2,i}(s) ds \tag{5.24}$$

where $\lim_{t\to\infty} \tilde{x}_i(t) = 0, i \in \mathbf{I}[1, N]$ is obvious and the expression of $Z_i(t)$ is explicit.

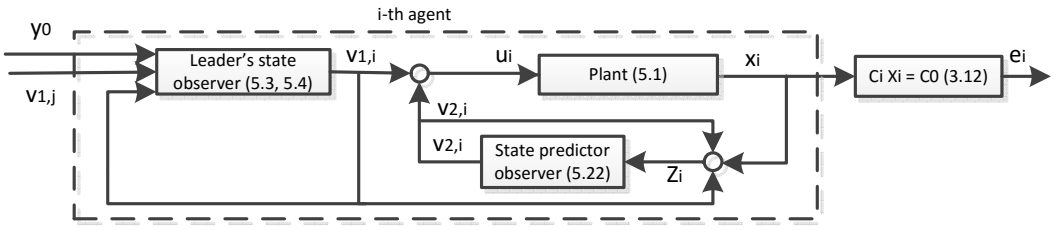

Figure 5.1: Block diagram of the proposed controller.

Theorem 5.7 *Consider Assumptions 3.12, 3.13, 5.2 and 5.3. The Problem 5.1 is solved by the fully distributed controller (see Fig. 5.1) consisting of the redesigned input (5.20), the redesigned state predictor (5.24) and its observer (5.22) with observers (5.3) and (5.4) constructed in Lemma 5.5, if K_{2i}, X_i and U_i are chosen as in Lemma 5.6.*

The proof is the same as in Lemma 5.6 and is omitted here.

Remark 5.8 *In Sections 5.1.1-5.1.4, three different kinds of observers are proposed and presented clearly in order to design the control input with the fully distributed property. We call it the **observer-based fully distributed controller**. In the next section, the novel APESO will be proposed to consider the input delay and disturbance effects for all followers at the same time.*

5.2 Consensus with the input delay and disturbances

The system (5.1) is changed as follows:

$$\begin{array}{rcl} \dot{x}_i(t) & = & A_i x_i(t) + B_i u_i(t-\tau) + E_i w_i(t), \\ \dot{w}_i(t) & = & S_i w_i(t), \quad i \in \mathbf{I}[1, N] \end{array} \tag{5.25}$$

where $w_i(t) \in \mathbb{R}^{s_i}$ is the external disturbance. $E_i = B_i F_i \in \mathbb{R}^{n_i \times s_i}$ and $S_i \in \mathbb{R}^{s_i \times s_i}$ are constant matrices.

Problem 5.9 *Given systems (5.2), (5.25) and a digraph $\mathcal{G}$, design the fully distributed control input $u_i(t)$ such that for any initial conditions $x_i(0), i \in \boldsymbol{I}[0, N]$, the OCT errors satisfy $\lim_{t\to\infty} e_i(t) = 0, i \in \boldsymbol{I}[1, N]$.*

In order to solve the Problem 5.9, the following assumptions are needed.

Assumption 5.10 *The heterogeneous followers have the same state dimension, which means n_i is an unchangeable constant, i.e., $rank(A_i) = rank(A_j) = n_i$ for $j \neq i$.*

Assumption 5.11 *$(S_i, E_i), i \in \boldsymbol{I}[1, N]$ are observable. The eigenvalues of S_i are distinct and on the imaginary axis.*

Assumption 5.10 enables us to calculate $x_i - x_j$, which is necessary for the APESO design in (5.32). Assumption 5.11 means $w_i(t)$ is matched and non-vanishing, which is common in the disturbance rejection literature (Ding, 2015b, Wang *et al.*, 2018a). The detailed explanation can be related to the Remark 1 in Ding (2015b).

Different from the state predictor (5.5), we adopt and modify the Artstein's reduction approach for each follower $i, i \in \mathbf{I}[1, N]$ as

$$\begin{aligned}\bar{Z}_i(t) =&\tilde{x}_i(t) + \int_{t-\tau}^{t} e^{A_i(t-\tau-s)}[B_i u_i(s) \\ &- B_i U_i e^{A_0\tau} v_{1,i}(s) + E_i e^{S_i\tau}\hat{w}_i(s)]ds\end{aligned} \tag{5.26}$$

where $\hat{w}_i$ is the disturbance observer used to estimate the disturbance signal w_i. Define the estimating error as $\tilde{w} = \hat{w}_i - w_i$. Similar as the derivative calculation of Z_i in Section 5.1.2 and the control input design in Section 5.1.4, we redesign the control input as

$$u_i = K_{3i} v_{3,i} + U_i e^{A_0\tau} v_{1,i} - F_i e^{S_i\tau}\hat{w}_i \tag{5.27}$$

such that

$$\dot{\bar{Z}}_i = (A_i + B_{3i}K_{3i})\bar{Z}_i + B_{3i}K_{3i}\tilde{v}_{3,i} - E_i e^{S_i\tau}\hat{w}_i(t-\tau) + \Omega_i'(t). \tag{5.28}$$

Here, $B_i F_i = E_i$ is used for the calculation, and $\tilde{v}_{3,i} = v_{3,i} - \bar{Z}_i$ is the error for the observer $v_{3,i}$ estimating $\bar{Z}_i$. Denote $B_{3i} = e^{-A_i\tau}B_i$ for writing convenience. We have proved in Lemma 1.9 that if Assumption 5.2 is satisfied, then $(A_i, B_{3i}), i \in \mathbf{I}[1, N]$ is controllable. After similar calculation as (5.15), we have

$$\begin{aligned}\Omega_i'(t) =&B_i U_i \int_{t-\tau}^{t} e^{A_0(t-s)} F(C_0 v_{1,i}(s) - y_0(s))ds \\ &+ X_i F(C_0 v_{1,i}(t) - y_0(t)), i \in \mathbf{I}[1, M] \\ \Omega_i'(t) =& - B_i U_i \int_{t-\tau}^{t} e^{A_0(t-s)} K(c_i(s) + \rho_i(s))C_0\varrho_i(s)ds \\ &- X_i K(c_i(t) + \rho_i(t))C_0\varrho_i(t), i \in \mathbf{I}[M+1, N],\end{aligned} \tag{5.29}$$

which equals $\Omega_i'(t) = e^{-A_i\tau}\Omega_i(t)$, meaning that $\lim_{t\to\infty}\Omega_i'(t) = 0, i \in \mathbf{I}[1, N]$.

Similar as the network measurement (4.11), based on relative states, denote

$$\xi_i = \sum_{j=1}^{N} a_{ij}(x_i - x_j), i \in \mathbf{I}[1, N]. \tag{5.30}$$

By using the above information ξ_i, denote a signal similar to (5.30) as

$$\begin{aligned}\varrho_{3i} =&a_{i0}(v_{3,i} - x_i + X_i v_{1,i}) - \sum_{j=0,j\neq i}^{N} a_{ij}\int_{t-\tau}^{t} e^{A_i(t-\tau-s)}\\ &\times (B_i u_i(s) - B_i U_i e^{A_0\tau} v_{1,i}(s) + E_i e^{S_i\tau}\hat{w}_i(s))ds\\ &+ \sum_{j=1,j\neq i}^{N} a_{ij}[\int_{t-\tau}^{t} e^{A_j(t-\tau-s)}(B_j u_j(s) - B_j U_j e^{A_0\tau} v_{1,j}(s)\\ &+ v_{3,i} - v_{3,j} + X_i v_{1,i} - X_j v_{1,j} + E_j e^{S_j\tau}\hat{w}_j(s))ds] - \xi_i.\end{aligned} \tag{5.31}$$

It is easy to calculate $\varrho_{3i} = a_{i0}\tilde{v}_{3,i} + \sum_{j=1}^{N} a_{ij}(\tilde{v}_{3,i} - \tilde{v}_{3,j}) = \sum_{j=1}^{N} l_{ij}\tilde{v}_{3,j}$. The observers $v_{3,i}$ and $\hat{w}_i$ are designed as follows:

$$\begin{aligned}\dot{v}_{3,i} =&(A_i + B_{3i}K_{3i})v_{3,i} + K_{3i}^{'}(c_{3i} + \rho_{3i})\varrho_{3i} + \Omega_i^{'},\\ \dot{\hat{w}}_i =&S_i\hat{w}_i + K_{4i}(c_{3i} + \rho_{3i})\varrho_{3i}, i \in \mathbf{I}[1, N].\end{aligned} \tag{5.32}$$

Remark 5.12 *The signal $\varrho_{3,i}$, which will be used in the APESO design, needs the relative state ξ_i, the matrices $A_j, B_j, E_j, S_j, U_j, X_j$, the observer states $v_{1,j}, v_{3,j}$, the stored history of control input $u_j(t-\tau)$, the leader's state observer $v_{1,j}(t-\tau)$ and disturbance observer state $\hat{w}_j(t-\tau)$ of its neighbor j via the digraph $\mathcal{G}$. The construction of ξ_i and ϱ_{3i} is based on the Assumption 5.10.*

Remark 5.13 *From (5.29), we can see that for each IF $i, i \in \boldsymbol{I}[1, M]$, it needs the leader's information $y_0(t-\tau)$ and $y_0(t)$ to construct $v_{3,i}$. In other words, the leader's historical output information is required by its neighboring followers to deal with the external disturbances.*

Then, from (5.28) and (5.32), the observer error dynamics is

$$\begin{aligned}\dot{\tilde{v}}_{3,i} =&A_i\tilde{v}_{3,i} + E_i e^{S_i\tau}\tilde{w}_i(t-\tau) + K_{3i}^{'}(c_{3i} + \rho_{3i})\varrho_{3i},\\ e^{S_i\tau}\dot{\tilde{w}}_i(t-\tau) =& S_i e^{S_i\tau}\tilde{w}_i(t-\tau) + e^{S_i\tau}K_{4i}(c_{3i}(t-\tau) + \rho_{3i}(t-\tau))\varrho_{3i}(t-\tau).\end{aligned}$$

Define the extended state $\zeta_i(t) = \begin{bmatrix}\tilde{v}_{3,i}(t)\\ e^{S_i\tau}\tilde{w}_i(t-\tau)\end{bmatrix}$. Then

$$\dot{c}_{3i} = \zeta_i^T\bar{\Gamma}\zeta_i,\ \rho_{3i} = \zeta_i^T\bar{P}\zeta_i. \tag{5.33}$$

Note that our objective is to prove $\lim_{t\to\infty} e_i = 0$ in Problem 5.9. Considering the components of c_{3i}, ρ_{3i} and ϱ_{3i}, it is reasonable to have $c_{3i}(t-\tau) = c_{3i}(t), \rho_{3i}(t-\tau) = \rho_{3i}(t)$ and $\varrho_{3i}(t-\tau) = \varrho_{3i}(t)$ when $t \to \infty$ considering the input delay τ is not very large, then

$$\dot{\zeta}_i = \underbrace{\begin{bmatrix} A_i & E_i \\ 0 & S_i \end{bmatrix}}_{\bar{A}_i} \zeta_i + \underbrace{\begin{bmatrix} K'_{3i} \\ e^{S_i\tau} K_{4i} \end{bmatrix}}_{\bar{K}_i} (c_{3i} + \rho_{3i}) \sum_{j=1}^{N} l_{ij} \underbrace{\begin{bmatrix} I & 0 \end{bmatrix}}_{T} \zeta_j \tag{5.34}$$

where $\bar{A}_i \in \mathbb{R}^{(n_i+s_i)\times(n_i+s_i)}, \bar{K}_i \in \mathbb{R}^{(n_i+s_i)\times n_i}$. Here, the following lemma is needed.

Lemma 5.14 *(Ding, 2015b) If (S_i, E_i) is observable, then the pair $(\bar{A}_i, T)$ is observable, with $\bar{A}_i, T$ defined in (5.34).*

Theorem 5.15 *Consider Assumptions 3.12, 3.13, 5.2, 5.3, 5.10 and 5.11. The Problem 5.9 is solved by the fully distributed controller consisting of the redesigned input (5.27), the redesigned state predictor (5.26) and the APESO (5.32) with (5.29)-(5.31) and (5.33), observers (5.3) and (5.4) constructed in Lemma 5.5, if (X_i, U_i) is chosen as in Lemma 5.6, $A_i + e^{-A_i\tau} B_i K_{3i}$ is Hurwitz, $\bar{\Gamma} = T^T T, \bar{K} = -\bar{P}^{-1} T^T$ and $\bar{P} > 0$ is a solution to the following LMI:*

$$\bar{P}_i \bar{A}_i + \bar{A}_i^T \bar{P}_i - 2T^T T < 0. \tag{5.35}$$

Besides, $c_{3i}(t), i \in \boldsymbol{I}[1, N]$ converge to some finite steady-state values.

Proof. Let

$$V_{11} = \frac{1}{2} \sum_{i=1}^{N} g_{3i}(2c_{3i} + \rho_{3i})\rho_{3i} + \frac{1}{2} \sum_{i=1}^{N} g_{3i}(c_{3i} - \beta)^2 \tag{5.36}$$

where $G_3 = \text{diag}\{g_{31}, g_{32}, \ldots, g_{3N}\} > 0$ has the similar property as G in (3.26). $\beta > 0$ is a constant to be determined. The derivative of V_{11} is

$$\begin{aligned} \dot{V}_{11} = & \sum_{i=1}^{N} \zeta_i^T g_{3i}(c_{3i} + \rho_{3i})[(\bar{P}_i \bar{A}_i + \bar{A}_i^T \bar{P}_i)\zeta_i + 2(c_{3i} + \rho_{3i})\bar{P}_i \bar{K}_i T \sum_{j=1}^{N} l_{ij}\zeta_j] \\ & + \sum_{i=1}^{N} \zeta_i^T g_{3i}(c_{3i} + \rho_{3i} - \beta)\bar{\Gamma}_i \zeta_i. \end{aligned} \tag{5.37}$$

Use the LMI (5.35) and $\bar{\Gamma} = T^T T, \bar{K} = -\bar{P}^{-1} T^T$, then

$$\begin{aligned}\dot{V}_{11} \leq & \sum_{i=1}^{N} \zeta_i^T g_{3i}(c_{3i} + \rho_{3i})[2T^T T\zeta_i - 2(c_{3i} + \rho_{3i})T^T T \sum_{j=1}^{N} l_{ij}\zeta_j] \\ & + \sum_{i=1}^{N} \zeta_i^T g_{3i}(c_{3i} + \rho_{3i} - \beta)T^T T\zeta_i \\ = & \zeta^T [2G_3(\hat{c}_3 + \hat{\rho}_3) \otimes T^T T + G_3(\hat{c}_3 + \hat{\rho}_3 - \beta I) \otimes T^T T \\ & - (\hat{c}_3 + \hat{\rho}_3)(G_3\mathcal{L}_3 + \mathcal{L}_3^T G_3)(\hat{c}_3 + \hat{\rho}_3) \otimes T^T T]\zeta \end{aligned} \tag{5.38}$$

where $\hat{c}_3 = \text{diag}\{c_{31}, \ldots, c_{3N}\}, \hat{\rho}_3 = \text{diag}\{\rho_{31}, \ldots, \rho_{3N}\}$. Since there exists $(G_3\mathcal{L}_3 + \mathcal{L}_3^T G_3) > \lambda_0^{'} I$ where $\lambda_0^{'} > 0$ is the smallest eigenvalue of $G_3\mathcal{L}_3 + \mathcal{L}_3^T G_3$, by using Young's inequality as follows:

$$\zeta^T [G_3(\hat{c}_3 + \hat{\rho}_3) \otimes T^T T]\zeta \leq \zeta^T [(\frac{\lambda_0^{'}}{2}(\hat{c}_3 + \hat{\rho}_3)^2 + \frac{G_3^2}{2\lambda_0^{'}}) \otimes T^T T]\zeta,$$

and by choosing $\beta \geq \frac{5}{2\lambda_0^{'}} \max g_{3i}, i \in \mathbf{I}[1, N]$, we obtain

$$\dot{V}_{11} \leq \zeta^T \{[2G_3(\hat{c}_3 + \hat{\rho}_3) - (\frac{\lambda_0^{'}}{2}(\hat{c}_3 + \hat{\rho}_3)^2 - \frac{G_3^2}{2\lambda_0^{'}} + \beta G)] \otimes T^T T\}\zeta \leq 0. \tag{5.39}$$

Similar as the analysis in Lemma 5.5, each coupling weight $c_{3i}(t)$ increases monotonically and converges to the finite value finally, which verifies $\lim_{t\to\infty} c_{3i}(t-\tau) = \lim_{t\to\infty} c_{3i}(t)$. Based on the LaSalle's Invariance principle (Krstic *et al.*, 1995), it follows $\lim_{t\to\infty} \zeta_i = 0$. So from (5.33), $\lim_{t\to\infty} \rho_{3i}(t) = 0$ which could verify $\lim_{t\to\infty} \rho_{3i}(t-\tau) = \lim_{t\to\infty} \rho_{3i}(t)$. Since $\varrho_{3i} = \sum_{j=1}^{N} l_{ij} T\zeta_j$ from (5.34), we could verify $\lim_{t\to\infty} \varrho_{3i}(t-\tau) = \lim_{t\to\infty} \varrho_{3i}(t)$. Recall from (5.28) that

$$\dot{\bar{Z}}_i = (A_i + B_{3i}K_{3i})\bar{Z}_i + \tilde{K}\zeta_i + \Omega_i^{'} \tag{5.40}$$

where $\tilde{K} = [B_{3i}K_{3i}, -E_i]$. As $A_i + B_{3i}K_{3i}$ is Hurwitz with $\lim_{t\to\infty} \zeta_i = 0$ and $\lim_{t\to\infty} \Omega_i^{'} = 0$, then $\lim_{t\to\infty} \bar{Z}_i = 0, i \in \mathbf{I}[1, N]$. Furthermore, there is $\lim_{t\to\infty} v_{3,i} = 0$ based on $\lim_{t\to\infty} \zeta_i = 0$. Integrating input (5.27) into (5.26) generates

$$\bar{Z}_i(t) = \tilde{x}_i(t) + \int_{t-\tau}^{t} e^{A_i(t-\tau-s)} B_i K_{3i} v_{3,i}(s) ds. \tag{5.41}$$

Then, we have $\lim_{t\to\infty} \tilde{x}_i = 0$ based on $\lim_{t\to\infty} \bar{Z}_i = 0$ and $\lim_{t\to\infty} v_{3,i} = 0$. Finally, to prove $\lim_{t\to\infty} e_i = 0$, the process is the same as in Lemma 5.6 and is omitted.

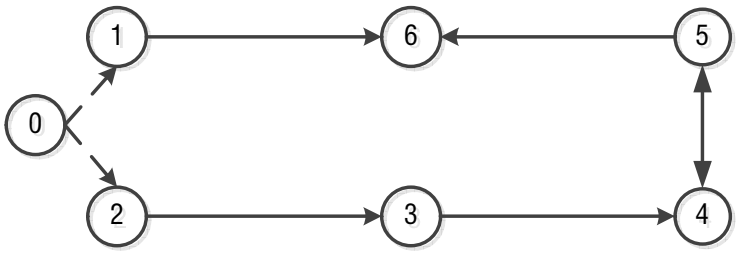

Figure 5.2: The directed communication topology $\mathcal{G}$.

Remark 5.16 *Since (S_i, E_i) is observable, the LMI (5.35) is guaranteed based on Lemma 5.14. To solve Problem 5.9, two fully distributed observers, i.e., the leader's state observer and the APESO, are proposed togethere, which is another main contribution of this chapter.*

5.3 Simulations

The Problems 5.1 and 5.9 are addressed by the following two examples respectively. All the initial conditions for the leader and followers are chosen as the same as in the Example 1 of Chapter 3.3.

Example 5. To solve the Problem 5.1, denote $M = 2, N = 6$ and the digraph $\mathcal{G}$ is shown in Fig. 5.2 satisfying Assumption 5.3. Choose the dynamics of IFs as $A_1 = A_1'', A_2 = A_2'$ and the dynamics of UFs as $A_3 = A_3', A_4 = A_4', A_5 = A_5''', A_6 = A_6'''$, which is the same as the dynamics (3.19) in the Example 1 of Chapter 3.3. The leader's dynamics (5.2) is

$$A_0 = \begin{bmatrix} 0_{2\times 2} & I_2 \\ \text{diag}\{-4,-4\} & 0_{2\times 2} \end{bmatrix}, C_0 = \begin{bmatrix} 1 & 0 & 0 & 0 \\ 0 & 1 & 0 & 0 \end{bmatrix}. \tag{5.42}$$

According to A_0 and ARE (3.10), $P, K = -P$ and $\Gamma = P^2$ can be calculated accordingly. Using pole placement method, assign eigenvalues of $A_0 - FC_0$ as -2,-5,-8,-10 and get $F = [10, 0; 0, 15; 12, 0; 0, 46]$. Similarly, assign poles -5,-8,-10 for agents 1, poles -5,-10 for agents 2,3,4, and poles -2,-5,-8,-10 for agents 5,6. Then we get $K_{2i}, i \in \mathbf{I}[1, 6]$ respectively. Fig. 5.3 shows the convergence of $\tilde{v}_{1,i}$ in (5.3) and (5.4), $v_{2,i}$ in (5.22) and heterogeneous OCT error e_i, meaning that the Problem 5.1 is indeed solved.

Example 6. To solve the Problem 5.9, we choose $n_i = 3$ to satisfy Assumption 5.10, i.e., $A_i = A_i'', i \in \mathbf{I}[1, 6]$. The leader's dynamics remains the same as

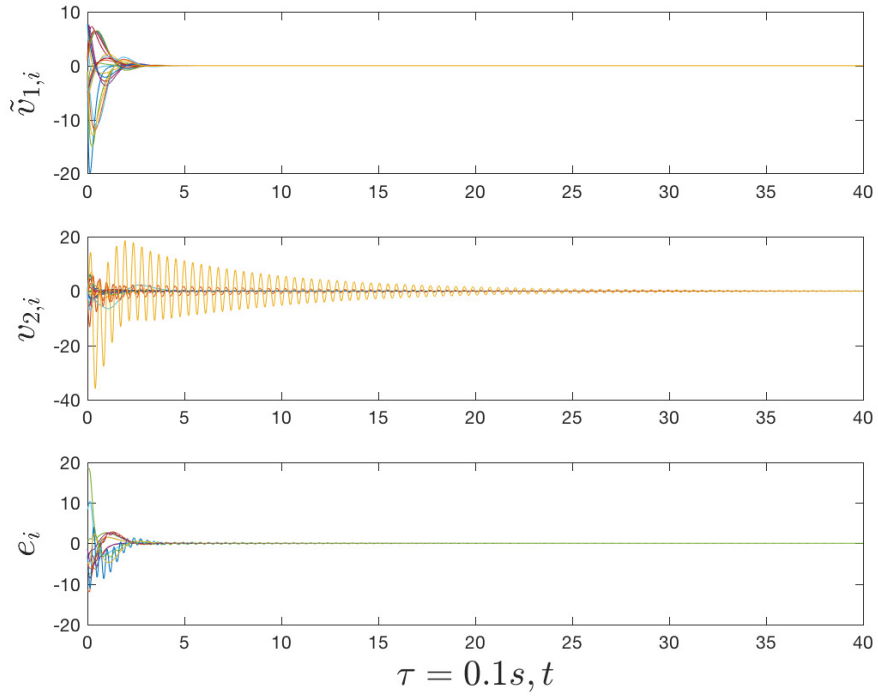

Figure 5.3: The leader's state observer error $\tilde{v}_{1,i} = v_{1,i} - x_0$ (top), the observer $v_{2,i}$ of the state predictor Z_i (middle), and the OCT error $e_i = y_i - y_0$ (bottom).

in Example 1. The disturbance w_i is generated by $w_i = \begin{bmatrix} 0 & f(i) \\ f(i) & 0 \end{bmatrix}, i \in \mathbf{I}[1,6]$ where $f = [1, 2, 0.1, 0.2, 0.5, 1.5]^T$. F_i is chosen as $F_i = [0; I_2], i \in \mathbf{I}[1,3]$ and $F_i = [I_2; 0], i \in \mathbf{I}[4,6]$. It is obvious that $(S_i, E_i), i \in \mathbf{I}[1,6]$ are observable. The $\bar{P}_i$, $K_{3i}, K'_{3i}, K_{4i}, i \in \mathbf{I}[1,6]$ can be calculates similarly as in Example 1. The input delay is chosen as $0.04s$.

Fig. 5.4(a) illustrates the OCT error converging to zero asymptotically, which means the Problem 5.9 is solved. Specifically, we choose agent 5 to analyze the observers' performances. Recall that both the leader's state observer $v_{1,i}$ and the APESO $v_{3,i}, \hat{w}_i$ are fully distributed and are verified by the Fig. 5.5 (a)-(c). The control input of agent 5 is drawn in Fig. 5.5 (d). Fig. 5.4(b) validates that $\lim_{t\to\infty} c_{3i}(t-\tau) = \lim_{t\to\infty} c_{3i}(t), \lim_{t\to\infty} \rho_{3i}(t-\tau) = \lim_{t\to\infty} \rho_{3i}(t)$ and $\lim_{t\to\infty} \varrho_{3i}(t-\tau) = \lim_{t\to\infty} \varrho_{3i}(t)$.

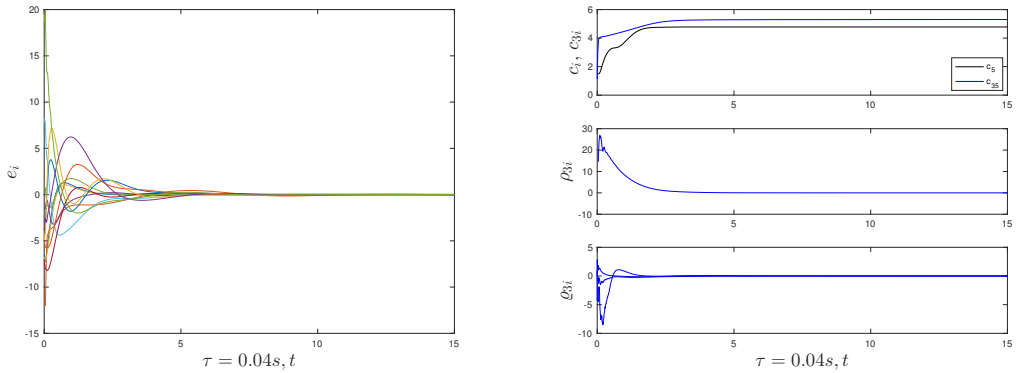

(a) $e_i = y_i - y_0$. (b)

Figure 5.4: (a) The output consensus tracking error; (b)c_i, c_{3i} (top), ρ_i (middle), ϱ_i (bottom) for agent $i = 5$.

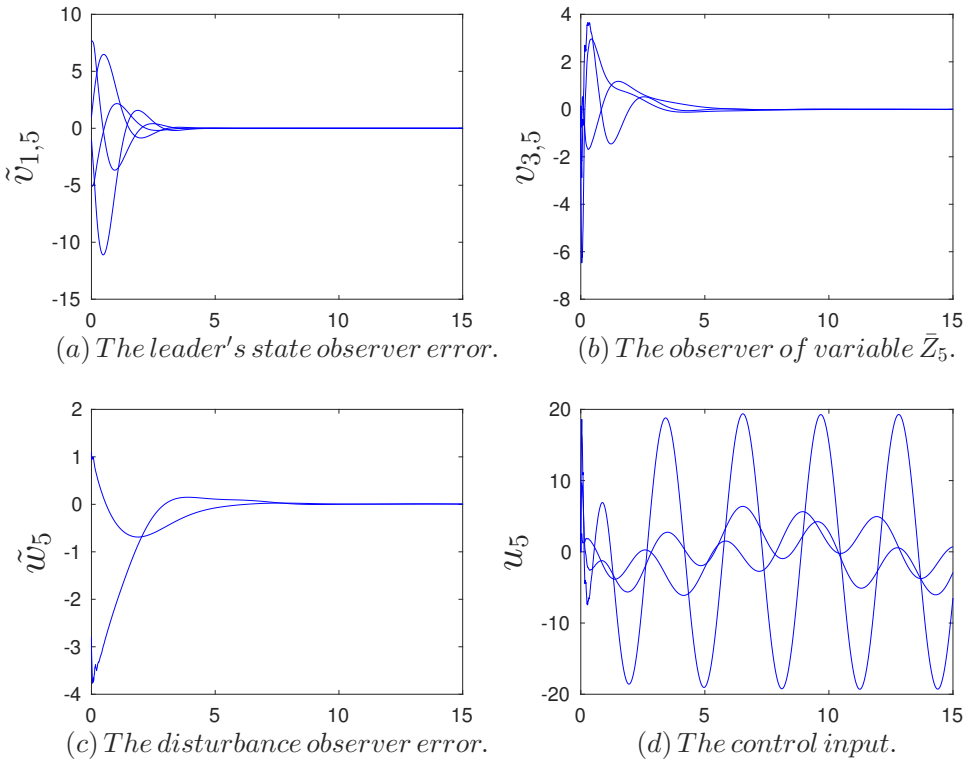

(a) *The leader's state observer error.* (b) *The observer of variable* $\bar{Z}_5$.

(c) *The disturbance observer error.* (d) *The control input.*

Figure 5.5: The observers' performances and the control input of agent $i = 5$.

5.4 Summary

Contributions

- √ Propose the novel state predictor (5.5).
- √ Design the novel adaptive predictive extended state observer in Section 5.2 to estimate the external disturbance and the redesigned state predictor (5.26) in a fully distributed fashion.
- √ Present the detailed and creative thinking about how to design fully distributed observers to construct the control input in order to achieve the control objective by a cooperative way in case of many constraints, e.g., heterogeneous dynamics, different state dimensions.

Chapter 6

Constant input & time-varying output delay

Contents

In the previous Chapters 4 and 5, the controllers are designed based on absolute/relative state information, and no output delay is considered. In this chapter, we extend the results in Chapters 5 to consider the time-varying output delay. The descriptor approach introduced in Chapter 1.3 is used to analyze the stability by means of Lyapunov-Krasovskii functionals (LKFs). Detailed comparisons about how to design parameters to have better control performance dealing with time-varying output delay is given. Finally, how to design fully distributed controllers dealing with cooperative control problems from consensus to TVF, then to time-varying FC for heterogeneous LTI MASs, is demonstrated.

Since there are many variables in this chapter, some may coincide with those in the previous chapter. Fortunately, these variables will be defined clearly here.

Similar as (5.1), consider a group of N followers with non-identical linear dynamics given by

$$\begin{aligned} \dot{x}_i(t) &= A_i x_i(t) + B_i u_i(t-\tau_u), \\ y_i(t) &= C_i x_i(t-\tau_y(t)), \quad i \in \mathbf{I}[1,N] \end{aligned} \tag{6.1}$$

τ_u is the known constant input delay and $\tau_y(t)$ is the time-varying output delay satisfying $0 \leq \tau_y(t) \leq \bar{\tau}, \dot{\tau}_y(t) \leq d < 1$.

The leader is indexed by 0 and its dynamics is

$$\dot{x}_0(t) = A_0 x_0(t), \quad y_0(t) = C_0 x_0(t-\tau_y(t)) \tag{6.2}$$

where $A_0 \in \mathbb{R}^{n\times n}, C_0 \in \mathbb{R}^{q\times n}$, and $x_0(t) \in \mathbb{R}^n$, $y_0(t) \in \mathbb{R}^q$ are the state and output of the leader, respectively. Note that only a portion of followers can get the leader's information.

Now, for each IF (see Chapter 5 for more details), similar as (5.3), design the Luenberger-like observer as

$$\dot{v}_{1,i}(t) = A_0 v_{1,i}(t) - F[y_0(t) - C_0 v_{1,i}(t-\tau_y(t))], i \in \mathbf{I}[1,M]. \tag{6.3}$$

Denote the observer error as $\tilde{v}_{1,i} = v_{1,i} - x_0, i \in \mathbf{I}[1,N]$. After some calculations, we have

$$\dot{\tilde{v}}_{1,i}(t) = A_0 \tilde{v}_{1,i}(t) + FC_0 \tilde{v}_{1,i}(t-\tau_y(t)), i \in \mathbf{I}[1,M], \tag{6.4}$$

where parameter matrix F will be designed in Section 6.1.

6.1 Observer with time-varying output delay

In this section, two approached are developed to decide the upper bound $\bar{\tau}$ of output delay $\tau_y(t)$. The detailed steps are provided.

6.1.1 Lyapunov-Krasovskii functional approach

Inspired by the work of Fridman (2014), we design the LKF to analysis the stability of observer estimating error dynamics (6.4) as follows:

$$\begin{aligned} V_{12} =& \tilde{v}_{1,i}^T(t) P \tilde{v}_{1,i}(t) + \int_{t-\bar{\tau}}^{t} \tilde{v}_{1,i}^T(s) S \tilde{v}_{1,i}(s) ds + \int_{t-\tau_y(t)}^{t} \tilde{v}_{1,i}^T(s) Q \tilde{v}_{1,i}(s) ds \\ &+ \bar{\tau} \int_{-\bar{\tau}}^{0} \int_{t+\theta}^{t} \dot{\tilde{v}}_{1,i}^T(s) R \dot{\tilde{v}}_{1,i}(s) ds d\theta \end{aligned} \tag{6.5}$$

where $P>0, S\geq 0, Q\geq 0, R\geq 0$ are symmetric matrices to be determined later. The derivative of V_{12} is

$$\begin{aligned}\dot{V}_{12} =&2\tilde{v}_{1,i}^T(t)P\dot{\tilde{v}}_{1,i}(t)+\tilde{v}_{1,i}^T(t)(S+Q)\tilde{v}_{1,i}(t)-\tilde{v}_{1,i}^T(t-\bar{\tau})S\tilde{v}_{1,i}(t-\bar{\tau})+\bar{\tau}^2\dot{\tilde{v}}_{1,i}^T(t)R\dot{\tilde{v}}_{1,i}(t)\\ &-(1-\dot{\tau}_y(t))\tilde{v}_{1,i}^T(t-\tau_y(t))Q\tilde{v}_{1,i}(t-\tau_y(t))-\bar{\tau}\int_{t-\bar{\tau}}^{t}\dot{\tilde{v}}_{1,i}^T(s)R\dot{\tilde{v}}_{1,i}(s)ds\\ \leq&2\tilde{v}_{1,i}^T(t)P\dot{\tilde{v}}_{1,i}(t)+\tilde{v}_{1,i}^T(t)(S+Q)\tilde{v}_{1,i}(t)-\tilde{v}_{1,i}^T(t-\bar{\tau})S\tilde{v}_{1,i}(t-\bar{\tau})+\bar{\tau}^2\dot{\tilde{v}}_{1,i}^T(t)R\dot{\tilde{v}}_{1,i}(t)\\ &-(1-d)\tilde{v}_{1,i}^T(t-\tau_y(t))Q\tilde{v}_{1,i}(t-\tau_y(t))-\bar{\tau}\int_{t-\bar{\tau}}^{t}\dot{\tilde{v}}_{1,i}^T(s)R\dot{\tilde{v}}_{1,i}(s)ds.\end{aligned} \tag{6.6}$$

Now, we regard V_{12} is a function of $\tilde{v}_{1,i}(t), \tilde{v}_{1,i}(t-\tau_y(t))$ and $\tilde{v}_{1,i}(t-\bar{\tau})$. So the integral term $\dot{\tilde{v}}_{1,i}(t)$ in (6.6) needs to be addressed. Applying Jensen's inequality (1.39), we have

$$\begin{aligned}-\bar{\tau}\int_{t-\bar{\tau}}^{t}\dot{\tilde{v}}_{1,i}^T(s)R\dot{\tilde{v}}_{1,i}(s)ds=&-\bar{\tau}\int_{t-\bar{\tau}}^{t-\tau_y(t)}\dot{\tilde{v}}_{1,i}^T(s)R\dot{\tilde{v}}_{1,i}(s)ds-\bar{\tau}\int_{t-\tau_y(t)}^{t}\dot{\tilde{v}}_{1,i}^T(s)R\dot{\tilde{v}}_{1,i}(s)ds\\ \leq&\frac{-\bar{\tau}}{\bar{\tau}-\tau_y(t)}\int_{t-\bar{\tau}}^{t-\tau_y(t)}\dot{\tilde{v}}_{1,i}^T(s)ds\,R\int_{t-\bar{\tau}}^{t-\tau_y(t)}\dot{\tilde{v}}_{1,i}(s)ds\\ &+\frac{-\bar{\tau}}{\tau_y(t)}\int_{t-\tau_y(t)}^{t}\dot{\tilde{v}}_{1,i}^T(s)ds\,R\int_{t-\tau_y(t)}^{t}\dot{\tilde{v}}_{1,i}(s)ds\\ =&\frac{-\bar{\tau}}{\bar{\tau}-\tau_y(t)}\xi_{i2}^TR\xi_{i2}+\frac{-\bar{\tau}}{\tau_y(t)}\xi_{i1}^TR\xi_{i1}\\ =&-\begin{bmatrix}\xi_{i1}^T & \xi_{i2}^T\end{bmatrix}\begin{bmatrix}\frac{1}{\frac{\tau_y(t)}{\bar{\tau}}}R & 0\\ 0 & \frac{1}{\frac{\bar{\tau}-\tau_y(t)}{\bar{\tau}}}R\end{bmatrix}\begin{bmatrix}\xi_{i1}\\ \xi_{i2}\end{bmatrix}\end{aligned} \tag{6.7}$$

where $\xi_{i1}=\tilde{v}_{1,i}(t)-\tilde{v}_{1,i}(t-\tau_y(t))$ and $\xi_{i2}=\tilde{v}_{1,i}(t-\tau_y(t))-\tilde{v}_{1,i}(t-\bar{\tau})$. Here, when $\tau_y(t)\to 0$, there exists the following limit:

$$\begin{aligned}\lim_{\tau_y(t)\to 0}\frac{-\bar{\tau}}{\tau_y(t)}\xi_{i1}^TR\xi_{i1}=&-\bar{\tau}\lim_{\tau_y(t)\to 0}\tau_y(t)\frac{\tilde{v}_{1,i}^T(t)-\tilde{v}_{1,i}^T(t-\tau_y(t))}{\tau_y(t)}R\frac{\tilde{v}_{1,i}(t)-\tilde{v}_{1,i}(t-\tau_y(t))}{\tau_y(t)}\\ &-\bar{\tau}\lim_{\tau_y(t)\to 0}\tau_y(t)\dot{\tilde{v}}_{1,i}^T(t)R\dot{\tilde{v}}_{1,i}(t)\\ =&0.\end{aligned}$$

Similarly, when $\tau_y(t)\to\bar{\tau}$, there exists the following limit:

$$\lim_{\tau_y(t)\to\bar{\tau}}\frac{-\bar{\tau}}{\bar{\tau}-\tau_y(t)}\xi_{i2}^TR\xi_{i2}=0.$$

Now we are ready borrow the following lemma.

Lemma 6.1 (Fridman (2014)) *Let $R_1 \in \mathbb{R}^{n_1 \times n_1}, \ldots, R_N \in \mathbb{R}^{n_N \times n_N}$ be positive matrices, Then for all $\xi_1 \in \mathbb{R}^{n_1}, \ldots, \xi_N \in \mathbb{R}^{n_N}$, for all $\alpha_i > 0$ with $\sum_i \alpha_i = 1$ and for all $S_{ij} \in \mathbb{R}^{n_i \times n_j}, i \in \boldsymbol{I}[1, N], j \in \boldsymbol{I}[1, i-1]$ such that*

$$\begin{bmatrix} R_i & S_{ij} \\ * & R_j \end{bmatrix} \geq 0, \tag{6.8}$$

the following inequality holds:

$$\sum_{i=1}^{N} \frac{1}{\alpha_i} \xi_i^T R_i \xi_i \geq \begin{bmatrix} \xi_1 \\ \xi_2 \\ \vdots \\ \xi_N \end{bmatrix}^T \begin{bmatrix} R_1 & S_{12} & \cdots & S_{1N} \\ * & R_2 & \cdots & S_{2N} \\ * & * & \ddots & \vdots \\ * & * & \cdots & R_N \end{bmatrix} \begin{bmatrix} \xi_1 \\ \xi_2 \\ \vdots \\ \xi_N \end{bmatrix}. \tag{6.9}$$

By applying Lemma 6.1, (6.7) becomes

$$-\bar{\tau} \int_{t-\bar{\tau}}^{t} \dot{\tilde{v}}_{1,i}^T(s) R \dot{\tilde{v}}_{1,i}(s) ds \leq - \begin{bmatrix} \xi_{i1}^T & \xi_{i2}^T \end{bmatrix} \begin{bmatrix} R & S_{12} \\ * & R \end{bmatrix} \begin{bmatrix} \xi_{i1} \\ \xi_{i2} \end{bmatrix}. \tag{6.10}$$

On the other hand, based on (6.4), we have

$$\begin{aligned} \bar{\tau}^2 \dot{\tilde{v}}_{1,i}^T(t) R \dot{\tilde{v}}_{1,i}(t) &= \bar{\tau}^2 [A_0 \tilde{v}_{1,i}(t) + FC_0 \tilde{v}_{1,i}(t - \tau_y(t))]^T R [A_0 \tilde{v}_{1,i}(t) + FC_0 \tilde{v}_{1,i}(t - \tau_y(t))] \\ &= \begin{bmatrix} \tilde{v}_{1,i}(t) \\ \tilde{v}_{1,i}(t - \tau_y(t)) \end{bmatrix}^T \begin{bmatrix} \bar{\tau} A_0^T \\ \bar{\tau} C_0^T F^T \end{bmatrix} R R^{-1} R \begin{bmatrix} \bar{\tau} A_0 & \bar{\tau} F C_0 \end{bmatrix} \begin{bmatrix} \tilde{v}_{1,i}(t) \\ \tilde{v}_{1,i}(t - \tau_y(t)) \end{bmatrix} \\ &= \begin{bmatrix} \tilde{v}_{1,i}(t) \\ \tilde{v}_{1,i}(t - \bar{\tau}) \\ \tilde{v}_{1,i}(t - \tau_y(t)) \end{bmatrix}^T \begin{bmatrix} \bar{\tau} A_0^T R \\ 0 \\ \bar{\tau} C_0^T F^T R \end{bmatrix} R^{-1} \begin{bmatrix} \bar{\tau} R A_0 & 0 & \bar{\tau} R F C_0 \end{bmatrix} \begin{bmatrix} \tilde{v}_{1,i}(t) \\ \tilde{v}_{1,i}(t - \bar{\tau}) \\ \tilde{v}_{1,i}(t - \tau_y(t)) \end{bmatrix}. \end{aligned} \tag{6.11}$$

We can see that the terms related to $\dot{\tilde{v}}_{1,i}(t)$ in (6.6) are transformed to relate to $\tilde{v}_{1,i}(t), \tilde{v}_{1,i}(t-\tau_y(t))$ and $\tilde{v}_{1,i}(t-\bar{\tau})$. Denote $\bar{\xi}_i = col\{\tilde{v}_{1,i}(t), \tilde{v}_{1,i}(t-\bar{\tau}), \tilde{v}_{1,i}(t-\tau_y(t))\}$. Then integrating (6.10) and (6.11) into (6.6), we get

$$\dot{V}_{12} \leq \bar{\xi}_i^T \Phi_1 \bar{\xi}_i + \bar{\xi}_i^T \begin{bmatrix} \bar{\tau} A_0^T R \\ 0 \\ \bar{\tau} C_0^T F^T R \end{bmatrix} R^{-1} \begin{bmatrix} \bar{\tau} R A_0 & 0 & \bar{\tau} R F C_0 \end{bmatrix} \bar{\xi}_i \tag{6.12}$$

where

$$\Phi_1 = \begin{bmatrix} PA_0 + A_0^T P + S + Q - R & S_{12} & PFC_0 + R - S_{12} \\ * & -S - R & R - S_{12}^T \\ * & * & -(1-d)Q - 2R + S_{12} + S_{12}^T \end{bmatrix}. \tag{6.13}$$

Applying Schur complement Lemma 1.8 to the right side of (6.12), then we get

$$\dot{V}_{12} \leq \bar{\xi}_i^T \Phi \bar{\xi}_i \tag{6.14}$$

where

$$\Phi = \begin{bmatrix} PA_0 + A_0^T P + S + Q - R & S_{12} & PFC_0 + R - S_{12} & \bar{\tau} A_0^T R \\ * & -S - R & R - S_{12}^T & 0 \\ * & * & -(1-d)Q - 2R + S_{12} + S_{12}^T & \bar{\tau} C_0^T F^T R \\ * & * & * & -R \end{bmatrix}. \tag{6.15}$$

Now we can conclude that given $\bar{\tau} \geq 0, d \in [0, 1)$, the observer error dynamics (6.4) is uniformly asymptotically stable for all output delays $\tau_y(t) \in [0, \bar{\tau}]$ such that $\dot{\tau}_y(t) \leq d \leq 1$, if there exists $n \times n$ matrices $P > 0, S > 0, Q > 0, R > 0$ and S_{12} such that $\Phi < 0$ and $\begin{bmatrix} R & S_{12} \\ * & R \end{bmatrix} \geq 0$.

Remind that objective is to calculate F. The problem is that in (6.15), there are two nonlinear terms PF and $F^T R$, and they are related because of F. Since the matrices P, F and R are unknown, we cannot calculate Φ in (6.15) by means of Yalmip in Matlab directly, which means the value of parameter F cannot be calculated directly. In fact, there are two ways to calculate F:

1. (1) In Matlab, using Yalmip to calculate $\Phi_1 < 0$ and $\begin{bmatrix} R & S_{12} \\ * & R \end{bmatrix} \geq 0$ at the same time to get F and other matrices P, S, Q, R and $S12$.
   (2) Set the value of $\bar{\tau}$ and verify whether $\Phi < 0$ is satisfied. By manual trials, we can get the almost maximum value of $\bar{\tau}$.

2. Set $R = \varepsilon P$ and the value of $\bar{\tau}$, then calculate $\Phi < 0$ directly. By manual trials, we can get the maximum value of $\bar{\tau}$ which is larger then the previous way.

The problem of the second way is that we introduce another constraint $R = \varepsilon P$, which means the calculation to get $\bar{\tau}$ is still conservative. In the next subsection, we will introduce the descriptor method to calculate $\bar{\tau}$ which can be less conservative.

6.1.2 LKF with descriptor approach

In previous subsection, the reason that we can calculate $\Phi_1 < 0$ but $\Phi < 0$ cannot, is the method we used to deal with the term $\bar{\tau}^2\dot{\tilde{v}}_{1,i}^T(t)R\dot{\tilde{v}}_{1,i}(t)$ in (6.6). In detail, the term $A_0\tilde{v}_{1,i}(t) + FC_0\tilde{v}_{1,i}(t-\tau_y(t))$ is used to replace $\dot{\tilde{v}}_{1,i}(t)$ in (6.11), and this generates the nonlinear term F^TR which is not wanted.

The idea is to employ the *descriptor model transformation* introduced in Fridman (2001) to regard $\dot{\tilde{v}}_{1,i}(t)$ as another state of the LKF V_{12} in addition to $\bar{\xi}_i$ in (6.14). Redesign the LKF as follows:

$$\begin{aligned} V_{13} =&\tilde{v}_{1,i}^T(t)P\tilde{v}_{1,i}(t) + \int_{t-\bar{\tau}}^{t} e^{2\delta(s-t)}\tilde{v}_{1,i}^T(s)S\tilde{v}_{1,i}(s)ds + \int_{t-\tau_y(t)}^{t} e^{2\delta(s-t)}\tilde{v}_{1,i}^T(s)Q\tilde{v}_{1,i}(s)ds \\ &+ \bar{\tau}\int_{-\bar{\tau}}^{0}\int_{t+\theta}^{t} e^{2\delta(s-t)}\dot{\tilde{v}}_{1,i}^T(s)R\dot{\tilde{v}}_{1,i}(s)dsd\theta. \end{aligned} \tag{6.16}$$

Following the similar calculation of (6.6), we get

$$\begin{aligned} \dot{V}_{13} + 2\delta V_{13} =&2\tilde{v}_{1,i}^T(t)P\dot{\tilde{v}}_{1,i}(t) + 2\delta\tilde{v}_{1,i}^T(t)P\tilde{v}_{1,i}(t) + \tilde{v}_{1,i}^T(t)(S+Q)\tilde{v}_{1,i}(t) \\ &- e^{-2\delta\bar{\tau}}\tilde{v}_{1,i}^T(t-\bar{\tau})S\tilde{v}_{1,i}(t-\bar{\tau}) \\ &- (1-\dot{\tau}_y(t))e^{-2\delta\tau_y(t)}\tilde{v}_{1,i}^T(t-\tau_y(t))Q\tilde{v}_{1,i}(t-\tau_y(t)) \\ &+ \bar{\tau}^2\dot{\tilde{v}}_{1,i}^T(t)R\dot{\tilde{v}}_{1,i}(t) - \bar{\tau}\int_{t-\bar{\tau}}^{t} e^{2\delta(s-t)}\dot{\tilde{v}}_{1,i}^T(s)R\dot{\tilde{v}}_{1,i}(s)ds \\ \leq&2\tilde{v}_{1,i}^T(t)P\dot{\tilde{v}}_{1,i}(t) + 2\delta\tilde{v}_{1,i}^T(t)P\tilde{v}_{1,i}(t) + \tilde{v}_{1,i}^T(t)(S+Q)\tilde{v}_{1,i}(t) \\ &- e^{-2\delta\bar{\tau}}\tilde{v}_{1,i}^T(t-\bar{\tau})S\tilde{v}_{1,i}(t-\bar{\tau}) \\ &- (1-d)e^{-2\delta\bar{\tau}}\tilde{v}_{1,i}^T(t-\tau_y(t))Q\tilde{v}_{1,i}(t-\tau_y(t)) \\ &+ \bar{\tau}^2\dot{\tilde{v}}_{1,i}^T(t)R\dot{\tilde{v}}_{1,i}(t) - \bar{\tau}e^{-2\delta\bar{\tau}}\int_{t-\bar{\tau}}^{t}\dot{\tilde{v}}_{1,i}^T(s)R\dot{\tilde{v}}_{1,i}(s)ds \\ &+ 2[\tilde{v}_{1,i}^T(t)P_2^T + \dot{\tilde{v}}_{1,i}^T(t)P_3^T][A_0\tilde{v}_{1,i}(t) + FC_0\tilde{v}_{1,i}(t-\tau_y(t)) - \dot{\tilde{v}}_{1,i}(t)]. \end{aligned} \tag{6.17}$$

The last term in (6.17), which is identically zero, comes from the descriptor method (see Fridman (2014) in detail). Here, denote $\bar{\xi}_i' = col\{\tilde{v}_{1,i}(t), \dot{\tilde{v}}_{1,i}(t), \tilde{v}_{1,i}(t-\bar{\tau}), \tilde{v}_{1,i}(t-\tau_y(t))\}$. So unlike (6.11), we leave $\bar{\tau}^2\dot{\tilde{v}}_{1,i}^T(t)R\dot{\tilde{v}}_{1,i}(t)$ unchanged. Integrating (6.10) into (6.17), we have

$$\dot{V}_{13} + 2\delta V_{13} \leq \bar{\xi}_i'^T\Phi_2\bar{\xi}_i' < 0 \tag{6.18}$$

if the following matrix inequality is feasible:

$$\Phi_2 = \begin{bmatrix} \Phi_2(1,1) & P - P_2^T + A_0^T P_3 & e^{-2\delta\bar{\tau}} S_{12} & P_2^T F C_0 + e^{-2\delta\bar{\tau}}(R - S_{12}) \\ * & \bar{\tau}^2 R - P_3 - P_3^T & 0 & P_3^T F C_0 \\ * & * & -e^{-2\delta\bar{\tau}}(S+R) & e^{-2\delta\bar{\tau}}(R - S_{12}^T) \\ * & * & * & \Phi_2(4,4) \end{bmatrix} < 0, \tag{6.19}$$

where

$$\begin{aligned} \Phi_2(1,1) =& 2\delta P + S + Q - e^{-2\delta\bar{\tau}} R + P_2^T A_0 + A_0^T P_2, \\ \Phi_2(4,4) =& -(1-d) e^{-2\delta\bar{\tau}} Q + e^{-2\delta\bar{\tau}}(-2R + S_{12} + S_{12}^T). \end{aligned} \tag{6.20}$$

Then we arrive at the following lemma.

Lemma 6.2 *Given $\delta > 0, \bar{\tau} \geq 0, d \in [0,1)$, the observer error dynamics (6.4) is exponentially stable with the decay rate δ for all output delays $\tau_y(t) \in [0, \bar{\tau}]$ such that $\dot{\tau}_y(t) \leq d \leq 1$, if there exist $n \times n$ matrices $P > 0, S > 0, Q > 0, R > 0$ and S_{12}, P_2, P_3 such that the LMIs (6.19) and $\begin{bmatrix} R & S_{12} \\ * & R \end{bmatrix} \geq 0$ are feasible. If $\delta = 0$ and LMI (6.19) is still feasible, then (6.4) is exponentially stable with a small enough decay rate.*

The above lemma just gives us the stability analysis of observer error dynamics (6.4). But the objective is to calculate F. To do that, set $P_3 = \varepsilon P_2, Y = P_2^T F$, then LMI (6.19) changes to

$$\Phi_3 = \begin{bmatrix} \Phi_2(1,1) & P - P_2^T + \varepsilon A_0^T P_2 & e^{-2\delta\bar{\tau}} S_{12} & Y C_0 + e^{-2\delta\bar{\tau}}(R - S_{12}) \\ * & \bar{\tau}^2 R - \varepsilon P_2 - \varepsilon P_2^T & 0 & \varepsilon Y C_0 \\ * & * & -e^{-2\delta\bar{\tau}}(S+R) & e^{-2\delta\bar{\tau}}(R - S_{12}^T) \\ * & * & * & \Phi_2(4,4) \end{bmatrix} < 0, \tag{6.21}$$

which is totally linear. Use Yalmip in Matlab to calculate Y, then $F = (P_2^T)^{-1} Y$.

6.1.3 Comparisons

In this subsection, the comparison with/without the descriptor approach, and the relation between exponential convergence rate and upper bound $\bar{\tau}$ are performed out by several simulations under the same initial conditions.

Choose (A_0, C_0) as (5.42) in Chapter 5.3. Choose $\delta = 0$, then $\Phi_3 < 0$ will guarantee the asymptotic stability of (6.4), which is the same stable performance as $\Phi < 0$ in (6.15). Set $\varepsilon = 0.3, d = 0$, then we get $\bar{\tau} = 0.37s$,

	Constant delay	Time-varying delay
Without descriptor	$d = 0, \bar{\tau} = 0.37s$	$d = 0.4, \bar{\tau} = 0.35s$
With descriptor	$\delta = 0, d = 0, \bar{\tau} = 0.49s$	$\delta = 0, d = 0.5, \bar{\tau} = 0.49s$
	$\delta = 0.1, d = 0, \bar{\tau} = 0.43s$	$\delta = 0.1, d = 0.45, \bar{\tau} = 0.43s$
	$\delta = 0.2, d = 0, \bar{\tau} = 0.38s$	$\delta = 0.2, d = 0.4, \bar{\tau} = 0.38s$
	$\delta = 0.6, d = 0, \bar{\tau} = 0.26s$	$\delta = 0.6, d = 0.3, \bar{\tau} = 0.26s$

Table 6.1: Comparisons of different $\bar{\tau}$ for with / without descriptor method and for asymptotic / exponential stability

$F = \begin{bmatrix} -0.2975 & 0.0000 & 0.0278 & -0.0000 \\ -0.0000 & -0.2975 & -0.0000 & 0.0278 \end{bmatrix}^T$ for $\Phi < 0$ and $\bar{\tau} = 0.49s, F = \begin{bmatrix} -1.2200 & -0.0000 & 0.7768 & -0.0000 \\ 0.0000 & -1.2200 & 0.0000 & 0.7768 \end{bmatrix}^T$ for $\Phi_3 < 0$. It means that using the descriptor method can guarantee a larger upper limit of the time-varying output delay. This is why we will adopt the descriptor method to design the observer (6.3).

By choosing $\delta > 0$, $\Phi_3 < 0$ will guarantee the exponential stability of (6.4), and the upper limit $\bar{\tau}$ will become smaller compared with $\delta = 0$. For example, after simulations, we get $\bar{\tau} = 0.43s$ for $\delta = 0.1$, $\bar{\tau} = 0.38s$ for $\delta = 0.2$ and $\bar{\tau} = 0.27s$ for $\delta = 0.6$, 10 simulation results are summarized in Table 6.1. it shows that with descriptor approach, the designed observer (6.3) can endure larger output delay. It also shows there is a trade-off between the exponential convergence rate δ and the value of upper bound $\bar{\tau}$. And no matter the output delay is constant or time-varying, the upper bound $\bar{\tau}$ does not change.

6.2 Heterogeneous consensus control

Following the similar design and analysis in Chapter 5, for each UF, the same adaptive distributed observer (5.4) is adopted to estimate the leader's state x_0 as follows:

$$\begin{aligned} \dot{v}_{1,i} =& A_0 v_{1,i} + K(c_i + \rho_i)\varrho_i, \\ \dot{c}_i =& \varrho_i^T \Gamma \varrho_i, \\ \varrho_i =& \sum_{j=1}^{N} a_{ij}(v_{1,i} - v_{1,j}), \\ \rho_i =& \varrho_i^T P \varrho_i, i \in \mathbf{I}[M+1, N]. \end{aligned} \tag{6.22}$$

Then, to solve the heterogeneous consensus problem, the controller is designed similarly as (5.5), (5.20), (5.22) as follows:

$$\begin{aligned} u_i =& K_{2i}v_{2,i} + U_i e^{A_0\tau_u} v_{1,i}, \\ \dot{v}_{2,i} =& (A_i + B_iK_{2i})v_{2,i} + B_iK_{2i}(v_{2,i} - Z_i) \\ Z_i(t) =& \int_{t-\tau_u}^{t} e^{A_i(t-s)} B_i(u_i(s) - U_i e^{A_0\tau_u} v_{1,i}(s))ds \\ &+ e^{A_i\tau_u}(x_i(t) - X_i v_{1,i}(t)), i \in \mathbf{I}[1, N]. \end{aligned} \tag{6.23}$$

Theorem 6.3 *Consider Assumptions 3.12, 3.13, 5.2 and 5.3. The OCT problem for heterogeneous MASs (6.1) considering constant input delay and time-varying output delay, is solved by the fully distributed controller consisting of (6.3), (6.22) and (6.23), if K_{2i}, X_i and U_i are chosen as in Lemma 5.6 and F is designed as in Lemma 6.2.*

Proof. The proof is mainly the same as in Chapter 5.1.2-5.1.4. The mathematical difference is that $\Omega_i(t), i \in \mathbf{I}[1, M]$ in (5.11) will become

$$\Omega_i(t) = e^{A_i\tau} B_i U_i \int_{t-\tau_u}^{t} e^{A_0(t-s)} F C_0 \tilde{v}_{1,i}(s - \tau_y(t))ds + e^{A_i\tau} X_i F C_0 \tilde{v}_{1,i}(t - \tau_y(t)), \tag{6.24}$$

and $e_i(t), i \in \mathbf{I}[1, N]$ in (5.19) becomes

$$e_i(t) = C_i\tilde{x}_i(t - \tau_y(t)) + C_0\tilde{v}_{1,i}(t - \tau_y(t)). \tag{6.25}$$

Thanks to $\lim_{t\to\infty} \tilde{x}_i(t) = 0$ and $\lim_{t\to\infty} \tilde{v}_{1,i}(t) = 0$, we conclude that $\lim_{t\to\infty} e_i(t) = 0$, i.e., the proof is finished.

Remark 6.4 *The output delay $\tau_y(t)$ is not used for the controller design here.*

Remark 6.5 *We can see that in the construction of state predictor $Z_i(t)$ in (6.23), the state $x_i(t)$ is used, which means that the state information is needed for the controller design. As it is known that in reality, sometimes the state information is not available, the output-based controller is preferred. So we redesign the state predictor as follows:*

$$\begin{aligned} Z_i(t) =& e^{A_i\tau_u}(\hat{x}_i(t) - X_i v_{1,i}(t)) + \int_{t-\tau_u}^{t} e^{A_i(t-s)} B_i K_{2i} v_{2,i}(s)ds, \\ \dot{\hat{x}}_i =& A_i\hat{x}_i(t) + B_i u_i(t - \tau_u) - F_i[y_i(t) - C_i\hat{x}_i(t - \tau_y(t))], i \in \boldsymbol{I}[1, N]. \end{aligned} \tag{6.26}$$

The stability analysis of Luenberger-like observer $\hat{x}_i(t)$ and the design of parameter matrix F_i is similar as $\tilde{v}_{1,i}(t)$ in Section 6.1. The convergence analysis of consensus error is quite straightforward based on (5.7) and (6.24), so the detail is omitted.

For the heterogeneous consensus problem considering constant input delay, time-varying output delay and matched disturbances, follow the work in Chapter 5.2, the controller can be designed as follows:

$$\begin{aligned}
u_i =&K_{3i}v_{3,i} + U_i e^{A_0\tau_u} v_{1,i} - F_i e^{S_i\tau_u}\hat{w}_i\\
\dot{v}_{3,i} =&(A_i + B_{3i}K_{3i})v_{3,i} + K_{3i}^{'}(c_{3i} + \rho_{3i})\varrho_{3i} + \Omega_i^{'},\\
\dot{\hat{w}}_i =&S_i\hat{w}_i + K_{4i}(c_{3i} + \rho_{3i})\varrho_{3i},\\
\dot{c}_{3i} =&\zeta_i^T\bar{\Gamma}\zeta_i,\ \rho_{3i} = \zeta_i^T\bar{P}\zeta_i,\\
\varrho_{3i} =&a_{i0}\tilde{v}_{3,i} + \sum_{j=1}^{N} a_{ij}(\tilde{v}_{3,i} - \tilde{v}_{3,j}) = \sum_{j=1}^{N} l_{ij}\tilde{v}_{3,j},\\
\tilde{v}_{3,i} =&v_{3,i} - \bar{Z}_i, \tilde{w} = \hat{w}_i - w_i, \zeta_i(t) = \begin{bmatrix} \tilde{v}_{3,i}(t) \\ e^{S_i\tau}\tilde{w}_i(t-\tau_u) \end{bmatrix},\\
\bar{Z}_i(t) =&x_i(t) - X_i v_{1,i}(t) + \int_{t-\tau_u}^{t} e^{A_i(t-\tau_u-s)}B_iK_{3i}v_{3,i}(s)ds, i \in \mathbf{I}[1,N],
\end{aligned} \tag{6.27}$$

where

$$\begin{aligned}
\Omega_i^{'}(t) =&B_iU_i\int_{t-\tau_u}^{t} e^{A_0(t-s)}F(C_0v_{1,i}(s-\tau_y(t)) - y_0(s))ds\\
&+ X_iF[C_0v_{1,i}(t-\tau_y(t)) - y_0(t)], i \in \mathbf{I}[1,M]\\
\Omega_i^{'}(t) =&-B_iU_i\int_{t-\tau_u}^{t} e^{A_0(t-s)}K(c_i(s) + \rho_i(s))C_0\varrho_i(s)ds\\
&- X_iK(c_i(t) + \rho_i(t))C_0\varrho_i(t), i \in \mathbf{I}[M+1,N].
\end{aligned} \tag{6.28}$$

Theorem 6.6 *Consider Assumptions 3.12, 3.13, 5.2, 5.3, 5.10 and 5.11. The OCT problem for heterogeneous MASs (6.1) considering constant input delay, time-varying output delay and matched disturbance, is solved by the fully distributed controller consisting of (6.3), (6.22), (6.27) and (6.28), if (X_i, U_i) is chosen as in Lemma 5.6, $A_i + e^{-A_i\tau}B_iK_{3i}$ is Hurwitz, $\bar{\Gamma} = T^TT, \bar{K} = -\bar{P}^{-1}T^T$ and $\bar{P} > 0$ is a solution to the LMI (5.35), and F is designed as in Lemma 6.2.*

The proof is similar as Chapter 5.2 and is omitted here.

Remark 6.7 *The time-varying output delay $\tau_y(t)$ is used for the controller design in (6.28) compared with Theorem 6.3, which is due to the integration of matched disturbance.*

6.2.1 Simulations

The Matlab function **"ddesd(ddefun,delays,history,tspan)"** is used to simulate the time-varying delay.

This subsection is to verify Theorem 6.6. Following the same initial conditions as in Example 6 of Chapter 5.3, Fig. 6.1 illustrates all the OCT errors converging to zero asymptotically, which verifies Theorem 6.6. Specifically, In Fig. 6.1, (a) shows that without using the descriptor approach, it takes about 35 seconds for the OCT error to converge to zero; (b) is about 14 seconds with the descriptor approach and $\delta = 0$; (c) is about 10 seconds with the descriptor approach and $\delta = 05$.. These differences come from the parameter matrix F calculation in the designed observer $v_{1,i}(t)$ in (6.3), whose observing error is demonstrated in Fig. 6.2. The results in Fig. 6.2 coincide with the comparisons in Subsection 6.1.3, i.e., the descriptor approach in Section 6.1.2 has better control performance.

It is known that different control input will lead to different tracking performance. Take the agent 1 as an example and its input is depicted in Fig.6.3. The main difference comes from the first control interval $[0, 10s]$.

In the following of this chapter, we will extend the OCT control result for heterogeneous MASs to TVF and time-varying FC control issues.

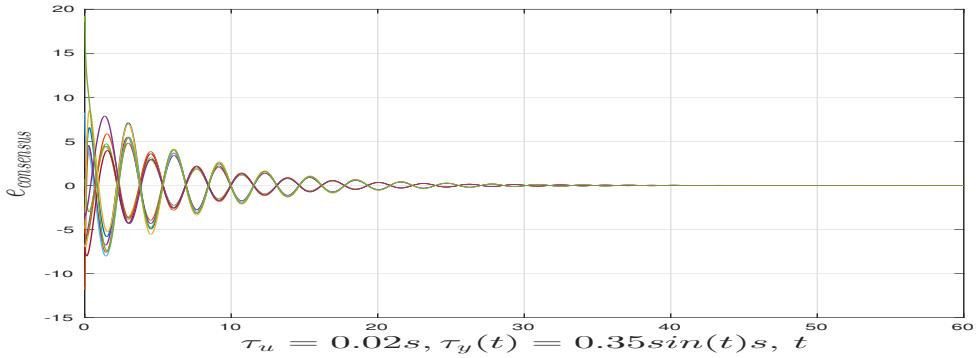

(a) Without descriptor approach.

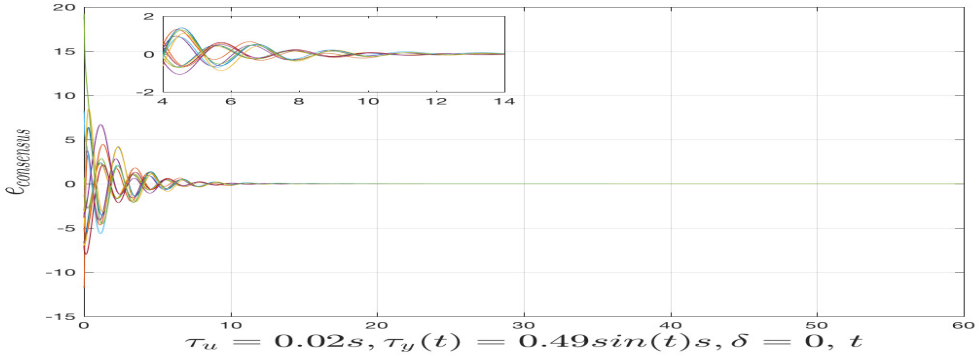

(b) With descriptor approach and $\delta = 0$.

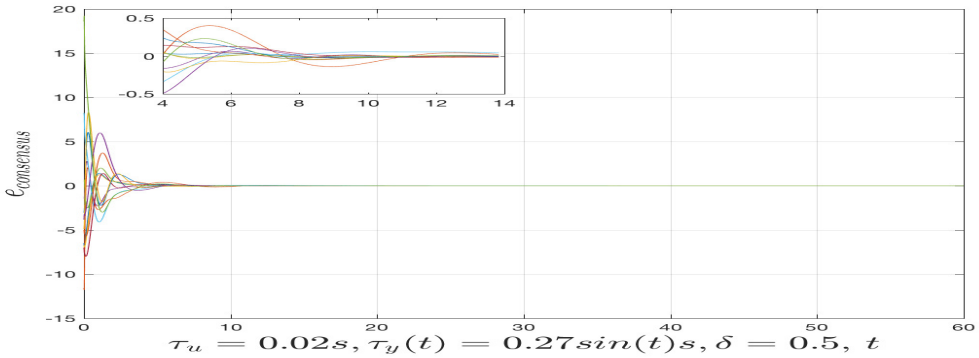

(c) With descriptor approach and $\delta = 0.5$.

Figure 6.1: Comparisons of output consensus tracking error evolutions.

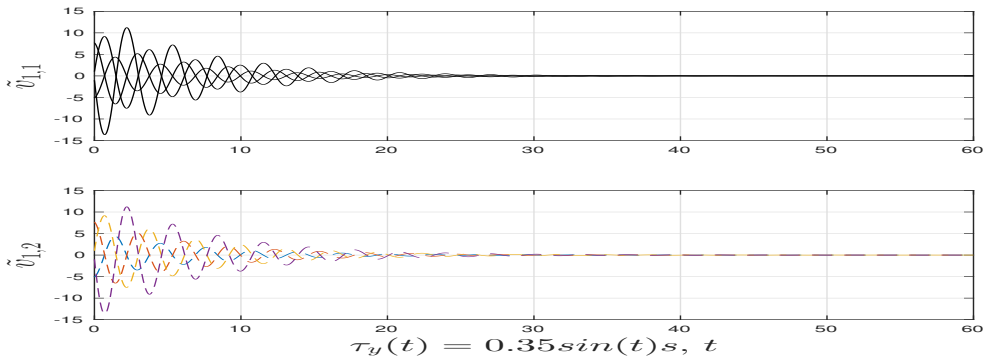

(a) Without descriptor approach.

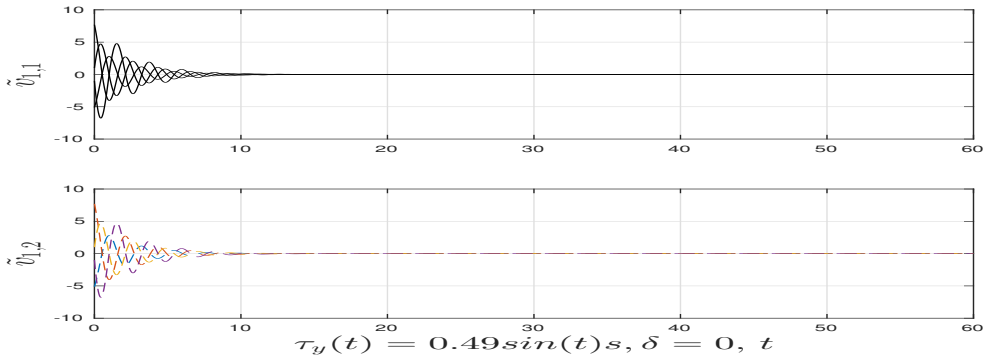

(b) With descriptor approach and $\delta = 0$.

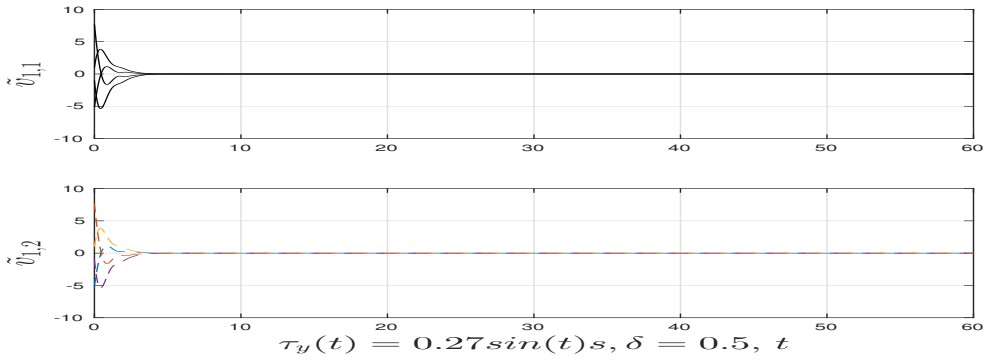

(c) With descriptor approach and $\delta = 0.5$.

Figure 6.2: Comparisons of observer error $\tilde{v}_{1,i} = v_{1,i} - x_0, i \in \mathbf{I}[1,2]$ in (6.4) evolutions.

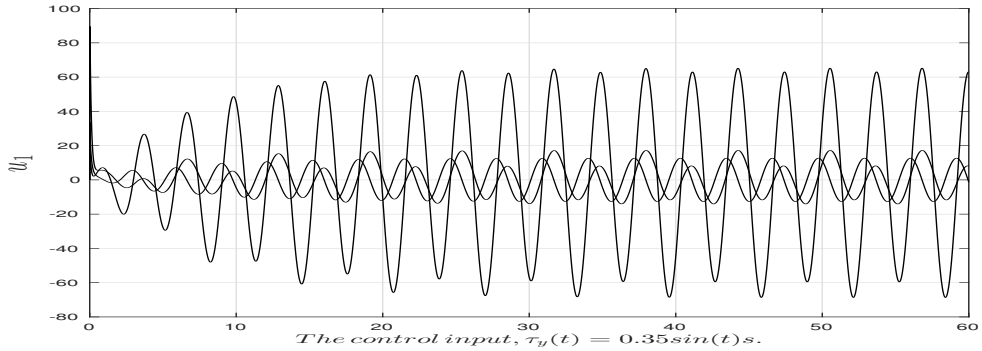

(a) Without descriptor approach.

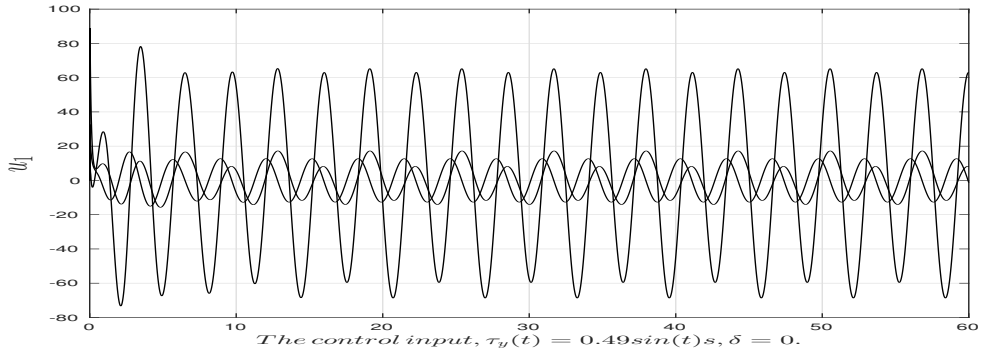

(b) With descriptor approach and $\delta = 0$.

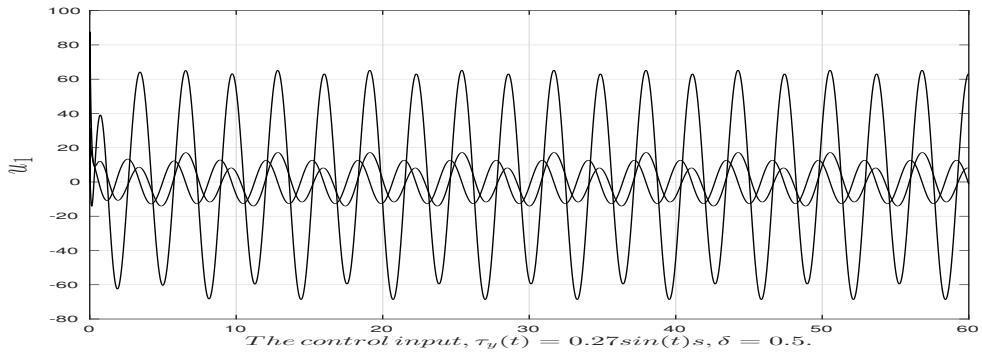

(c) With descriptor approach and $\delta = 0.5$.

Figure 6.3: Control input differences for agent 1.

6.3 Heterogeneous TVF tracking control

In this section, the controller design is based on the results of Section 6.2, Chapter 1.6.2 and Chapter 3.1. First, the TVF shape definition for heterogeneous MASs is the same as (1.47) and (1.48), which is rewritten here for the reading convenience as follows:

$$\begin{aligned} \dot{h}_i(t) =& A_h h_i(t),\ y_{hi}(t) = C_i h_i(t-\tau_y(t)) \\ X_{hi}A_h =& A_i X_{hi} + B_i U_{hi},\ C_0 = C_i X_{hi}, \quad i \in \mathbf{I}[1,N]. \end{aligned} \tag{6.29}$$

Similar as (6.23) and (6.26), the output-based controller is designed as

$$\begin{aligned} u_i =& K_{2i}v_{2,i} + U_i e^{A_0\tau_u} v_{1,i} + U_{hi} e^{A_h\tau_u} h_i, \\ \dot{v}_{2,i} =& (A_i + B_i K_{2i}) v_{2,i} + B_i K_{2i}(v_{2,i} - Z_i) \\ Z_i(t) =& \int_{t-\tau_u}^{t} e^{A_i(t-s)} B_i (u_i(s) - U_i e^{A_0\tau_u} v_{1,i}(s) - U_{hi} e^{A_h\tau_u} h_i(s)) ds \\ &+ e^{A_i\tau_u}(\hat{x}_i(t) - X_i v_{1,i}(t) - X_{hi} h_i(t)) \\ \dot{\hat{x}}_i =& A_i\hat{x}_i(t) + B_i u_i(t-\tau_u) - F_i[y_i(t) - C_i\hat{x}_i(t-\tau_y(t))], i \in \mathbf{I}[1,N]. \end{aligned} \tag{6.30}$$

It is not difficult to prove that $\lim_{t\to\infty}(\hat{x}_i(t) - X_i v_{1,i}(t) - X_{hi} h_i(t)) = 0$ and $\lim_{t\to\infty}(\hat{x}_i(t) - x_i(t)) = 0$ based on the previous results. As it is stated out in (3.32), the TVF tracking error is defined as $e_i = y_i - y_0 - y_{hi}$. The convergence proof is similar as the proof of Theorem 3.15 and is omitted here.

Theorem 6.8 *Consider Assumptions 3.12, 3.13, 5.2 and 5.3. The TVF tracking problem for heterogeneous MASs (6.1) considering constant input delay and time-varying output delay, is solved by the fully distributed controller consisting of (6.3), (6.22) and (6.30), if K_{2i}, X_i and U_i are chosen as in Lemma 5.6, F is designed as in Lemma 6.2, and F_i is designed similar as F by replacing (A_0, C_0) as (A_i, C_i) in (6.21).*

The proof is similar as Chapters 3.1 and 5.1 and is omitted here.

Moreover, the controller design to solve the heterogeneous TVF tracking problem considering constant input delay, time-varying output delay and matched disturbances can be completed based on (6.27) and (6.30).

6.4 Heterogeneous time-varying FC control

Based on the results in Chapter 3, the controller design for heterogeneous time-varying FC control problem is quite straightforward after we have solved the TVF tracking problem in the previous section.

Based on the same analysis in Chapter 3.2, for the agent $i, i \in \mathbf{I}[N+1, N+L]$, first, the following fully distributed adaptive observer $v_{1,i}(t) \in \mathbb{R}^n$ is proposed to estimate the $(-\mathcal{L}_4^{-1}\mathcal{L}_3 \otimes I_n)(\mathbf{1} \otimes x_0)$ information

$$\begin{aligned}
\dot{v}_{4,i} =& A_0 v_{4,i} + K^{'}(d_i + \varrho_i)\theta_i, \\
\dot{d}_i =& \theta_i^T \Gamma^{'} \theta_i, \\
\theta_i =& \sum_{j=1}^{N} a_{ij}(v_{4,i} - v_{1,j}) + \sum_{j=N+1}^{N+L} a_{ij}(v_{4,i} - v_{4,j}) \\
\varrho_i =& \theta_i^T P^{'} \theta_i, i \in \mathbf{I}[N+1, N+L].
\end{aligned} \tag{6.31}$$

Then, to estimate the $(-\mathcal{L}_4^{-1}\mathcal{L}_3 \otimes I_n)h$, the fully distributed adaptive observer $\hat{h}_i \in \mathbb{R}^n$ is proposed the same as (3.16). Now the output-based controller can be designed as

$$\begin{aligned}
u_i =& K_{2i} v_{2,i} + U_i e^{A_0 \tau_u} v_{4,i} + U_{hi} e^{A_h \tau_u} \hat{h}_i, \\
\dot{v}_{2,i} =& (A_i + B_i K_{2i}) v_{2,i} + B_i K_{2i}(v_{2,i} - Z_i) \\
Z_i(t) =& \int_{t-\tau_u}^{t} e^{A_i(t-s)} B_i (u_i(s) - U_i e^{A_0 \tau_u} v_{4,i}(s) - U_{hi} e^{A_h \tau_u} \hat{h}_i(s)) ds \\
&+ e^{A_i \tau_u}(\hat{x}_i(t) - X_i v_{1,i}(t) - X_{hi} \hat{h}_i(t)) \\
\dot{\hat{x}}_i =& A_i \hat{x}_i(t) + B_i u_i(t - \tau_u) - F_i[y_i(t) - C_i \hat{x}_i(t - \tau_y(t))], i \in \mathbf{I}[N+1, N+L].
\end{aligned} \tag{6.32}$$

Theorem 6.9 *Consider Assumptions 3.7, 3.12, 3.13 and 5.2. The time-varying FC control problem for heterogeneous MASs (6.1) considering constant input delay and time-varying output delay, is solved by the fully distributed controller consisting of (3.16), (6.3), (6.22), (6.31) and (6.32), if $(K^{'}, \Gamma^{'}, P^{'})$ are designed in Lemma 3.18, $\hat{h}_i$ is designed in Lemma 3.19 , (K_{2i}, X_i, U_i) are chosen as in Lemma 5.6, F is designed in Lemma 6.2, and F_i is designed similar as F by replacing (A_0, C_0) as (A_i, C_i) in (6.21).*

The proof is similar as Chapters 3.2 and 5.1 and is omitted here. Moreover, the controller design to solve the time-varying FC control problem considering

constant input delay, time-varying output delay and matched disturbances can be completed based on (6.27), (6.31) and (6.32).

6.4.1 Simulations

Since we have provided detailed comparison simulating results for the OCT control problem in Section 6.2, the simulations for TVF and time-varying FC control are omitted here because they are also similar as in Chapter 3.3.

6.5 Summary

Contributions

- √ Use LKF and descriptor approach to analyze the leader's state observer estimating error $\tilde{v}_{1,i}(t)$ in (6.4).
- √ Provide detailed comparisons about how to design parameter matrix F inside leader's state observer $v_{1,i}(t)$ in (6.3).
- √ Design the output-based fully distributed controllers for heterogeneous MASs to deal with consensus, TVF and time-varying FC control, step by step.

A

Time-varying delays & mismatched disturbances

Contents

In Chapters 4-6, only the matched disturbances which are in the same channels as the control inputs (e.g., $E = BF$ in (4.1) and $E_i = B_iF_i$ in (5.25)) and the constant input delay, are considered. Another common characteristic is the integral terms inside the controllers of Chapters 4-6. As it has stated out clearly in Chapter 1.3 that the integral term discretization should be carefully executed in real applications, especially for open-loop unstable systems because the bad discretization may make systems become unstable, inspired by Najafi *et al.* (2013), we drop the integral term off in this chapter.

Since there are many variables in this chapter, some may coincide with those in the previous chapter. Fortunately, these variables will be defined clearly here.

The research objective is to develop distributed controllers to solve the consensus control problem for homogeneous MASs considering time-varying input / output delays and mismatched disturbances. Consider a group of N identical

single input MAS with time-varying input and output delays as following:

$$\begin{aligned} \dot{\mathcal{X}}_i(t) &= A\mathcal{X}_i(t) + Bu_i(t-\tau_u(t)) + \Delta_l f_i(t), \\ y_i(t) &= C\mathcal{X}_i(t-\tau_y(t)), \quad i \in \mathbf{I}[1,N] \end{aligned} \tag{A.1}$$

where $\mathcal{X}_i(t) \in \mathbb{R}^n$, $u_i(t) \in \mathbb{R}$ and $y_i(t) \in \mathbb{R}^q$ are respectively the state, control input and measured output of the i-th follower. $A \in \mathbb{R}^{n\times n}, B \in \mathbb{R}^n$ and $C \in \mathbb{R}^{q\times n}$ are constant and known matrices. $\tau_u(t)$ and $\tau_y(t)$ are respectively the time-varying input and output delays satisfying $0 \leq \tau_u(t) \leq \bar{\tau}_1, \dot{\tau}_u(t) \leq d_1 < 1$, $0 \leq \tau_y(t) \leq \bar{\tau}_2, \dot{\tau}_y(t) \leq d_2 < 1$ and $d_1 + d_2 = d < 1, \bar{\tau}_1 + \bar{\tau}_2 = \bar{\tau}$. $\Delta_l \in \mathbb{R}^n$ is a vector whose l-th entry is equal to one and the rest are zero. $f_i : \mathbb{R}_{\geq 0} \to \mathbb{R}$ is an unknown external disturbance satisfying the follow assumption.

Assumption A.1 *$f_i(t)$ can be described as $f_i(t) = \iota_i(t) + \varpi_i(t)$ with*

$$\begin{aligned} \dot{\varsigma}_{1i}(t) &= S_1\varsigma_{1i}(t), \\ \iota_i(t) &= S_2\varsigma_{1i}(t), \end{aligned} \tag{A.2}$$

where the exogenous system ($S_1 \in \mathbb{R}^{s\times s}, S_2 \in \mathbb{R}^{1\times s}$) is known and observable, $\varsigma_{1i}(t) \in \mathbb{R}^s$ with unknown initial condition $\varsigma_{1i}(0)$, and $\varpi_i(t) : \mathbb{R}_{\geq 0} \to \mathbb{R}$ is an unknown bounded signal which represents the unmodeled disturbance component satisfying $\varpi_i(t) \in L_2[0,\infty), i \in \boldsymbol{I}[1,N]$

Assumption A.2 *(A, B) is controllable and (A, C) is observable.*

A.1 Model transformation

Based on Assumption A.2, without loss of generality, we consider the pair (A, B) in the canonical controllable form as follows:

$$A = \begin{bmatrix} 0 & 1 & 0 & \cdots & 0 \\ 0 & 0 & 1 & \cdots & 0 \\ \vdots & \vdots & \vdots & \ddots & \vdots \\ 0 & 0 & 0 & \cdots & 1 \\ a_1 & a_2 & a_3 & \cdots & a_n \end{bmatrix}, \qquad B = \begin{bmatrix} 0 \\ 0 \\ \vdots \\ 0 \\ b \end{bmatrix}. \tag{A.3}$$

If $l \neq n$, the disturbance $f_i(t)$ will be mismatched, meaning that $f_i(t)$ affect the state through channels in which the input has no direct influence (Sanz *et al.*, 2018). Inspired by the above chapters about the matched disturbances and have

analyzed the components of $f_i(t)$ in (A.2), we would like to put $\iota_i(t)$ in the input channel. So the following state transformation (Ding, 2003) is employed:

$$\left.\begin{array}{l} x_{ij}(t) = \mathcal{X}_{ij}(t),\ j \in \mathbf{I}[1,l] \\ x_{ij}(t) = \mathcal{X}_{ij}(t) + \iota_i^{j-l-1}(t),\ j \in \mathbf{I}[l+1,n] \end{array}\right\} i \in \mathbf{I}[1,N], \tag{A.4}$$

where $x_i(t) \in \mathbb{R}^n, i \in \mathbf{I}[1,N]$. Then the system (A.1) can be transformed into

$$\begin{array}{rcl} \dot{x}_i(t) & = & Ax_i(t) + B[u_i(t-\tau_u(t)) + w_i(t)] + \Delta_l \varpi_i(t), \\ y_i(t) & = & Cx_i(t-\tau_y(t)), \quad i \in \mathbf{I}[1,N] \end{array} \tag{A.5}$$

with

$$w_i(t) = \frac{1}{b}\left(\iota_i^{n-l}(t) - \sum_{j=l+1}^{n} a_j \iota_i^{j-l-1}(t)\right). \tag{A.6}$$

The mathematical detail about the state transformation is given in the following:

$$\begin{array}{rcl} j = 1, \dot{x}_{i1} & = & \mathcal{X}_{i2}, \\ & \vdots & \\ j = l-1, \dot{x}_{i(l-1)} & = & \mathcal{X}_{il}, \\ j = l, \dot{x}_{il} & = & \dot{\mathcal{X}}_{il} = \mathcal{X}_{i(l+1)} + \iota_i + \varpi_i = x_{i(l+1)} + \varpi_i, \\ j = l+1, \dot{x}_{i(l+1)} & = & \dot{\mathcal{X}}_{i(l+1)} + \dot{\iota} = \mathcal{X}_{i(l+2)} + \dot{\iota}_i = x_{i(l+2)}, \\ & \vdots & \\ j = n-1, \dot{x}_{i(n-1)} & = & \dot{\mathcal{X}}_{i(n-1)} + \iota_i^{n-1-l-1+1} = \mathcal{X}_{in} + \iota_i^{n-l-1} = x_{in}, \\ j = n, \dot{x}_{in} & = & \dot{\mathcal{X}}_{in} + \iota_i^{n-l-1+1} \\ & = & a_1\mathcal{X}_{i1} + a_2\mathcal{X}_{i2} + \ldots + a_n\mathcal{X}_{in} + bu_i(t-\tau_u(t)) + \iota_i^{n-l} \\ & = & a_1 x_{i1} + \ldots + a_l x_{il} + a_{l+1}(x_{i(l+1)} - \iota_i) + \ldots + a_n(x_{in} - \iota_i^{n-l-1}) \\ & + & bu_i(t-\tau_u(t)) + \iota_i^{n-l} \\ & = & a_1 x_{i1} + \ldots + a_n x_{in} + b[u_i(t-\tau_u(t)) + w_i(t)]. \end{array}$$

In addition, from (A.6) and (A.2), we have

$$w_i(t) = \frac{1}{b}\left(S_2\varsigma_{1i}^{n-l}(t) - \sum_{j=l+1}^{n} a_j S_2 \varsigma_{1i}^{j-l-1}(t)\right) = S_2\varsigma_{2i}(t)$$

with $\varsigma_{2i}(t) = \frac{1}{b}\left(\varsigma_{1i}^{n-l}(t) - \sum_{j=l+1}^{n} a_j \varsigma_{1i}^{j-l-1}(t)\right)$ and

$$\dot{\varsigma}_{2i}(t) = \frac{1}{b}\left(S_1\varsigma_{1i}^{n-l}(t) - \sum_{j=l+1}^{n} a_j S_1 \varsigma_{1i}^{j-l-1}(t)\right) = S_1\varsigma_{2i}(t).$$

So we can see that the component $\iota_i(t)$ in (A.2) of the external disturbance $f_i(t)$ can be viewed as the generator of the equivalent input disturbance $w_i(t)$ in (A.5), which can be described as

$$\begin{aligned} \dot{\varsigma}_{2i}(t) &= S_1\varsigma_{2i}(t), \\ w_i(t) &= S_2\varsigma_{2i}(t), \end{aligned} \tag{A.7}$$

where $w_i(t) \in \mathbb{R}$ and $\varsigma_{2i}(t) \in \mathbb{R}^s$ with unknown initial condition $\varsigma_{2i}(0)$.

The leader is indexed by 0 and its dynamics is

$$\dot{x}_0(t) = Ax_0(t), \quad y_0(t) = Cx_0(t - \tau_y(t)). \tag{A.8}$$

Note that only a portion of followers can get the leader's information. Denote the state and output consensus tracking error for follower i as $\tilde{x}_i(t) = x_i(t) - x_0(t)$ and $\tilde{y}_i(t) = y_i(t) - y_0(t)$, respectively. The dynamics of $(\tilde{x}_i(t), \tilde{y}_i(t))$ is

$$\begin{aligned} \dot{\tilde{x}}_i(t) =& A\tilde{x}_i(t) + B[u_i(t - \tau_u(t)) + w_i(t)] + \Delta_l\varpi_i(t), \\ \tilde{y}_i(t) =& C\tilde{x}_i(t - \tau_y(t)), \quad i \in \mathbf{I}[1, N]. \end{aligned} \tag{A.9}$$

A.2 Predictive ESO design

Similar as Chapter 4.1, let us define an augmented state $Z_i(t) = [\tilde{x}_i^T(t), \varsigma_{2i}^T(t)]^T$ and based on (A.7) and (A.9), we have

$$\begin{aligned} \dot{Z}_i(t) &= \underbrace{\begin{bmatrix} A & BS_2 \\ 0 & S_1 \end{bmatrix}}_{A_z} Z_i(t) + \underbrace{\begin{bmatrix} B \\ 0 \end{bmatrix}}_{B_z} u_i(t - \tau_u(t)) + \underbrace{\begin{bmatrix} \Delta_l \\ 0 \end{bmatrix}}_{B_w} \varpi_i(t) \\ \tilde{y}_i(t) &= \underbrace{\begin{bmatrix} C & 0 \end{bmatrix}}_{C_z} Z_i(t - \tau_y(t)), \quad i \in \mathbf{I}[1, N] \end{aligned} \tag{A.10}$$

where $A_z \in \mathbb{R}^{(n+s)\times(n+s)}$, $B_z \in \mathbb{R}^{(n+s)}$, $B_w \in \mathbb{R}^{(n+s)}$ and $C_z \in \mathbb{R}^{q\times(n+s)}$.

The idea is to use the relative output measurements to design the predictive ESO as $\hat{Z}_i(t) = [\hat{x}_i^T(t), \hat{\varsigma}_{2i}^T(t)]^T \in \mathbb{R}^{(n+s)}$ to estimate the extended state $Z_i(t)$. Recall that in Chapter 4.1, we adopted the FSA approach to transform the system (4.1) with a delayed input into a delay-free system by the help of variable transformation (4.6) in which there exits an integral term. The small drawback is that the integral calculation is very time-consuming. So we would like to design an ESO without any integral term. Inspired by the work of Najafi *et al.* (2013), $\hat{Z}_i(t)$ is

proposed as follows:

$$\begin{aligned}\dot{\hat{Z}}_i(t) =& A_z\hat{Z}_i(t) + B_z u_i(t)\\ &+ L\left\{\sum_{j=1,j\neq i}^{N} a_{ij}\left[y_i - y_j + \hat{x}_j(t-\tau(t))\right] + a_{i0}(y_i - y_0) - \sum_{j=0,j\neq i}^{N} a_{ij}\hat{x}_i(t-\tau(t))\right\}\\ =& A_z\hat{Z}_i(t) + B_z u_i(t) + L\sum_{j=1}^{N} l_{ij}\left[\tilde{y}_j(t) - C_z\hat{Z}_j(t-\tau(t))\right]\\ =& A_z\hat{Z}_i(t) + B_z u_i(t) + LC_z\sum_{j=1}^{N} l_{ij}\left[Z_j(t-\tau_y(t)) - \hat{Z}_j(t-\tau(t))\right]\end{aligned} \tag{A.11}$$

where $\tau(t) = \tau_u(t) + \tau_y(t)$, a_{ij} is the ij-th entry of the adjacent matrix $\mathcal{A}$ of the communication topology satisfying Assumption 2.6, and $L \in \mathbb{R}^{(n+s)\times q}$ will be designed in Section A.3. The relative output measurements and the historical values $\hat{x}_j(t-\tau(t)), j \in \mathbf{I}[1, N]$ are used to design this ESO. The term $a_{i0}(y_i - y_0)$ means not all followers need to get the leader's information. Compared with (A.10), there is no input delay in (A.11). It means this ESO can predict the value of $Z_i(t)$ with $\tau_u(t)$ unites of time in advance. Define the ESO estimating error as $\tilde{Z}_i(t) = Z_i(t) - \hat{Z}_i(t-\tau_u(t))$. Then the error dynamics $\tilde{Z}_i(t) \in \mathbb{R}^{(n+s)}$ is

$$\dot{\tilde{Z}}_i(t) = A_z\tilde{Z}_i(t) - LC_z\sum_{j=1}^{N} l_{ij}\tilde{Z}_j(t-\tau(t)) + B_w\varpi_i(t). \tag{A.12}$$

In order to prove the stability of $\tilde{Z}_i(t)$, we need to guarantee that when $\tau(t) = 0$ and $\varpi_i(t) = 0$, $\tilde{Z}_i(t)$ can be controlled to converge to zero. Similar as the error dynamics in (2.20) and (4.15), to guarantee that, the following assumption is required.

Assumption A.3 $\left(\begin{bmatrix} A & BS_2 \\ 0 & S_1 \end{bmatrix}, \begin{bmatrix} C & 0 \end{bmatrix}\right)$ *is detectable.*

Assumption A.3 does not imply the loss of generality since it could always be satisfied if (A, C) is observable in Assumption A.2 by changing the dimension of the exogenous model(Isidori & Byrnes, 1990, Sanz *et al.*, 2018).

Similar as the control input design (4.8), to deal with the mismatched disturbance, the control law can be designed as

$$u_i(t) = -K\hat{x}_i(t) - S_2\hat{\varsigma}_{2i}(t) = -[K,\ S_2]\hat{Z}_i(t), \tag{A.13}$$

where $K \in \mathbb{R}^{1\times n}$ will be designed in Section A.3. Integrating (A.13) into the consensus tracking error dynamics (A.9), we get

$$\dot{\tilde{x}}_i(t) = (A - BK)\tilde{x}_i(t) + [BK,\ BS_2]\tilde{Z}_i(t) + \Delta_l \varpi_i(t). \tag{A.14}$$

The Kronecker product format of (A.12) and (A.14) is

$$\begin{cases} \dot{\tilde{x}}(t) = [I_N \otimes (A - BK)]\tilde{x}(t) + (I_N \otimes [BK,\ BS_2])\tilde{Z}(t) + (I_N \otimes \Delta_l)\varpi(t), \\ \dot{\tilde{Z}}(t) = (I_N \otimes A_z)\tilde{Z}(t) - (\mathcal{L}_1 \otimes LC_z)\tilde{Z}(t - \tau(t)) + (I_N \otimes B_w)\varpi(t). \end{cases} \tag{A.15}$$

Let us define another augmented variable $\zeta(t) = [\tilde{x}^T(t), \tilde{Z}^T(t)]^T \in \mathbb{R}^{N(2n+s)}$ and rewrite (A.15) as

$$\begin{aligned} \dot{\zeta}(t) = &\underbrace{\begin{bmatrix} I_N \otimes (A - BK) & I_N \otimes [BK,\ BS_2] \\ 0 & I_N \otimes A_z \end{bmatrix}}_{A_\zeta} \zeta(t) \\ &+ \underbrace{\begin{bmatrix} 0 & 0 \\ 0 & -\mathcal{L}_1 \otimes LC_z \end{bmatrix}}_{A_{\zeta 1}} \zeta(t - \tau(t)) + \underbrace{\begin{bmatrix} I_N \otimes \Delta_l \\ I_N \otimes B_w \end{bmatrix}}_{B_\zeta} \varpi(t) \end{aligned} \tag{A.16}$$

where $A_\zeta \in \mathbb{R}^{N(2n+s)\times N(2n+s)}$, $A_{\zeta 1} \in \mathbb{R}^{N(2n+s)\times N(2n+s)}$ and $B_\zeta \in \mathbb{R}^{N(2n+s)\times N}$.

Now the original problem is transformed into the H_∞ stabilization problem of (A.16). we can see that the format of (A.16) is quite similar as (6.4), so the descriptor method will be used to design protocol parameters L and K.

A.3 Stability analysis

Design the LKF as follows:

$$\begin{aligned} V_{14} =& \zeta^T(t)P\zeta(t) + \int_{t-\bar{\tau}}^{t} e^{2\delta(s-t)}\zeta^T(s)S\zeta(s)ds + \int_{t-\tau(t)}^{t} e^{2\delta(s-t)}\zeta^T(s)Q\zeta(s)ds \\ &+ \bar{\tau}\int_{-\bar{\tau}}^{0}\int_{t+\theta}^{t} e^{2\delta(s-t)}\dot{\zeta}^T(s)R\dot{\zeta}(s)dsd\theta \end{aligned} \tag{A.17}$$

where $P \in \mathbb{R}^{N(2n+s)\times N(2n+s)} > 0, S \in \mathbb{R}^{N(2n+s)\times N(2n+s)} \geq 0, Q \in \mathbb{R}^{N(2n+s)\times N(2n+s)} \geq 0, R \in \mathbb{R}^{N(2n+s)\times N(2n+s)} \geq 0$. Following the similar calculation of (6.17), denote

$\gamma = \text{diag}\{\gamma_1, \ldots, \gamma_N\}, \gamma_i > 0, i \in \mathbf{I}[1, N]$, then we have

$$\begin{aligned}
\dot{V}_{14}+2\delta V_{14} - \varpi^T(t)\gamma\varpi(t) =& 2\zeta^T(t)P\dot{\zeta}(t) + 2\delta\zeta^T(t)P\zeta(t) \\
&+ \zeta^T(t)(S+Q)\zeta(t) - e^{-2\delta\bar{\tau}}\zeta^T(t-\bar{\tau})S\zeta(t-\bar{\tau}) \\
&- (1-\dot{\tau}(t))e^{-2\delta\tau(t)}\zeta^T(t-\tau(t))Q\zeta(t-\tau(t)) - \varpi^T(t)\gamma\varpi(t) \\
&+ \bar{\tau}^2\dot{\zeta}^T(t)R\dot{\zeta}(t) - \bar{\tau}\int_{t-\bar{\tau}}^{t} e^{2\delta(s-t)}\dot{\zeta}^T(s)R\dot{\zeta}(s)ds \\
\leq& 2\zeta^T(t)P\dot{\zeta}(t) + 2\delta\zeta^T(t)P\zeta(t) - (1-d)e^{-2\delta\bar{\tau}}\zeta^T(t-\tau(t))Q\zeta(t-\tau(t)) \\
&+ \zeta^T(t)(S+Q)\zeta(t) - e^{-2\delta\bar{\tau}}\zeta^T(t-\bar{\tau})S\zeta(t-\bar{\tau}) \\
&+ \bar{\tau}^2\dot{\zeta}^T(t)R\dot{\zeta}(t) - \bar{\tau}e^{-2\delta\bar{\tau}}\int_{t-\bar{\tau}}^{t}\dot{\zeta}^T(s)R\dot{\zeta}(s)ds - \varpi^T(t)\gamma\varpi(t) \\
&+ 2[\zeta^T(t)P_2^T + \dot{\zeta}^T(t)P_3^T][A_\zeta\zeta(t) + A_{\zeta 1}\zeta(t-\tau(t)) + B_\zeta\varpi(t) - \dot{\zeta}(t)] \\
=& \bar{\zeta}^T\Phi_4\bar{\zeta}
\end{aligned} \tag{A.18}$$

where $\bar{\zeta} = col\{\zeta(t), \dot{\zeta}(t), \zeta(t-\bar{\tau}), \zeta(t-\tau(t)), \varpi(t)\}, P_2 \in \mathbb{R}^{N(2n+s)\times N(2n+s)}, P_3 \in \mathbb{R}^{N(2n+s)\times N(2n+s)}$ and

$$\Phi_4 = \begin{bmatrix}
\Phi_4(1,1) & \Phi_4(1,2) & e^{-2\delta\bar{\tau}}S_{12} & P_2^TA_{\zeta 1} + e^{-2\delta\bar{\tau}}(R - S_{12}) & P_2^TB_\zeta \\
* & \Phi_4(2,2) & 0 & P_3^TA_{\zeta 1} & P_3^TB_\zeta \\
* & * & -e^{-2\delta\bar{\tau}}(S+R) & e^{-2\delta\bar{\tau}}(R - S_{12}^T) & 0 \\
* & * & * & \Phi_4(4,4) & 0 \\
* & * & * & * & -\gamma
\end{bmatrix}, \tag{A.19}$$

$$\begin{aligned}
\Phi_4(1,1) =& 2\delta P + S + Q - e^{-2\delta\bar{\tau}}R + P_2^TA_\zeta + A_\zeta^TP_2, \\
\Phi_4(1,2) =& P - P_2^T + A_\zeta^TP_3,\ \gamma = \text{diag}\{\gamma_1, \ldots, \gamma_N\} \\
\Phi_4(2,2) =& \bar{\tau}^2R - P_3 - P_3^T, \\
\Phi_4(4,4) =& -(1-d)e^{-2\delta\bar{\tau}}Q + e^{-2\delta\bar{\tau}}(-2R + S_{12} + S_{12}^T).
\end{aligned}$$

Following the Proposition 1 in Fridman & Dambrine (2009), solving (A.18) gets

$$\zeta^T(t)P\zeta(t) < e^{-2\delta t}\zeta^T(0)P\zeta(0) + [1 - e^{-2\delta t}]\frac{\lambda_{max}(\gamma)}{2\delta}|\varpi(t)|^2 \tag{A.20}$$

with $\varpi_i(t) \in L_2[0,\infty), i \in \mathbf{I}[1,N]$ if $\Phi_4 < 0$ is feasible. Because of $\zeta(t) = [\tilde{x}^T(t), \tilde{Z}^T(t)]^T$, we can conclude that

$$\|\tilde{x}(t)\|^2 < \frac{\lambda_{max}(\gamma)}{2\delta\lambda_{min}(P)}|\varpi(t)|^2, t \to \infty. \tag{A.21}$$

Theorem A.4 *Consider Assumptions 2.6, A.1, A.2, A.3 hold. Given* $\bar{\tau} \geq 0, d \in [0,1), \gamma = \text{diag}\{\gamma_1, \ldots, \gamma_N\} > 0$ *and tuning parameters* $\kappa > 0, , \delta > 0, \varepsilon > 0$*, the consensus control problem for homogeneous MASs considering time-varying input / output delays and mismatched disturbances is solved by the distributed controller consisting of (A.11) and (A.13), if there exist* $N(2n+s) \times N(2n+s)$ *matrices* $P > 0, S > 0, Q > 0, R > 0, S_{12}$*,* $n \times n$ *matrix* $U > 0$*, and matrices* $P_{21} \in \mathbb{R}^{Nn \times Nn}, P_{22} \in \mathbb{R}^{(n+s)\times(n+s)}, P'_{22} \in \mathbb{R}^{N(n+s)\times Nn}, X \in \mathbb{R}^{1\times n}, Y \in \mathbb{R}^{(n+s)\times q}$ *such that the following LMIs are feasible:*

$$\Phi_5 = \begin{bmatrix} \Phi_4(1,1) & \Phi_5(1,2) & e^{-2\delta\bar{\tau}}S_{12} & \Phi_5(1,4) & P_2^T B_\zeta \\ * & \Phi_5(2,2) & 0 & \varepsilon \begin{bmatrix} 0 & 0 \\ 0 & -\mathcal{L}_1 \otimes YC_z \end{bmatrix} & \varepsilon P_2^T B_\zeta \\ * & * & -e^{-2\delta\bar{\tau}}(S+R) & e^{-2\delta\bar{\tau}}(R - S_{12}^T) & 0 \\ * & * & * & \Phi_4(4,4) & 0 \\ * & * & * & * & -\gamma \end{bmatrix} < 0, \tag{A.22}$$

$$AU + UA^T - BX - X^T B^T + \kappa U < 0 \tag{A.23}$$

$$\begin{bmatrix} R & S_{12} \\ * & R \end{bmatrix} \geq 0 \tag{A.24}$$

where

$$\begin{aligned} \Phi_5(1,2) =& P - P_2^T + \varepsilon A_\zeta^T P_2, \\ \Phi_5(1,4) =& \begin{bmatrix} 0 & 0 \\ 0 & -\mathcal{L}_1 \otimes YC_z \end{bmatrix} + e^{-2\delta\bar{\tau}}(R - S_{12}), \\ \Phi_5(2,2) =& \bar{\tau}^2 R - \varepsilon(P_2 + P_2^T), \end{aligned}$$

$P_2 = \begin{bmatrix} P_{21} & 0 \\ P'_{22} & (I_N \otimes P_{22}) \end{bmatrix}$ *and the controller parameters are designed as* $K = XU^{-1}, L = (P_{22}^T)^{-1}Y$*. The consensus error dynamics (A.14) is exponentially stable with the decay rate* δ *for any delay* $0 \leq \tau_u(t) \leq \bar{\tau}_1, 0 \leq \tau_y(t) \leq \bar{\tau}_2, \bar{\tau}_1 + \bar{\tau}_2 = \bar{\tau}$ *if* $\lim_{t\to\infty} \varpi_i(t) = 0, i \in \boldsymbol{I}[1,N]$*, and achieves (A.21) if* $0 \neq \varpi_i(t) \in L_2[0,\infty), i \in \boldsymbol{I}[1,N]$*.*

Proof. From (A.16) and (A.19), we can see that the the terms $P_2^T A_{\zeta 1}, P_3^T A_{\zeta 1}$

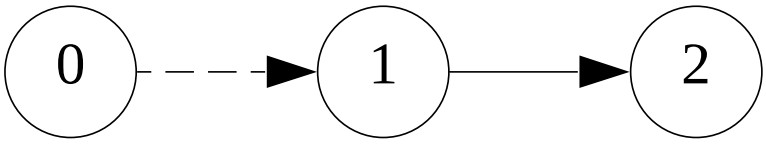

Figure A.1: The directed communication topology $\mathcal{G}$ satisfying Assumption 2.6.

in LMI (A.19) are nonlinear. In order to linearize Φ_4, we set $P_2 = \text{diag}\{P_{21}, (I_N \otimes P_{22})\}$ and $P_3 = \varepsilon P_2$, and define $Y = P_2^T L$. Then LMI (A.19) can be transformed into (A.22) directly. By analyzing the structure of A_ζ in (A.16), the $(A - BK)$ should be Hurwitz, which can be guaranteed by (A.23).

To apply Theorem A.4, the following steps should be followed.

1. Set parameter κ in (A.23) to get matrices X, U, then calculate $K = XU^{-1}$ for control input protocol (A.13).

2. Calculate A_ζ in (A.16) based on K, set the decay rate δ and parameters $\varepsilon, \bar{\tau}, d, \gamma = \text{diag}\{\gamma_1, \ldots, \gamma_N\}$, use Yalmip in Matlab to solve LMIs (A.22) and (A.24) to get matrices P_{22}, Y, then calculate $L = (P_{22}^T)^{-1} Y$ for predictive ESO (A.11).

A.4 Simulations

This example verifies Theorem A.4. Set system (A.1) and (A.2) as

$$A = \begin{bmatrix} 0 & 1 & 0 \\ 0 & 0 & 1 \\ 0 & 0 & -2 \end{bmatrix}, B = \begin{bmatrix} 0 \\ 0 \\ -2 \end{bmatrix}, \Delta_l = \begin{bmatrix} 0 \\ 1 \\ 0 \end{bmatrix}, S_1 = \begin{bmatrix} 0 & 0.1 \\ -0.1 & 0 \end{bmatrix} S_2 = \begin{bmatrix} 1 & 0 \end{bmatrix}$$

and $C = [1\,0\,0]$. Then (A, B) is controllable, (A, C) and (S_1, S_2) are observable. The digraph $\mathcal{G}$ is shown in Fig. A.1. The input/output delays are taken as $\tau_u(t) = 0.05\cos(t), \tau_y(t) = 0.05\sin(t)$ and $\bar{\tau} = 0.1$. The initial conditions for control input is $u_i(t) = 0, t \in \mathbf{I}[-\bar{\tau}, 0], i \in \mathbf{I}[1, 2]$. Set parameter $\kappa = 0.5$, then solving LMI (A.23) gets $K = \begin{bmatrix} -0.6863 & -1.7969 & 0.2283 \end{bmatrix}$. Now set $\delta = 0.01, \varepsilon = 0.3, d = 0.2, \gamma = \text{diag}\{\gamma_1, \gamma_2\} \leq \text{diag}\{0.7, 0.7\}$ and $P \geq 0.2I$, then solving LMIs (A.22) and (A.24) gets $L = \begin{bmatrix} 4.8249 & 5.8709 & 0.5147 & -0.6095 & -0.0054 \end{bmatrix}^T$.

First, we provide the simulation where there is no unmodeled disturbance component, i.e., $\varpi_i(t) = 0, i \in \mathbf{I}[1, 2]$. Fig. A.2 (a) shows the consensus error convergent to zero, indeed when there exists no unmodeled disturbance component $\varpi_i(t)$. Fig. A.2 (b) describes agents' state trajectories tracking the leader's corresponding state. Denote $\hat{w}_i(t) = S_2 \hat{\varsigma}_{2i}$ where $\hat{\varsigma}_{2i}$ is the designed predictive disturbance

observer in (A.11). Then the function of $\hat{w}_i(t)$ is to estimate disturbance $w_i(t)$ in (A.9), which is illustrated in Fig. A.2 (c) where the input delay is set to be constant for the convenience of plotting historical data, i.e., $\hat{w}_i(t-\tau)$.

Second, the unmodeled disturbance component is added to the previous disturbance signal after $t = 100s$. From Fig A.3 (a) to (b), there exist two points to state. (i), the unmodeled disturbance components are well attenuated. (ii) From (a) to (b), $\varpi_2(t)$ does not change, but the amplitude of $\varpi_1(t)$ changes from 13 to 1.3. One can see that the unmodeled disturbance attenuation performance of agent 2 is better in (b) than in (a), meaning that agents are influenced by each other in cooperative control of MASs. And from the performance of agent 1, it is clear that the smaller the amplitude of unmodeled disturbance is, the smaller the consensus tracking error is. Note that compared with the values of initial states, the values of unmodeled disturbances are quite large.

From A.3 (b) to (c), one can see that the values of $\gamma_i, i = 1, 2$ are not the only factor to influence the consensus tracking performance. This can be partially verified in (A.21). In fact, in order to have the best control performance, the problem can be casted into optimization seeking, i.e., minimize $\frac{\lambda_{max}(\gamma)}{2\delta\lambda_{min}(P)}$ in (A.21) subject to LMIs (A.22)-(A.24) where $\gamma = \text{diag}\{\gamma_1, \ldots, \gamma_N\}$.

Remark A.5 *Compared with the work in Wang et al. (2018a) where the constant input/output delay and matched disturbance are considered, the work in this chapter is an improvement. Compared with previous chapters in this thesis, the controller is without integral terms and can be easily implemented in real applications. The regret is that the controller is not fully distributed, meaning it is nearly impossible to apply to large-scale systems, as we have stated out clearly the reason in Chapter 1.1.2. This problem is one of the future research objectives.*

A.5 Summary

Contributions

- √ Design a new distributed controller without integral terms to deal with time-varying input/output delays and mismatched disturbances.
- √ Present the method about how to solve complicated LMIs by linearizing the nonlinear terms into linear ones.
- √ Provide detailed comparisons to show how to obtain better robust control performance.

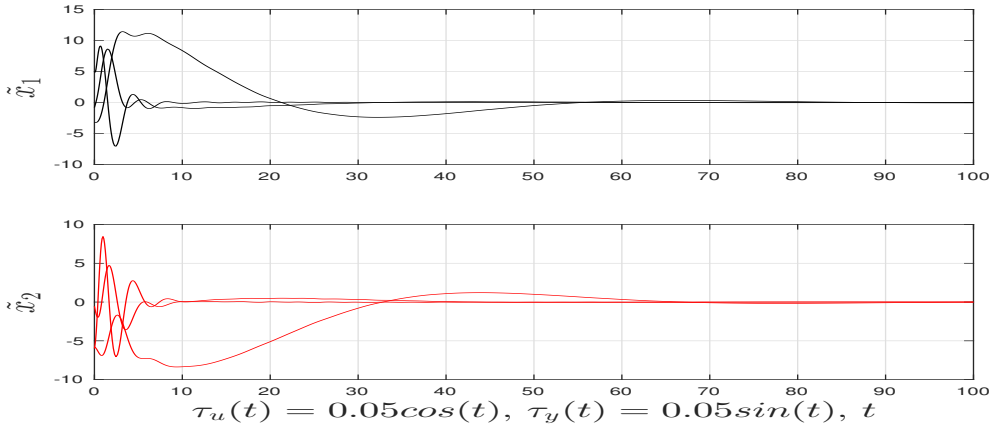

(a) The consensus tracking error for agnets 1 and 2.

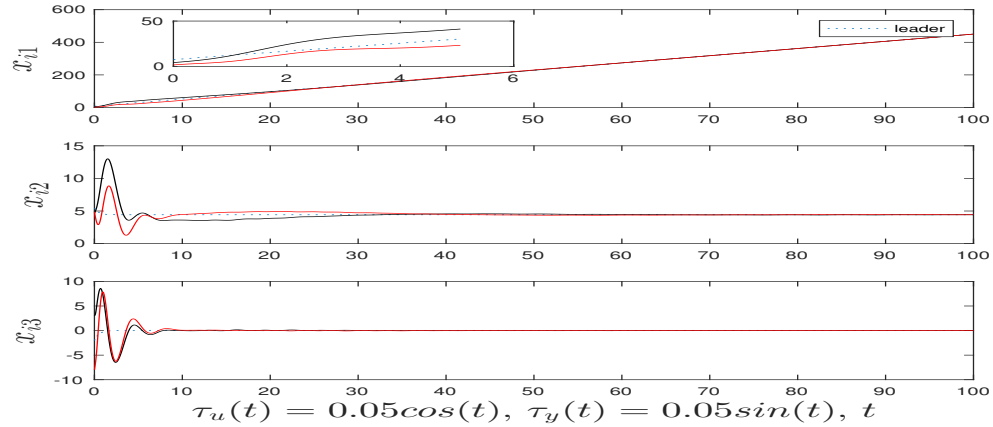

(b) The trajectories of agent $i = 1, 2$ tracking the leader 0.

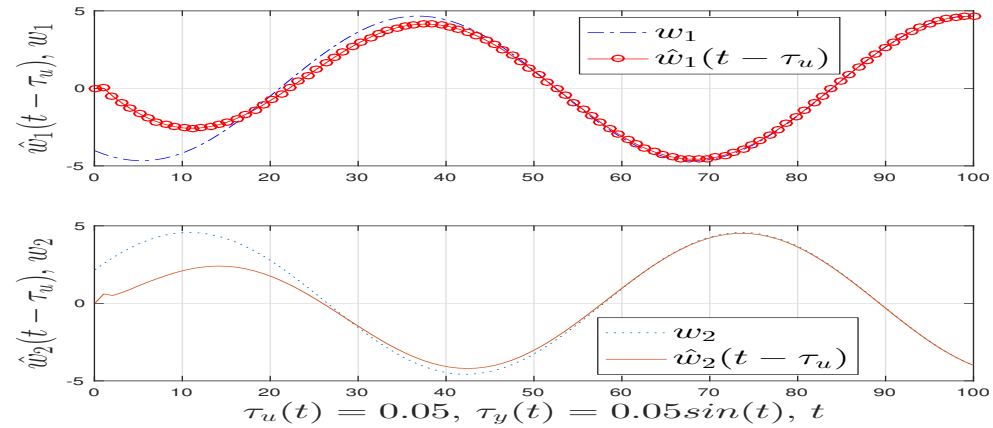

(c) Disturbance observer estimating error.

Figure A.2: Control performance with the unmodeled disturbance component $\varpi_i(t) = 0, i = 1, 2$.

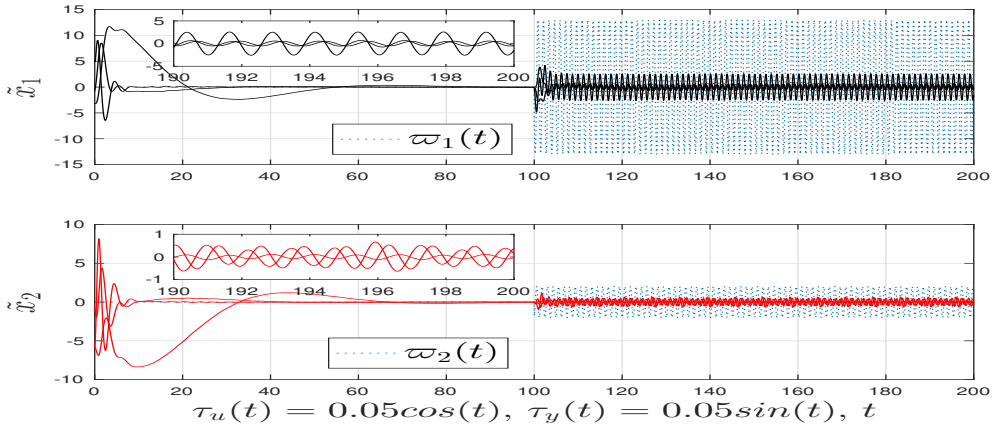

(a) $\varpi_1(t) = 13\sin(5t), \varpi_2(t) = 2\sin(5t), \gamma_1 = 0.6938, \gamma_2 = 0.6955.$

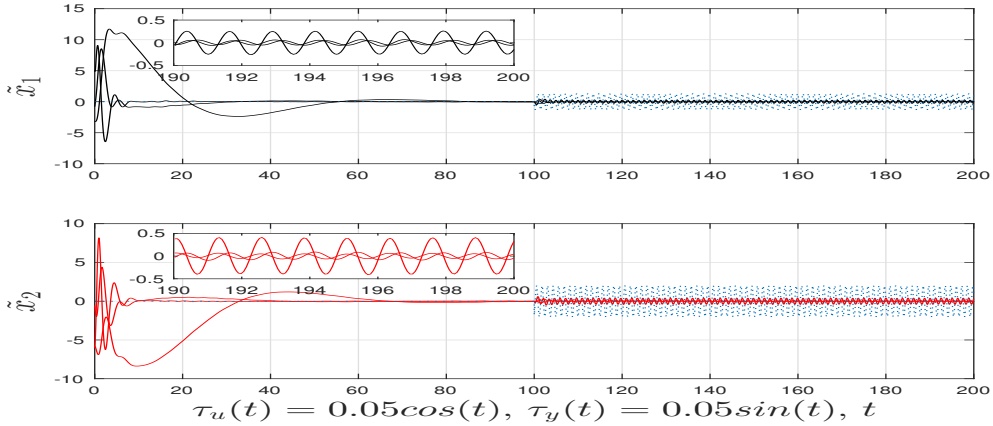

(b) $\varpi_1(t) = 1.3\sin(5t), \varpi_2(t) = 2\sin(5t), \gamma_1 = 0.6938, \gamma_2 = 0.6955.$

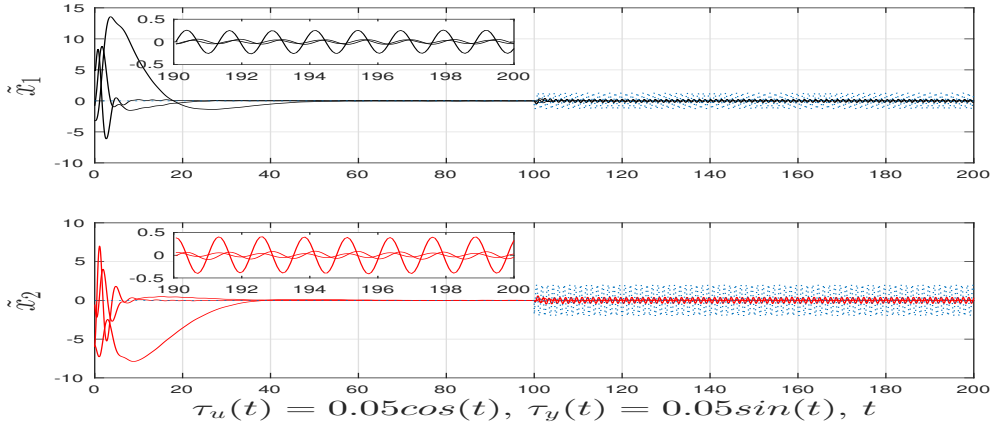

(c) $\varpi_1(t) = 1.3\sin(5t), \varpi_2(t) = 2\sin(5t), \gamma_1 = 1.9008, \gamma_2 = 1.9183.$

Figure A.3: Comparisons with different $\varpi_i(t)$ and $\gamma_i, i = 1, 2.$

Conclusions and future works

This thesis has mainly focuses on the following two aspects:

- fully distributed output-based adaptive controller design for the time-varying formation (TVF)/formation-containment (FC) control problems of general linear MASs with heterogeneity under the directed communication topology containing a spanning tree,
- furthermore, controller design considering constant/time-varying input/output delays and matched/mismatched disturbances.

The main contributions are restated in the following with some future work directions.

Part I: In Chapter 2, a new TVF shape format is proposed for homogeneous LTI MASs, and a unified framework about how to design fully distributed controllers based on the output measurements is provided.

Then for heterogeneous LTI MASs in Chapter 3, another new TVF shape format is re-proposed and the fully distributed controller is redesigned to address the time-varying FC issue. The application to multiple mobile robots systems is also provided to validate the theory in Section 3.3.2. The limitation is that the leader's system matrix A_0 in (1.46) should be known in advance for each follower to design the observer. This constraint can be relieved that A_0 needs only be known to its neighboring followers by the work of Zuo, Song, Lewis & Davoudi (2018). **So how to design fully distributed controller for time-varying FC control of heterogeneous MASs considering A_0 only known to its neighboring followers could be one of the future work.**

Part II: In Chapter 4, the fully distributed controllers to solve the consensus tracking control problem for homogeneous MASs considering the constant input delay and matched disturbance with/without the leader's input $u_0(t)$ are investigated in Sections 4.1 and 4.2, respectively. The finite spectrum assignment (FSA) method is adopted and modified to design the controller with absolute/relative state information. As the state measurements are not always available in reality, the output measurements are preferred for the controller. The controller design based on output measurements is solved in Chapter 6.3.

In Chapter 5, the fully distributed controller is redesigned based on Arstein's reduction approach for heterogeneous LTI MASs by proposing a new state predictor considering the constant input delay and matched disturbance without the leader's input $u_0(t)$. And then, the factor of time-varying output delay is considered by proposing Lyapunov-Krasovskii functionals with using the descriptor approach in Chapter 6. The detail about how to design fully distributed controllers based on output measurements to solve cooperative problems from consensus to TVF, then to time-varying FC is demonstrated. All the above works dealing with the constant input delay are based on the predictive control method with integral terms inside control protocols. Since the discretization of integral term is very time-consuming and needs to be executed very carefully in real applications, it is **very interesting to develop alternative fully distributed controllers without the integral term calculation.**

In Appendix A, an attempt to design the controllers without the integral term calculation is completed to solve the consensus tracking control problem for homogeneous LTI MASs considering the time-varying input/output delays and mismatched disturbances. Unfortunately, this controller is not full distributed, meaning that it will be difficult to applied this controller to large-scale systems. **Future efforts will aim at developing fully distributed controllers without integral term to solve the TVF and time-varying FC issues for heterogeneous LTI MASs considering the time-varying input/output delays and mismatched disturbances.**

During this three-year research career, I spent tremendous time thinking what I am doing and where I am in the world research of MASs domain of automatic control. Before finishing this thesis, I would like to share my thinkings as follows:

- The main difference between the multi-agent systems and single agent system is that MASs can do formation/containment, flocking, etc., to complete cooperative tasks and that MASs can have the communication network and the heterogeneity. This is the root reason I choose to work on the time-varying FC control for heterogeneous systems.

- Cooperative control should be capable of applying on large-scale systems where the fully distributed controller design in this thesis is one option.

- During the time of working on input/output delays, one can see those works introduced in Chapter 1.3 are developed for single agent system. So I told myself: working on homogeneous MASs which can be regarded consisting of different numbers of single same agent system, does not produce a big difference. Standing on the shoulders of those works introduced in Chapter 1.3, my main attention focuses on the heterogeneous MASs dealing with time-varying input/output delays.

- In terms of dealing with input delay, in Chapters 4-6, the controllers are fully distributed with integral term calculation while in Appendix A, not fully distributed but without integral term calculation. It seems there is a trade-off between the ability of applying on large-scale systems and the convenience of implementation in reality. It is very interesting to research deeper to make clear of this point.
- Nowadays, artificial intelligence (AI) is nearly everywhere in the world. Since MASs execute cooperative tasks in a distributed way, it would be very beneficial if each agent is equipped with AI ability, then the whole MASs can complete much more complicated tasks with good efficiency. A good example of using deep reinforcement learning method to developing TVF controllers can be referred to Conde *et al.* (2017).
- Implementing the results in this thesis to real experiments in laboratory is necessary. The work on the robot operating system (ROS) is undergoing.

Bibliography

Abreu, P.C., Bayat, M., Botelho, J., Góis, P., Gomes, J., Pascoal, A., Ribeiro, J., Ribeiro, M., Rufino, M., Sebastião, L. *et al.* (2015). Cooperative formation control in the scope of the ec morph project: Theory and experiments. In *OCEANS 2015-Genova*, 1–7, IEEE. 2, 3, 5, 13

Alami, R., Fleury, S., Herrb, M., Ingrand, F. & Robert, F. (1998). Multi-robot cooperation in the martha project. *IEEE Robotics & Automation Magazine*, **5**, 36–47. 2

Albea, C., Seuret, A. & Zaccarian, L. (2016). Activation and consensus control of a three-node server network cluster via hybrid approach. *Nonlinear Analysis: Hybrid Systems*, **22**, 16–30. 2

Almeida, J., Silvestre, C. & Pascoal, A.M. (2014). Output synchronization of heterogeneous lti plants with event-triggered communication. In *Decision and Control (CDC), 2014 IEEE 53rd Annual Conference on*, 3572–3577, IEEE. 2, 7, 69, 118

Antonelli, G., Arrichiello, F., Caccavale, F. & Marino, A. (2014). Decentralized time-varying formation control for multi-robot systems. *The International Journal of Robotics Research*, **33**, 1029–1043. 3, 5, 12, 38, 70

Aranda, M., Mezouar, Y., López-Nicolás, G. & Sagüés, C. (2018). Scale-free vision-based aerial control of a ground formation with hybrid topology. *IEEE Transactions on Control Systems Technology, in press*. 2

Artstein, Z. (1982). Linear systems with delayed controls: a reduction. *IEEE Transactions on Automatic Control*, **27**, 869–879. 15, 17, 115

Bai, H. & Wen, J.T. (2010). Cooperative load transport: A formation-control perspective. *IEEE Transactions on Robotics*, **26**, 742–750. 5

Banks, H.T., Jacobs, M.Q. & Latina, M. (1971). The synthesis of optimal controls for linear, time-optimal problems with retarded controls. *Journal of Optimization Theory and Applications*, **8**, 319–366. 17

Bernstein, D.S. (2009). *Matrix Mathematics: Theory, Facts, and Formulas*. Princeton University Press. 31

Boyd, S., El Ghaoui, L., Feron, E. & Balakrishnan, V. (1994). *Linear Matrix Inequalities in System and Control Theory*, vol. 15. Siam. 31

Brinón-Arranz, L., Pascoal, A. & Aguiar, A.P. (2014a). Adaptive leader-follower formation control of autonomous marine vehicles. In *Decision and Control (CDC), 2014 IEEE 53rd Annual Conference on*, 5328–5333, IEEE. 5, 12

Brinón-Arranz, L., Seuret, A. & Canudas-de Wit, C. (2014b). Cooperative control design for time-varying formations of multi-agent systems. *IEEE Transactions on Automatic Control*, **59**, 2283–2288. 12

Cai, H., Lewis, F.L., Hu, G. & Huang, J. (2017). The adaptive distributed observer approach to the cooperative output regulation of linear multi-agent systems. *Automatica*, **75**, 299–305. 39, 65, 91

Cao, W., Zhang, J. & Ren, W. (2015). Leader–follower consensus of linear multi-agent systems with unknown external disturbances. *Systems & Control Letters*, **82**, 64–70. 92

Cao, Y., Stuart, D., Ren, W. & Meng, Z. (2011). Distributed containment control for multiple autonomous vehicles with double-integrator dynamics: algorithms and experiments. *IEEE Transactions on Control Systems Technology*, **19**, 929–938. 10

Cao, Y., Ren, W. & Egerstedt, M. (2012). Distributed containment control with multiple stationary or dynamic leaders in fixed and switching directed networks. *Automatica*, **48**, 1586–1597. 10

Cao, Y., Yu, W., Ren, W. & Chen, G. (2013). An overview of recent progress in the study of distributed multi-agent coordination. *IEEE Transactions on Industrial Informatics*, **9**, 427–438. 10

Chen, W.H. (2003). Nonlinear disturbance observer-enhanced dynamic inversion control of missiles. *Journal of Guidance, Control, and Dynamics*, **26**, 161–166. 93

Chen, W.H., Yang, J., Guo, L. & Li, S. (2016). Disturbance-observer-based control and related methods—an overview. *]IEEE Transactions on Industrial Electronics*, **63**, 1083–1095. 92

Chu, H., Gao, L. & Zhang, W. (2016). Distributed adaptive containment control of heterogeneous linear multi-agent systems: an output regulation approach. *IET Control Theory & Applications*, **10**, 95–102. 11, 64

Conde, R., Llata, J.R. & Torre-Ferrero, C. (2017). Time-varying formation controllers for unmanned aerial vehicles using deep reinforcement learning. *arXiv preprint arXiv:1706.01384*. 163

Corless, M. & Leitmann, G. (1981). Continuous state feedback guaranteeing uniform ultimate boundedness for uncertain dynamic systems. *IEEE Transactions on Automatic Control*, **26**, 1139–1144. 30

DARPA (2006). Formation-flying satellites. https://www.wired.com/2013/05/formation-flying-satellites/. 5

Dimarogonas, D.V., Egerstedt, M. & Kyriakopoulos, K.J. (2006). A leader-based containment control strategy for multiple unicycles. In *Decision and Control, 2006 45th IEEE Conference on*, 5968–5973, IEEE. 13

Ding, Z. (2003). Global stabilization and disturbance suppression of a class of nonlinear systems with uncertain internal model. *Automatica*, **39**, 471–479. 151

Ding, Z. (2015a). Adaptive consensus output regulation of a class of nonlinear systems with unknown high-frequency gain. *Automatica*, **51**, 348–355. 13

Ding, Z. (2015b). Consensus disturbance rejection with disturbance observers. *IEEE Transactions on Industrial Electronics*, **62**, 5829–5837. 96, 97, 104, 123, 125

Ding, Z. (2017). Distributed adaptive consensus output regulation of network-connected heterogeneous unknown linear systems on directed graphs. *IEEE Transactions on Automatic Control*, **62**, 4683–4690. 2

Dong, X. (2015). *Formation and containment control for high-order linear swarm systems*. Springer. 5, 6

Dong, X. & Hu, G. (2016). Time-varying formation control for general linear multi-agent systems with switching directed topologies. *Automatica*, **73**, 47–55. 5, 12, 38, 40, 53, 70

Dong, X., Li, Q., Ren, Z. & Zhong, Y. (2016). Output formation-containment analysis and design for general linear time-invariant multi-agent systems. *Journal of the Franklin Institute*, **353**, 322–344. 13, 38

Dong, X., Xiang, J., Han, L., Li, Q. & Ren, Z. (2017). Distributed time-varying formation tracking analysis and design for second-order multi-agent systems. *Journal of Intelligent & Robotic Systems*, **86**, 277–289. 12, 39, 40, 70

Dong, X., Hua, Y., Zhou, Y., Ren, Z. & Zhong, Y. (2018). Theory and experiment on formation-containment control of multiple multirotor unmanned aerial vehicle systems. *IEEE Transactions on Automation Science and Engineering*, 1–12. 4

Encarnaçao, P. & Pascoal, A. (2001). Combined trajectory tracking and path following: an application to the coordinated control of autonomous marine craft. In *Decision and Control, 2001. Proceedings of the 40th IEEE Conference on*, vol. 1, 964–969, IEEE. 12

Engelborghs, K., Dambrine, M. & Roose, D. (2001). Limitations of a class of stabilization methods for delay systems. *IEEE Transactions on Automatic Control*, **46**, 336–339. 21

Everett, H., Laird, R., Carroll, D., Gilbreath, G. & Heath-Pastore, T. (2000). Multiple resource host architecture (mrha) for the mobile detection assessment response system (mdars) revision a. Tech. rep., Space and Naval Warfare Systems Center San Diego CA. 2

Ferrari-Trecate, G., Egerstedt, M., Buffa, A. & Ji, M. (2006). Laplacian sheep: A hybrid, stop-go policy for leader-based containment control. In *International Workshop on Hybrid Systems: Computation and Control*, 212–226, Springer. 13

Flanders, H. (1973). Differentiation under the integral sign. *The American Mathematical Monthly*, **80**, 615–627. 31

Fridman, E. (2001). New lyapunov–krasovskii functionals for stability of linear retarded and neutral type systems. *Systems & Control Letters*, **43**, 309–319. 22, 136

Fridman, E. (2014). Introduction to time-delay and sampled-data systems. In *2014 European Control Conference (ECC)*, 1428–1433. 20, 21, 132, 134, 136

Fridman, E. & Dambrine, M. (2009). Control under quantization, saturation and delay: An lmi approach. *Automatica*, **45**, 2258–2264. 155

Furukawa, T. & Shimemura, E. (1983). Predictive control for systems with time delay. *International Journal of Control*, **37**, 399–412. 20

Ghabcheloo, R., Aguiar, A.P., Pascoal, A., Silvestre, C., Kaminer, I. & Hespanha, J. (2009). Coordinated path-following in the presence of communication losses and time delays. *SIAM journal on control and optimization*, **48**, 234–265. 9

Ghommam, J., Luque-Vega, L.F., Castillo-Toledo, B. & Saad, M. (2016). Three-dimensional distributed tracking control for multiple quadrotor helicopters. *Journal of the Franklin Institute*, **353**, 2344–2372. 12, 38, 70

Godsil, C. & Royle, G.F. (2001). *Algebraic Graph Theory*. Springer Science & Business Media, New York, NY, USA. 29

Gu, K. & Niculescu, S.I. (2003). Survey on recent results in the stability and control of time-delay systems. *Journal of Dynamic Systems, Measurement, and Control*, **125**, 158–165. 21

Gu, K., Chen, J. & Kharitonov, V.L. (2003). *Stability of Time-delay Systems*. Springer Science & Business Media. 31

Guo, L. & Cao, S. (2014). Anti-disturbance control theory for systems with multiple disturbances: A survey. *ISA transactions*, **53**, 846–849. 92

Gupta*, V., Hassibi, B. & Murray, R.M. (2005). A sub-optimal algorithm to synthesize control laws for a network of dynamic agents. *International Journal of Control*, **78**, 1302–1313. 79

Haghshenas, H., Badamchizadeh, M.A. & Baradarannia, M. (2015). Containment control of heterogeneous linear multi-agent systems. *Automatica*, **54**, 210–216. 6, 11, 64, 69

Han, L., Dong, X., Li, Q. & Ren, Z. (2016). Formation-containment control for second-order multi-agent systems with time-varying delays. *Neurocomputing*, **218**, 439–447. 13

Hazard, C.J., Wurman, P.R. & D'Andrea, R. (2006). Alphabet soup: A testbed for studying resource allocation in multi-vehicle systems. In *Proceedings of AAAI Workshop on Auction Mechanisms for Robot Coordination*, 23–30, Citeseer. 2

Henry, J. (2016). Dead time compensation (smith predictor). https://slideplayer.com/slide/10740178/. vii, 14, 15

Hong, Y., Hu, J. & Gao, L. (2006). Tracking control for multi-agent consensus with an active leader and variable topology. *Automatica*, **42**, 1177–1182. 45

Huang, J. (2004). *Nonlinear Output Regulation: Theory and Applications*. SIAM. 69, 70

Hurtado, J., Robinett III, R.D., Dohrmann, C.R. & Goldsmith, S.Y. (2004). Decentralized control for a swarm of vehicles performing source localization. *Journal of Intelligent and Robotic Systems*, **41**, 1–18. 5

Isidori, A. (2013). *Nonlinear Control Systems*. Springer Science & Business Media. 96

Isidori, A. & Byrnes, C.I. (1990). Output regulation of nonlinear systems. *IEEE transactions on Automatic Control*, **35**, 131–140. 153

Jadbabaie, A., Lin, J. & Morse, A.S. (2003). Coordination of groups of mobile autonomous agents using nearest neighbor rules. *IEEE Transactions on Automatic Control*, **48**, 988–1001. 2, 10

Jenabzadeh, A. & Safarinejadian, B. (2018). Tracking control of nonholonomic mobile agents with external disturbances and input delay. *ISA transactions*, **76**, 122–133. 9

Ji, M., Ferrari-Trecate, G., Egerstedt, M. & Buffa, A. (2008). Containment control in mobile networks. *IEEE Transactions on Automatic Control*, **53**, 1972–1975. 10

Jiang, W., Wen, G., Meng, Y. & Rahmani, A. (2017). Distributed adaptive time-varying formation tracking for linear multi-agent systems: A dynamic output approach. In *Control Conference (CCC), 2017 36th Chinese*, 8571–8576, IEEE. 23, 26, 34, 41, 59, 182, 184

Jiang, W., Peng, Z., Rahmani, A., Hu, W. & Wen, G. (2018a). Distributed consensus of linear mass with an unknown leader via a predictive extended state observer considering input delay and disturbances. *Neurocomputing*, **315**, 465–475. 25, 26, 97, 102, 105, 183, 184

Jiang, W., Rahmani, A. & Wen, G. (2018b). Fully distributed time-varying formation-containment control for large-scale nonholonomic vehicles with an unknown real leader. *International Journal of Control (submitted)*. 26, 184

Jiang, W., Wen, G., Peng, Z., Huang, T. & Rahmani, A. (2018c). Fully distributed formation-containment control of heterogeneous linear multi-agent systems. *IEEE Transactions on Automatic Control, in press*. 25, 26, 70, 72, 182, 184

Jiang, W., Wen, G., Rahmani, A., Huang, T., Li, Z. & Peng, Z. (2018d). Observer-based fully distributed output consensus tracking of heterogeneous linear multi-agent systems with input delay and disturbances. *IEEE Transactions on Cybernetics (submitted)*. 25, 26, 183, 184

Khalil, H.K. (1996). *Noninear Systems*. Prentice-Hall, New Jersey. 31, 56

Kim, H., Shim, H. & Seo, J.H. (2011). Output consensus of heterogeneous uncertain linear multi-agent systems. *IEEE Transactions on Robotics and Automation*, **56**, 200–206. 3, 7, 91

Krstic, M. (2009). *Delay Compensation for Nonlinear, Adaptive, and PDE Systems*. Springer. 15, 17, 18, 19, 21

Krstic, M. (2010). Lyapunov stability of linear predictor feedback for time-varying input delay. *IEEE Transactions on Automatic Control*, **55**, 554–559. 20

Krstic, M., Kokotovic, P.V. & Kanellakopoulos, I. (1995). *Nonlinear and Adaptive Control Design*. John Wiley & Sons, Inc, 1st edn. 43, 45, 84, 103, 126

Kwon, W. & Pearson, A. (1980). Feedback stabilization of linear systems with delayed control. *IEEE Transactions on Automatic Control*, **25**, 266–269. 15

Lawton, J.R.T., Beard, R.W. & Young, B.J. (2003). A decentralized approach to formation maneuvers. *IEEE Transactions on Robotics and Automation*, **19**, 933–941. 80, 81, 82

Léchappé, V. (2015). *Predictive control and estimation of uncertain systems with an input delay*. Ph.D. thesis, Ecole Centrale de Nantes (ECN). 9, 21, 100

Léchappé, V., Moulay, E., Plestan, F., Glumineau, A. & Chriette, A. (2015). New predictive scheme for the control of lti systems with input delay and unknown disturbances. *Automatica*, **52**, 179–184. 20

Li, Z., Duan, Z., Chen, G. & Huang, L. (2010). Consensus of multiagent systems and synchronization of complex networks: A unified viewpoint. *IEEE Transactions on Circuits and Systems I: Regular Papers*, **57**, 213–224. 2, 10, 91

Li, Z., Ren, W., Liu, X. & Fu, M. (2013). Distributed containment control of multi-agent systems with general linear dynamics in the presence of multiple leaders. *International Journal of Robust and Nonlinear Control*, **23**, 534–547. 11

Li, Z., Wen, G., Duan, Z. & Ren, W. (2015). Designing fully distributed consensus protocols for linear multi-agent systems with directed graphs. *IEEE Transactions on Automatic Control*, **60**, 1152–1157. 102

Li, Z., Chen, M.Z.Q. & Ding, Z. (2016). Distributed adaptive controllers for cooperative output regulation of heterogeneous agents over directed graphs. *Automatica*, **68**, 179–183. 66, 68, 69

Lin, Z. & Fang, H. (2007). On asymptotic stabilizability of linear systems with delayed input. *IEEE Transactions on Automatic Control*, **52**, 998–1013. 21

Lin, Z., Francis, B. & Maggiore, M. (2005). Necessary and sufficient graphical conditions for formation control of unicycles. *IEEE Transactions on Automatic Control*, **50**, 121–127. 5, 12

Liu, C.L. & Liu, F. (2011). Stationary consensus of heterogeneous multi-agent systems with bounded communication delays. *Automatica*, **47**, 2130–2133. 91

Liu, C.L. & Liu, F. (2013). Dynamical consensus seeking of heterogeneous multi-agent systems under input delays. *International Journal of Communication Systems*, **26**, 1243–1258. 91, 93

Liu, H., Xie, G. & Wang, L. (2012). Necessary and sufficient conditions for containment control of networked multi-agent systems. *Automatica*, **48**, 1415–1422. 6, 10

Liu, K. & Fridman, E. (2014). Delay-dependent methods and the first delay interval. *Systems & Control Letters*, **64**, 57–63. 22

Liu, T. & Jiang, Z.P. (2013). Distributed formation control of nonholonomic mobile robots without global position measurements. *Automatica*, **49**, 592–600. 5, 12, 38

López-Nicolás, G., Aranda, M. & Mezouar, Y. (2017). Formation of differential-drive vehicles with field-of-view constraints for enclosing a moving target. In *Robotics and Automation (ICRA), 2017 IEEE International Conference on*, 261–266, IEEE. 5

Lunze, J. (2012). Synchronization of heterogeneous agents. *IEEE Transactions on Robotics and Automation*, **57**, 2885–2890. 7, 91

Lv, Y., Li, Z., Duan, Z. & Chen, J. (2015). Fully distributed adaptive output feedback protocols for linear multi-agent systems with directed graphs: a sequential observer design approach. *arXiv preprint arXiv:1511.01297*. 58

Madoński, R. & Herman, P. (2015). Survey on methods of increasing the efficiency of extended state disturbance observers. *ISA Transactions*, **56**, 18–27. 92

Manitius, A. & Olbrot, A. (1979). Finite spectrum assignment problem for systems with delays. *IEEE Transactions on Automatic Control*, **24**, 541–552. 15

Mei, J., Ren, W. & Chen, J. (2014). Consensus of second-order heterogeneous multi-agent systems under a directed graph. In *American Control Conference (ACC), 2014*, 802–807, IEEE. 30

Mellinger, D.W. (2012). *Trajectory generation and control for quadrotors*. Ph.D. thesis, University of Pennsylvania. 8

Meng, M., Liu, L. & Feng, G. (2017). Output consensus for heterogeneous multiagent systems with markovian switching network topologies. *International Journal of Robust and Nonlinear Control*, **28**, 1049–1061. 3, 7, 91, 118

Mirkin, L. & Raskin, N. (2003). Every stabilizing dead-time controller has an observer–predictor-based structure. *Automatica*, **39**, 1747–1754. 21

Mu, B. & Shi, Y. (2018). Distributed lqr consensus control for heterogeneous multi-agent systems: theory and experiments. *IEEE/ASME Transactions on Mechatronics*, **23**, 434 – 443. 7, 91

Murphy, R.R. (2000). Marsupial and shape-shifting robots for urban search and rescue. *IEEE Intelligent Systems*, 14–19. 2

Najafi, M., Hosseinnia, S., Sheikholeslam, F. & Karimadini, M. (2013). Closed-loop control of dead time systems via sequential sub-predictors. *International Journal of Control*, **86**, 599–609. 22, 94, 149, 152

Nakao, M., Ohnishi, K. & Miyachi, K. (1987). A robust decentralized joint control based on interference estimation. In *Robotics and Automation. Proceedings. 1987 IEEE International Conference on*, vol. 4, 326–331, IEEE. 92

Ni, J., Liu, L., Liu, C. & Liu, J. (2017). Fixed-time leader-following consensus for second-order multi-agent systems with input delay. *IEEE Transactions on Industrial Electronics*. 9

Nigam, N., Bieniawski, S., Kroo, I. & Vian, J. (2012). Control of multiple uavs for persistent surveillance: algorithm and flight test results. *IEEE Transactions on Control Systems Technology*, **20**, 1236–1251. 5

Nihtila, M.T. (1989). Adaptive control of a continuous-time system with time-varying input delay. *Systems & control letters*, **12**, 357–364. 20

Nihtila, M.T. (1991). Finite pole assignment for systems with time-varying input delays. In *Decision and Control, 1991., Proceedings of the 30th IEEE Conference on*, 927–928, IEEE. 20

Oh, K.K., Park, M.C. & Ahn, H.S. (2015). A survey of multi-agent formation control. *Automatica*, **53**, 424–440. 11

Olbrot, A. (1978). Stabilizability, detectability, and spectrum assignment for linear autonomous systems with general time delays. *IEEE Transactions on Automatic Control*, **23**, 887–890. 15

Olfati-Saber, R. & Murray, R.M. (2004). Consensus problems in networks of agents with switching topology and time-delays. *IEEE Transactions on Automatic Control*, **49**, 118–173. 2, 10, 49, 91

Parker, L.E. (2008). Multiple mobile robot systems. In *Springer Handbook of Robotics*, 921–941, Springer. 2, 3, 7

Parker, L.E. *et al.* (1998). Alliance: An architecture for fault tolerant multirobot cooperation. *IEEE Transactions on Robotics and Automation*, **14**, 220–240. 2

Pascoal, A., Oliveira, P., Silvestre, C., Bjerrum, A., Ishoy, A., Pignon, J.P., Ayela, G. & Petzelt, C. (1997). Marius: An autonomous underwater vehicle for coastal oceanography. *IEEE Robotics & Automation Magazine*, **4**, 46–59. 12

Peng, Z., Wen, G., Rahmani, A. & Yu, Y. (2013). Leader–follower formation control of nonholonomic mobile robots based on a bioinspired neurodynamic based approach. *Robotics and Autonomous Systems*, **61**, 988–996. 5, 12

Peymani, E., Grip, H.F., Saberi, A., Wang, X. & Fossen, T.I. (2014). H∞ almost output synchronization for heterogeneous networks of introspective agents under external disturbances. *Automatica*, **50**, 1026–1036. 13, 38, 50, 70

Ponomarev, A., Chen, Z. & Zhang, H.T. (2018). Discrete-time predictor feedback for consensus of multi-agent systems with delays. *IEEE Transactions on Automatic Control*, **63**, 498–504. 92

Qu, Z. (2009). *Cooperative Control of Dynamical Systems: Applications to Autonomous Vehicles*. Springer Science & Business Media. 32, 67

Rahimi, R., Abdollahi, F. & Naqshi, K. (2014). Time-varying formation control of a collaborative heterogeneous multi agent system. *Robotics and Autonomous Systems*, **62**, 1799–1805. 5, 13, 38, 64, 70

Ren, W. (2007). Consensus strategies for cooperative control of vehicle formations. *IET Control Theory & Applications*, **1**, 505–512. 10, 91

Ren, W. & Beard, R.W. (2005). Consensus seeking in multiagent systems under dynamically changing interaction topologies. *IEEE Transactions on Automatic Control*, **50**, 655–661. 2, 10, 29

Rezaei, M.H. & Menhaj, M.B. (2018). Stationary average consensus protocol for a class of heterogeneous high-order multi-agent systems with application for aircraft. *International Journal of Systems Science*, **49**, 284–298. 7, 91

Richard, J.P. (2003). Time-delay systems: an overview of some recent advances and open problems. *Automatica*, **39**, 1667–1694. 8, 21

Rockafellar, R.T. (2015). *Convex Analysis*. Princeton university press. 66

Sakurama, K. (2016). Multi-robot formation control over distance sensor network. *IFAC-PapersOnLine*, **49**, 198–203. 38

Sanz, R., Garcia, P., Fridman, E. & Albertos, P. (2018). Rejection of mismatched disturbances for systems with input delay via a predictive extended state observer. *International Journal of Robust and Nonlinear Control*, **28**, 2457–2467. 150, 153

Scardovi, L. & Sepulchre, R. (2009). Synchronization in networks of identical linear systems. *Automatica*, **45**, 2557–2562. 91

Seyboth, G.S., Dimarogonas, D.V., Johansson, K.H., Frasca, P. & Allgöwer, F. (2015). On robust synchronization of heterogeneous linear multi-agent systems with static couplings. *Automatica*, **53**, 392–399. 91

Seyboth, G.S., Ren, W. & Allgöwer, F. (2016). Cooperative control of linear multi-agent systems via distributed output regulation and transient synchronization. *Automatica*, **68**, 132–139. 3, 7, 91, 93

Smith, O.J. (1957). Close control of loops with dead time. *Chemical Engineering Progress*, **53**, 217–219. 14

Smith, O.J. (1959). A controller to overcome dead time. *ISA J.*, **6**, 28–33. 14

Soares, J.M., Aguiar, A.P., Pascoal, A.M. & Martinoli, A. (2016). A graph-based formation algorithm for odor plume tracing. In *Distributed Autonomous Robotic Systems*, 255–269, Springer. 12

Su, Y. & Huang, J. (2012). Cooperative output regulation with application to multi-agent consensus under switching network. *IEEE Transactions on Systems, Man, and Cybernetics, Part B (Cybernetics)*, **42**, 864–875. 13, 14

Su, Y., Hong, Y. & Huang, J. (2013). A general result on the robust cooperative output regulation for linear uncertain multi-agent systems. *IEEE Transactions on Automatic Control*, **58**, 1275–1279. 13, 14

Sukhatme, G., Montgomery, J.F. & Vaughan, R.T. (2001). Experiments with cooperative aerial-ground robots. *Robot Teams: From Diversity to Polymorphism*, 345–368. 8

Sun, J., Geng, Z., Lv, Y., Li, Z. & Ding, Z. (2018). Distributed adaptive consensus disturbance rejection for multi-agent systems on directed graphs. *IEEE Transactions on Control of Network Systems*, **5**, 629–639. 92

Tanner, H.G. (2004). On the controllability of nearest neighbor interconnections. In *Decision and Control, 2004. CDC. 43rd IEEE Conference on*, vol. 3, 2467–2472, IEEE. 5, 12

Tanner, H.G. & Christodoulakis, D.K. (2007). Decentralized cooperative control of heterogeneous vehicle groups. *Robotics and Autonomous Systems*, **55**, 811–823. 91

Tanner, H.G., Jadbabaie, A. & Pappas, G.J. (2005). Flocking in teams of nonholonomic agents. In *Cooperative Control*, 229–239, Springer. 77

Tian, Y.P. & Liu, C.L. (2009). Robust consensus of multi-agent systems with diverse input delays and asymmetric interconnection perturbations. *Automatica*, **45**, 1347–1353. 9, 92

Tian, Y.P. & Zhang, Y. (2012). High-order consensus of heterogeneous multi-agent systems with unknown communication delays. *Automatica*, **48**, 1205–1212. 7, 91

Van Assche, V., Dambrine, M., Lafay, J.F. & Richard, J.P. (1999). Some problems arising in the implementation of distributed-delay control laws. In *Decision and Control, 1999. Proceedings of the 38th IEEE Conference on*, vol. 5, 4668–4672, IEEE. 21

Wang, C. & Ding, Z. (2016). H∞ consensus control of multi-agent systems with input delay and directed topology. *IET Control Theory & Applications*, **10**, 617–624. 92

Wang, C., Sun, J., Zuo, Z. & Ding, Z. (2017a). Consensus disturbance rejection of network-connected dynamic systems with input delay and unknown network connectivity. *IFAC-PapersOnLine*, **50**, 10357–10362. 92, 103

Wang, C., Zuo, Z., Qi, Z. & Ding, Z. (2018a). Predictor-based extended-state-observer design for consensus of mass with delays and disturbances. *IEEE Transactions on Cybernetics 10.1109/TCYB.2018.2799798*. 9, 92, 116, 123, 158

Wang, J. & Xin, M. (2013). Integrated optimal formation control of multiple unmanned aerial vehicles. *IEEE Transactions on Control Systems Technology*, **21**, 1731–1744. 5, 12, 38

Wang, Q., Fu, J. & Wang, J. (2017b). Fully distributed containment control of high-order multi-agent systems with nonlinear dynamics. *Systems & Control Letters*, **99**, 33–39. 11

Wang, R., Dong, X., Li, Q. & Ren, Z. (2016a). Distributed adaptive time-varying formation for multi-agent systems with general high-order linear time-invariant dynamics. *Journal of the Franklin Institute*, **353**, 2290–2304. 39

Wang, W., Wen, C. & Huang, J. (2017c). Distributed adaptive asymptotically consensus tracking control of nonlinear multi-agent systems with unknown parameters and uncertain disturbances. *Automatica*, **77**, 133–142. 93

Wang, X., Hong, Y., Huang, J. & Jiang, Z.P. (2010). A distributed control approach to a robust output regulation problem for multi-agent linear systems. *IEEE Transactions on Automatic Control*, **55**, 2891–2895. 13, 14

Wang, X., Li, S. & Lam, J. (2016b). Distributed active anti-disturbance output consensus algorithms for higher-order multi-agent systems with mismatched disturbances. *Automatica*, **74**, 30–37. 92, 93

Wang, X., Li, S., Yu, X. & Yang, J. (2017d). Distributed active anti-disturbance consensus for leader-follower higher-order multi-agent systems with mismatched disturbances. *IEEE Transactions on Automatic Control*, **62**, 5795–5801. 92

Wang, X., Li, S. & Chen, M.Z. (2018b). Composite backstepping consensus algorithms of leader–follower higher-order nonlinear multiagent systems subject to mismatched disturbances. *IEEE Transactions on Cybernetics*, **48**, 1935–1946. 92, 93

Wang, Y., Song, Y. & Krstic, M. (2017e). Collectively rotating formation and containment deployment of multi-agent systems: a polar coordinate based finite time approach. *IEEE Transactions on Cybernetics*, **47**, 2161–2172. 13, 64

Wang, Y.W., Liu, X.K., Xiao, J.W. & Lin, X. (2017f). Output formation-containment of coupled heterogeneous linear systems under intermittent communication. *Journal of the Franklin Institute*, **354**, 392–414. 13, 64, 73

Wang, Y.W., Liu, X.K., Xiao, J.W. & Shen, Y. (2018c). Output formation-containment of interacted heterogeneous linear systems by distributed hybrid active control. *Automatica*, **93**, 26–32. 13, 64, 73

Watanabe, K. & Ito, M. (1981). A process-model control for linear systems with delay. *IEEE Transactions on Automatic Control*, **26**, 1261–1269. 21

Wen, G., Zhao, Y., Duan, Z., Yu, W. & Chen, G. (2016). Containment of higher-order multi-leader multi-agent systems: a dynamic output approach. *IEEE Transactions on Automatic Control*, **61**, 1135–1140. 6, 11, 39, 40, 71

Wieland, P. & Allgöwer, F. (2009). An internal model principle for consensus in heterogeneous linear multi-agent systems. *IFAC Proceedings Volumes*, **42**, 7–12. 13

Wieland, P., Sepulchre, R. & Allgöwer, F. (2011). An internal model principle is necessary and sufficient for linear output synchronization. *Automatica*, **47**, 1068–1074. 7, 13, 65, 91

Wu, Y., Lu, R., Shi, P., Su, H. & Wu, Z.G. (2017). Adaptive output synchronization of heterogeneous network with an uncertain leader. *Automatica*, **76**, 183–192. 3, 39, 65, 91

Yaghmaie, F.A., Lewis, F.L. & Su, R. (2016). Output regulation of linear heterogeneous multi-agent systems via output and state feedback. *Automatica*, **67**, 157–164. 3, 4, 39, 65, 91

Yoon, S.Y. & Lin, Z. (2013). Truncated predictor feedback control for exponentially unstable linear systems with time-varying input delay. *Systems & Control Letters*, **62**, 837–844. 21, 22

Yuan, C. (2018). Leader-following consensus control of general linear multi-agent systems with diverse time-varying input delays. *Journal of Dynamic Systems, Measurement, and Control*, **140**, 061010. 9

Zeng, H. & Sepehri, N. (2005). Non-linear position control of cooperative hydraulic manipulators handling unknown payloads. *International Journal of Control*, **78**, 196–207. 93

Zhang, B., Jia, Y. & Du, J. (2018a). Adaptive synchronization control of networked robot systems without velocity measurements. *International Journal of Robust and Nonlinear Control*, **28**, 3606–3622. 9

Zhang, D., Xu, Z., Karimi, H.R., Wang, Q.G. & Yu, L. (2018b). Distributed output-feedback control for consensus of heterogeneous linear multiagent systems with aperiodic sampled-data communications. *IEEE Transactions on Industrial Electronics*, **65**, 4145–4155. 3, 7, 39, 65, 91, 118

Zhang, H., Yue, D., Dou, C., Zhao, W. & Xie, X. (2018c). Data-driven distributed optimal consensus control for unknown multiagent systems with input-delay. *IEEE Transactions on Cybernetics*, 1–11. 9

Zhang, M. & Liu, H.H. (2016). Cooperative tracking a moving target using multiple fixed-wing uavs. *Journal of Intelligent & Robotic Systems*, **81**, 505–529. 5

Zheng, Y. & Wang, L. (2014). Containment control of heterogeneous multi-agent systems. *International Journal of Control*, **87**, 1–8. 11, 64

Zheng, Y., Zhu, Y. & Wang, L. (2011). Consensus of heterogeneous multi-agent systems. *IET Control Theory & Applications*, **5**, 1881–1888. 91

Zhong, Q.C. (2006). *Robust Control of Time-delay Systems*. Springer Science & Business Media. 21

Zhou, B. & Lin, Z. (2014). Consensus of high-order multi-agent systems with large input and communication delays. *Automatica*, **50**, 452–464. 9, 21, 92

Zhu, W. & Jiang, Z.P. (2015). Event-based leader-following consensus of multi-agent systems with input time delay. *IEEE Transactions on Automatic Control*, **60**, 1362–1367. 9

Zuo, S., Song, Y., Lewis, F.L. & Davoudi, A. (2018). Adaptive output containment control of heterogeneous multi-agent systems with unknown leaders. *Automatica*, **92**, 235–239. 161

Zuo, Z., Wang, C. & Ding, Z. (2017). Robust consensus control of uncertain multi-agent systems with input delay: a model reduction method. *International Journal of Robust and Nonlinear Control*, **27**, 1874–1894. 9, 92

Contexte et organisation

Cette thèse est divisée en deux parties:

- La première partie est consacrée à la présentation de deux points: (i) les nouveaux formats de forme variant dans le temps proposés pour les MAS homogènes et hétérogènes respectivement; (ii) comment concevoir des contrôleurs entièrement distribués pour les systèmes à grande échelle par la

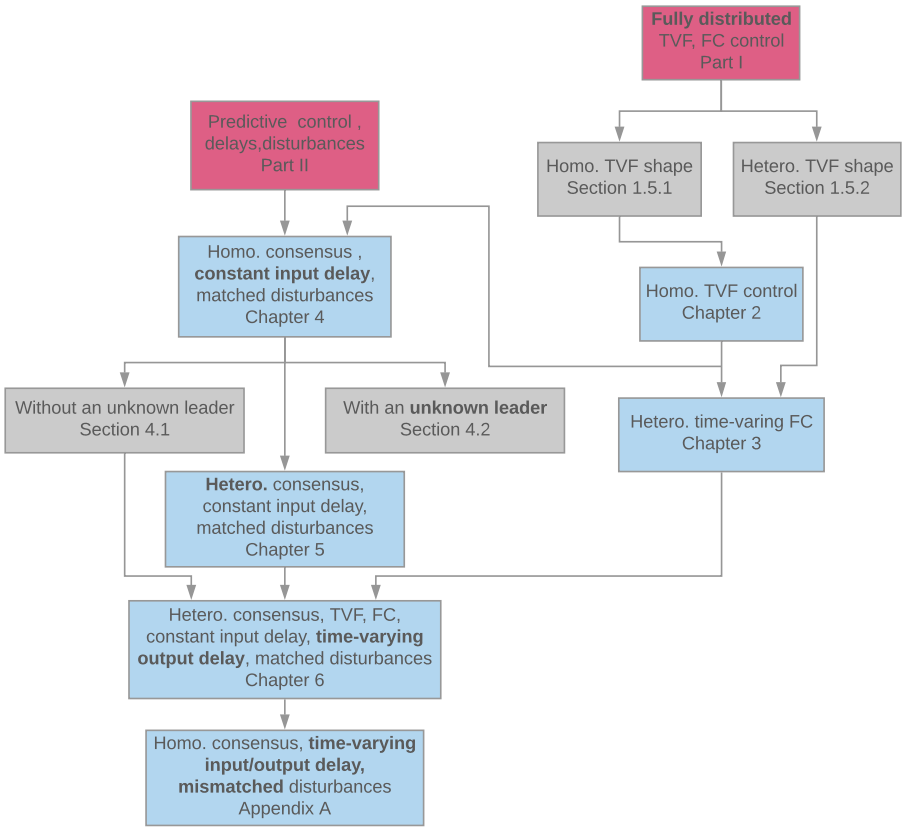

Figure A.4: Organisation (Homo.:homogeneous; Hetero.:heterogeneous).

méthode de l'observateur basée sur la sortie.

- La deuxième partie révèle une technologie de base derrière le contrôle TVF et FC — consensus, et étudie ses comportements en tenant compte des retards d'entrée / sortie variables en fonction de la constante / dans le temps, perturbations corrélées / non concordantes en concevant des contrôleurs prédictifs et adaptatifs avec la propriété entièrement distribuée.

Une organisation détaillée est montrée à la Fig. A.4. Les contributions sont indiquées tout au long de la présentation de chaque chapitre. **Notez que les théorèmes dans les encadrés sont les contributions principales de ce travail**.

La **Partie** I est dédiée à la présentation des nouvelles définitions du contrôle TVF avec la propriété entièrement distribuée, qui est l'une des contributions principales. Une autre contribution principale consiste à révéler l'essence de la relation entre le contrôle TVFT et le contrôle de confinement afin d'obtenir le contrôle FC variable dans le temps pour des systèmes MAS / MRS à grande échelle hétérogènes.

Dans le **Chapitre** 2, un cadre unifié de conception de contrôleurs TVF pour les MAS linéaires généraux basé sur un point de vue d'observateur, allant de la topologie non dirigée à dirigée et de la stabilisation au suivi, est proposé. La première version de cette méthode a été publiée pour la topologie de communication non dirigée dans Jiang *et al.* (2017). Une extension de la topologie dirigée du contrôle de stabilisation au contrôle de suivi est également donnée en détail. L'idée initiale réside dans la proposition d'une nouvelle définition du format de forme TVF (voir Fig. 1.10 (a)) et de la méthodologie de conception de contrôleurs entièrement distribués pour des MAS homogènes. La méthode basée sur l'observateur avec des mesures de sortie est utilisée et des preuves de convergence formelles sont données. Une simulation numérique est fournie pour vérifier les résultats théoriques.

Dans le **Chapitre** 3, le problème de contrôle FC variable dans le temps de sortie distribuée pour les MAS linéaires hétérogènes sous la topologie de communication dirigée basée sur le cadre de régulation de sortie du point de vue de l'observateur est étudié. Tous les agents peuvent avoir différentes dynamiques et différentes dimensions d'état. Tout d'abord, un autre nouveau format de forme TVF est proposé, qui diffère du format pour les MAS homogènes dans le **Chapitre** 2. Ensuite, le problème du contrôle TVFT pour les MAS hétérogènes est résolu en concevant le nouvel observateur entièrement distribué. Après cela, le problème de FC variable dans le temps est résolu. Une contribution importante réside dans la recherche du lien entre le TVFT et le FC variable dans le temps, les contrôleurs étant toujours entièrement distribués. Des simulations comprenant une application à de multiples robots mobiles hétérogènes non holonomiques sont démontrées pour vérifier l'efficacité des résultats théoriques. Une analyse du taux de convergence est également fournie. Le contenu de ce chapitre est partiellement résumé dans Jiang *et al.* (2018c).

La **Partie** II indique que le contrôle par consensus pourrait être considéré comme l'une des techniques principales du contrôle de la formation et du confinement variant dans le temps après l'analyse des résultats de la **Partie** I. L'objectif principal est d'abord de développer des contrôleurs prédictifs et adaptatifs afin d'obtenir de meilleures performances de contrôle par consensus en tenant compte des retards d'entrée / sortie variant constamment / dans le temps et des perturbations appariées / asymétriques externes, puis d'étendre les résultats au-dessus des contrôles TVF et FC dans le temps. L'analyse stable est présentée par la fonction de Lyapunov ou fonctionnelle de Lyapunov-Krasovskii avec des conditions suffisantes dérivées de l'équation algébrique de Riccati et de l'inégalité linéaire de la matrice. Tous les résultats de cette partie fonctionnent pour la topologie de communication dirigée.

Le **Chapitre** 4 traite du problème de suivi du consensus de réjection / atténuation de perturbations pour les MAS linéaires à retard d'entrée constant. Premièrement, dans la **Section** 4.1, lorsque le leader n'a aucune entrée de contrôle, un nouvel observateur d'état étendu prédictif adaptatif, utilisant uniquement les informations d'état relatives des agents voisins, est conçu sur la base de l'approche de la FSA afin d'obtenir un suivi du consensus de perturbations rejetées. Ensuite, dans la **Section** 4.2, le résultat est étendu au cas atténué par la perturbation où le leader a une entrée de contrôle délimitée qui n'est connue que par une partie des suiveurs (le leader inconnu). L'idée de base est de concevoir un nouveau prédicteur d'état pour transformer le MAS retardé en un système sans retard et de concevoir un nouvel observateur de perturbation pour compenser l'effet de perturbation. Les procédures détaillées pour traiter avec le chef inconnu sont également présentées. La contribution principale porte sur la conception de protocoles APESO avec la propriété entièrement distribuée. Ce travail est présenté dans Jiang *et al.* (2018a).

Le **Chapitre** 5 étend le résultat de la Section 4.1 en liant le résultat du Chapitre 3 à la résolution du problème de suivi du consensus de sortie pour les MAS linéaires hétérogènes utilisant l'approche par observateur. Tout d'abord, dans la **Section** 5.1, nous étudions le problème OCT en ne considérant que le délai d'entrée constant. Sur la base de l'approche FSA et de la théorie de la régulation de sortie, un autre prédicteur d'état innovant et un protocole adaptatif, qui requiert uniquement les états d'observateurs désignés des voisins et les informations de sortie du leader, sont proposés pour lutter contre l'effet de retard d'entrée. Ensuite, dans la **Section** 5.2, afin de réaliser le rejet de perturbation, les suiveurs sont contraints d'avoir la même dimension d'état afin que le protocole ci-dessus puisse être redéfini en fonction de l'approche de réduction d'Arstein, en ajoutant un nouvel APESO pour estimer la perturbation et le prédicteur d'état remodelé simultanément. Ce travail est donné dans Jiang *et al.* (2018d). Tous les résultats sont vérifiés par des simulations de MAS et de systèmes multi-véhicules.

Le **Chapitre** 6 étend les résultats du Chapitre 5 pour prendre en compte le délai de sortie variable dans le temps. L'approche descriptive introduite au Chapitre 1.3

permet d'analyser la stabilité au moyen de fonctionnelles de Lyapunov-Krasovskii. Des comparaisons détaillées sur la façon de concevoir des paramètres pour obtenir de meilleures performances de contrôle en ce qui concerne le retard de sortie variant dans le temps sont présentées. Enfin, nous montrons comment concevoir des contrôleurs entièrement distribués traitant des problèmes de contrôle coopératif, du consensus à la TVF, puis à la FC variable dans le temps pour des MAS LTI hétérogènes.

Dans **l'Annexe** A, une tentative pour résoudre le contrôle de suivi par consensus pour les MAS LTI homogènes en prenant en compte les retards d'entrée / sortie variables dans le temps et les perturbations asymétriques est complétée par la proposition du protocole de contrôle distribué sans termes intégraux. Les comparaisons détaillées sont fournies pour réfléchir à la manière d'améliorer les performances d'atténuation des perturbations face à des perturbations asymétriques.

Certains des résultats présentés dans cette thèse ont été publiés ou sont en cours de révision pour publication dans des revues et conférences.

Revues internationales

1. Wei Jiang, Zhaoxia Peng, Ahmed Rahmani, Wei Hu and Guoguang Wen, *Distributed consensus of linear MASs with an unknown leader via a predictive extended state observer considering input delay and disturbances*, Neurocomputing, 315, 465-476, 2018.
   Jiang *et al.* (2018a)

2. Wei Jiang, Guoguang Wen, Zhaoxia Peng, Tingwen Huang and Ahmed Rahmani, *Fully distributed formation-containment control of heterogeneous linear multi-agent systems*, IEEE Transactions on Automatic Control, accepted.
   Jiang *et al.* (2018c)

3. Wei Jiang, Guoguang Wen, Ahmed Rahmani, Tingwen Huang, Zhongkui Li and Zhaoxia Peng, *Observer-based fully distributed output consensus tracking of heterogeneous linear multi-agent systems with input delay and disturbances*, IEEE Transactions on Cybernetics, submitted.
   Jiang *et al.* (2018d)

4. Wei Jiang, Ahmed Rahmani and Guoguang Wen, *Fully distributed time-varying formation-containment control for large-scale nonholonomic vehicles with an unknown real leader*, International Journal of Control, submitted.
   Jiang *et al.* (2018b)

Conférences internationales

1. Wei Jiang, Guoguang Wen, Yunhe Meng and Ahmed Rahmani, *Distributed adaptive time-varying formation tracking for linear multi-agent systems: A dynamic output approach*, Chinese Control Conference, Dalian, China, 2017.
   Jiang *et al.* (2017)

Titre

Contrôle de la formation et du confinement variable dans le temps et entièrement distribué pour les systèmes multi-agents/ multi-robots

Résumé

Cette thése traite du contrôle de la formation et du confinement variant dans le temps pour les systèmes multi-agents linéaires invariants avec hétérogénéité en tenant compte des délais d'entrée / sortie constants / variables dans le temps et des perturbations adaptées / incompatibles sous topologie de communication dirigée et fixe. De nouveaux formats de formes de formation variables dans le temps pour des systèmes homogènes et hétérogènes sont proposés. Les contrôleurs, conçus sur la base de techniques prédictives et adaptatives avec une technique d'observation, sont entièrement distribués et peuvent être appliqués à des systèmes à grande échelle. L'application sur les systèmes robotisés multi hétérogènes linéarisés est vérifiée.

Mots-clefs

Systèmes multi-agents hétérogènes, formation et confinement variant dans le temps, contrôleurs entièrement distribués, systèmes de délai d'entrée et de sortie, rejet et atténuation des perturbations.

Title

Fully Distributed Time-varying Formation and Containment Control for Multi-agent / Multi-robot Systems

Abstract

This thesis deals with the time-varying formation and containment control for linear time-invariant multi-agent systems with heterogeneity considering constant / time-varying input / output delays and matched / mismatched disturbances under directed and fixed communication topology. New formats of time-varying formation shapes for homogeneous and heterogeneous systems are proposed. The controllers, which are designed based on predictive and adaptive techniques with observer technique, are fully distributed and can be applied to large-scale systems. The application on linearized heterogeneous multi mobile robot systems is verified.

Key words

Heterogeneous multi-agent systems, time-varying formation-containment, fully distributed controller, input and output delay systems, disturbance rejection and attenuation.